ISTANBUL TECHNICAL UNIVERSITY ★ GRADUATE SCHOOL

COMPREHENSIVE TRANSCRIPTOMIC and GENOMIC ANALYSIS of OXIDATIVE STRESS-RESISTANT SACCHAROMYCES CEREVISIAE

Ph.D. THESIS

Nazlı KOCAEFE ÖZŞEN

Department of Molecular Biology-Genetics and Biotechnology

Molecular Biology-Genetics and Biotechnology Programme

JULY 2023

ISTANBUL TECHNICAL UNIVERSITY ★ GRADUATE SCHOOL

COMPREHENSIVE TRANSCRIPTOMIC and GENOMIC ANALYSIS of OXIDATIVE STRESS-RESISTANT SACCHAROMYCES CEREVISIAE

Ph.D. THESIS

Nazlı KOCAEFE ÖZŞEN
(521122107)

Department of Molecular Biology-Genetics and Biotechnology

Molecular Biology-Genetics and Biotechnology Programme

Thesis Advisor: Prof. Dr. Zeynep Petek ÇAKAR

JULY 2023

ISTANBUL TEKNİK ÜNİVERSİTESİ ★ LİSANSÜSTÜ EĞİTİM ENSTİTÜSÜ

OKSİDATİF STRESE DİRENÇLİ SACCHAROMYCES CEREVISIAE SUŞUNUN TRANSKRİPTOMİK ve GENOMİK ANALİZİ

DOKTORA TEZİ

Nazlı KOCAEFE ÖZŞEN
(521122107)

Moleküler Biyoloji-Genetik ve Biyoteknoloji Anabilim Dalı

Moleküler Biyoloji-Genetik ve Biyoteknoloji Programı

Tez Danışmanı: Prof. Dr. Zeynep Petek ÇAKAR

MAYIS 2023

Nazlı KOCAEFE ÖZŞEN, a Ph.D. student of İTU Graduate School student ID 521122107, successfully defended the thesis/dissertation entitled "COMPREHENSIVE TRANSCRIPTOMIC and GENOMIC ANALYSIS of OXIDATIVE STRESS-RESISTANT SACCHAROMYCES CEREVISIAE", which she prepared after fulfilling the requirements specified in the associated legislations, before the jury whose signatures are below.

Thesis Advisor :	**Prof. Dr. Zeynep Petek ÇAKAR** İstanbul Technical University	.....
Jury Members :	**Prof. Dr. Ayten KARATAŞ** Istanbul Technical University	.....
	Prof. Dr. Emine Şeküre Nazlı ARDA Istanbul University	.....
	Prof. Dr. Tuba GÜNEL Istanbul University	.....
	Assoc. Prof. Dr. Ceren ÇIRACI MUĞAN Istanbul Technical University	.....

Date of Submission : 18 May 2023
Date of Defense : 25 July 2023

To my family,

FOREWORD

I would like to convey my gratitude to my supervisor Prof. Dr. Zeynep Petek ÇAKAR for her guidance and support throughout my thesis.

I would also like to thank to my thesis steering committee members, Prof. Dr. Nazlı ARDA and Prof. Dr. Ayten KARATAŞ, for their valuable contributions.

I am also very grateful to Dr. Ceren Alkım for her support and contribution. She always encouraged me not only in laboratory but also in all life.

I would like to thank to Dr. Bahtiyar Yılmaz for his succesful experiments. The mutant I worked on for my thesis was obtained by his successful experiments.

I am also thankful to my colleagues Dr. Berrak Gülçin Balaban, Dr. Mevlüt Arslan, Halil İbrahim Kısakesen, Erdinç Gülsev, Can Holyavkin, Alican Topaloğlu for their support, the times we spent and shared. I also need to thank to them for their technical assistance. I also would like to thank to Levent Üge for maintenance of laboratory equipments.

I would like to remember and thank to my thesis steering committe member and one of the best professors, Prof. Dr. Fatma Neşe KÖK. Your teachings will forever live with your students.

Finally, I would like to thank to my family being with me all the time.

May 2023

Nazlı KOCAEFE ÖZŞEN
(M.Sc.)

TABLE OF CONTENTS

Page

ABBREVIATIONS

AP : Apurine/Apyrimidine
BAM : Binary Alignment Map
cDNA : Complementary Deoxyribonucleic Acid
cRNA : Complementary Ribonucleic Acid
CLS : Chronological Life Span
DNA : Deoxyribonucleic Acid
dsDNA : Double Stranded Deoxyribonucleic Acid
DTT : Dithiothreitol
EDTA : Ethylenediaminetetraacetic acid
EMS : Ethyl Methanesulfonate
ER : Endoplasmic Reticulum
ESR : Environmental Stress Response
et al, : And Others
FAD : Flavin Adenine Dinucleotide
HOG : High Osmolarity Glycerol
HPLC : High Performance Liquid Chromatography
IGV : Integrative Genomics Viewer
KEGG : Kyoto Encyclopedia of Genes and Genomes
NAD : Nicotinamide Adenine Dinucleotide
PCR : Polymerase Chain Reaction
RIN : RNA Integrity Number
RNA : Ribonucleic Acid
rRNA : Ribosomal Ribonucleic Acid
ROS : Reactive Oxygen Species
RPM : Revolution Per Minute
RS : Reactive Species
SNP : Single Nucleotide Polymorphism
SOD : Superoxide Dismutase
STRE : Stress-Response Elements
TE : Tris EDTA

VCF **:** Variant Caller File

YMM **:** Yeast Minimal Medium

YPD **:** Yeast Extract Peptone – Dextrose

SYMBOLS

atm	**:** Atmospheric Pressure
bp	**:** Base Pair
µg	**:** Microgram
µL	**:** Microliter
g	**:** Gravity
h	**:** Hour
M	**:** Molar
min	**:** Minute
mL	**:** Milliliter
mM	**:** Millimolar
ng	**:** Nanogram
OD	**:** Optical Density

LIST OF TABLES

Page

LIST OF FIGURES

Page

COMPREHENSIVE TRANSCRIPTOMIC and GENOMIC ANALYSIS of OXIDATIVE STRESS-RESISTANT SACCHAROMYCES CEREVİSİAE

SUMMARY

Oxidative stress occurs as the oxidant and antioxidant balance in an organism is disrupted in the direction of oxidants, and oxidants come to a position that can potentially cause damage.

All aerobic organisms use oxygen for respiration and oxidation of nutrients for producing energy. For this reason, while oxygen is necessary for aerobic organisms to live, it is also harmful because of the reactive oxygen species (ROS) that emerge during these processes that are necessary for life. Lipid, protein and DNA molecules, which form the basis of life, can be damaged directly or indirectly due to oxidative stress caused by ROS.

Aerobic organisms have developed various mechanisms to protect themselves from the harmful effects of oxidative stress. These mechanisms involve enzymatic and non-enzymatic (antioxidants) systems. In addition to these mechanisms, organisms use various repair mechanisms, especially to repair damaged DNA.

Oxidative stress from ROS is biomedically important and widely researched, as it causes many neurodegenerative and autoimmune diseases, as well as cardiovascular diseases, cancer, and aging in mammals.

The yeast *Saccharomyces cerevisiae* is used as a model organism, because of its beneficial characteristics. *S. cerevisiae*, which is a eukaryotic organism, has a short-life span. It is a single cell organism and can be found as haploid, diploid or polyploid in nature. Thus, *S. cerevisiae* is an important model organism for elucidating the processes in eukaryotic complex organisms.

The aim of this study was to characterize an oxidative stress-resistant mutant *S. cerevisiae* strain at genetic and transcriptomic levels. The main idea, however, was to comprehensively examine the complex molecular infrastructure of oxidative stress resistance. In addition, as a physiological analysis, the cell wall properties of the mutant strain was also tested and information was obtained about the effect of stress on the cell wall structure.

In this thesis study, transcriptomic analysis of the mutant *S. cerevisiae* was performed by comparing the transcriptomic profiles of the oxidative stress-resistant, evolved *S. cerevisiae* and the reference strain. Transcriptomic data of the strains were obtained by microarray analysis.

As a genomic analysis, the entire genomes of the oxidative stress-resistant strain and the reference strain were sequenced and the differences in the genome were determined to find the mutations in the evolved srain that are related to oxidative stress resistance.

In addition, cell wall analyses of the reference strain and the mutant strain were performed, using lyticase susceptibility test.

As a result of transcriptomic analysis, it was observed that the expression level of 869 genes changed by at least 2-fold, 349 genes changed by at least 3-fold, 144 genes changed by at least 4-fold, and 67 genes changed by at least 5-fold in the oxidative stress-resistant mutant. Among these 869 genes that were differentially regulated by 2 times or more, 459 genes were upregulated and 410 genes were downregulated. The genes whose expression were decreased are generally related with ribosomal RNA, nuclear transport, organelle integration, tRNA cell cycle, mitosis and RNA polymerase. Expression levels of stress response genes, carbohydrates, lipid, protein, precursor metabolites and ion/metabolite transport-related genes were generally increased in the mutant strain.

According to the ESR analysis results, a positive correlation was observed between the ESR-induced genes and the genes of the oxidative stress- resistant mutant with increased expression, according to the database. In addition, a positive correlation was observed between ESR-suppressed genes and genes of the mutant with decreased expression. The expression levels of two genes related to oxidative stress decreased and twenty three of them increased in the oxidative stress-resistant, evolved strain.

The expression levels of six autophagy-related genes in the oxidative stress-resistant mutant decreased and 30 of them increased.

According to whole genome sequencing results, 34 missense, 2 nonsense, 1 deletion and 12 silent mutations were found in the genes of the mutant strain, and 13 mutations were detected in chromosomal regions outside the coding regions. A nonsense mutation in the *NRG1* gene, which is a transcriptomic regulator, results in the formation of a truncated protein. Further genomic and proteomic studies would be necessary to clarify the role of these genes and mutations in the oxidative stress resistance.

OKSİDATİF STRESE DİRENÇLİ SACCHAROMYCES CEREVİSİAE SUŞUNUN TRANSKRİPTOMİK ve GENOMİK ANALİZİ

ÖZET

Oksidatif stres; organizmadaki oksidant ve antioksidant dengesinin oksidantlar yönünde bozularak oksidantların potansiyel olarak hasara neden olabilecek konuma gelmesi olarak nitelendirilmektedir.

Aerobik organizmalar oksijen kullanarak solunum yapmakta ve enerji ihtiyacına yönelik olarak besinleri okside etmek için oksijen kullanmaktadırlar. Bu sebepten ötürü oksijen, aerobik canlılar için gerekli olmakla birlikte, bu süreçte oluşan reaktif oksijen türleri (ROS) nedeni ile zararlı da olabilmektedir. Canlılığın temelini oluşturan lipid, protein ve DNA molekülleri ROS'ların oluşturduğu oksidatif stres nedeniyle doğrudan veya dolaylı olarak zarar görebilmektedir.

ROS, dioksijenin (O_2) farklı durumlarından meydana gelmektedir. Oksijenli solunum süresince üretilen en önemli ROS'lar süperoksit anyonu, hidrojen peroksit ve reaktif hidroksil radikalleridir.

Aerobik canlılar oksidatif stresin zararlı etkilerinden korunmak amacıyla çeşitli mekanizmalar geliştirmişlerdir. Bu mekanizmalar; enzimatik ve enzimatik olmayan (antioksidanlar) mekanizmalar olarak ikiye ayrılır. Organizmalar, bu mekanizmaların yanında özellikle DNA hasarını gidermek için çeşitli tamir mekanizmaları da kullanırlar.

ROS'tan kaynaklı oksidatif stres memelilerde bir çok nörodejeneratif ve otoimmün hastalıklara neden olduğu gibi, kardiyovasküler hastalıklar, kanser ve yaşlanmaya da sebebiyet verdiği için biyomedikal açıdan önemlidir ve geniş kapsamlı olarak araştırılmaktadır.

Saccharomyces cerevisiae mayası, kısa yaşam süresine sahip olması ve tek hücreli olması dolayısıyla kolaylıkla genetik olarak manipüle edilebilir ve bu nedenle bilimsel çalışmalarda model organizma olarak sıklıkla kullanılmaktadır. Bunun yanında *S. cerevisiae*'nin ökaryotik bir organizma olması ve doğada diploid, haploid, ya da poliploid olarak bulunabilmesi de ökaryotik kompleks organizmalardaki proseslerin aydınlatılması için *S. cerevisiae*'yi önemli bir model organizma konumuna getirmektedir.

Metabolik mühendislik, 1991 yılında Bailey tarafından, hücrelerin enzimatik, taşınım ve regülasyon fonksiyonlarının rekombinant DNA teknolojisinin kullanılmasıyla değiştirilerek, hücresel aktivitelerin geliştirilmesi olarak tanımlanmıştır. Evrimsel mühendislik ise, bir tersine metabolik mühendislik yaklaşımı olup, istenen fenotipik özelliklerin çevresel stres uygulamaları ve uygun seçilim stratejisi kullanılarak yapay bir evrimsel süreç ile elde edilmesine dayanmaktadır. Bu yöntem ile elde edilen, özellikleri iyileştirilmiş mikroorganizmanın fenotipi karakterize edilip, incelenen

özellikler genetik, transkriptomik, fizyolojik ve proteomik çalışmalarla aydınlatılabilir.

Bu çalışmanın amacı; bir tersine metabolik mühendislik stratejisi olan evrimsel mühendislik ile daha önceki çalışmalar ile elde edilmiş olan, oksidatif strese dirençli bir *S. cerevisiae* mutant mayasının genomik ve transkriptomik düzeyde karakterize edilmesidir. Asıl amaç ise, oksidatif stres direncinin karmaşık moleküler altyapısının kapsamlı olarak incelenmesidir. Ayrıca fizyolojik analiz olarak hücre duvarı yapısına dair de analiz gerçekleştirilmiş ve stresin hücre duvarı yapısı üzerindeki etkisi hakkında bilgi sahibi olunmuştur.

Çalışmada kullanılan mutant maya, daha önceki çalışmalarda evrimsel mühendislik ile elde edilmiştir. Kısaca, önce başlangıç kültürü EMS'ye (etil metan sülfonat) tabi tutularak genomda rastgele mutasyonlar oluşması sağlanmış, daha sonra kültürlerden alınan pasajlar sürekli ve giderek artan düzeyde hidrojen peroksit stresine (oksidatif stres) maruz bırakılmıştır. EMS ile oluşturulan rastgele mutasyonlar, hidrojen peroksit uygulaması ve stres direnç testleri ile seleksiyon sağlanmış, oksidatif strese dirençli bir birey seçilmiştir.

Bu süreçte oksidatif strese dirençli mutant *S. cerevisiae* suşu ve referans suşun mikroarray yöntemiyle oluşturulan transkriptomik profillerinin karşılaştırılması ile mutant *S. cerevisiae*'nin transkriptomik analizleri gerçekleştirilmiştir.

Genomik analiz olarak, oksidatif strese dirençli suş ile referans suşun tüm genomları dizilenmiş ve mutant suşun genomunda evrimsel mühendislik sürecinde oluşmuş olan farklılıklar belirlenmiştir.

Genomik ve transkriptomik analizler ile birlikte ESR (çevresel stres direnci) analizleri, KEGG analizi ile yolak analizleri gerçekleştirilmiştir. Ayrıca transkriptomik verileri ile otofaji genleri analizi yapılmıştır. Mutant suşta nonsense (anlamsız) mutasyona uğramış bir transkripsiyon baskılayıcı gen olan *NRG1* geni tarafından regüle edilen genler de analiz edilmiştir.

Bunun yanında litikaz duyarlılık testi ile, referans suş ile mutant suşun hücre duvarı analizleri gerçekleştirilmiştir.

Transkriptomik analiz sonucunda oksidatif strese dirençli mutantta 869 genin 2 kat ve üzerinde, 349 genin 3 kat ve üzerinde, 144 genin 4 kat ve üzerinde, 67 genin 5 kat ve üzerinde ekspresyon değişimi gösterdiği gözlenmiştir. 2 kat ve üzeri değişen 869 genden 459 genin ekspresyonu artmış, 410 genin ekspresyonu da azalmıştır.

Ekspresyonu azalan genler genellikle; ribozomal RNA, nukleus taşınımı, organel bütünleşmesi, tRNA hücre döngüsü, mitoz ve RNA polimeraz ile ilgilidir.

Stres cevap genleri, kabronhidrat, lipit, protein, öncül metabolitler ile iyon ve metabolit taşınımı ile ilgili genlerin ekspresyonları ise mutant suşta genellikle artmıştır.

ESR analiz sonucuna göre ise veri tabanı bilgilerine göre ESR ile indüklenen genler ile oksidatif strese dirençli mutantın ekspresyon düzeyi artmış genleri arasında pozitif korelasyon gözlenmiştir. Ayrıca ESR ile baskılanan genler ile mutantın ekspresyonu azalmış olan genleri arasında da pozitif korelasyon belirlenmiştir.

Beklenildiği üzere, stres cevap genleri analizine göre kimyasal stres, oksidatif stres, sıcaklık stresi, osmotik stres, glikoz limitasyonu stresi ve açlık stresine cevap genlerinin ekspresyonu artmıştır.

Oksidatif strese dirençli mutant mayanın, ekpresyon düzeyleri 2 kat ve üstü değişen genleri oksidatif stres genleri açısından incelendiğinde, bunların iki tanesinin ekspresyonun azaldığı yirmiüç tanesinin ise ekspresyonun arttığı gözlenmiştir.

Oksidatif strese dirençli mutantta otofaji ile ilişkili olan altı adet genin ekpresyonu azalmış, otuz adedinin ise artmıştır.

Genomik analizler incelendiğinde; mutant suşta genler üzerinde 34 yanlış anlamlı (missense), 2 anlamsız (nonsense), 1 delesyon, 12 adet de sessiz (silent) mutasyon bulunmuş olup, 13 adet mutasyon da genlerin dışında kalan kromozomal bölgelerde saptanmıştır. Bir transkriptomik regülatör olan *NRG1* genindeki anlamsız mutasyon ise, yarım kalmış (truncated) bir protein oluşmasına neden olmaktadır.

Mutant suşta anlamsız mutasyonun görüldüğü diğer gen ise *DUF1* genidir. Bu gen, fonksiyonu tam olarak bilinmeyen bir ubikitine bağlanan protein (ubiquitine-binding protein) kodlamakta olup, mutasyonun gerçekleştiği ve protein sentezinin durduğu nokta, proteinin işlevinin esas gerçekleştirildiği WD40 domeynine oldukça uzaktır. Gelecek çalışmalarda tek başına bu mutasyona uğratılmış referans suş ile mutasyonun işlevi ve hatta proteinin işlevi konusunda bilgi sahibi olunabilir. Benzer şekilde, *DUF1* gibi diğer mutasyonlar da, özellikle gen içerisinde meydana gelen yanlış anlamlı ve sessiz mutasyonlar ile delesyonlar referans suşta birer birer veya çeşitli kombinasyonlarla meydana getirilip fizyolojik ve/veya genomik, transkriptomik ve proteomik çalışmalar ile incelenebilir. Yolaklar daha kesin bilgiler ile aydınlatılabilir ve böylelikle fonksiyonları tam bilinmeyen proteinler ve genler hakkında bilgi sahibi olunabilir.

1. INTRODUCTION

1.1 Oxidative Stress

Oxidative stress was defined as “an imbalance between oxidants and antioxidants in favor of the oxidants, potentially leading to damage” (Sies, 1997). Oxidative damage was described as “the biomolecular damage caused by attack of reactive species (RS) during constituents of living organisms” (Halliwell & Whiteman, 2004). There are two reasons for oxidative stress. The first one is a reduced level of antioxidants due to a mutation on a gene related to an antioxidant defense enzyme. The second one is the escalated production of reactive species, for instance, exposure of cells or organisms to high levels of molecular oxygen or other toxins, which are RS (Halliwell & Whiteman, 2004) (Figure 1.1) .

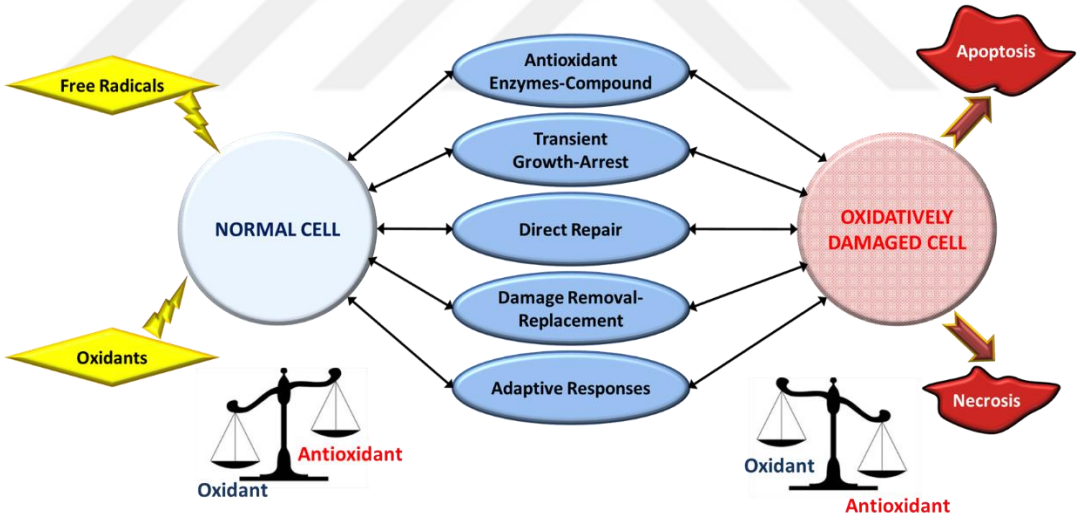

Figure 1.1 : The balance between oxidative stress and antioxidant defense mechanisms (modified from Davies, 2000).

1.1.1 Oxidative stress elements

Molecular oxygen is used by all aerobic organisms for oxidation of nutrients and respiration in order to produce energy efficiently. While molecular oxygen is reduced to water through the acceptance of four electrons, active oxygen species such as

superoxide anion radical, hydrogen peroxide and hydroxyl radical are produced during the processes required for living (Ames et al., 1993; Toyokuni et al., 1995).

Hydrogen peroxide, a major oxidative stress factor, causes increased DNA strand breakage within minutes accompanied by an increase in base modification products. However, hydrogen peroxide does not damage DNA or RNA molecules directly. The pattern of DNA damage (raises of the levels of multiple products of all four bases) indicates attack by OH•. If DNA is attacked by this RS, it could be speculated that it must be produced very close to DNA. Because OH• is highly reactive, it cannot diffuse from its site of formation. Fenton chemistry is responsible for this situation. OH• is generated during Fenton chemistry in the nucleus, then the iron ions must be in close proximity to DNA. Copper/ H_2O_2 reactions may also generate oxo-copper complexes in addition to OH• which are DNA-damaging molecules. Iron and copper normally exist in the nucleus. However, they are not in a molecular form that will cause OH• formation. Another possibility is that oxidative stress causes release of intracellular iron and/or copper ions that bind readily to DNA, making it a target of H_2O_2 attack. Either way the presence of the metal ions on DNA favors'site-specific' OH• generation, leading to DNA damage. Another reason for lack of protection by scavengers is that some of the scavengers-derived radicals themselves cause DNA damage period. Radicals derived from formate, propane-2-ol, glycerol and dimethylthysulphoxide cause single-strand breaks in DNA (Halliwell & Gutteridge, 2007).

Generally, during the Fenton reaction hydrogen peroxide occurs via hydroxyl radicals produced and it can damage the cellular products. Oxidation of arginine, lysine, proline and histidine causes division at proline, aspartate and glutamate residues forming carbonyl derivatives. Degradation of the proteins occurs by proteasomes from the polypeptide chains of the proteins (V. Costa & Moradas-Ferreira, 2001) (Figure 1.2).

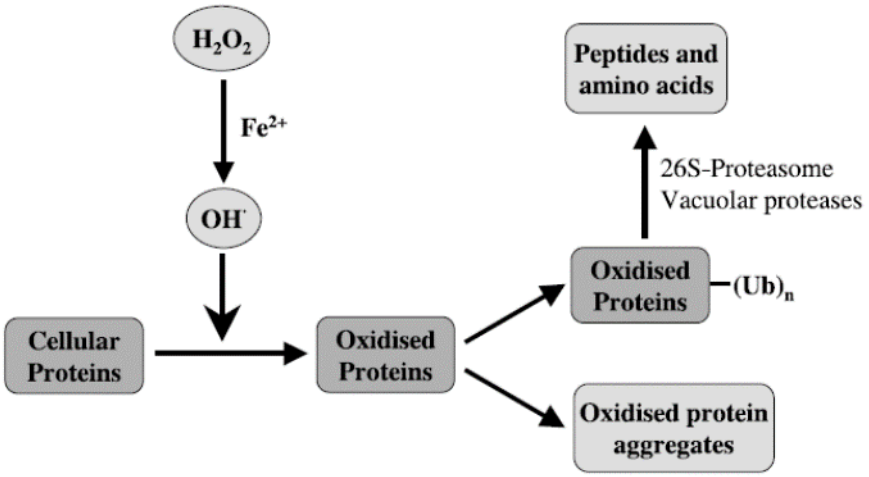

Figure 1.2 : Generation of hydroxyl radical via protein oxidation during Fenton reaction (Costa and Moradas-Ferreira, 2001).

DNA-related copper ions might also react with certain phenols to produce ROS at oxidized phenols. This could form a range of oxidative DNA lesions and phenol adducts to the DNA bases, which may contribute to the carcinogenicity of certain phenolic compounds (Brunelli et al., 2001; DeMaster et al., 1998).

1.1.2 Effects of oxidative stress on organisms

Oxygen and oxygen-derived oxidants are the first causes of cellular damage and ROS related diseases. Oxidants are tried to be balanced by antioxidants and repair systems in all organisms. Oxidative stress is highly important in biomedicine, as the process of aging, neurodegenerative, inflammatory and cardiovascular diseases and cancer are related with this stress (Ames et al., 1993; Hohmann & Mager, 2003). High levels of iron accumulation-related oxidative damage causes the pathogenesis of cardiovascular diseases and cancer (Nordberg et al., 2002).

Modification of DNA bases are induced by reactive oxygen species generated from hydrogen peroxide. ROS can cause strand breaks or intrachromosomal recombination on DNA helix. If those mutations cannot be repaired, modifications may cause degenerative diseases or cancer which can be lethal for an organism (V. Costa & Moradas-Ferreira, 2001). It is known that mammalian mitochondrial rRNAs are degraded as a response to oxidative stress (Crawford, 2002).

ROS appear as natural derivatives in mitochondrial respiration. The accumulation of oxidative damage in mitochondria can cause autophagy of the damaged mitochondria. This process is defined as mitophagy and it is quite well conserved from yeast to

humans. Mitophagy can cause aging and several neurodegenerative diseases such as Parkinson's (Bhatia-Kiššová & Camougrand, 2010).

1.2 *Saccharomyces cerevisiae* as a Model Organism

As a model organism, *Saccharomyces cerevisiae* is a unicellular eukaryotic organism with short life cycle and has an uncomplicated structure. Its genome contains approximately 6000 genes, which have been sequenced and mapped. These all-basic features are important for scientific studies to understand life processes. Especially, the uncomplicated structure of this yeast allows researchers to work on and understand the major processes in more complex organisms. For instance signal transduction pathways, cell cycle control progression, the basis of switch from mitosis to meiosis, genetic recombination, intracellular trafficking of proteins in cell, protein degradation processes and general stress response such as heat shock, ethanol resistance, oxidative stress and heavy metal resistance, which are essential processes for complex living organisms, are studied using this yeast as a model organism (Gershon & Gershon, 2000; Glover & Lindquist, 1998; Goffeau et al., 1996; Stahl, 1996; Whitmarsh & Davis, 1998).

The yeast *S. cerevisiae* is one of the mostly used microorganisms in the various industrial biotechnological product manufacturing processes (Berterame et al., 2018). Biotechnological processes often require robust strains. Thus, it is expected that these strains are tolerant to at least one or several stress conditions such as extreme pH, high temperature and osmotic pressure levels, shearing forces, organic acids and/or toxic substances (Kavščček et al., 2015). Also, during the biotechnological production processes in industry, yeasts are faced with different stress factors which often include oxidative stress. These products can cause the disruption of the cell growth. Consequently, to increase production and yield, the development of robust strains is necessary (Berterame et al., 2018).

The yeast *S. cerevisiae* has been greatly utilized to explain the mechanisms of oxidative stress response. Many aspects of the responses of *S. cerevisiae* to environmental stressors have already been elucidated (Wallace-Salinas et al., 2015). The yeast *S. cerevisiae* is the most suitable eukaryotic model organism for the analysis of core molecular mechanisms of the oxidative stress response. As *S. cerevisiae* can be easily manipulated genetically through defined mutations, and physiologically via

manipulation of growth and environmental conditions, it is a well-known species and one of the most studied organisms. In addition, the genome whole sequence of *S. cerevisiae* is already known. Besides, DNA microarray data in databases allow the analysis of changes in the entire transcriptome during cellular adaptation to stress conditions (Moradas-Ferreira & Costa, 2001).

In the past, researches using the yeast *S. cerevisiae*, as model organism, have provided great development to have knowladge about crucial cellular and molecular processes (Botstein & Fink, 2011). Recently, the studies on yeasts is undergoing a 'rebirth' in both fundamental and applied research. Research on budding yeast contributed significantly to the knowledge about the aging process. It has been particularly useful in adopting classical and molecular genetic approaches to associate genes with proteins, which are produced under certain conditions, and to understand the functions of these proteins within the cell (Rona et al., 2015).

1.2.1 Effects of oxidative stress on *S. cerevisiae*

Oxidative stress has been connected to the pathogenesis of several diseases. There are different producers of oxidative stress. In addition, aging is the most common risk factor for particular diseases. However, most theories about aging processes concentrate on the levels of cumulative oxidative stress, the aging mechanism and the diseases related with age (Gandhi & Abramov, 2012; Mariani et al., 2005).

It is also shown that oxidative damage on DNA by ROS is the cause of multiple lesions such as single-strand breaks, double-strand breaks, apurine/apyrimidinic sites and modified pyrimidines and purines (Potukuchi et al., 2018; Woodbine et al., 2011).

The reactive oxygen species such as hydrogen peroxide, superoxide anion and hydroxyl radical are causes of cellular death, mutagenesis and carcinogenesis, aging, arthritis, ischaemic damage and emphysema in multicellular organisms (Mello Filho et al., 1984).

According to the studies of Hoffmann and Meneghini (1979), H_2O_2 causes single-strand breaks on DNA. But H_2O_2 does not attack DNA directly. It was suggested that the Fenton reaction occurred in cells to remove H_2O_2. During the Fenton reaction, hydroxyl radicals occur. Hoffmann and Meneghini (1979) found that Fenton reaction did not occur in the absence of iron. Hydroxyl radicals, which are more reactive than hydrogen peroxide, do not appear. Thus, they showed that DNA was not damaged by

H_2O_2 attacks, but hydroxyl radicals made single-strand breaks on DNA (Mello Filho et al., 1984).

$$H_2O_2 + Fe^{+2} = OH^{\cdot} + OH^{-} + Fe^{+3} \quad (1.1)$$

Generally, lipids and amino acid residues are not damaged by hydrogen peroxide. Hydroxyl radicals, which are produced by Fenton reactions, attack lipids, PUFA (Polyunsaturated Fatty Acids), head groups of phospholipids and amino acid residues. Hydrogen peroxide can attack certain easily-oxidizable accessible –SH groups such as G3PDH and caspase enzyme. Hydrogen peroxide does not attack or it attacks indirectly at the physiological level (Halliwell & Gutteridge, 2007).

Molecular oxygen is used as an electron acceptor for aerobic respiration and oxidation of nutrients by aerobic organisms to generate energy (Zhao et al., 2015). During these metabolic processes by reduction of molecular oxygen not only water is produced, but also some ROS including superoxide anion, hydrogen peroxide, and hydroxyl radicals appear (Figure 1.1). ROS cause serious damages in cellular components, such as DNA, proteins and membrane lipids. As an example for a nucleic acid damage, ROS damage can cause oxidative DNA damage by altering purine and pyrimidine structures as well as cleave the phosphodiester bonds (Halliwell & Gutteridge, 2007).

When proteins that bind to metals are exposed to hydrogen peroxide, as a result of some reactions, especially the Fenton reaction, hydroxyl radicals come out and damage the amino acid residues easily (Halliwell & Gutteridge, 2007).

1.2.2 Response to oxidative stress in *S. cerevisiae*

All organisms including fungi, plants, microorganisms and the other multicellular organisms use different signal transduction mechanisms to take and reply to various environmental stress conditions (Hong et al., 2013a). During alcoholic fermentation and other conditions, *S. cerevisiae* cells work on to overcome various environmental stress conditions which affect their growth and development (Zuzuarregui et al., 2006). The theories and the perspectives related with the oxidative stress response were developed, based on yeast research. These studies have shown that modulation of transcription of response-related antioxidant genes helps with the survival of the organism (Hong et al., 2013b). Yeasts have a sensing mechanism to detect changes in the living space (existence of the required or toxic substance, nitrogen and carbon

starvation, physical situations of environment such as pressure, osmolarity, temperature, pH, etc.). This sensing step is necessary for the activation of signal transduction pathways. The signal transduction pathway of stress response causes the changes in particlar gene expression. Besides, protective molecules are synthesized, and/or modulation of the protein activity by posttranslational modifications or subcellular localization changes occurs (Hohmann & Mager, 2003). Ultimately, alteration in the activity levels of yeast proteins has an important role in the adaptation of the cell to various environmental conditions (Zuzuarregui et al., 2006).

Numerous transcription factors are related with the stress-activated protein kinase/mitogen-activated protein kinase (SAPK/MAPK) pathway. These transcription factors adjust the schedule and transcription level of particular genes coding the proteins responsible for antioxidants and secondary metabolism like trehalose and glycogen, thus controlling metabolic processes with cellular stress response (Hong et al., 2013a). Additionally, it is indicated that oxidative stress treatments stimulate the yeast osmosensing high-osmolarity glycerol (HOG) pathway (Bilsland et al., 2004). The fact remains that ROS could be also a trigger for the stimulation of stress response specific signaling pathways (Finkel & Holbrook, 2000).

Antioxidant defenses minimized the oxidative damages by scavenging or preventing the ROS generation, and repairing or degrading oxidatively damaged molecules (Costa et al., 2002). Organisms cope with oxidative stress via enzymatic and nonenzymatic defense systems to protect cellular constituents and maintain cellular redox state. Glutathione, trehalose, glycogen, thioredoxin, and glutaredoxin family are non-enzymatic systems which are used by *S. cerevisiae* to overcome oxidative stress. Besides, catalase, superoxide dismutase (SOD), glutathione peroxidase and reductase, thioredoxin peroxidase and reductase, methionine reductase, pentose phosphate pathway (PPP) enzymes, and Apn1 endonuclease are used as enzymatic stress response by *S. cerevisiae* for protection against oxidative stress (Jamieson, 1998).

Trehalose is important for the protection of cell membrane integrity. Autooxidation of membrane fatty acids can be prevented by the two-carbon sugar named trehalose (Doğan et al., 2014). Besides, glutathione is also important both as a nonenzymatic response to the defense of the cell and as an enzymatic response to degrade hydrogen peroxide to H_2O via glutathione peroxidase (Okada et al., 2014).

As mentioned earlier, *S. cerevisiae* has been known and studied as a eukaryotic model organism to understand the molecular mechanisms of oxidative stress resistance/response. In addition, evaluation of the antioxidant potential of dietary extracts and phenolic compounds are researched using budding yeast. Studies have shown that resveratrol (a secondary metabolite with an antioxidant effect, found in red grape, pineapple and peanut, etc.) and catechin (a secondary metabolite which is an antioxidant and found in tea, apple, pear, peach, vinegar, etc.) increase oxidative stress resistance of yeast by joining the catalase activation mechanisms. Delphinidin 3-glucoside (an anthocyanin found in berries) and petunidin 3-glucoside (a phenolic compond found in wine) protect yeast cells via activation of the stress response regulators Msn2p and Msn4p. Moreover, according to recent stdies, the sirtuin (signaling protein family work on metabolic regulation) Hst3p was shown to have a role in protection against oxidative stress, provided by a polyphenol-enriched cocoa powder (Mendes et al., 2015).

From the genomic perspective, oxidative stress response of the *S. cerevisiae* is regulated by transcription factors. The transcription factors have a major role in triggering response pathways. *YAP1* gene encodes a significant transcription factor and the Yap1p protein regulates the environmental stress response, both enzymatically and non-enzymatically. *GSH1*, regulated by Yap1p protein, encodes Gamma glutamylcysteine synthetase. The first step of glutathione biosynthesis is catalyzed by Gamma glutamylcysteine synthetase. Besides thioredoxin metabolism; SOD, catalase and cytochrome c peroxidase are also controlled by Yap1p transcription factor. After the expression of Yap1p, activated by H_2O_2 in oxidative stress conditions, it is oxidized to a disulphide bridge by peroxides and goes to the nucleus and increases gene expression. Finally, it is degraded in the nucleus when oxidative stress is over (Hon et al., 2003; Moye-Rowley et al., 1989; Okazaki et al., 2007). Deletion studies of the *YAP1* gene showed that yeast cultures with *YAP1* null mutation had hypersensitivity to hydrogen peroxide and could not induce 32 proteins (Lee et al., 1999).

MSN2 and *MSN4* genes are stress-responsive transcriptional activators. While the expression of *MSN2* is constitutive, *MSN4* gene expression is dependent on Msn2/4p complex and is induced by stress conditions. They are functionally related to each other and they bind to STRE (stress-response elements) sequence and have a role as the binding factor of STRE. Approximately two-hundred genes related with stress

response are regulated by Msn2/4 (Hasan et al., 2002; Martinez-Pastor et al., 1996; Schmitt & McEntee, 1996).

1.3 Metabolic Engineering

Metabolic engineering was defined as “the improvement of cellular activities by manipulation of enzymatic, transport, and regulatory functions of the cell with the use of recombinant DNA technology” (Bailey, 1991).

Genetic modifications with systematic manipulations are needed to obtain desired microbial phenotypes. This requires extensive knowledge about metabolic pathways and chemical networks. The major limitation in rational metabolic engineering is this need for extensive knowledge about the metabolic pathways of interest and/or regulatory systems. Besides, the complexity of the cellular physiological responses could be another limitation to overcome. Modification of a certain pathway may regulate changes in a high number of genes. Especially in industrial strains, this situation can make genetic manipulation very difficult (Bailey et al., 1996; Çakar et al., 2012).

1.3.1 Inverse metabolic engineering

As explained in Section 1.3, rational metabolic engineering has some limitations. Thus, inverse metabolic engineering was suggested and explained as a “bottom-up” approach. The aim of the inverse metabolic engineering method is to obtain an organism with the desired phenotype first, and then characterize and analyze this organism with the desired properties. The characterization of this organism is performed by using genomic, transcriptomic and proteomic methods. The major advantage of inverse metabolic engineering is that there is no need for extensive information about the metabolic pathways of interest. Any identified genetic factor related to the desired phenotype can then be transferred to the target organism (Bailey et al., 1996).

1.3.2 Evolutionary engineering

Evolutionary engineering involves obtaining the particular desired microbial phenotypes by use of random mutagenesis, environmental treatment and selection strategies (Çakar et al., 2012). Evolved strains are obtained with this strategy via

physical or chemical mutagenesis treatment followed by cultivation of the microorganism in medium containing particular selective treatment which could be high salt concentration, oxidative agent presence, high metal concentrations, high/low temperatures or freeze-thaw conditions. The application of selective strategy in repeated cycles provides selection highly resistant evolved strains. Evolutionary engineering strategy example for producing oxidative stress resistant evolved strain via EMS (Ethyl Methanesulfonate) and hydrogen peroxide (oxidative stress) treantment is shown in Evolutionary engineering strategy example for producing oxidative stress resistant evolved strain via EMS (Ethyl Methanesulfonate) and hydrogen peroxide (oxidative stress) treatment..

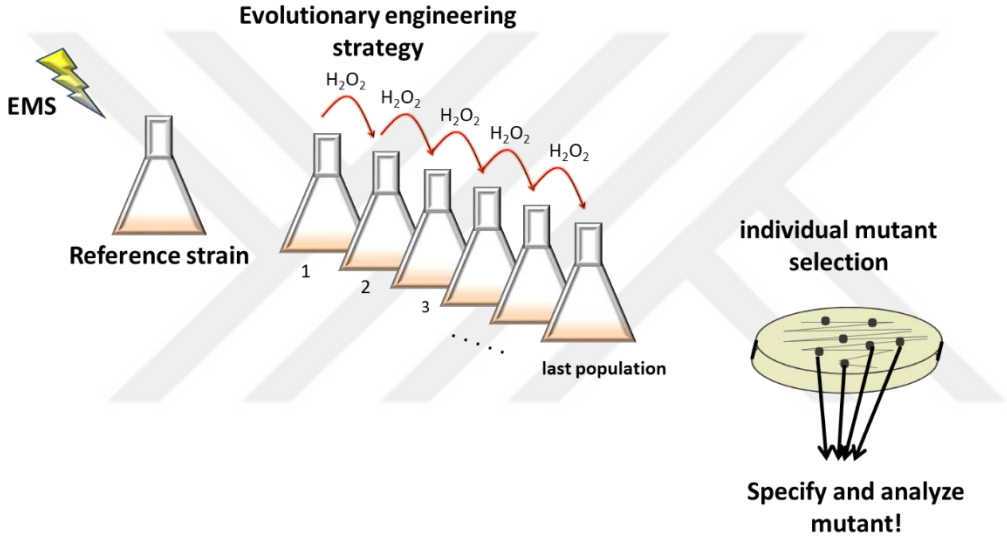

Figure 1.3 : Evolutionary engineering strategy example for producing oxidative stress resistant evolved strain via EMS (Ethyl Methanesulfonate) and hydrogen peroxide (oxidative stress) treatment.

1.4 Aim of the Study

The aim of this thesis study was to investigate the molecular basis of oxidative stress resistance in *S. cerevisiae*, by using comparative transcriptomic and genomic analysis of an oxidative stress-resistant *S. cerevisiae* strain and its reference strain, CEN.PK 113-7D (MATa, MAL2-8c, *SUC2*). The oxidative stress-resistant *S. cerevisiae* strain had been previously obtained by evolutionary engineering (Yılmaz, 2009), by applying selection in the presence of oxidative stress (hydrogen peroxide). The transcriptomic analyses were perfomed using DNA microarray technology, and genomic analyses were performed using whole genome sequencing technology. The

transcriptomic and genomic analysis results of the study will help understand the complex molecular basis of oxidative stress- resistance in *S. cerevisiae.*

2. MATERIALS and METHODS

2.1 Materials

2.1.1 Strains

S. cerevisiae CEN.PK 113-7D (MATα, MAL2-8c, SUC2) was used as the reference strain which was kindly provided by Dr. L. Benbadis from INSA-Toulouse, France. Hydrogen peroxide-resistant evolved strain 'H7' obtained previously via evolutionary engineering was also used, which has *S. cerevisiae* CEN.PK 113-7D background (Kocaefe-Özşen et al., 2022; Yılmaz, 2009).

2.1.2 Culture media and preservation conditions of strains

Media preparation and ingredients are described in Section 2.1.2.1 and 2.1.2.2. After media preparation, sterilization was performed via autoclaving at 121 °C and 1.2 atmospheric pressure (atm).

Yeast strains were stored in microcentrifuge tubes in 30% (v/v) glycerol at -80 °C for a long period of time. For the storage, strains were grown on solid complex medium, inoculated in the liquid complex medium in 50 mL culture tubes overnight at 30 °C. The next day, cultures were centrifuged, supernatant was thrown away, and precipitated yeast cells were resuspended in 30% (v/v) glycerol for long-term storage.

Yeast strains were cultured on agar medium on Petri plates and kept at 4 °C to store for a short period.

2.1.2.1 YPD (Yeast Extract Peptone Dextrose) medium

Yeast Extract Peptone Dextrose Medium, also abbreviated as YPD, is a complete, complex medium for yeast growth. YPD medium was used as both solid and liquid medium. It contains 2% D-glucose, 1% yeast extract, 1% peptone and 2% agar (if it is used as solid media), (w/w). YPD ingredients are listed in Table 2.1.

Table 2.1 : Yeast Extract Peptone Dextrose Medium ingredients.

Content "w/v"	Amount
2% D-Glucose	20 g
1% Peptone	10 g
1% YeastExtract	10 g
2% Agar*	20 g
dH_2O	up to 1000 mL final volume
*When solid medium is desired, agar was added to medium as indicated above.	

2.1.2.2 YMM (Yeast Minimal Medim)

Yeast Minimal Medium was used for regular growth. YMM includes 2% D-glucose, 1% Yeast Nitrogen Base without amino acids and agar (if solid media is used). YMM constituents are given in Table 2.2.

Table 2.2 : Yeast Minimal Medium ingredients.

Content "w/v"	Amount
2% D-Glucose	20 g
0.67% Yeast Nitrogen Base (without amino acids)	6.7 g
2% Agar*	20 g
dH_2O	up to 1000 mL final volume
*When solid medium is desired, agar was added to medium as indicated above.	

2.1.3 Laboratory equipment, chemicals, kits, enzymes, software programs and databases

Laboratory equipment, chemicals, kits, enzymes, software and databases used in this study are indicated in Table 2.3, Table 2.4, Table 2.5 and Table2.6 respectively, with their trademarks, and country of origin.

Table 2.3 : Laboratory equipment used in the thesis experiments.

Equipment	Company (Country)
UV-Visible Spectrophotometer	NanoDrop2000, ThermoScientific (USA)
Laminar Flow Cabinet	Faster BH-EN 2003 (Italy)
Rotary Shaker	Techne- Roller Blot Hybridizer HB-3D (UK)
Centrifuge	Eppendorf Microcentrifuge 5424 (Germany) BeckmanCoulterAllegraTM 25R Centrifuge (USA) Hettich Universal 220 (Germany)
Centrifuge/Vortex	BiosanFVL-2400N Europlug (Latvia)
Orbital Shaker	Sartorius-cermotat SII (Germany)
Thermomixer	Eppendorf Thermomixer Compact
Thermoshaker	Biosan-TS-100C (Latvia)
Pipette- Multichannel pipette	Eppendorf (Germany)
Thermal Cycler	Applied Biosystems Veriti™ Thermal Cycler (USA)
Bioanalyzer	Agilent 2100 Bioanalyzer (USA)
Hybridization Chamber	Agilent (USA)
Hybridization oven rotator for Agilent Microarray Hybridization Chambers	Agilent (USA)
Autoclave	TOMY SX700E (Japan)
-80 °C Refrigerator	Sanyo Ultra Low (Japan)
-20 °C Refrigerator	Arçelik 2031D (Turkey)
+4 °C Refrigerator	Arçelik 3061 Plus (Turkey)
Magnetic Stirrer	Labworld-Online (German)
Vortex Mixer	Heidolph (Germany)
Ion S5™ System	ION Torrent/ Thermo Fischer Scientific (USA)
Ion Chef System	ION Torrent/ Thermo Fischer Scientific (USA)
E-Gel® Safe Imager™ Real-Time Transilluminator	Invitrogen/ Thermo Fischer Scientific (USA)
DynaMag™-2 Magnet	Thermo Fischer Scientific (USA)
Qubit® 3.0 Fluorometer	Invitrogen/Thermo Fischer Scientific (USA)
Glass Slides	Agilent Biotechnologies (USA)
pH-meter	MettlerToledo MP220 (Switzerland)
UV-Vis Spectrophotometer	Shimadzu UV-1700 (Japan)

Table 2.4 : Chemicals used in the thesis experiments.

Chemicals	Company (Country)
Peptone	MERCK (Germany)
Yeast Extract	MERCK (Germany)
D-Glucose	VWR BDH PROLABO (UK)
Agar	AppliChem (Germany)
Glycerol	Duchefa Biochemie (Holland)
Yeast Nitrogen Base without Amino acid	BD Difco™ (USA)
Ethanol (≥ 99.8)	J. T. Baker (the Netherland) Sigma-Aldrich (USA)
Agencourt™ AMPure™ XP Reagent	Beckman-Coulter (USA)
DNA Ladder	50 bp DNA Ladder/ Thermo Fisher Scientific (USA)
H_2O	Eczacıbaşı (Turkey)
E-Gel EX with SYBR® Gold II %2	Invitrogen/Thermo Fischer Scientific (USA)
SizeSelect	
Cleaning reagent for removing RNase RNaseZAP	Sigma Aldrich (USA)
β-mercaptoethanol	Merck, Hohenbrunn (Germany)
Hydrogen peroxide	MERCK (Germany)
Tris/HCl Buffer	MERCK (Germany)

Table 2.5 : Kits and enzymes used in the thesis study.

Kit/ Enzyme Name	Company (Country)
Epicentre MasterPure™ DNA Purification Kit	Illumina (USA)
Qiagen RNeasy Mini Kit	Qiagen (Germany)
Low Input Quick Amp Labeling Kit, One-Color	Agilent Technologies (USA)
RNA Spike-In Kit, One-Color	Agilent Technologies (USA)
Gene Expression Hybridization Kit	Agilent Technologies (USA)
Gene Expression Wash Buffer Kit	Agilent Technologies (USA)
Absolutely RNA Nanoprep Kit	Agilent Technologies (USA)
Quick Amp Labeling Kit, One-Color	Agilent Technologies (USA)
Qubit™ dsDNA HS Assay Kit	Thermo Fisher Scientific (USA)
Ion Xpress™ Plus Fragment Library Kit	Thermo Fisher Scientific (USA)
Ion Shear™ Plus Reagents Kit	Thermo Fisher Scientific (USA)
Ion Xpress™ Barcode Adapters 1-16 Kit	Thermo Fisher Scientific (USA)
Ion 540™ Chip Kit	Thermo Fisher Scientific (USA)
Ion 540™ Kit-Chef (Ion S5™ Chef Supplies, Ion S5™ Chef Solutions, Ion 540™ Chef Reagents, Ion S5™ Sequencing Solutions, Ion S5™ Sequencing Reagents)	Thermo Fisher Scientific (USA)
Lyticase	Sigma-Aldrich (USA)

Table 2.6 : Softwares, databases and websites with their functions used in this study

Softwares, Databases and Websites	Data and Result Order
2100 Expert (Agilent Technologies)	Program of Bioanalyzer for RIN measurement
NanoDrop 2000 / 2000c Operating Software (ThermoScientific)	Program of Nanodrop for DNA quality and quantity measurement
GeneSpring (Agilent Technologies)	Microarray data analysis software
Torrent Suite Software and Torrent Server (Thermo Fisher Scientific)	NGS management; plan, monitor, view sequencing and data analysis
IGV (Integrative Genomics Viewer)	Visualization of sequenced genome data
SGD Saccharomyces Genome Database (*URL-1*)	Genome and gene database of *S. cerevisiae*, GO analysis
Ensembl Fungi (*URL-2*)	Domain and classification analysis
Ensembl (*URL-3*)	Genome database of *S. cerevisiae*
Yeast growth rate analyze (*URL-4*)	Genome database
Wikipathways (*URL-5*)	Environmental Stress Response (ESR) gene analysis
DAVID 6.8 (*URL-6*)	Pathway analysis
YEASTRACT (*URL-7*)	The Database for Annotation, Visualization and Integrated Discovery-KEGG analysis
	Yeast Search for Transcriptional Regulators and Consensus Tracking Transcriptional regulator finding

2.2 Methods

2.2.1 Cultivation and strain procedure

Reference strain and the oxidative stress-resistant evolved strain cells, collected from glycerol stock solutions at -80 °C, were inoculated into YPD medium to revive cells and grown at 30 °C and 150 rpm overnight. The cells were then collected and cultured on solid YPD medium for short-time storage.

Strains were inoculated to 20 mL of YMM in 100 mL flasks at 30 °C 150 rpm overnight as precultures. The following day, each strain was incubated in 100 mL YMM in 500 mL flasks to an initial OD_{600} of approximately 0.1 (6-8 x 10^5 cells mL^{-1}). Cultures were grown at 30ºC, 150 rpm up to 1 OD_{600} unit ($5x10^7$ cells mL^{-1}).

2.2.2 Transcriptome profiling

The transcriptomic analysis was performed by microarray technology. Firstly, all strains were grown. The total RNA was then isolated, measured and cDNA was constructed. cRNA was synthesized from the constructed cDNA. Samples were

prepared for hybridization. Hybridization was carried out with the chip. After a wash step, chip was scanned to detect hybridized probe fluorescence.

Microarray workflow is shown in Figure 2.1 with schematic cRNA production.

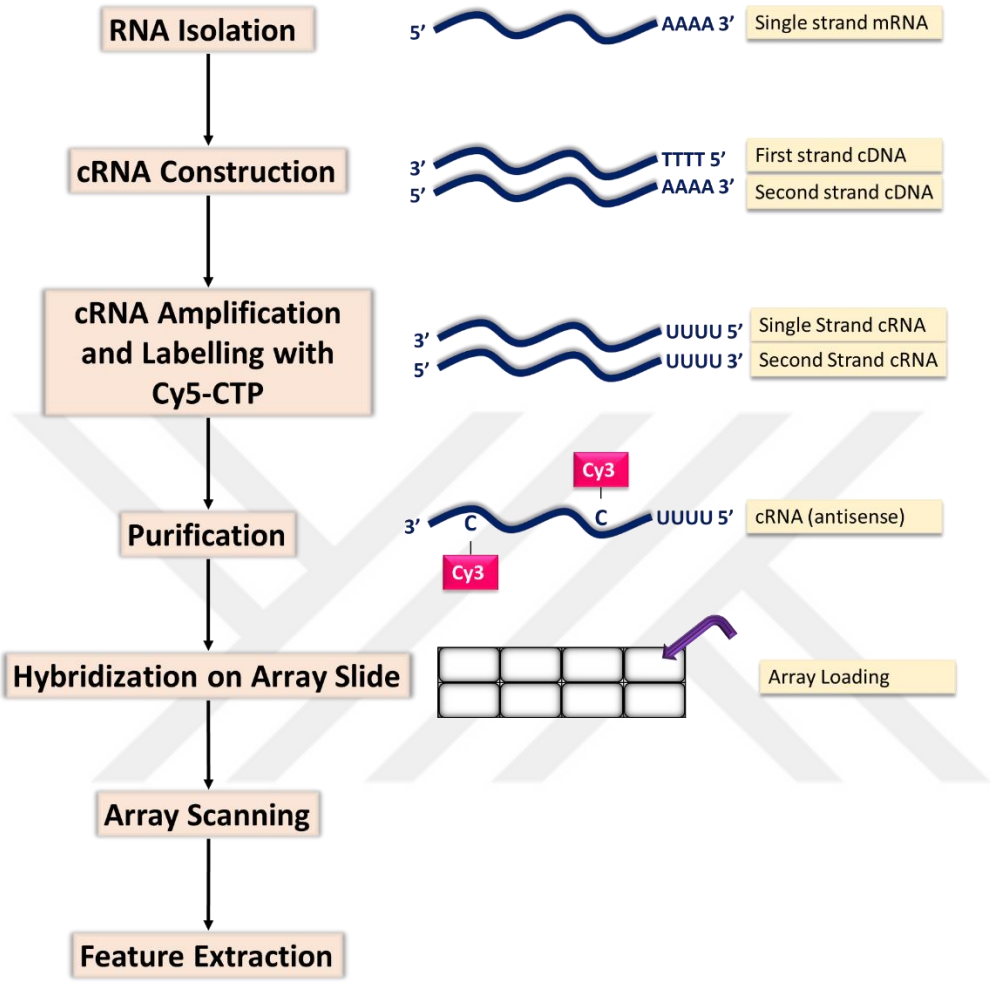

Figure 2.1 : Microarray workflow with schematic mRNA isolation to array loading.

2.2.2.1 Cell preparation/harvesting and total RNA isolation

One mL of cells, grown up to 1 OD_{600} unit ($5x10^7$ cells mL^{-1}), were transferred to microcentrifuge tubes and centrifuged at 1'000 *g* for 5 min at room temperature to harvest cells. The supernatant was thrown away, and the pellet, which contained yeast cells, was resuspended in 1.5 mL of freshly prepared Y1 buffer including lyticase enzyme (Sigma). Y1 buffer is the component of Qiagen RNA Extraction Kit and it is ready for use by adding the lyticase enzyme. Adding of this enzyme to Y1 buffer was done immediately before use, as a fresh enzyme. The preparation of Y1 buffer and other buffers used in RNA isolation is given in Table 2.7. Lyticase enzyme works to

disturb the yeast cell wall and Y1 buffer provides the required environment for working of the enzyme. Cells in the buffer were incubated at 30 °C for 30 min with shaking, to disrupt cell wall. Spheroplast structures were obtained at the end of this step.

Spheroplast including disrupted cell wall was centrifuged at 300 *g* for 5 min and the supernatant was removed to throw away the cell wall particles. 350 µL of RLT Buffer was added to spheroplast and vortexed to lysis. 350 µl of 70 % (v/v) ethanol was added to the homogenized lysate and pipetted.

The lysate was transferred into the RNeasy spin column placed in a 2 mL collection tube and centrifuged at 8'000 *g* for 15 sec. 700 µL of RW1 Buffer was added onto the spin column and centrifuged at 8'000 *g* for 15 sec. 500 µl of Buffer RPE was added into the spin column and centrifuged for 15 seconds at 8'000 *g* to wash the column filter. Once again, 500 µl of Buffer RPE was added into the spin column and centrifuged for 2 minutes at 8'000 *g* to re-wash the column filter. Spin column was replaced into the new collector tube and centrifuged at maximum speed for 1 min to remove waste residue. At the last step, spin column was replaced into a new 1.5 mL microcentrifuge tube and 40 µl of RNase free water was added onto the spin column filter and centrifuged at 8'000 *g* for 1 min to dilute RNA.

Table 2.7 : Ingredients and preparation of Qiagen RNeasy® Mini Kit buffers

Buffer Name	Content/Preparation (amount)
RLT Buffer	10 µl β-mercaptoethanol was added per 1 mL RLT buffer
Y1 Buffer	1 M sorbitol and 0.1 M EDTA (Ethylenediaminetetraacetic acid) was mixed and adjusted to pH 7.4. 0.1% β-mercaptoethanol and lyticase were added to Y1 Buffer just before use.
RPE Buffer	4 volumes of ethanol (molecular grade) were added to RPE buffer

2.2.2.2 Measurement of RNA quality, integrity, and quantity

Concentrations and quality of RNA isolates were measured by Nanodrop 2000 (ThermoScientific). RNA concentration in isolates was given in terms of µg / µL. Besides, Nanodrop measured 260/280 and 230/280 absorbance ratios to show the purity of RNA against DNA and another aromatic component contamination.

Quality and integrity analysis of isolated RNA samples was performed by BioAnalyzer 2100 (Agilent Technologies). RIN (RNA Integrity Number) were measured and calculated by BioAnalyzer 2100.

2.2.2.3 Microarray experiment set-up

The microarray experiment process could be summarized as three steps: cRNA construction, cRNA amplification/labeling, and purification of amplified/labeled cRNA were the first step of the microarray procedure. Hybridization of the cRNA to probes on the microarray and washing of microarrays after hybridization were the second step. In these experiments, Agilent yeast microarrays, including probes specific to *S. cerevisiae*, were used. As the last step, microarrays were scanned and signal detection was provided by the Scanner (Agilent Technologies). All steps were carried out according to producers manual and explained in this section in detail. Raw data rising from signal detection were analyzed by GeneSpring software.

At the first step, cRNA construction was carried out by One-Color Microarray-Based Gene Expression Analysis (Low Input Quick Amp Labeling) Kit (Agilent Technologies).

1.5 µL of isolated RNA samples were put in the microcentrifuge tubes as 200 ng total volume. Then, 2 µL of three times diluted Spike-in RNA was added into RNA samples. Two µL of Spike-in was added to 38 µL of Dilution Buffer as the first dilution (1:20). Two µL of the first dilution of Spike-in was added to 48 µL of Dilution Buffer as the second dilution (1:25). Two µL of the first dilution of Spike-in was added to 8 µL of Dilution Buffer as the third dilution (1:10). By this way, the total volume reached 3.5 µL. Spike-in includes ten synthetic oligos which provide the positive control for the assay.

After that, 1.8 µL of diluted T7 primer mix was added to the total 3.5 µL volume. 0.8 µL of T7 primer and 1 µL of nuclease-free water were mixed to dilute the T7 Primer. The total volume reached 5.3 µL. Incubation at 65 °C for 10 min was then applied to denaturate the template and anneal the primers to template RNA. The mix was chilled on ice for 5 min. At the same time, 5X First-Strand Buffer was heated at 80 °C for 4 min to prepare cDNA Master Mix. cDNA Master Mix ingredients are listed in Table 2.8.

Table 2.8 : Ingredients (and amounts) required to prepare cDNA Master Mix.

Ingredient	Amount (µL)
5X First Strand Buffer (heated)	2 µL
0.1 M Dithiothreitol (DTT)	1 µL
10 mM each dNTP Mix	0.5 µL
Affinity Script RNase Block Mix	1.2 µL
Total Volume	4.7 µL

4.7 µL of cDNA Master Mix was added onto the mix which included RNA, Spike-in and T7 primer. Each tube then contained a total volume of 10 µL. Samples were incubated at 40 °C for 2 h. Incubation at 70 °C for 5 min was then applied, followed by chilling for 5 min.

After cDNA construction, cRNA was produced by using Transcription Master Mix. 6 µL of Transcription Master Mix (contents given in Table 2.9) was added to cDNA samples. In this step, while cRNA was being produced, it was labelled with Cyanine 3-CTP. Each tube then contained a total volume of 16 µL. Samples were incubated at 40 °C for 2 h.

Table 2.9 : Ingredients (and amounts) required to prepare Transcription Master Mix.

Ingredient	Amount
Nuclease-free water	0.75 µL
5× Transcription Buffer	3.2 µL
0.1 M DTT	0.6 µL
NTP Mix	1 µL
T7 RNA Polymerase Blend	0.21 µL
Cyanine 3-CTP	0.24 µL
Total Volume	6 µL

Purification was carried out by Absolutely RNA Nanoprep Kit (Agilent). While the samples were kept at -20 °C, 80% sulfolane solution and the other wash buffers provided by the kit were prepared. As 100% sulfolane was solid at room temperature, it was incubated in a 37 °C water bath until liquefied, and then it was diluted to 80% with DNase/RNase-free distilled water. Wash buffers were prepared by adding particular amounts of molecular grade ethanol for each wash buffer, as indicated in the users guide.

100 µL of the Lysis buffer was put in the bottom of microcentrifuge tubes. 16 µL of the cRNA samples were then added onto the Lysis buffer in microcentrifuge tubes. Then, 116 µL of the 80 % sulfolane solution was added to the mix and vortexed for 5 sec. All 232 µL of the total volume of each samples were transferred to RNA-binding nano-spin cup in the collection tubes. The nano-spin columns in collection tubes were centrifuged at 12'000 rpm for 60 sec. The liquid was then thrown away from the collection tubes. 300 µL of 1× High-Salt Wash Buffer was added to the RNA-binding nano-spin cup and the RNA-binding nano-spin cups in collection tubes were centrifuged at 12'000 rpm for 60 sec. The liquid was then thrown away from collection tubes. 300 µL of 1× Low-Salt Wash Buffer was added to the RNA-binding nano-spin cup and the RNA-binding nano-spin cups in collection tubes were centrifuged at 12'000 rpm for 60 sec. After that, liquid was thrown away from collection tubes. 1× Low-Salt Wash Buffer was applied again. Finally, 300 µL of 1× Low-Salt Wash Buffer was added to the RNA-binding nano-spin cup and the RNA-binding nano-spin cups in collection tubes were centrifuged at 12'000 rpm for 3 min to dry fiber matrix. RNA-binding nano-spin cups were put into the new collection tube and 20 µL of Elution Buffer, heated to 60 °C, was added onto the directly fiber matrix inside the RNA-binding nano-spin cup and incubated at room temperature for 2 min. Tubes were centrifuged at 12'000 rpm for 5 min and eluted cRNA samples were transferred into the new DNase/RNase-free microcentrifuge tubes. Cyanine 3-labeled, linearly amplified cRNA samples were obtained purely.

cRNA concentration and dye concentration were measured by Nanodrop 2000. According to the measurements, samples were diluted with distilled water to 100 ng/ µL concentration.

Hybridization was performed as the last step. Firstly, fragmentation was carried out by preparing the fragmentation mix, as specified in Table 2.10. Fragmentation mixes were incubated at 60 °C for 30 min in a thermal cycler for fragmentation of cRNA samples and then cooled and incubated on ice immediately for 1 min.

Table 2.10 : Fragmentation mix ingredients and their amounts.

Ingredients	Amounts
Cyanine 3-labeled, linearly amplified cRNA samples (100 ng/ µL concentration)	6 µL (600 ng total amount)
10× Gene Expression Blocking Agent	5 µL
Nuclease-free water	13 µL (up to 25 µL)
25× Fragmentation Buffer	1 µL
Total Volume	25 µL

25 µL of the 2× Hi-RPM Hybridization Buffer was added onto the samples and pipetted carefully to stop the fragmentation reaction. Samples were centrifuged at 13'000 rpm for 1 min to drive the sample off the walls and the lid, and to aid in bubble reduction. Samples were put on ice immediately. Finally, 40 µL of each sample were loaded onto the array slide immediately and microarray slides were incubated at 65 °C in the hybridization oven for 17 h to hybridize labeled cRNA to probes on array slides.

The washing procedure was applied after hybridization. Gene Expression Wash Buffer 1 was added to slide-staining dish #1 completely. Slide was opened in this buffer. Then, it was incubated in Slide-staining dish #2 filled with Gene Expression Wash Buffer 1 with a magnetic stirrer bar on a magnetic stirrer plate for 1 min at room temperature. After that, the slide was washed at 37 °C pre-heated slide-staining dish #3 filled with Gene Expression Wash Buffer 2. Slide was put in a slide holder, and then scanned with Agilent Scanner.

2.2.2.4 Microarray data analysis

Raw data analysis procedure began with raw data extracted from the scanner. Until reaching usable and biologically meaningful data; quality control, normalization of raw data, filtering and clustering were performed by using GeneSpring Software. Besides, GeneSpring was used for the interpretation of results. In addition to this, Saccharomyces Genome Database (*URL-1*) and Yeast Growth Rate (*URL-4*) were used to analyze results.

Firstly, raw data was normalized by using Percentile algorithm. Quality control results were extracted. A filter was created and applied on sample data based on their signal intensity values. By the way, probe-set filtering was created and applied by detection of coefficient value as 50. Bonferroni correction was applied to obtain more stringent test by statistically. Different cut-off values (2, 10, 25, 100, 150, 200, 250, 500) were

applied on data sets as threshold values. By this filtration, up and down-regulated genes were determined, listed and imaged graphically.

Gene Ontology analysis was performed GO Slimmapper of Saccharomyces Genome Database ($p \leq 0.05$ and fold change ≥ 2) (*URL-1*). In addition, Environmental Stress Response (ESR) genes were analyzed (*URL-4*). Transcription factors that regulate the up-regulated and down-regulated genes, were analyzed by YEASTRACT (*URL-7*). Pathway analysis was carried out by GeneSpring Software.

2.2.3 Whole genome sequencing

Whole genome sequencing of the reference and the evolved strain were carried out by Next Generation Sequencing. Basically, the growth of the cultures, total genomic DNA isolation, measurement of DNA quality and quantity, library preparation, template preparation and sequencing of the whole genome were performed in this experiment. The workflow of the resequencing of the reference and the oxidative stress-resistant evolved strain is given in Figure 2.2. All steps were are explained in detail in this section.

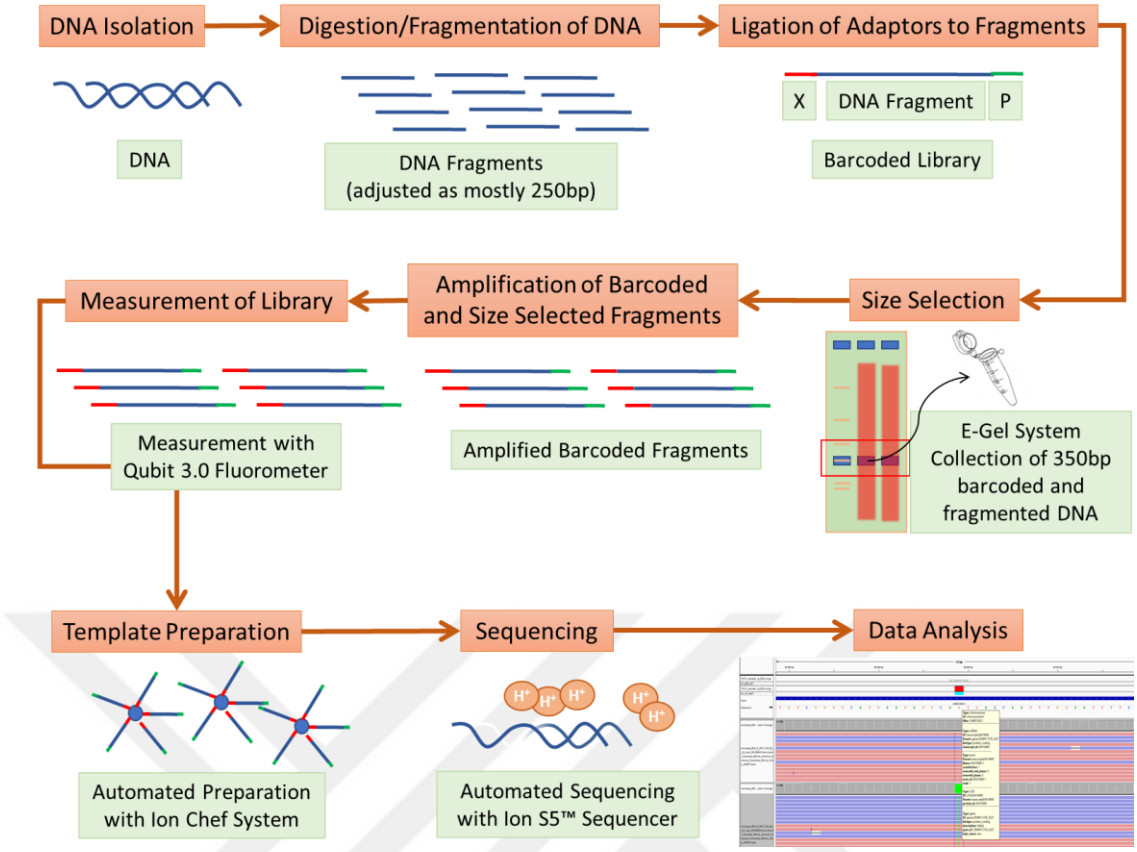

Figure 2.2 : Next Generation Sequencing Workflow
The first step is the DNA isolation from the yeast cells in culture. Then, isolated DNA samples were digested by a sharing enzyme. After that, barcode and adaptor oligonucleotide acid structures were ligated to shared DNA fragments. Following the selection of the fragment with the required size by e-gel system, fragments were amplified by PCR. After the measuring and dilution of amplified fragments, template preparation and chip filling with diluted fragments was carried out by an automated system. Finally, sequencing was performed by an automated sequencer as the last step of the wet lab procedure. Raw data obtained from the sequencer were analyzed by the same sequencer device. Finally, post data analysis was performed.

2.2.3.1 Cell preparation for DNA isolation

Cultivations of the reference and evolved strain cultures was carried out as described in Section 2.2.1., cells were then harvested and prepared for DNA isolation. When the cultures reached an OD_{600} of approximately 1, 1 mL of 1 OD_{600} ($5x10^7$ cells mL^{-1}) for each sample was transferred to 1.5 mL microcentrifuge tubes for isolation procedure. Strain samples in microcentrifuge tubes were centrifuged at 10’000 g for 3 min, the supernatant was removed and the yeast cells were then washed twice. Pellets were resuspended with 1 mL of sterilized distilled water, centrifuged at 10’000 g for 3 min

and the supernatants were removed by pipetting to wash yeast cells. 25 µL of supernatant was left on the pellet during washing for the second time.

2.2.3.2 DNA isolation

After preparing cells, DNA isolation was carried out by MasterPure™ DNA Purification Kit (Epicentre). As the first step, 300 µL of Tissue Cell Lysis Solution was added to cell pellet in 25 µL of supernatant. Then 1 µL of Proteinase K was added into the cell and Tissue Cell Lysis Solution mix and incubated for 15 min at 65 °C. During incubation, the mixture was vortexed once every 5 min. At the next step, the mixture was cooled to 37 °C. 1 µL of RNase A (5 µg/ µL) was added to cooled mixture and vortexed. The mixture was incubated at 37 °C for 30 min.

DNA precipitation was then started by chilling on ice during 5 min. 175 µL of MPC Protein Precipitation Reagent was put in the 300 µL of sample lysate and vortexed for 10 sec. Microcentrifuge tubes including lysate and the precipitation mixture were centrifuged for 10 min at 10’000 g at 4 °C.

The supernatant was transferred a to new and clean microcentrifuge tube. 500 µL of isopropanol, stored at -20 °C, was added into the supernatant for purification. The tube was shaken by up and down movements for 40 times. DNA pellet was obtained by centrifugation of the mixture for 10 min at 10’000 g at 4 °C. Isopropanol was removed carefully without lifting the DNA pellet.

DNA pellet was washed twice with 70 % (v/v) ethanol. One mL of 70 % (v/v) ethanol was added onto the DNA pellet, vortexed, centrifuged for 10 min at 10’000 g at 4 °C. Ethanol was removed by pipetting. When the second wash was finished, microcentrifuge tube containing the pellet was kept in laminar flow hood with open caps for 3 h to remove the remaining ethanol.

As the last step, DNA was eluted in 35 µL of TE Buffer. Total genomic DNA was obtained to use for sequencing stages. After isolation, isolates were measured and the amounts to be used for whole genome sequencing were determined.

2.2.3.3 Measurement of DNA quality and quantity

The concentration and purity of isolated DNA was evaluated by Nanodrop 2000 spectrophotometer (Thermo Fisher Scientific) and Qubit® Fluorometer 3.0 (Thermo Fisher Scientific).

Nanodrop computed the concentration information of DNA samples in terms of µg / µL. In addition, 260/280 and 230/280 absorbance ratios were measured and calculated by Nanodrop. 2 µL of DNA in TE buffer was placed in the Nanodrop device and measured using the Nanodrop software.

Besides, DNA was measured by the Qubit® Fluorometer 3.0 to determine DNA concentration exactly. 200 µL of tQubit® dsDNA HS Reagent and Buffer and 1 µL of The Qubit® dsDNA HS Reagent were mixed for each sample and standard. Qubit Standard solutions were 1/20 diluted in dsDNA HS Reagent and Buffer mix in the 200 µL last volume. Samples were diluted to 1/5 with distilled water, because the DNA amount was too high for measurement with Qubit 3.0. Diluted DNA samples were then 1/100 diluted in dsDNA HS Reagent and Buffer mix in the 200 µL last volume. Appropriate 0.5 mL test tubes, special for Qubit measurements, were used. Firstly, Qubit Standard 1 and Qubit Standard 2 were measured for calibration of the assay. Then the tubes containing the samples were put in the Qubit® Fluorometer 3.0 and measured.

2.2.3.4 Sequencing of whole genome

The Ion Torrent Sequencing Systems were used for sequencing the whole genome of the strains. The whole genome sequencing strategy has three massive steps: library preparation, template preparation and sequencing. Library preparation from DNA was carried out manually by using appropriate kits. Template preparation was performed using Ion Chef™ Instrument (ThermoScientific, USA), automatically. As the last step, high-throughput sequencing was performed by Ion S5 Sequencing System (ThermoScientific, USA).

2.2.3.5 Library preparation for next generation sequencing (NGS)

Library preparation involves four main phases, which are digestion and fragmentation, adaptor ligation, size selection and amplification/purification.

Ion Shear™ Plus Reagents Kit (ThermoScientific, USA) was used for digestion and fragmentation, and adaptor ligation was performed by use of IonXpress™ Plus Fragment Library Kit (ThermoScientific, USA) and Ion Xpress™ Barcode Adapters. As the third step, E-Gel System (ThermoScientific, USA) was used for size selection. Finally, amplification and purification was perfomed by Ion Xpress™ Plus Fragment

Library Kit (ThermoScientific, USA) and Agencourt AMPure XP (Beckman Coulter, ABD) reagent.

The first stage, which is the digestion of total genomic DNA was started by preparing the fragmentation mix. Fragmentation mix was prepared by adding 200 ng of DNA, as shown in Table 2.11. Then, immediately Ion Shear™ Plus Enzyme Mix II was added to the mix including reaction buffer and DNA. The mix was pipetted by avoiding bubble formation and incubated at 37 °C for 14 min in a thermal cycler (Veriti, Thermo Fisher Scientific). The incubation time was determined according to the desired fragment size. As approximately 250 bp fragmented DNA was desired for sequencing, sharing time was determined as 14 min.

Table 2.11 : Fragmentation reaction mix contents.

Component	Volume of Component for the reference strain	Volume of Component for the evolved strain
Ion Shear™ Plus 10X Reaction Buffer	5 µL	5 µL
Total gDNA	2 µL (200 ng of total gDNA)	5 µL (200 ng of total gDNA)
Nuclease-free Water	33 µL	30 µL
Total	40 µL	40 µL

After incubation, immediately 5 µL of Ion Shear™ Stop Buffer was added and vortexed for 5 sec to stop fragmentation. Later, the total volume (55 µL) of digested DNA samples was transferred to microcentrifuge tubes. 99 µL of Agencourt™ AMPure™ XP Reagent (1.8X of last total volume) was added to the sample mix, pipetted and incubated at room temperature for 5 min for purification. Microcentrifuge tubes were placed in the DynaMag™-2 magnet rack for 3 min or until the solution became clear of the brown tint when viewed at an angle. Supernatant was removed without disturbing the bead pellet. 500 µL of freshly prepared 70% (v/v) ethanol was added onto the pellets for washing the beads. After incubation for 30 sec, microcentrifuge tubes were turned 3-4 times in the magnet to agitate the beads. When the solution was clear, supernatant was removed without disturbing the bead pellets containing the fragments. This washing step was applied twice. To remove residual ethanol, microcentrifuge tubes were pulse-centrifuged and placed back in the magnetic rack. Supernatant was removed very carefully by a pipette without disturbing the pellet which includes magnetic beads. Microcentrifuge tubes were kept on the magnet, the beads were left for air-drying at room temperature for 5 min. After the beads became

dry, 25 µL of Low TE (Ion Plus Fragment Library Kit ingredient) was added onto the pellet directly and vortexed for 10 sec. After pulse-spin, tubes were kept on the DynaMag™-2 magnet rack until obtaining a clear solution. Finally, eluted purified fragments were transferred into the new 0.2 mL PCR tubes without beads.

Ligation reaction was performed in order to ligate adaptors to fragments. For this purpose, ligation reaction was prepared and incubated in a thermal cycler (Veriti, Thermo Fisher Scientific). Ligation reaction contents and incubation conditions are given in Table 2.12 and Table 2.13, respectively.

Table 2.12 : Ligation reaction mix composition for ligation of the adaptor and barcode to amplicons.

Component	Amount
Fragmented DNA	25 µL
10X Ligase Buffer	10 µL
Ion P1 Adapter	2 µL
Ion Xpress™ Barcode X (different Barcode for each sample)	2 µL
dNTP Mix	2 µL
Nuclease Free Water	49 µL
DNA Ligase	2 µL
Nick Repair Polymerase	8 µL
Total	100 µL

Table 2.13 : Ligation reaction incubation stages for ligation of the adaptor and barcode to amplicons.

Temperature	Time
25 °C	15 min
72 °C	5 min
4 °C	up to 1 h

After ligation incubation, reaction products were carried to new microcentrifuge tubes and 120 µL of Agencourt™ AMPure™ XP Reagent (1.2X of total volume) was added. Microcentrifuge tubes were put in the DynaMag™-2 magnet rack for 3 min or until the solution got clear of brown tint at an angle view. Supernatant again was removed without disturbing the pellet. 500 µL of freshly prepared 70% (v/v) ethanol was added onto the pellets for washing the beads. After incubation for 30 sec, microcentrifuge tubes were turned 3-4 times in the magnet to agitate the beads. When the solution was clear, supernatant was removed without disturbing the bead pellets containing

fragments. This washing step was applied twice. To remove residual ethanol, microcentrifuge tubes were pulse-centrifuged and placed back in the magnetic rack. Supernatant was carefully removed using a pipette without disturbing the pellet. When the beads were dry, 20 µL of Low TE (Kit ingredient) was added onto the pellet directly; vortexed for 10 sec and incubated for 1 min. After pulse-spin, tubes were kept on the DynaMag™-2 magnet rack until a clear solution was obtained. Finally, the eluted barcoded and purified fragments were transferred into new 1.5 mL microcentrifuge tubes without disturbing bead pellets.

The next stage was size selection. For this purpose, E-Gel™ SizeSelect™ Agarose Gels System was used. Firstly, 50 bp DNA Ladder (Thermo Fisher Scientific) including 350 bp fragment was prepared to load the gel system in order to determine and obtain 350 bp fragments (350 base pair contains approximately 200-250 bp amplicons with adaptors and barcodes with approximate sizes of 100bp) in the genomic DNA fragment bulk to be sequenced. Ladder and barcoded amplicons were loaded to up-wells on e-gel and 25 µL of distilled water was loaded to down-wells. Approximately 15 min later, when the 450 bp fragment size of the marker was observed in the down-well, 25 µL of distilled water containing ~350 bp barcoded fragments was collected by a pipette and transferred to clean microcentrifuge tubes.

As the third step, amplification was carried out by using the ingredients given in Table 2.14. and applying a thermal cycler protocol, as shown in Table 2.15.

Table 2.14 : Amplification reaction ingredients.

Component	Amount
Platinum™ PCR Super Mix High Fidelity	100 µL
Library Amplification Primer Mix	5 µL
Unamplified library (size-selected by E-Gel™ SizeSelect™ Agarose Gels)	~25 µL

Table 2.15 : Thermal cycler protocol for amplification.

	Temperature	Time
1 cycle	95 °C	5 min.
	95 °C	15 sec.
10 cycle	58 °C	15 sec.
	70 °C	1 min.
Hold	4 °C	Hold

Purification was carried out as the last step in order to produce the library. As 200 ng gDNA was used as the template and ~250 bp fragments were selected, the Agencourt AMPure XP (Beckman Coulter, ABD) reagent amount to be used for purification was calculated. Accordingly, 156 µL of Agencourt AMPure XP (Beckman Coulter, ABD) reagent (1.8X of last total volume) was added to the microcentrifuge tubes, which included size-selected and barcoded fragments, and then pipetted and incubated at room temperature for 5 min for purification. After spin-down, the microcentrifuge tubes were put in the DynaMag™-2 magnet rack for 3 min until the solution got clear when viewed at an angle. The supernatant was removed without disturbing the bead magnetic pellet. 500 µL of freshly prepared 70 % (v/v) ethanol was added onto the pellets for washing the beads. After incubation for 30 sec, microcentrifuge tubes were turned 3-4 times in the magnet to agitate the beads. When the solution was clear, the supernatant was removed without disturbing the bead pellets containing fragments. This washing step was applied twice. To remove residual ethanol, microcentrifuge tubes were pulse-centrifuged and placed back in the magnetic rack, and the remaining supernatant was carefully removed via pipetting, without disturbing the pellet. Microcentrifuge tubes were kept on the magnet; the beads were left for air-drying at room temperature for 5 min. After the beads got dry, 30 µL of Low TE was added onto the pellet directly and vortexed for 10 sec. After pulse-spin, tubes were kept on the DynaMag™-2 magnet rack until obtaining a clear solution. Finally, 30 µL of the eluted, purified size-selected and barcoded fragments were obtained. 10 µL of purified size selected and barcoded fragments were measured via Qubit® Fluorometer 3.0 (Thermo Fisher Scientific).

200 µL of The Qubit® dsDNA HS Reagent and Buffer and 1 µL of The Qubit® dsDNA HS Reagent were mixed for each sample and the standard. Purified size selected and barcoded fragment samples were 1/20 diluted in dsDNA HS Reagent and Buffer mix in the 200 µL final volume. 10 µL of purified size-selected and barcoded fragments were put in the 190 µL of dsDNA HS Reagent and Buffer mix. Then the tubes containing the samples and dsDNA HS Mix were put in the Qubit® Fluorometer 3.0 and measured.

2.2.3.6 Template preparation

The Ion Chef™ Instrument (Thermo Fisher Scientific) was used for template preparation in the automatical process.

Samples were diluted to 20 ng/ mL and pooled in order to load the Ion Chef™ Instrument (Thermo Fisher Scientific). 25 µL of sample pool was pipetted to the microcentrifuge tubes of the Ion 540™ Kit-Chef (Thermo Fisher Scientific).

Beside the template preparation, the Ion Chef System was used for loading the chip. Ion 540™ Chip Kit (Thermo Fisher Scientific) was used for sample tracking and sequencing runs via the Ion S5™ Sequencer (Thermo Fisher Scientific). All cartridges, consumables, solutions, chip and tube containing library pools were loaded to the right position in Ion Chef™ Instrument. Samples and run conditions were entered and a plan was created on Torrent Suite Software on computer. The Ion Chef™ Instrument (Thermo Fisher Scientific) and the Ion S5™ Sequencer (Thermo Fisher Scientific) use this software. The system was then started to work for preparing the template and loading the Ion 540™ Chip.

2.2.3.7 Sequencing

During template preparation and chip loading by the Ion Chef™ Instrument (Thermo Fisher Scientific), the Ion S5™ Sequencer was prepared. The Ion S5™ Sequencing Reagents, Ion S5™ Wash solution, the Ion S5™ Cleaning solution bottle, and the Ion S5™ Sequencing Reagents cartridge were placed in the sequencer appropriately. Then the Ion S5™ Sequencer reagents were initialized. Initializing was completed in approximately 30-40 minutes. After initializing, the chip was placed on the Ion S5™ Sequencer and sequencing was started.

2.2.3.8 Data analysis

Next Generation Sequencing data were analyzed using the Ion Torrent Suit Software. ASM26988v1 genome assembly data (provided by https://fungi.ensembl.org) was used as the reference genome of *S. cerevisiae* CEN.PK113-7D (GCA_000269885).

Binary Alignment Map (BAM) files and Variant Caller Files (VCF) were obtained from the Ion Torrent Suit Software as raw data. BAM files provided the raw data of genome sequencing. It consisted of data which are a binary alignment of the fragment

to the reference sequence. VCF contained information about the position of mutated regions in the genome.

VCF files of the reference strain and the evolved strain were compared and the differences were found. BAM and VCF files of the reference strain and H7 were imported to IGV (Integrative Genomic Viewer) software. Data obtained (VCF of the reference strain and H7) were visualized, using the IGV software.

Mutations were determined and named by their location in the genes via the use of Ensembl and Ensembl Fungi (*URL-2*; *URL-3*). Yeast Genome Database (*URL-1*) was used for finding information about genes, pathways, processes, and functions of the genes. Besides, GO Slimmapper function ($p \leq 0.05$ and fold change ≥ 2), and the gene domain classification function of the Yeast Genome Database were used for the analysis of both microarray data and re-sequencing data. KEGG pathway analysis was performed using DAVID Bioinformatics Resources (v6.8) (Huang et al., 2008, 2009a) for the genes with significantly different expression levels ($p \leq 0.05$ and fold change ≥ 2). Pathway analysis of expression data was performed by PathVisio Software and pathways were obtained from WikiPathways database (*URL-5*). Transcription factors, which regulate the up-regulated and down-regulated genes with a SNP on H7 genome, were analyzed by YEASTRACT (*URL-7*).

2.2.4 Lyticase sensitivity assay

Lyticase sensitivity assay was modified and adapted from a previously described method (Kuranda et al. 2006). Briefly, the cultures of the reference strain (905) and the oxidative stress-resistant evolved strain (H7) grown overnight, were inoculated in 50 mL YMM in 250 mL-shake flasks. Both of the cultures were initiated at an OD_{600} of 0.2 (approximately 2.8×10^6 cells mL^{-1}), in the presence and absence (control) of stress treatment (0.5 mM hydrogen peroxide). Cultivation was continued at 30°C, 150 rpm until the cultures reached the stationary phase. The cultured cells were harvested by centrifugation at 10,000 *g* for 10 min. Cultures at an approximate OD_{600} of 0.9 per mL were harvested and resuspended in 10 mL of 10 mM Tris/HCl buffer (pH 7.4), including 40 mM of β-mercaptoethanol (Merck, Germany). Then the respended samples were incubated at 25°C for 30 min, and 2 U/mL^{-1} of lyticase enzyme (Sigma-Aldrich, USA) was added onto each resuspended sample. The samples were incubated at 30°C, 150 rpm. The lyticase sensitivity of the cultures was determined via

spectrophotometric measurements by the decrease in the OD_{600} values. Spectrophotometric measurements were performed every 20 min during the first two hours and half-hourly in the third hour. The OD_{600} values of each sample for each culture were divided by the initial OD_{600} values. Calculated ratio was multiplied by 100 to determine the lyticase resistance of the cultures. The test was carried out as three biological repeats.

3. RESULTS and DISCUSSION

3.1 Microarray Analysis

3.1.1 Microarray quality control results

Microarray experiments and analysis of the results were performed by using kits and microarrays from Agilent Microarray Technology which also included bioinformatic software for analysis. RNA isolation was carried out from the reference strain and oxidative stress-resistant evolved strain samples at their exponential phase (OD_{600} ~1). Reference and evolved strain were grown as three parallel cultures each, as biological replicates. OD_{600} values of the cultures are given in Table 3.1.

Table 3.1 : Initial OD_{600} values and the OD_{600} values of the cultures before RNA isolation.

Strain name	Initial OD_{600} of the cultures	OD_{600} of the cultures just before the RNA extraction		
		Culture 1	Culture 2	Culture 3
Reference Strain	0.12	1.16	1.09	1.12
H7	0.16	1.18	1.10	1.12

Amount and quality values of the RNA samples were measured and evaluated by NanoDrop and BioAnalyser spectrophotometric devices, respectively. RNA concentration, and potential protein/DNA and ethanol contamination of the samples were determined by Nanodrop. RNA concentration and integrity of RNA information (RIN value) were also determined via BioAnalyser. RNA concentration and their RIN values of the RNA samples are given in Table 3.2 and Table 3.3, respectively.

Table 3.2 : RNA concentrations (ng/µl) of the cultures' RNA isolates, as measured by Nanodrop.

Strain name	RNA concentrations of cultures (ng/µl)		
	Culture 1	Culture 2	Culture 3
Reference Strain	625	595	455
H7	180	206	220

Table 3.3 : RNA Integrity Numbers (RIN) of isolated RNA samples

Strain Name	RIN values of RNA isolates		
	Culture 1	Culture 2	Culture 3
Reference Strain	9,9	9,7	9,6
H7	9,7	9,5	10,0

The Quality control graphics of the microarray results of the samples is shown in Figure 3.1. Principal Component Analysis (PCA) calculated the PCA scores and the software represented them visually them in a 3D scatter plot. Red points indicate H7 samples and blue points indicate reference strain samples. The chosen algorithm and parameters are shown at the right bottom of Figure 3.1.

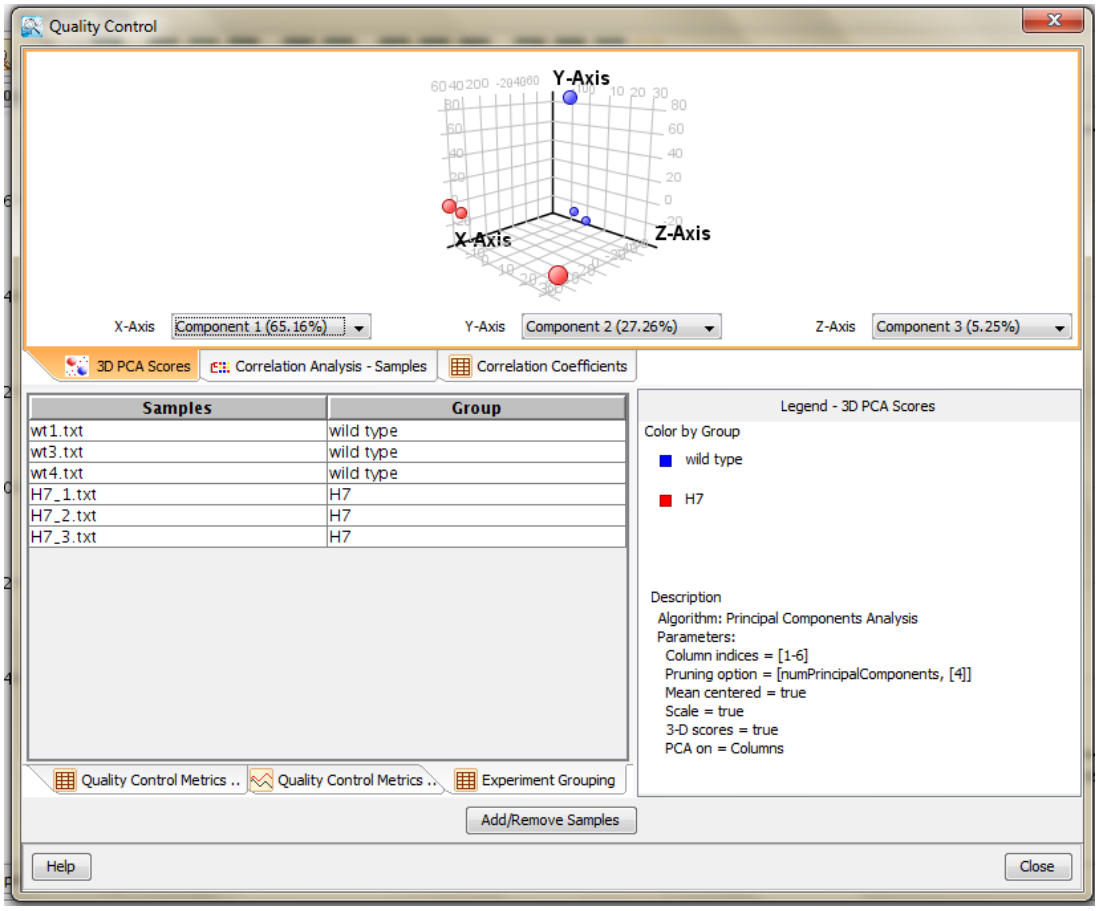

Figure 3.1 : Quality control graphics of the microarray results obtained from GeneSpring software.

The Box Whisker plot is given in Figure 3.2. The Box Whisker plot shows the distribution of both strains in the active interpretation with respect to the determined entity list in this experiment. The x-axis indicates samples in the experiment, and the y-axis indicates normalized intensity values.

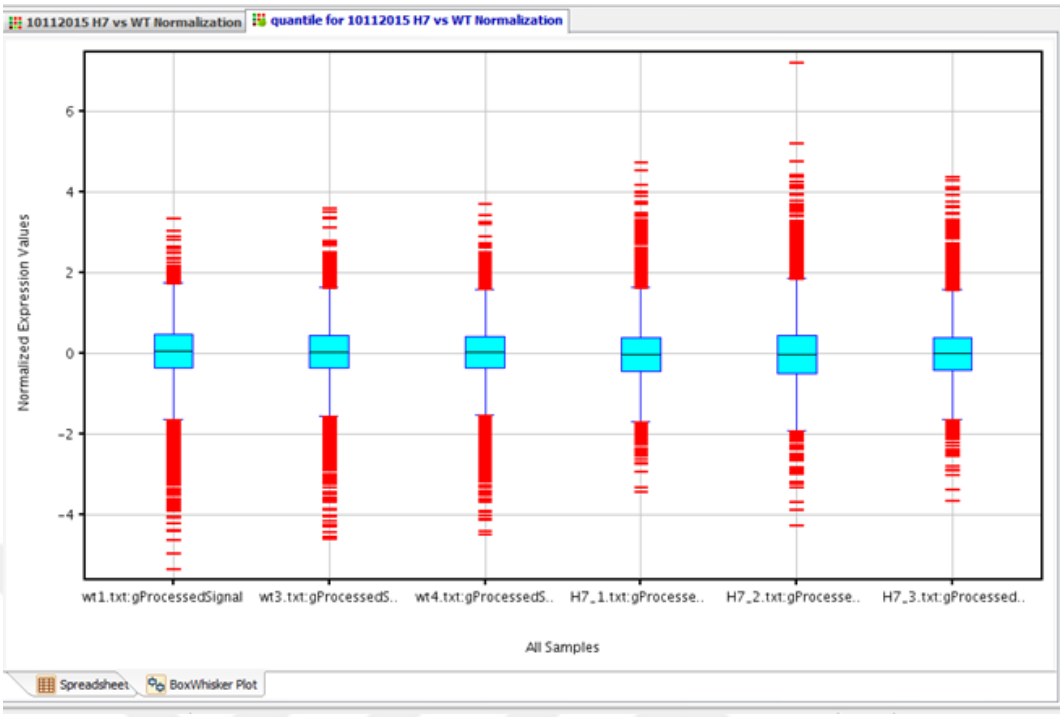

Figure 3.2 : The Box Whisker Plot of all samples.

The Profile Plot is given for all active samples in Figure 3.3. The Profile Plot provides visualization of normalized transcription data against the determined interpretation. The x-axis indicates samples in the experiment, and the y-axis indicates normalized intensity values.

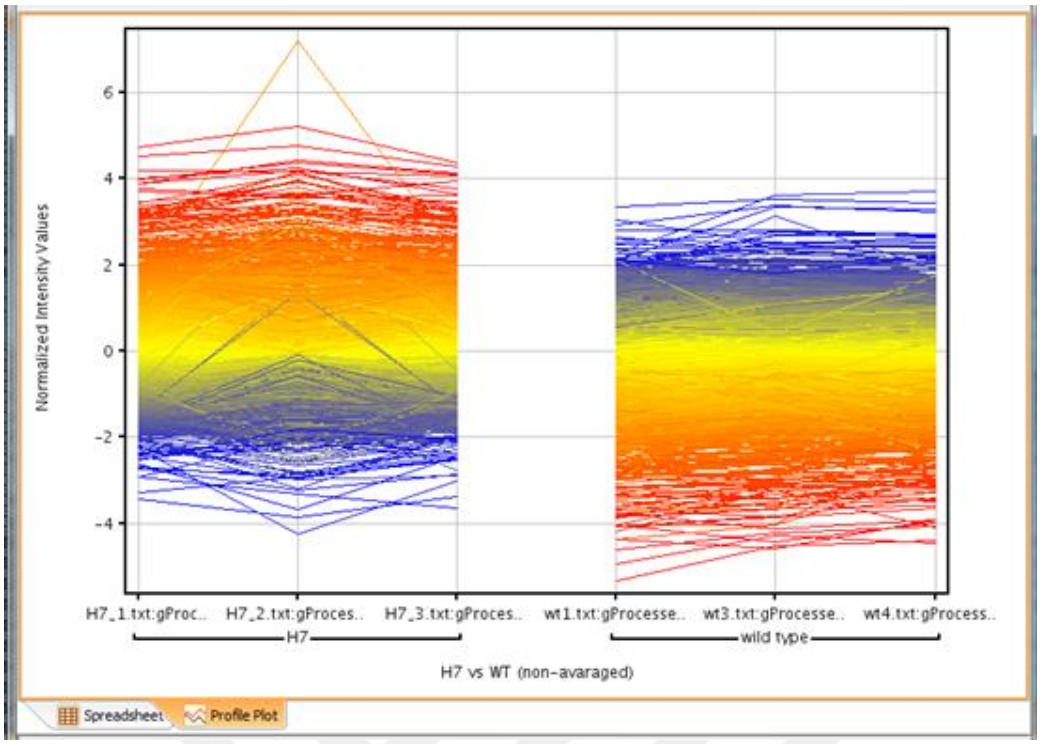

Figure 3.3 : The Profile Plot of all samples.

The Matrix Plot of H7 samples against each other is given in Figure 3.4 and the Matrix Plot of all samples is given in Figure 3.5. Matrix plot gives an overview of the correlation between selected samples (cut-off = 0.05).

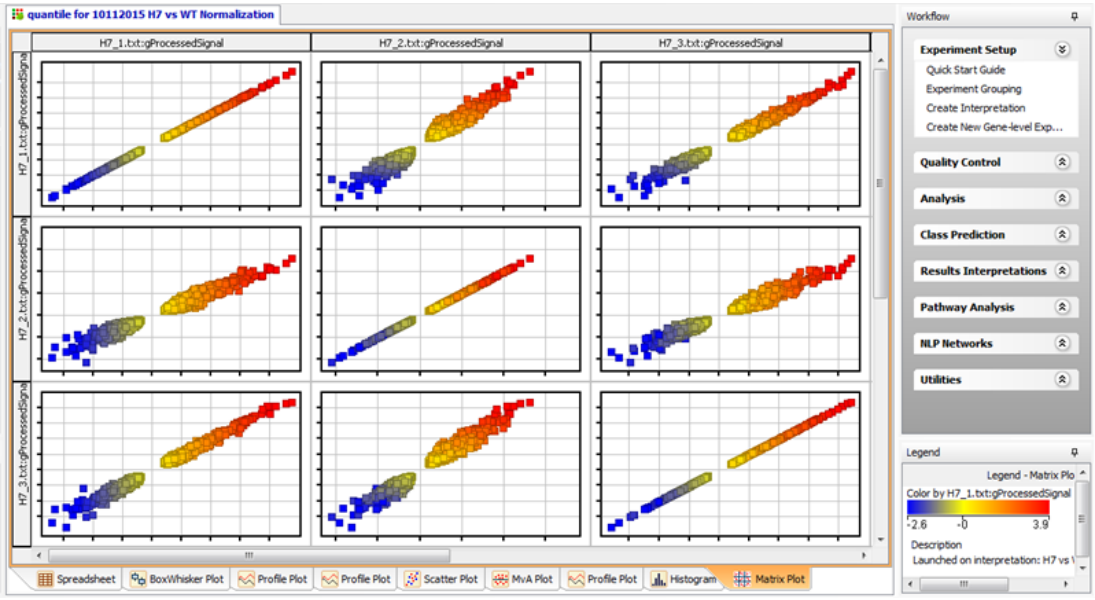

Figure 3.4 : The Matrix Plot of H7 samples.

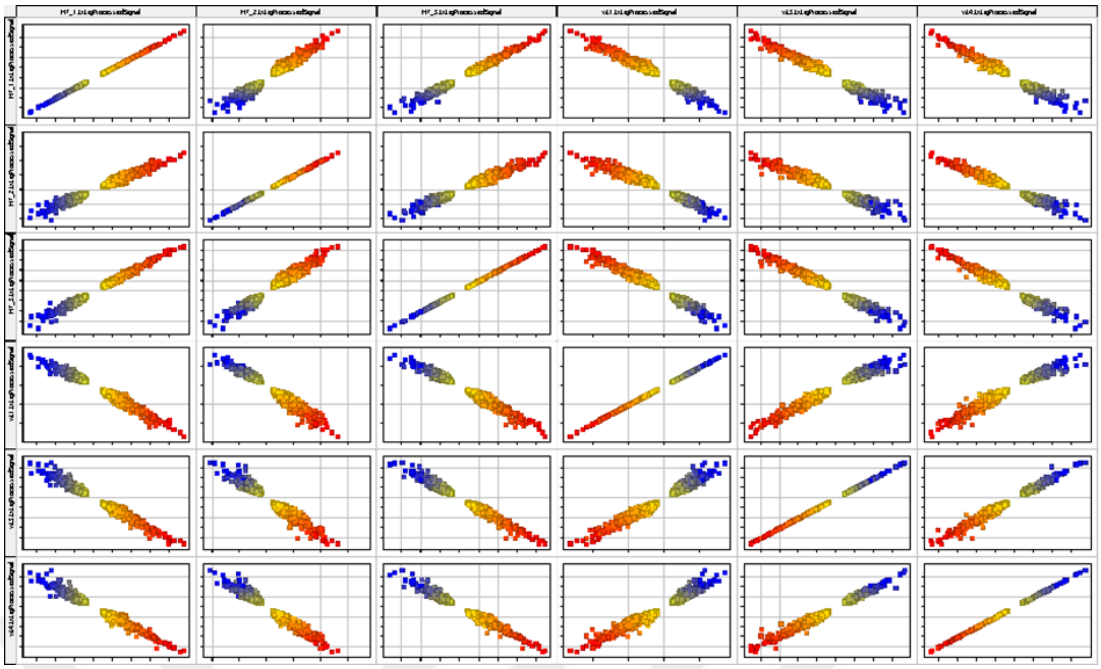

Figure 3.5 : The Matrix Plot of all samples.

The Venn diagram of the differentially expressed gene lists of fold changes ≥2, ≥10, ≥25 and ≥50 is shown in Figure 3.6 (results are given according to fold change calculation, not the absolute quantification calculations of the fold change in this Venn diagram). In this diagram, it could be observed that the expression levels of 1911 genes were changed by 2-or more fold, the expression levels of 265 genes were changed by 10- or more fold, the expression levels of 87 genes were changed by 25- or more fold and the expression levels of 44 genes were changed by 50- or more fold (Figure 3.6).

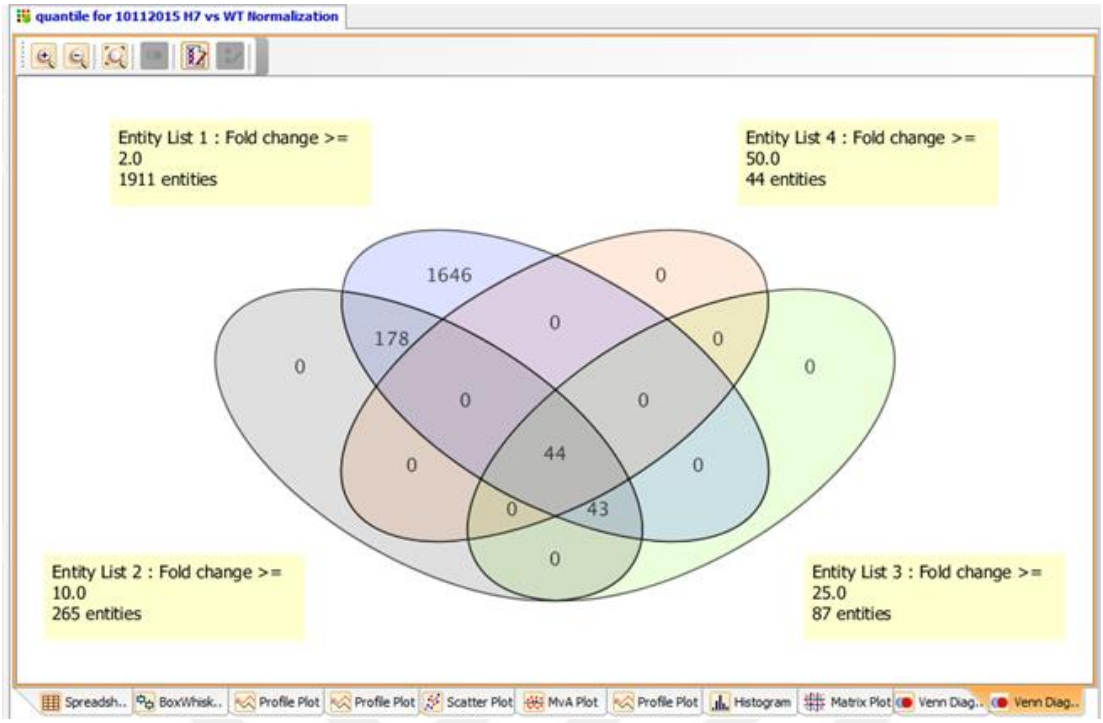

Figure 3.6 : The Venn diagram of the differentially expessed gene list (entity list). Fold change ≥2, ≥10, ≥25 and ≥50 lists were used.

Heatmaps of expression levels of all samples for at least 2, 10, 25, 50, 100 and 150-fold changes are given in Figure 3.7 (results are given according to fold change calculation, not the absolute quantification calculations of the fold change in this Heatmap graphics). The Heatmap shows the normalized values of signals of both strains in the determined interpretation for all the entities in the determined entity list.

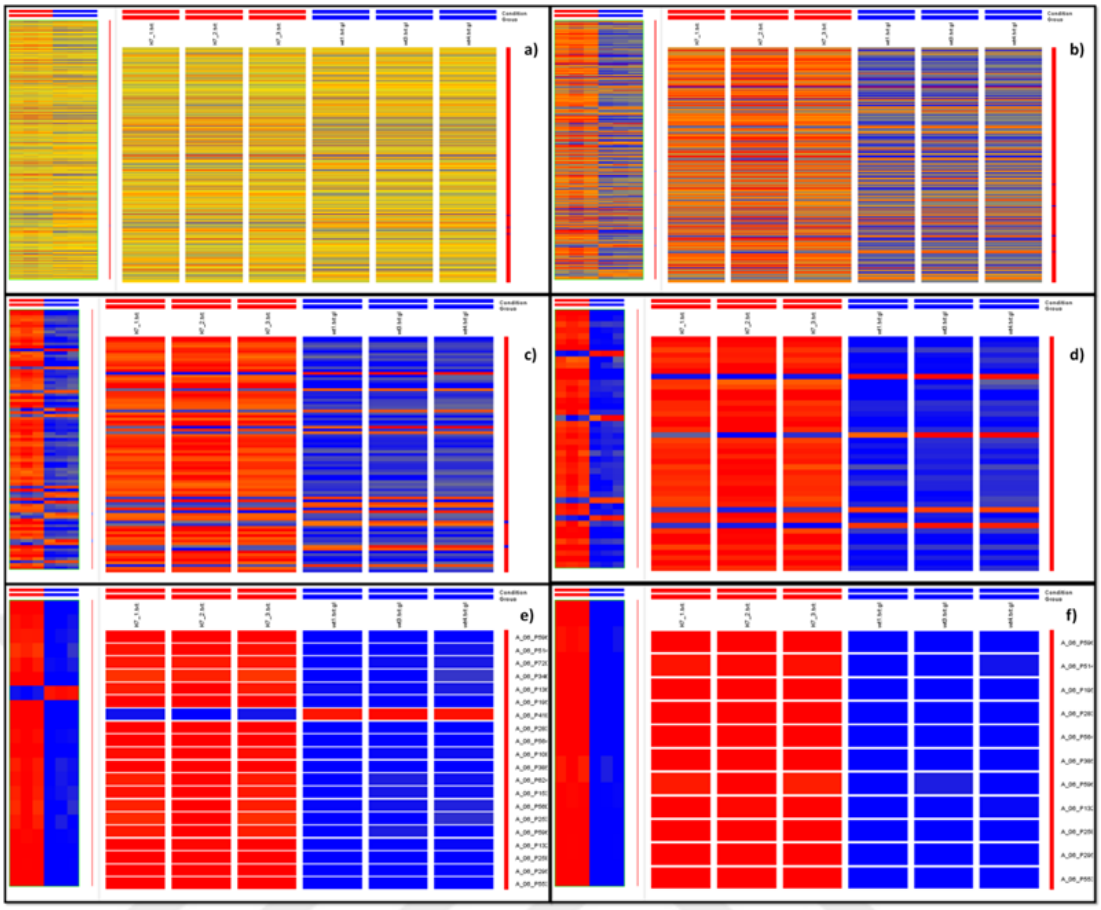

Figure 3.7 : The Heatmaps of expression levels of all samples.
a) Fold change ≥2, b) Fold change ≥10, c) Fold change ≥25, c) Fold change ≥50, d) Fold change ≥100, e) Fold change ≥150.

3.1.2 Microarray analysis results of the reference strain and the oxidative stress-resistant evolved strain H7

Comparison of the expression levels of genes in the oxidative stress-resistant strain H7 and the reference strain was carried out by whole genomic transcriptomic analysis via microarray. Analysis of microarray raw data and clustering of these up-regulated and down-regulated genes was performed using GeneSpring GX 12.5 software. Yeast Genome Database Gene Ontology Slim Mapper (*URL-1*) was used for the categorization of up-regulated and down-regulated genes, according to molecular function and biological process. In addition, Environmental Stress Response (ESR) genes were analyzed by comparing induced and repressed ESR genes, according to the web site (*URL-4*).

In view of GeneSpring software analysis, 1014 genes were down-regulated, and 897 genes were up-regulated with two-fold expression change (log2 (fold change ≥2),

t-test p<0.05). In Figure 3.8, Heatmap graphics of the up- and down-regulated genes are given, according to fold-change calculations, but not the absolute quantification calculations of the fold change.

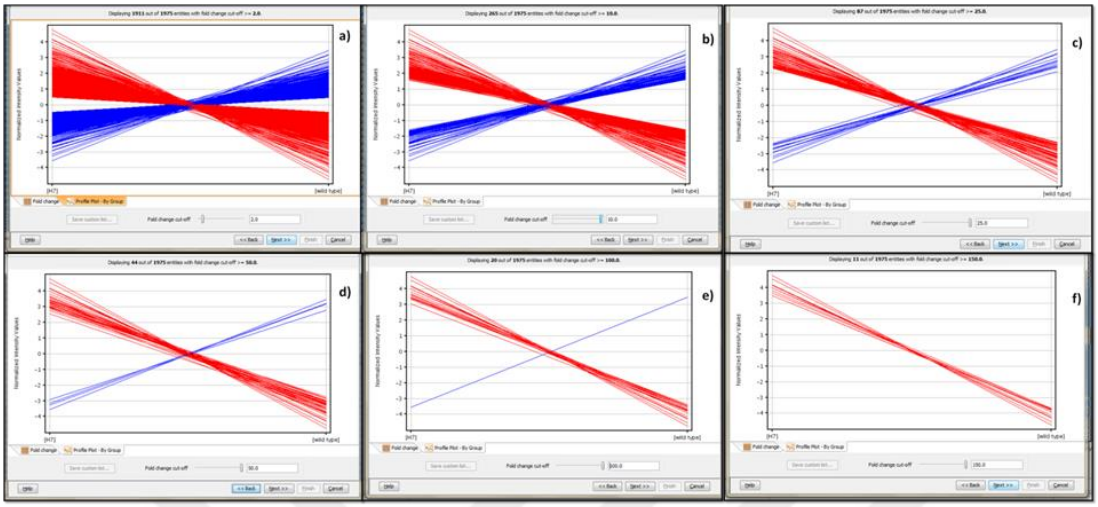

Figure 3.8 : The Profile plot of expression levels of all samples.
Red lines indicate the up-regulated genes of H7. Blue lines indicate the down-regulated genes of H7. a) Fold change ≥2, b) Fold change ≥10, c) Fold change ≥25, c) Fold change ≥50, d) Fold change ≥100, and e) Fold change ≥150.

Comparison of up-regulated and down-regulated genes according to metabolic processes, given in Table 3.4, gave indications about the metabolic situation of the oxidative stress-resistant strain, H7. It could be seen that the expression of the genes that belong to processes related with ribosomal RNA, nuclear transport, organelle assembly, tRNA, cell cycle, mitosis and transcription from RNA polymerases were generally down-regulated. On the other hand, expression of genes related to stress response, carbohydrate, lipid, protein and other precursor metabolites, transportation of metabolites and ions were up-regulated.

Table 3.4 : Comparison of up-regulated and down-regulated genes according to metabolic processes.

Metabolic Process Name	At least 5-Fold Changed Genes	At least 5-Fold Up-regulated Genes	At least 5-Fold Down-regulated Genes
rRNA processing	99	-	99
ribosomal small subunit biogenesis	58	-	58
response to chemical	51	40	11
ribosomal large subunit biogenesis	50	-	50
carbohydrate metabolic process	48	45	3
generation of precursor metabolites and energy	36	31	5
nucleobase-containing small molecule metabolic process	36	24	12
RNA modification	28	2	26
transmembrane transport	26	19	7
nuclear transport	25	2	23
response to oxidative stress	25	23	2
cellular amino acid metabolic process	23	12	11
ion transport	23	16	7
meiotic cell cycle	22	18	4
transcription from RNA polymerase II promoter	22	14	8
signaling	20	10	10
organelle assembly	19	1	18
ribosome assembly	18	-	18
monocarboxylic acid metabolic process	18	17	1
cofactor metabolic process	18	15	3
organelle fission	17	9	8
protein targeting	16	14	2
ribosomal subunit export from nucleus	16	-	16
regulation of cell cycle	15	5	10
lipid metabolic process	15	11	4
cellular respiration	15	14	1
tRNA processing	15	-	15
regulation of organelle organization	14	7	7
protein phosphorylation	14	10	4
mitochondrion organization	14	12	2
mitotic cell cycle	14	4	10
protein complex biogenesis	13	9	4
sporulation	13	10	3
conjugation	12	4	8
cell wall organization or biogenesis	12	8	4
transcription from RNA polymerase I promoter	12	-	12
RNA catabolic process	11	3	8
response to osmotic stress	11	9	2
oligosaccharide metabolic process	11	11	-
carbohydrate transport	11	11	-

Table 3.4 (continued) : Comparison of up-regulated and down-regulated genes according to metabolic processes.

Metabolic Process Name	At least 5-Fold Changed Genes	At least 5-Fold Up-regulated Genes	At least 5-Fold Down-regulated Genes
response to heat	11	11	-
protein modification by small protein conjugation or removal	11	9	2
cytoskeleton organization	10	5	5
regulation of protein modification process	9	4	5
protein folding	9	7	2
DNA replication	8	2	6
DNA recombination	8	6	2
peptidyl-amino acid modification	8	1	7
protein alkylation	8	1	7
chromosome segregation	8	3	5
proteolysis involved in cellular protein catabolic process	8	5	3
peroxisome organization	8	8	-
cellular response to DNA damage stimulus	7	4	3
regulation of DNA metabolic process	7	3	4
pseudohyphal growth	7	4	3
DNA repair	6	3	3
chromatin organization	6	4	2
endosomal transport	6	4	2
response to starvation	6	4	2
nucleobase-containing compound transport	6	1	5
invasive growth in response to glucose limitation	6	5	1
endocytosis	6	5	1
mRNA processing	5	-	5
RNA splicing	5	-	5
snoRNA processing	5	-	5
vacuole organization	5	4	1
cytoplasmic translation	5	1	4
Golgi vesicle transport	5	5	-
regulation of translation	5	-	5
histone modification	4	2	2
membrane invagination	4	4	-
telomere organization	4	2	2
membrane fusion	4	4	-
translational initiation	3	-	3
lipid transport	3	3	-
cellular ion homeostasis	3	1	2
cytokinesis	3	-	3
transcription from RNA polymerase III promoter	3	-	3
translational elongation	3	-	3

Table 3.4 (continued) : Comparison of up-regulated and down-regulated genes according to metabolic processes.

Metabolic Process Name	At least 5-Fold Changed Genes	At least 5-Fold Up-regulated Genes	At least 5-Fold Down-regulated Genes
DNA-templated transcription, elongation	3	-	3
protein dephosphorylation	3	1	2
amino acid transport	3	3	-
organelle fusion	3	3	-
DNA-templated transcription, termination	2	-	2
cell morphogenesis	2	2	-
cell budding	2	-	2
nucleus organization	1	1	-
organelle inheritance	1	1	-
mitochondrial translation	1	1	-
regulation of transport	1	1	-
protein maturation	1	1	-
vitamin metabolic process	1	-	1
tRNA aminoacylation for protein translation	1	-	1

3.1.3 Analysis of down-regulated genes

The at least 2-fold down-regulated genes of the evolved strain according to metabolic process categories are shown in Figure 3.9 (The cut-off value is set to ≥ 2-fold). Gene names are given in Table A.1 in detail.

According to Figure 3.9, it could be clearly seen that the majority of the down-regulated genes belong to ribosome biosynthesis. A key result about the down-regulated genes is that they have a role in RNA biosynthesis and modification processing such as tRNA biosynthesis, snoRNA processing, RNA modification, translation and RNA splicing. Many of the down-regulated genes have a role in processes that are involved in nucleotide metabolism including production, assembly and transport processes. Genes of H7 which are related to nuclear and nucleobase-containing transport metabolites were generally down-regulated. Transcription of organelle and ribosome assembling process related genes were also down-regulated. Some of the down-regulated genes were related to mitosis and the cell cycle.

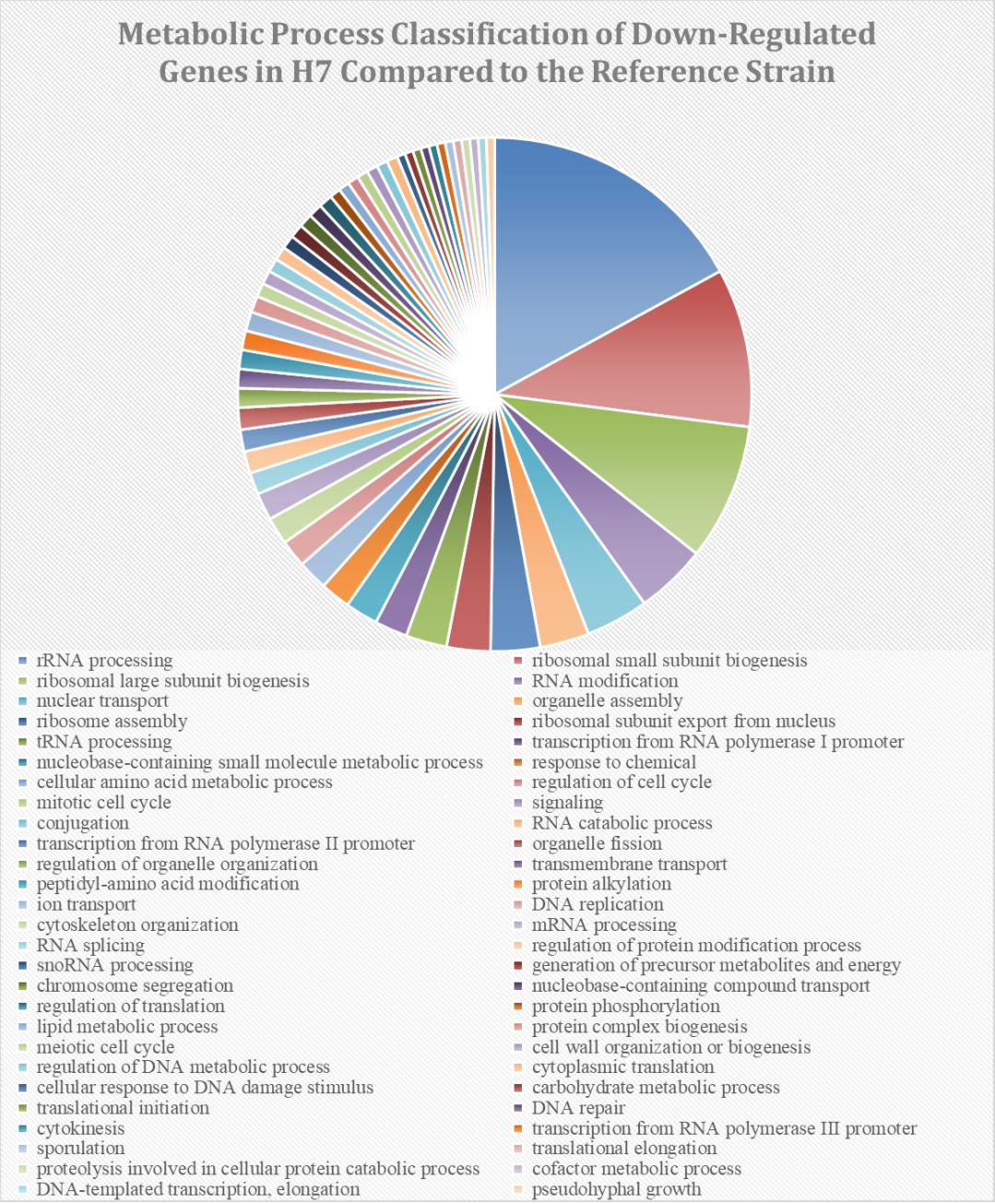

Figure 3.9 : At least 2-fold down-regulated genes of the evolved strain according to metabolic process categories (The cut-off value was set to ≥ 2-fold).

Stress response genes are generally related with growth rate (Brauer et al., 2008). Microarray data of H7 and its reference strain were analyzed by the search tool at ESR gene analysis web site (*URL-4*). This database includes information about the analysis of biomolecules in the yeast *S. cerevisiae* as a function of the growth rate and the limiting nutrient. The distribution of transcriptional changes of environmental stress response genes graphics was obtained by this search tool via analyzing the down-regulated genes (Figure 3.10). The bar chart indicates the expression level of cells that

live in normal condition without any stress. Genes induced with stress conditions are shown as the red curve and the repressed genes are represented by the green curve. The black curve indicates the down-regulated gene set of this study. It could be seen that the down-regulated ESR genes of H7 and ESR-repressed genes that were determined in the database share almost the same pattern. The ESR is initiated as a response to a wide variety of environmental alterations, as indicated by the changes in the expression of the genes in this response (Gasch, 2003).

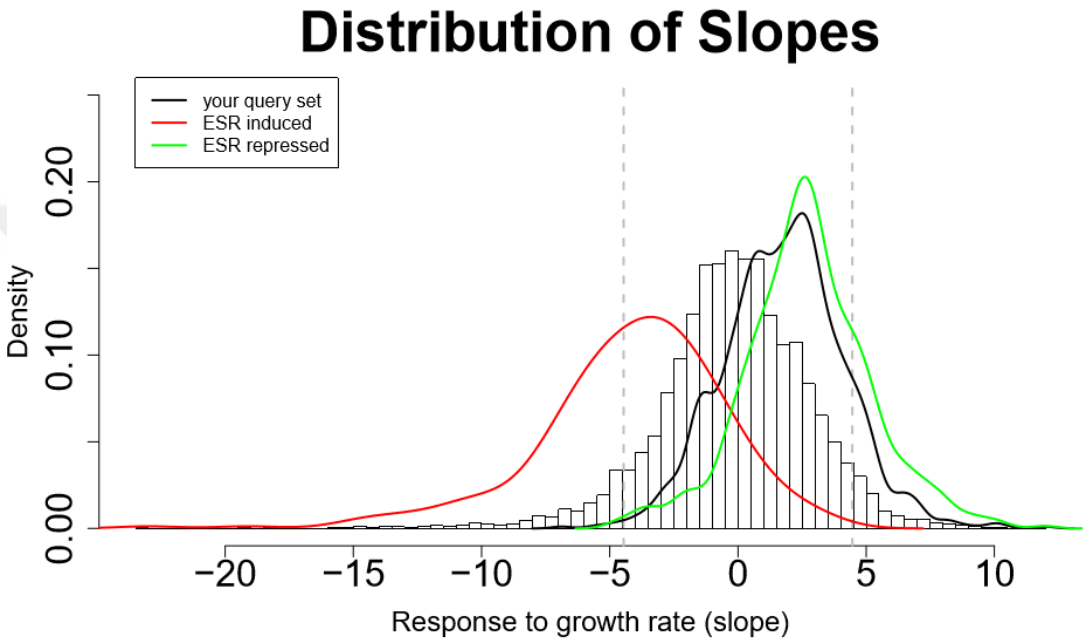

Figure 3.10 : The distribution of transcriptional changes of environmental stress response genes. The induced ESR genes are shown as the red curve and the repressed ESR genes are indicated with the green curve under environmental stress conditions. The bar chart shows the genes that were expressed under normal growth conditions. The black curve indicates the down-regulated genes of H7 under normal growth condition.

The list of the down-regulated genes (two-fold and higher) of H7 classified by metabolic processes can be found in Table A-1. Categorization was performed by Yeast Genome Database Gene Ontology Slim Mapper.

3.1.4 Analysis of up-regulated genes

At least 2-fold up-regulated genes of H7 according to metabolic process categories is shown in Figure 3.11 (The cut-off value was set to ≥ 2-fold). Gene names are provided in Table A.2.

According to Figure 3.11, it could be seen that the up-regulated genes were related with response to stress conditions which included oxidative, heat, chemical, osmotic and starvation stress. Besides, the genes related with metabolite production and modification processes such as carbohydrate metabolic process, generation of precursor metabolites and energy, monocarboxylic acid metabolic process, cofactor metabolic process, lipid metabolic process, protein phosphorylation, protein complex biogenesis, cell wall organization or biogenesis, oligosaccharide metabolic process, protein modification by small protein conjugation or removal and protein folding were up-regulated in the oxidative stress-resistant, evolved strain. Only mitochondrion and peroxisome organization-related genes were up-regulated among the organelles. It could also be observed that the transportation-related genes were generally up-regulated. These genes included ion transport, transmembrane transport, protein targeting, carbohydrate transport, Golgi vesicle transport, membrane invagination, membrane fusion, lipid transport, amino acid transport and organelle fusion. Besides, expression levels of genes related with cellular respiration were also up-regulated. Another key result was that the expression levels of genes related to meiotic cell cycle and sporulation increased.

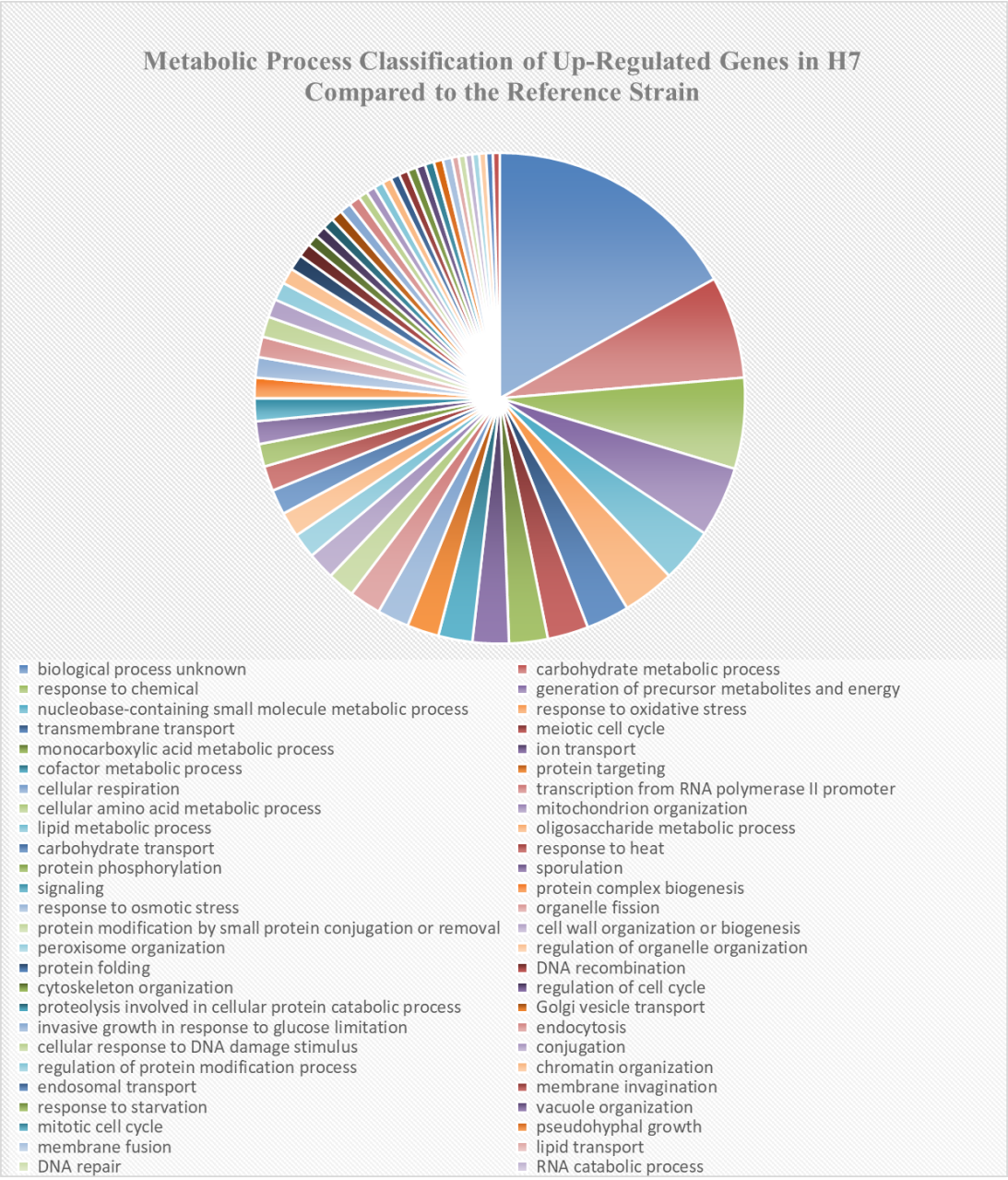

Figure 3.11 : At least 2-fold up-regulated genes of the evolved strain according to metabolic process categories (The cut-off value was set to ≥ 2-fold).

Up-regulated genes of H7 were also analyzed by the search tool in ESR analysis web site (*URL-4*). Distribution of transcriptional changes of environmental stress response genes graphics was obtained by this search tool via analyzing the up-regulated genes (Figure 3.12). The bar chart points out the expression levels of cells under normal conditions without any stress. Genes induced with stress conditions are indicated as the red curve and the repressed genes are represented by the green curve. The black curve indicates the down-regulated gene set of this study. It could be seen that the up-

regulated ESR genes of H7 and the ESR-induced genes of the database share almost the same profile.

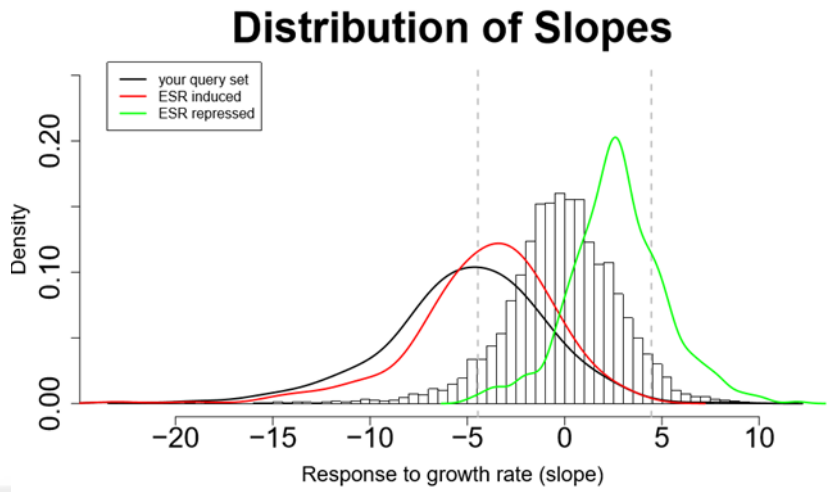

Figure 3.12 : The distribution of transcriptional changes of environmental stress response genes.The induced ESR genes are shown as the red curve and the repressed ESR genes are indicated with a green curve under environmental stress conditions. The bar chart indicates the genes which were expressed under normal growth situation. The black curve indicates the down-regulated genes of H7 under normal growth condition.

The list of the up-regulated genes (two-fold and higher) of H7 classified by metabolic processes is given in Table A.2. Categorization was performed by Yeast Genome Database Gene Ontology Slim Mapper.

One of the most critical results is that there were 34 genes which were up-regulated by about 6-fold and higher. These genes are listed in Table 3.5.

Hxk1p and Hxk2p are hexokinases and Glk1p is a glucokinase, having a main role in the first irreversible step of glycolysis that involves the glucose phosphorylation at C6 in the intracellular metabolism (Walsh et al., 1983). *HXK2* (has no significant expression level change in this study) is expressed at a high level during yeast growth on a fermentable medium with glucose, fructose or mannose as the carbon source. But *HXK1* (7.63-fold up-regulated in H7) and *GLK1* (3.90-fold up-regulated in H7) are expressed when organisms were shifted to a non-fermentable carbon source (Rodríguez, 2001). *MPC3* gene was up-regulated in H7 (6.77-fold). Mpc3p is a highly conserved subunit of a two-subunit carrier complex which is a mitochondrial pyruvate carrier in the mitochondrial inner membrane. *MPC3* gene is expressed during growth on a non-fermentable medium. A deletion study on MPC showed that the *MPC3*

deletion mutant displayed no-growth on a medium with non-fermentable carbon source (Bricker et al., 2012). In light of this information, it can be speculated that H7 may behave as if it is growing on non-fermentable medium. This is supported by the finding that H7 used glycerol and acetate, which were produced during exponential phase, at the stationary phase of growth (Kocaefe-Özşen et al., 2022).

CYC7 encodes cytochrome c isoform 2 and has a role as an electron carrier of the mitochondrial intermembrane space (Downie et al., 1977). *CYC7* and *COX5B* are hypoxic genes. These two genes are not expressed until the oxygen concentration is below 0.5 mM O_2 (Burke et al., 1997). In the present study, it was observed that the *CYC7* gene expression in the H7 strain increased to 9.09-fold and *COX5B* gene expression level increased to 3.99-fold. Besides, *CYC1* and *COX5A* genes are paralog genes of *CYC7* and *COX5B*. While *CYC1* and *COX5A* are expressed aerobically, *CYC7* and *COX5B* are expressed under hypoxic condition. *CYC7* gene is known as a global response gene (Zitomer et al., 1997). In light of this information, it can be considered that H7 strain behaves like under hypoxic condition.

HSP12, *HSP26*, and *DDR2* are important for the environmental stress response of organisms. H7 behaves as it is always under oxidative stress conditions, according to the gene expression results and the previous metabolic analysis results with growth analysis (Kocaefe-Özşen et al., 2022). This observation is clearly expected for the oxidative stress-resistant evolved strain.

YMR206W (8.44-fold up-regulated), *YBR285W* (7.13-fold up-regulated), *TMA10* (7.23-fold up-regulated), and *RGI2* are putative genes and it is known that they are not essential (Byrne & Wolfe, 2005). It has been observed that *YMR206W, TMA10, GPH1* and *ALD3* genes were up-regulated in the diauxic shift (Murphy et al., 2015). A significant increase in the expression levels of these genes was also observed in H7.

YNL194C and *FMP45* genes are paralog genes. They encode an integral membrane protein and are required for sporulation and induced during whole-genome duplication (Young et al., 2002). *SLZ1* gene is also required for sporulation (Briza et al., 2002).

Gph1 is required for the mobilization of glycogen. *GPH1* is regulated by stress response elements (Hwang et al., 1989). According to the trehalose and glycogen metabolite studies, glycogen production of the oxidative stress-resistant strain H7 was substantially high (Kocaefe-Özşen et al., 2022).

SPG4 encodes the protein required for high-temperature survival during the stationary phase (Martinez et al., 2004). *SPG4* gene expression level is known to increase slightly during post-diauxic shift. However, significant increase in *SPG4* expression level was observed in the stationary phase (Bisschops et al., 2015).

YBR116C is a dubious open reading frame. According to previous studies, high sugar stress, sorbic acid and 1M sorbitol (as osmotic stress), and imino acid analog azetidine 2-carboxylic acid (AZC) induce *YBR116C* expression (Chang et al., 2018; de Nobel et al., 2001; Erasmus et al., 2003; Schuller et al., 2004; Trotter, 2002). Further studies on this gene may be necessary, as a 6.93-fold increase in its expression in H7 seems to be critical.

Table 3.5 : Genes which were up-regulated in H7 by about 6-fold and higher.

Systematic Gene Symbol	Standard Gene Symbol	Gene Name	Fold Change	Regulatory Genes
YFR053C	*HXK1*	HeXoKinase	7.63	*BUR6, CYC8, GCN4, GCN5, HSF1, IXR1, MED2, MED4, RAP1, SFP1, SIN4, SPN1, SPT6, STP1, SUA7, TUP1, YAP1*
YEL039C	*CYC7*	CYtochrome C	9.09	*TUP1, HAP1, HIR3, MSN2, PHD1, SFP1, SIR2, SIR3, SIR4, SUA7, TFC7*
YMR206W			8.44	*GCR2, SFP1, SIR2, SIR3, SIR4, SUA7, UGA3, UME6, XBP1*
YMR107W	*SPG4*	Stationary Phase Gene	9.52	*CST6, GCR1, LEU3, MED2, RAP1, SPT10, SRB5, UME6, YAP5*
YDL222C	*FMP45*	Found in Mitochondrial Proteome	7.89	*BUR6, MED4, STE12, SUA7, TEC1, XBP1*
YIL057C	*RGI2*	Respiratory growth induced	7.69	*RAP1, SPT10*
YFL014W	*HSP12*	Heat Shock Protein	8.44	*BAS1, CBF1, CSE2, CST6, GCN5, GCR1, HAL9, HCM1, HSF1, IXR1, MED4, MSN2, NCB2, RAP1, REB1, RPN4, SFP1, SIR2, SIR3, SIR4, SPT10, SPT3, SRB8, SUA7, TUP1, UME6, XBP1, YAP5, YAP6, ZAP1*
YNL194C			8.30	*AFT2, CYC8, MSN2, NCB2, RPD3, SPT3, SUA7, UME6, YAP5*
YLR327C	*TMA10*	Translation Machinery Associated	7.23	*BUR6, CAD1, CST6, CUP2, CYC8, FKH1, FKH2, FLO8, GCR1, HSF1, MED2, MED4, MET32, MET4, NCB2, RAP1, RGM1, RDR1, SFP1, SPT10, SPT3, SPT7, SRB5, SUA7S, WI4, SWI6, TUP1, YAP1*
YNL196C	*SLZ1*		7.27	*SPT10*
YBR072W	*HSP26*	Heat Shock Protein	7.32	*HCM1, BUR6, CIN5, CST6, CYC8, FKH2, GCN5, HSF1, IFH1, MED2, MED4, MET32, MET4, MSN2, MSN4, NCB2, NHP6A, PHO2, RAP1, REB1, SFP1, SPN1, SPT10, SPT20, SPT3, SPT7, SRB5, SUA7, TOA2, TUP1, XBP1, ZAP1*
YPR160W	*GPH1*	Glycogen PHosphorylase	6.83	*CYC8, MSN2, NHP6A, SUA7, TUP1*
YOL052C-A	*DDR2*	DNA Damage Responsive	7.00	*CBF1, CST6, GCR1, HSF1, IXR1, LEU3, MET32, MET4, RAP1, REB1, SIR2, SIR3, SIR4, SPT10, SRB8, SSN2, SUA7*
YGR243W	*MPC3*	Mitochondrial Pyruvate Carrier	6.77	*FHL1, MED2, MIG1 REB1, RGR1, RPD3, SIR2, SIR3, SIR4, SPT3, SUA7, TUP1, UME6, ZAP1*
YBR116C			6.93	*ACE2, ARO80, CDC73, CST6, MET32, SFP1, SPT10*

Table 3.5 (Continued): Genes which were up-regulated in H7 by about 6-fold and higher.

Systematic Gene Symbol	Standard Gene Symbol	Gene Name	Fold Change	Regulatory Genes
YDR536W	*STL1*	Sugar Transporter-Like protein	6.91	*HOG1, HOT1, DAL82, SFP1, SPT10, YAP6*
YMR169C	*ALD3*	Aldehyde Dehydrogenase	6.75	*DEP1, HOG1, MSN2, MSN4, PHO23, RPD3, SAP30, SDS3, SIN3, UME1, BUR6, CAD1, CST6, GCN5, HSF1, IXR1, MED2, MED6, SFP1, SUA7, XBP1, ZAP1*
YAL061W	*BDH2*		7.15	*BUR6, CST6, CYC8, MET32, MET4, SOK2, SPT10, SUA7, YAP1*
YBR285W			7.13	*FKH1, GCN5, LEU3, RPD3, SFP1, SPT10, SUA7, UME6, ZAP1*
YER067W	*GRI1*	Respiratory Growth Induced	6.00	*BUR6, CHA4, CUP2, CYC8, FLO8, GAT3, HSF1, MAC1, MED2, NCB2, RGM1, RPD3, SRB5, SUA7, TUP1*
YER121W			6.09	*FKH1, SFP1, SPT10*
YKL217W	*JEN1*		6.12	*BUL1, ROD1, BAS1, FKH1, FKH2, GCR1, IFH1, RPD3, SPT10, STP1, UME6*
YPR151C	*SUE1*		6.23	*AFT1, AFT2, FKH1, FKH2, HAP1, SPT6, SUA7, XBP1*
YCR010C	*ADY2*	Accumulation of DYads	6.24	*USV1, MSN2, MSN4, SFP1, SIN3, SPT10, UME6, YAP5, YAP6*
YDL204W	*RTN2*	ReTiculoN-like	6.27	*GIS1, MOT3, MSN2, MSN4, CAD1, FKH1, GCN5, IXR1, MED4, SFP1, SPT10*
YDR342C	*HXT7*	HeXose Transporter	6.30	*BUR6, FKH1, FKH2, IXR1, REB1, SOK2, TUP1*
YDL079C	*MRK1*	Mds1p Related Kinase	6.31	*BUR6, CYC8, MED2, MET32, RPD3, SUA7, UME6, YAP6*
YPL223C	*GRE1*	Genes de Respuesta a Estres (spanish for stress responsive genes)	6.34	*HAA1, HOT1, MOT3, MSN2, MSN4, SKO1, CST6, GCN4, GCN5, IXR1, MET32, MET4, REB1, RGR1, SFP1, SPT10*
YGR043C	*NQM1*	Non-Quiescent Mutant	6.36	*BUR6, GCN4, GLN3, IXR1, REB1, SFP1, SPT10, SWI4, UME6*
YDR343C	*HXT6*	HeXose Transporter	6.38	*FKH1, HFI1, MIG1, MSN2, RAP1, TUP1*
YBR117C	*TKL2*	TransKetoLase	6.52	*ZAP1, CST6, FHL1, FKH1, FKH2, IXR1, MED2, MED4, MET32, RAP1, SPT10*
YHR096C	*HXT5*	HeXose Transporter	6.62	*CAD1, CST6, FKH1, HSF1, IXR1, RAP1, SKO1*
YDR070C	*FMP16*	Found in Mitochondrial Proteome	6.63	*BUR6, IXR1, SUA7, XBP1*

3.1.5 Stress response genes

Because the transcriptional response of H7 was in line with the ESR, the frequencies of genes that were up or down-regulated as a metabolic response were evaluated. Figure 3.13 indicates upregulated and downregulated gene counts for metabolic processes which are related to the response of organism to various metabolic processes, including stress response.

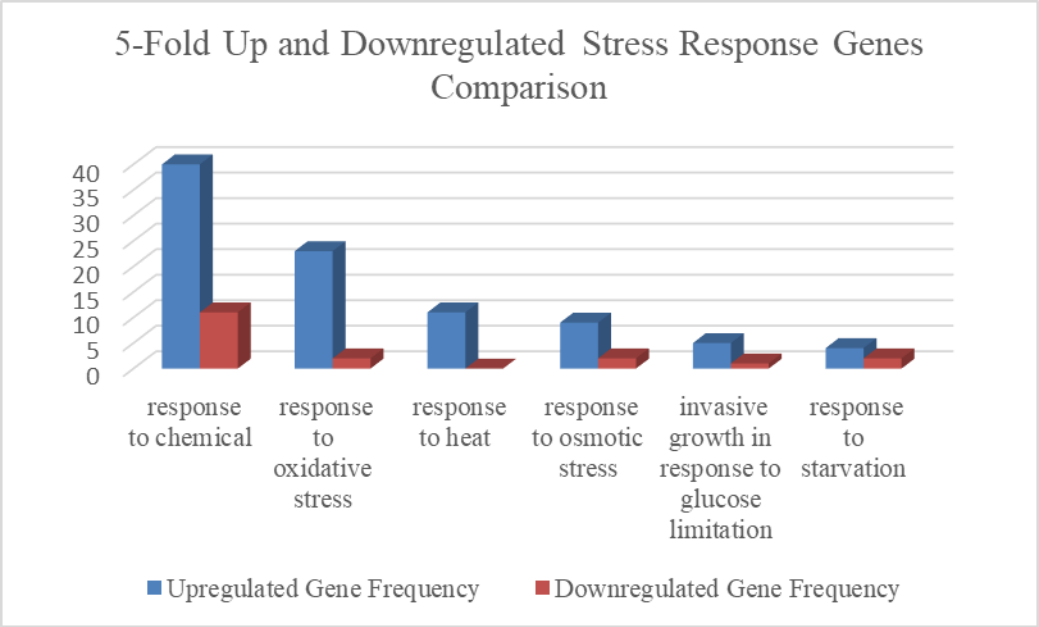

Figure 3.13 : Up-regulated and down-regulated gene counts in H7.
Cut off value is ≥ 5-fold. Blue bars show up-regulated gene numbers for each response to metabolic processes. Red bars indicate down-regulated gene numbers for each response to metabolic processes.

Figure 3.14 gives the percentage of the up-regulated and down-regulated genes to total genes whose expression level changed for each different metabolic process.

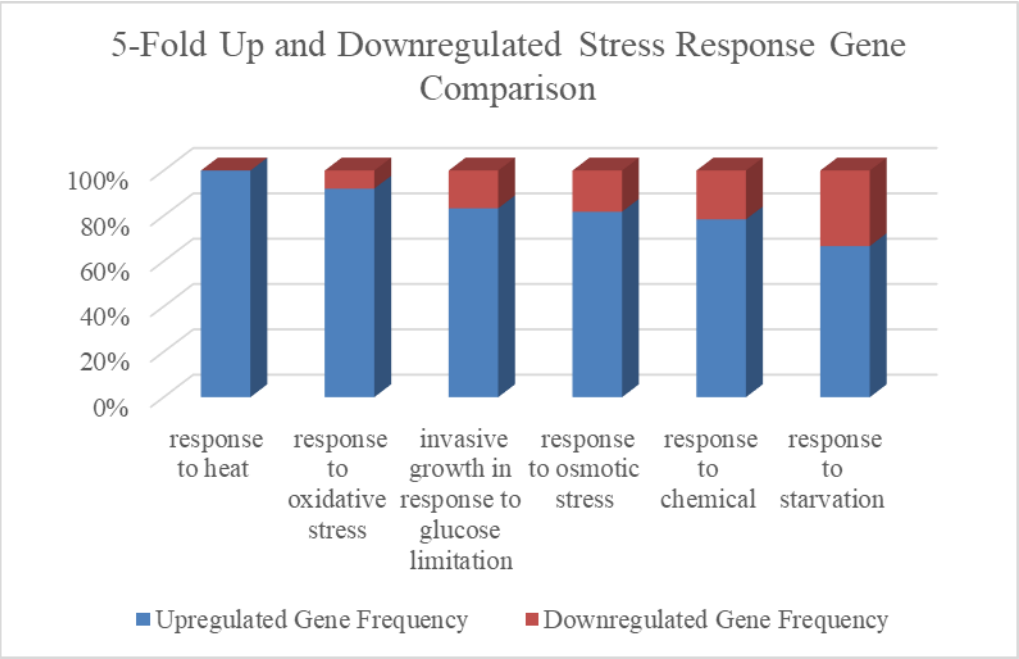

Figure 3.14 : The percentage of up-regulated and down-regulated genes to total genes in H7 whose expression level changed for each different response process. Cut off value is ≥ 5 fold. Blue bars show up-regulated gene numbers for each response to metabolic processes. Red bars indicate down-regulated gene numbers for each response to metabolic processes.

3.1.6 Oxidative stress response genes of H7

As shown in Table 3.6, there were 23 oxidative stress response genes which were at least 2-fold up-regulated in H7. In addition, there were 2 such genes that were at least 2-fold down-regulated (*NCL1* and *RLI1*) in H7. The expression level of *HSP12* in H7 was 8.44-fold of the reference strain. *HSP12* gene encodes heat shock protein as a plasma membrane protein. It has a role in membrane organization maintainence. Besides, membrane organization maintainence continues during stress conditions such as heat shock, oxidative stress, osmostress, stationary phase, glucose depletion, oleate and alcohol; by the plasma membrane protein encoded by *HSP12*. Additionally, Heat Shock Protein amount in the cells increases in response to DNA replication stress and dietary restriction. Expression of *HSP12* is regulated by the HOG and Ras-Pka pathways. It is required for caloric restriction-induced lifespan extension (Sales et al., 2000).

Table 3.6 : Up-regulated oxidative stress response genes (two-fold and higher) in H7 based on microarray results.

Systematic Gene Symbol	Standard Gene Symbol	Gene Name	Fold Change
YKR066C	*CCP1*	Cytochrome c Peroxidase	2.48
YGR088W	*CTT1*	CaTalase T	5.37
YHR053C	*CUP1-1*	Cu, copper, CUPrum	2.77
YHR055C	*CUP1-2*	Cu, copper, CUPrum	2.71
YOL052C-A	*DDR2*	DNA Damage Responsive	7.00
YMR250W	*GAD1*	GlutAmate Decarboxylase	4.03
YOR120W	*GCY1*	Galactose-inducible Crystallin-like Yeast protein	3.86
YKL026C	*GPX1*	Glutathione PeroXidase	3.45
YHR104W	*GRE3*	Genes de Respuesta a Estres (stress responsive genes)	2.78
YCL035C	*GRX1*	GlutaRedoXin	3.91
YDR513W	*GRX2*	GlutaRedoXin	3.59
YFL014W	*HSP12*	Heat Shock Protein	8.44
YKL150W	*MCR1*	Mitochondrial NADH-Cytochrome b5 Reductase	2.50
YNL036W	*NCE103*	NonClassical Export	4.86
YGR043C	*NQM1*	Non-Quiescent Mutant	6.86
YPL196W	*OXR1*	OXidation Resistance	2.39
YBL064C	*PRX1*	PeroxiRedoXin	3.73
YKL086W	*SRX1*	SulfiRedoXin	4.31
YBR126C	*TPS1*	Trehalose-6-Phosphate Synthase	2.45
YDR453C	*TSA2*	Thiol-Specific Antioxidant	3.45
YIL101C	*XBP1*	XhoI site-Binding Protein	4.12
YJR096W	-	Xylose and Arabinose Reductase	4.27
YBR046C	*ZTA1*	ZeTA-crystallin	3.11

The regulation network of *HSP12* gene is given in Figure 3.15. These data were provided by the Saccharomyces Genome Database (*URL-1*). According to this database, *HSF1* gene is a positive regulator for *HSP12*. *IXR1* contributes as both positive and negative regulators for *HSP12*. The other genes in Figure 3.15 negatively regulate the *HSP12* gene. *HCM1* gene was approximately 2.01-fold down-regulated in H7. However, the expression levels of *CSE2* and *RPN4* did not change in H7. According to these data, there is no significant change in the expression level of *HSF1* that is single positive regulator. But there are 2 genes that were up-regulated and 2 genes that were down-regulated as negative regulators of *HSP12*. Considering the 8.44-fold up-regulation of *HSP12* in H7, it can be said that *HCM1* could be more effective on *HSP12* gene expression.

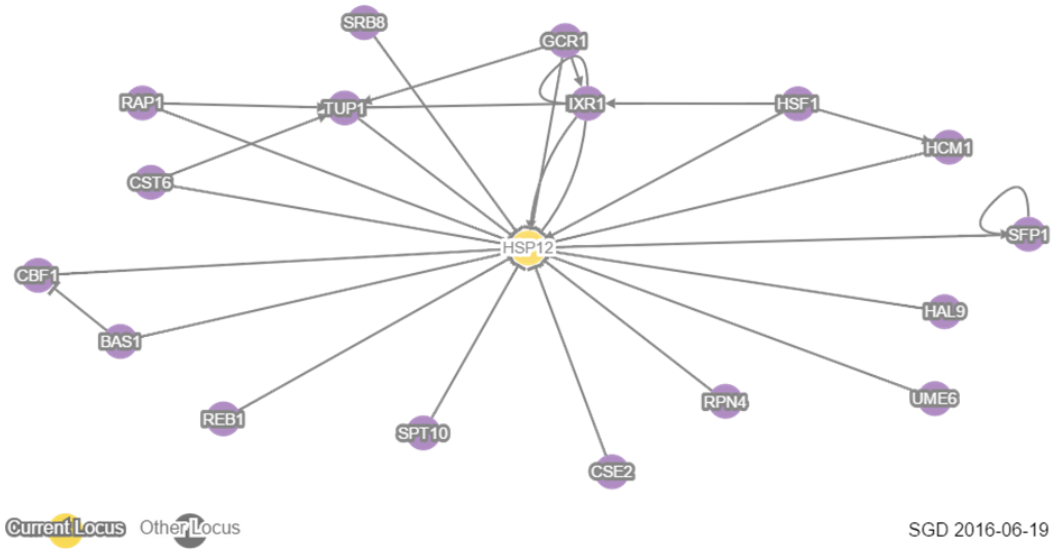

Figure 3.15 : *HSP12* gene regulation network (data provided by Saccharomyces Genome Database).

Another important gene for oxidative stress response is *DDR2*. The expression level increase of *DDR2* was 7.00-fold in H7. *DDR2* encodes a multi-stress response protein and expression of this gene is especially situmulated by particular xenobiotic agents, in environmental/physiological stress conditions (Kobayashi and McEntee, 1990).

The regulation network of *DDR2* gene is given in Figure 3.16. These data were provided by Saccharomyces Genome Database (*URL-1*). According to this database, *HSF1* gene has only one positive regulator. The other genes contribute as negative regulators. However, there were no significant expression level changes in the regulators of *DDR2,* based on the evaluations of expression level changes that were 2-fold and higher.

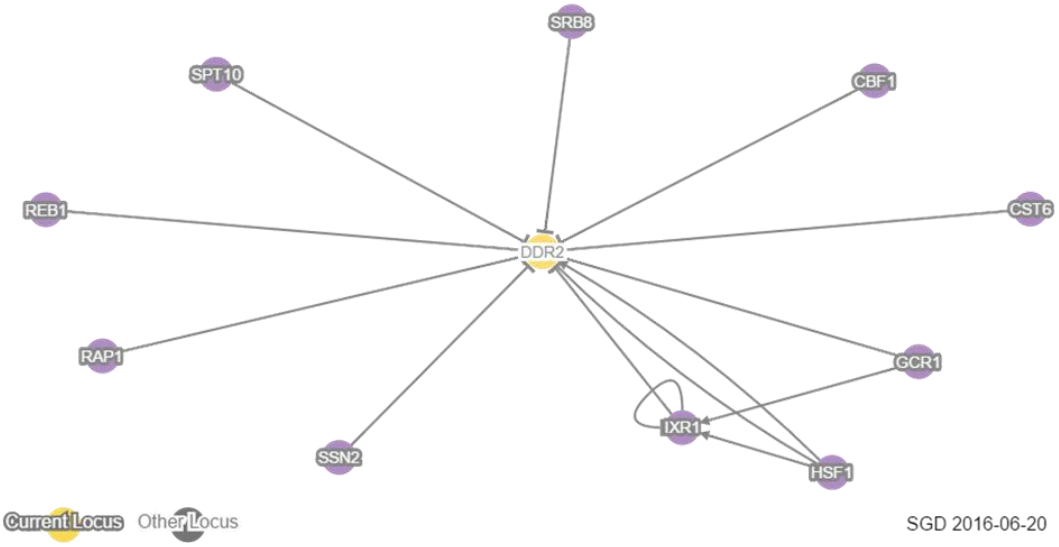

Figure 3.16 : *DDR2* gene regulation network (data provided by Saccharomyces Genome Database).

When the regulation network map of these two genes were compared, it could be observed that *CBF1, CST6, GCR1, HSF1, RAP1, REB1, SRB8, IXR1* and *SPT10* genes regulate both genes, and all of these genes did not have a significant expression level change. *CST6, GCR1, HSF1, RAP1, IXR1* and *SPT10* genes are transcription regulators, acting as repressors or activators. Thus, *CST6, GCR1, HSF1, RAP1, IXR1* and *SPT10* genes could be responsible for the upregulation of *HSP12* and *DDR2*.

3.1.7 KEGG analysis

The KEGG (Kyoto Encyclopedia of Genes and Genomes) pathway mapping analysis was performed using the up- and down-regulated gene data sets via DAVID v6.8 Bioinformatics Resources (*URL-6*) in order to classify their biological significance (Huang et al., 2009b, 2009a). KEGG has a comprehensive database that includes genomes, biological pathways, diseases, drugs, and chemical substances data. The analysis showed that nucleobase metabolism, RNA polymerase and ribosome biogenesis, amino acid biosynthesis and steroid biosynthesis as significantly enriched pathways in the down-regulated genes set. Pathway analysis results further identified that the up-regulated genes were enriched mainly in carbon metabolism, oxidative phosphorylation, peroxisome, fatty acid degradation, endocytosis pathways, citrate metabolism and biosynthesis of the antibiotics and secondary metabolites (Table 3.7).

Table 3.7 : KEGG pathway analysis results of up- and down-regulated genes in the oxidative stress-resistant strain H7, as compared to the reference strain.

Term	Count[a]	Fold Enrichment[b]	Corrected p-value[c]
Pathways enriched in down-regulated genes set			
Ribosome biogenesis in eukaryotes	49	3.25	2.76×10^{-16}
Purine metabolism	44	2.71	5.10×10^{-11}
Pyrimidine metabolism	36	3.04	8.20×10^{-11}
Biosynthesis of amino acids	49	2.35	1.26×10^{-9}
RNA polymerase	18	3.54	7.51×10^{-7}
Metabolic pathways	155	1.34	1.83×10^{-6}
Lysine biosynthesis	10	4.92	1.40×10^{-5}
Biosynthesis of antibiotics	59	1.62	5.84×10^{-5}
RNA transport	32	2.03	5.84×10^{-5}
Biosynthesis of secondary metabolites	72	1.44	2.35×10^{-4}
DNA replication	13	2.48	2.95×10^{-3}
2-Oxocarboxylic acid metabolism	14	2.36	3.06×10^{-3}
Phenylalanine, tyrosine and tryptophan biosynthesis	9	3.12	3.64×10^{-3}
Valine, leucine and isoleucine biosynthesis	7	3.44	8.30×10^{-3}
One carbon pool by folate	7	2.75	2.86×10^{-2}
Arginine and proline metabolism	8	2.25	5.02×10^{-2}
Steroid biosynthesis	7	2.43	5.26×10^{-2}
Base excision repair	7	3.30	6.82×10^{-2}
Cysteine and methionine metabolism	11	1.80	6.87×10^{-2}
Glycine, serine and threonine metabolism	10	1.84	7.67×10^{-2}
Pathways enriched in up-regulated genes set			
Carbon metabolism	44	3.39	3.12×10^{-14}
Starch and sucrose metabolism	25	5.48	8.88×10^{-14}
Metabolic pathways	126	1.62	1.69×10^{-11}
Citrate cycle (TCA cycle)	20	5.48	5.22×10^{-11}
Biosynthesis of antibiotics	55	2.24	1.55×10^{-9}
Biosynthesis of secondary metabolites	66	1.96	8.56×10^{-9}
Peroxisome	18	4.15	1.63×10^{-7}
Galactose metabolism	13	4.75	2.76×10^{-6}
Oxidative phosphorylation	23	2.80	6.28×10^{-6}
Glyoxylate and dicarboxylate metabolism	13	4.38	7.97×10^{-6}
Glycolysis / Gluconeogenesis	20	3.02	9.00×10^{-6}
Pyruvate metabolism	16	3.60	9.04×10^{-6}
Glycerolipid metabolism	10	3.51	1.07×10^{-3}
Fructose and mannose metabolism	9	3.76	1.34×10^{-3}
Valine, leucine and isoleucine degradation	7	4.73	1.73×10^{-3}
Pentose phosphate pathway	9	2.82	1.01×10^{-2}
beta-Alanine metabolism	6	4.05	1.08×10^{-2}
Lysine degradation	6	3.76	1.53×10^{-2}
Amino sugar and nucleotide sugar metabolism	9	2.47	2.28×10^{-2}
Arginine and proline metabolism	7	2.93	2.51×10^{-2}
Methane metabolism	8	2.51	3.26×10^{-2}
Nitrogen metabolism	4	5.01	3.28×10^{-2}
Butanoate metabolism	5	3.37	5.07×10^{-2}
Fatty acid degradation	6	2.77	5.55×10^{-2}
Endocytosis	13	1.61	9.96×10^{-2}

[a] Number of input genes involved in each term.
[b] Ratio between frequencies of the query and the reference gene set.
[c] p values were adjusted with Benjamini-Hochberg false discovery rate correction.

3.1.8 Expression level analysis of autophagy genes

It was observed that 12 of the autophagy system-associated genes were up-regulated by more than 2-fold in H7 (Table 3.8). In addition, there were no down-regulated genes in H7 which were related with the autophagy system. Especially, *ATG39* gene was 5.62-fold up-regulated in H7. Atg39 is located in the perinuclear ER (or the nuclear envelope) and stimulates the autophagic sequestration of part of the nucleus. Atg39-dependent autophagy of the perinuclear ER/nucleus has a role in cell survival under nitrogen-deprivation conditions. Atg39 is required in perinuclear ER-phagy (Mochida et al., 2015).

Table 3.8 : Up-regulated autophagy genes in H7.

Systematic Name	Standard Name	Symbol	Fold Change
YBL078C	AuTophaGy related	*ATG8*	+2.99
YOR019W	-		+3.41
YPL166W	AuTophaGy related	*ATG29*	+2.34
YBR128C	AuTophaGy related	*ATG14*	+2.79
YCR068W	AuTophaGy related	*ATG15*	+2.92
YDR022C	AuTophaGy related	*ATG31*	+2.06
YJL164C	Takashi's Protein Kinase	*TPK1*	+2.95
YLR312C	AuTophaGy related	*ATG39*	+5.62
YAL008W	Function Unknown Now	*FUN14*	+2.22
YLR423C	AuTophaGy related	*ATG17*	+2.04
YDR435C	Protein Phosphatase Methyltransferase	*PPM1*	+2.21
YJL185C	AuTophaGy related	*ATG36*	+3.36

3.2 Whole Genome Sequencing Analysis of the Reference Strain and the Oxidative Stress-Resistant Strain H7

3.2.1 DNA measurement and quantification

Nanodrop measurement and quantification results of the isolated DNA samples are given in Table 3.9.

Table 3.9 : Nanodrop measurement results. DNA concentration, 260/280 and 260/280 ratios are given for both reference strain (905) and the oxidative stress resistant strain (H7).

Strain Name	DNA Concentration	260/280 Ratio	260/230 Ratio
905 (Reference Strain)	745.8 ng/µl	2.17	2.29
H7 (H_2O_2-Resistant Strain)	540.6 ng/µl	2.19	2.25

DNA quantification was done by using Qubit® Fluorometer 3.0. Results are shown in Table 3.10.

Table 3.10 : Qubit 3.0 measurement results for DNA concentrations of the reference strain (905) and the oxidative stress resistant strain (H7).

Strain Name	DNA Concentration
905 (Reference Strain)	122 ng/µl
H7 (H_2O_2-Resistant Strain)	47.2 ng/µl

3.2.2 Library measurement

Prepared libraries were measured by Qubit 3.0. Measurement values are given in Table 3.11.

Table 3.11 : Qubit 3.0 measurement results of the prepared libraries.

Purified size selected and barcoded fragment sample DNA concentrations are given for both reference strain (905) and the oxidative stress-resistant strain (H7).

Purified Size Selected and Barcoded Fragment Sample	Purified Size Selected and Barcoded Fragment Sample Concentration
905 (Reference Strain)	714 ng/mL
H7 (H_2O_2-Resistant Stain)	1402 ng/mL

3.2.3 NGS quality control data

The genome sequencing of the reference strain and the oxidative stress resistant evolved strain was performed by Ion S5 sequencing system. Coverage and quality data are given in Table 3.12. Besides, coverage of chromosomes is given in Figure 3.17 and Figue 3.18.

Table 3.12 : Coverage data and quality information of the NGS results.

Total mapped reads, average base coverage depth, 1x, 20 x and 100 x coverage of genome are shown.

	905 (Reference Strain)	H7 (H_2O_2-Resistant Strain)
Number of Mapped Reads	20,972,820	20,174,500
Average Base Coverage Depth	368.1	349.1
Uniformity of Base Coverage	98.36%	97.96%
Genome Base Coverage at 1x	99.52%	99.50%
Genome Base Coverage at 20x	99.09%	99.08%
Genome Base Coverage At 100x	97.37%	95.54%

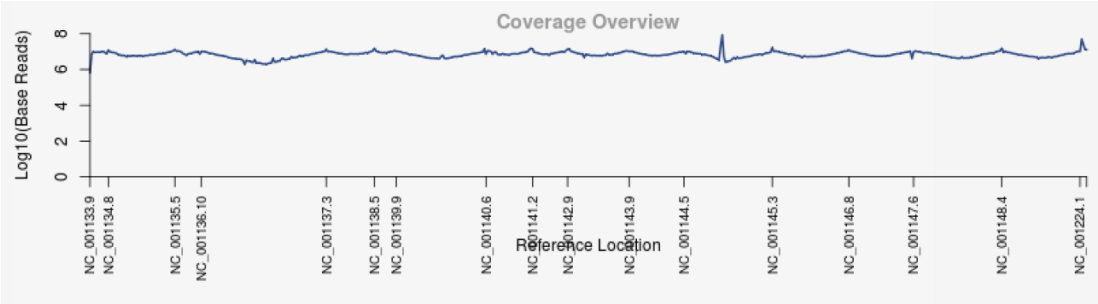

Figure 3.17 : Coverage overview of all chromosomes of the reference strain. Chromosomes are indicated as NC numbers. Base reads are given as log10.

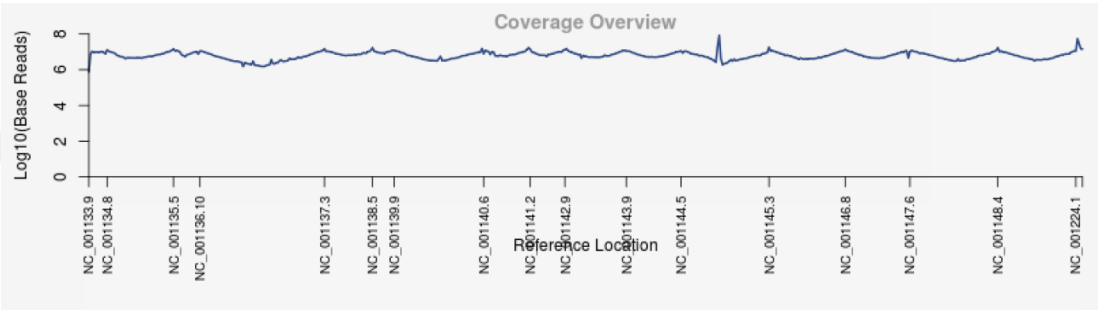

Figure 3.18 : Coverage overview of all chromosomes of the evolved strain H7. Chromosomes are indicated as NC numbers. Base reads were given as log10.

3.2.4 Mutation data analysis

Mutations were determined by comparing reference strain and the evolved strain's whole genome sequencing data files. All mutations were observed on IGV software. Information about the genes in *S. cerevisiae* genome was obtained from https://www.yeastgenome.org/ (*URL-1*).

Mutations were classified according to mutation types. IGV images of the mutations are given in the Appendices section (Figure B.1- Figure B.61).

To summarize, 34 missense mutations, 2 nonsense mutations, 1 frameshift deletion mutation, 13 mutations out of the coding sequence and 12 silent mutations were observed in the H7 genome. Mutations are indicated in Table 3.13- 3.17, and they were classified according to mutation types.

The function of the protein coded by *AIM19*, which had a missense mutation in H7, is unknown. It is known that Aim19 protein is located in the mitochondrion (Hess et al., 2009). According to Lee at al. (2007), *AIM19* gene expression was induced by MMS

(methyl methanesulphonate). In this study, EMS (ethyl methanesulphonate) was used to obtain the stress-resistant strain. The reason for the mutation in *AIM19* and the up-regulation of this gene could possibly be EMS. The missense mutation in *AIM19* was in the non-cytoplasmic domain.

FIS1 encodes a mitochondrial fission protein. It is located in the outer mitochondrial membrane with its amino terminus exposed to the cytoplasm (Kitagaki et al., 2007; Mozdy et al., 2000). In addition, Fis1p has a role in peroxisome proliferation. Although *FIS1* is not an essential gene, it is known that it has a positive regulatory role in mitophagy. Together with other other three genes, which are *DNM1*, *MDV1* or *CAF4*, they are involved in the maintenance of the mitochondrial shape by fission and fusion. In this study, the mutation (p.L65F) in *FIS1* is in the tetratricopeptide-like helical domain of the Fis1p protein. Both expression level increase in *FIS1* gene and the presence of the mutation in the corresponding region of Fis1p, the tetratricopeptide-like helical domain, could be important for the selective autophagy and the chronological life span (CLS).

IRC15 encodes a microtubule associated protein. Irc15 regulates microtubule dynamics (Keyes & Burke, 2009). This protein is required for accurate chromosome segregation during meiosis (Jordan et al., 2007). According to the findings of Koch et al (2018), Irc15p is a flavoprotein and works with FAD as the cofactor and the thermal stability of this protein is high (Tm = 70 °C). The presence of the mutation (p.L73F) at the FAD/NAD(P)-binding domain of this protein could affect the stabiliy of this zone and the affinity of the domain to the cofactor in the evolved strain H7.

IKS1 encodes a putative serine–threonine kinase and suppresses the Ira1 kinase activity. According to a previous study, deletion of *IKS1* gene causes the phenotypical changes on organism. It brings a sorbate-resistant phenotype and causes hypersensitivity to copper sulfate (Dastidar et al., 2012; Rieger et al., 1999). Iks1 may be involved in the regulation of key pathways in acute stress defense (Ma et al., 2015). When the mutation that occurred in the protein kinase domain in this protein in H7 is considered, according to domain classification databases, the reason for upregulation of *IKS1* could be this mutation or the enhanced activation of the enzyme by the mutation that affects the protein kinase domain. Thus, this mutation may be involved in resistance to oxidative stress.

Gdh2, the NAD^+-dependent GDH (NAD-GDH; Gdh2) encoded by *GDH2* gene, catalyzes reversible oxidative deamination of glutamate to α-ketoglutarate and ammonia (Miller & Magasanik, 1990). Gdh2-dependent NAD^+ supply stimulates the growth at low temperature (Ballester-Tomás et al., 2015). In H7 genome, the mutation occurred at the Leu/Phe/Val dehydrogenases active site in this gene. Even though there are no previous studies on the description of this condition, this change could be providing high resistance to hydrogen peroxide in H7 by affecting the activation level with a different active site configuration.

YGL052W is a putative gene with a missense mutation in H7. There is limited information on this gene. Interestingly, in a previous study in our laboratory, *YGL052W* was found to be up-regulated in a boron stress-resistant mutant (3.22-fold up-regulated) (Tartik, 2013). This putative gene was also 3.29-fold up-regulated in the oxidative stress-resistant mutant, H7. According to the *YGL052W* expression changes in these two different stress-resistant strains, it can be suggested that this gene may be important for the response to a particular group of stresses.

Nop9p is an essential subunit of U3-containing 90S pre-ribosome. A missense mutation was found in *NOP9* gene in H7. According to a study, in which 6300 deleted heterozygous yeast mutants were grown in a medium with and without hydrogen peroxide, 331 genes were found to be required for oxidative stress resistance. Besides, when these genes were classified according to their localization, it was observed that 71 essential genes for oxidative stress tolerance were enriched in nucleus and nucleolus. Classification of the essential genes based on functional categories showed that rRNA synthesis and tRNA synthesis were over-represented. It was suggested that nuclear function, such as RNA synthesis, is important in response to oxidative stress (Okada et al., 2014). However, the present study seems to have opposite results. Generally, the expression levels of tRNA synthesis and rRNA synthesis genes in H7 were down-regulated. The reason for this might be related to the differences in the ploidy levels of the strains used in these studies: while the reference and the evolved yeast strains used in the present study were haploid, the deleted yeast strains in the above-mentioned study were diploid.

HOM3 gene encodes an aspartate kinase. Hom3 catalyses the first step of the methionine and threonine biosynthesis pathway (Rafalski & Falco, 1988). *HOM3* gene

had a missense mutation in H7 genome, and the amino acid change corresponded to the catalytic site on the enzyme. In addition, this gene was down-regulated in H7.

RPF2 gene protein is an essential protein involved in rRNA maturation and ribosomal assembly. Rpf2, which is a highly conserved protein in eukaryotic organisms, is required for growth and is localized predominantly in nucleolus (Morita et al., 2002). Obviously, the observed mutation in this gene is not lethal for H7, but the low transcription level of *RPF2* in H7 and its mutation could play a role in oxidative stress resistance.

Ies1p, which is encoded by *IES1*, is a subunit of the INO80 chromatin remodeling complex (Dastidar et al., 2012). Despite the missense mutation *IES1*, there is no significant expression level change in *IES1* gene in H7 genome. The amout of this protein could be sufficient for H7, however, the mutation may alter the protein features.

Rrp6p, encoded by *RRP6* gene, is a nuclear exosome exonuclease component and it has 3'-5' exonuclease activity (Briggs et al., 1998; Hieronymus, 2004). Although there was no significant change in the expression level of *RRP6* in H7, the missense mutation in this gene may be critical for protein function and the oxidative stress resistance of H7.

Rtt10p is a WD40 domain-containing protein involved in endosomal recycling and it works with Rtt2p (Shi et al., 2011). *RTT10* had a missense mutation in H7. Both *RTT10* and *RTT2* genes of H7 were down-regulated. In light of this information, it could be inferred that endosomal recycling may not be critical for the survival of the yeast in the presence of hydrogen peroxide.

Another gene with a missense mutation in H7, *MAK10*, encodes a noncatalytic subunit of N-terminal acetyltransferase (Fujimura & Wickner, 1987). In a study on the global analysis of gene function in yeast by quantitative phenotypic profiling, the investigators found that the homozygous diploid null mutant of *MAK10* had decreased oxidative stress resistance (Brown et al., 2006). In the present study, it was observed that the *MAK10* expression level was reduced in H7.

Pig1p, encoded by the *PIG1* gene, is the putative targeting subunit for type-1 protein phosphatase Glc7. *PIG1* gene had a missense mutation in H7. According to a study which is related to the yeast *PIG* genes, researchers showed that the deletion of *PIG1* gene on its own had little effect on glycogen storage, but the combination with the loss of *GAC1* (encodes regulatory subunit for Glc7 type-1 protein phosphatase) caused a more severe glycogen-deficient phenotype than seen in gac1-deleted mutants. Thus, they indicated that Pig1 was functionally related to Gac1 and suggested that Pig1 might be a type 1 phosphatase regulatory subunit (Cheng et al., 1997). *PIG1* gene expression level was 4.83-fold decreased in H7. On the other hand, *GAC1* gene was up-regulated (3.78-fold). Besides, the glycogen level of H7 was considerably higher than that of the reference strain. It could be suggested that, although Pig1 is functionally related with Gac1, Gac1 as a regulatory subunit of Glc7 seems to be significantly more important for glycogen storage in H7.

HPT1 gene product is the dimeric hypoxanthine-guanine phosphoribosyltransferase which catalyzes the transfer of the phosphoribosyl portion of 5-phosphoribosyl-alpha-1-pyrophosphate to a purine base to form pyrophosphate and a purine nucleotide. In higher organisms, mutations in hypoxanthine-guanine phosphoribosyltransferase genes cause a deficiency in this enzyme. Mutations in the human homolog *HPRT1* can cause Lesch-Nyhan syndrome and Kelley-Seegmiller syndrome (Woods et al., 1983). Interestingly, null mutation of *HPT1* gene causes an increase in the oxidative stress resistance of *S. cerevisiae* (Brown et al., 2006). The missense mutation in the *HPT1* gene of H7 may alter the phosphoribosyltransferase domain of the Hpt1 protein and it may affect the enzymatic activity.

Table 3.13 : Missense mutations found in H7. Chromosome locations, gene (with the systematic name), changed nucleotide and amino acid and information about the mutated gene of H7 are listed.

Chromosome	Gene name, nucleotide and amino acid location	Information about gene
X:400045	*NOP9 / YJL010C* c.1939A>C, p.S647A	Essential subunit of U3-containing 90S preribosome
IX:191303	*AIM19 / YIL087C* c.154G>A, p.P52S	Protein of unknown function; mitochondrial protein that physically interacts with Tim23p
II:484630	*MEO1 / YBR126W-A* c.11C>T, p.T4I	Putative protein of unknown function; WAT-GFP, seamless-GFP and mCherry fusion proteins localize to the endoplasmic reticulum
V:255011	*HOM3 /YER052C* c.801G>A, p.P267L	Aspartate kinase (L-aspartate 4-P-transferase)
IX:233632	*FIS1 / YIL065C* c.193G>A, p.L65F	Protein involved in mitochondrial fission and peroxisome abundance
XI:591763	*RPF2 / YKR081C* c.453C>T p.G145S	Essential protein involved in rRNA maturation and ribosomal assembly
XVI:519978	*IRC15 / YPL017C* c.217G>A, p.L73F	Microtubule associated protein
XII:364951	*CFT2 / YLR115W* c.1945G>A, p.G145S	Subunit of the mRNA cleavage and polyadenylation factor (CPF)
VII:590178	*UFD1 / YGR048W* c.634G>A, p.A212T	Substrate-recruiting cofactor of the Cdc48p-Npl4p-Ufd1p segregase
VI:105954	*IES1 / YFL013C* c.307C>T, p.G103R	Subunit of the INO80 chromatin remodeling complex
X:312036	*IKS1 / YJL057C* c.554C>T, p.G185D	Protein kinase of unknown cellular role; putative serine/threonine kinase
XVI:528563	*CIP1 / YPL014W* c.1010G>A, p.R337K	Cyclin-dependent kinase inhibitor
II:687892	*PRP5 / YBR237W* c.2147A>T, p.K716M	RNA helicase in the DEAD-box family; necessary for prespliceosome formation
XII:372405	*YPS1 / YLR120C* c.838G>A, p.P280S	Aspartic protease
XV:328232	*RRP6 / YOR001W* c.1720A>G, p.K574E	Nuclear exosome exonuclease component; involved in RNA processing, maturation, surveillance, degradation, tethering, and export; role in sn/snoRNAs precursor degradation
IV:1390336	*SPP41 / YDR464W* c.2769G>A, p.M923I	Protein of unknown function; involved in negative regulation of expression of spliceosome components *PRP4* and *PRP3*
V:300881	*VTC1 / YER072W* c.248G>A, p.R83K	Regulatory subunit of the vacuolar transporter chaperone (VTC) complex
XVI:199921	*RTT10 / YPL183C* c.2498G>A, p.S833L	WD40 domain-containing protein involved in endosomal recycling;Regulator of Ty1 Transposition
IV:70705	*GDH2 / YDL215C* c.1880C>T, p.G627D	NAD(+)-dependent glutamate dehydrogenase
XI:654269	*NFT1 / YKR103W* c.2186C>T, p.T729M	Putative transporter of the MRP subfamily
XI:599762	*PRP16 / YKR086W* c.251C>T, p.A84V	DEAH-box RNA helicase involved in the second catalytic step of splicing and in exon ligation
VII:335155	*SPC105 / YGL093W* c.83G>A, p.S28N	Subunit of a kinetochore-microtubule binding complex
VIII:493763	*PPX1 / YHR201C* c.567C>T, p.M189I	Exopolyphosphatase
XI:536858	*DYN1 / YKR054C* c.10724C>T, p.G3575E	Cytoplasmic heavy chain dynein
XII:740006	*CDC25 / YLR310C* c.1601A>T, p.I534K	Membrane-bound guanine nucleotide exchange factor

Table 3.13 (continued): Missense mutations found in H7. Chromosome locations, gene (with the systematic name), changed nucleotide and amino acid and information about the mutated gene of H7 are listed.

Chromosome	Gene name, nucleotide and amino acid location	Information about gene
XII:99458	*CDC25 / YLR310C* c.2204G>A, p. G735D	Membrane-bound guanine nucleotide exchange factor
V:52037	*MAK10 / YEL053C* c.1906G>A, p.R636K	Non-catalytic subunit of the NatC N-terminal acetyltransferase
III:301974	*YCR101C* c.250C>T, p.P84S	Putative protein of unknown
V:45899	*HAT2 / YEL056W* c.892G>A, p.V298M	Subunit of the Hat1-Hat2 histone acetyltransferase complex;
XII:673770	*PIG1 / YLR273C* c.1892C>T, p.S631N	Putative targeting subunit for type-1 protein phosphatase Glc7; tethers Glc7 to Gsy2 glycogen synthase
VIII:209596	*RSC30 / YHR056C* c.1402C>T, p. E68K	Component of the RSC chromatin remodeling complex
VIII:459947	*YHRWdelta13* c.211C>T	long_terminal_repeat
IV:1268909	*HPT1* / *YDR399W* c.179G>A, p.R60K	Dimeric hypoxanthine-guanine phosphoribosyltransferase
VII:403389	*YGL052W* c. 112G>A, p.A38T	Dubious open reading frame; unlikely to encode a functional protein

Table 3.14 : Nonsense mutations found in H7. Chromosome locations, gene (with the systematic name), changed nucleotide and amino acid and information about the mutated gene of H7 are listed.

Chromosome	Gene name, nucleotide and amino acid location	Information about gene
XV:150439	*DUF1 / YOL087C* c.2164G>A, p.Q722*	Ubiquitin-binding protein of unknown function; contains one WD40 repeat in a beta-propeller fold
IV:542210	*NRG1 / YDR043C* c.245C>T, p.W82*	Transcriptional repressor; recruits the Cyc8p-Tup1p complex to promoters; mediates glucose repression and negatively regulates a variety of processes including filamentous growth and alkaline pH response

Table 3.15 : Frameshift mutation found in H7. Chromosome location, gene (with the systematic name), changed nucleotide and amino acid and information about the mutated gene of H7 are listed.

Chromosome	Gene name, nucleotide and amino acid location	Information about gene
II:629134	*FTH1 / YBR207W* c.211delC, p.Q71Kfs	Putative high-affinity iron transporter; involved in the transport of intravacuolar stores of iron; forms complex with Fet5; expression is regulated by iron; proposed to play an indirect role in endocytosis

As mentioned in Section 3.1.8, almost all ATG genes were up-regulated in H7 strain. Although there was no significant difference in the expression level of *ATG40* gene in

H7, the presence of a mutation in the upstream region, at the c.-602G>A position, was identified (Table 3.16). This mutation may be the reason why there was no increase in the expression level of *ATG40,* despite the expression level increase in almost all *ATG* genes.

The *ATG* genes have different responsibilities in selective autophagy. Although *ATG39* and *ATG40* have roles in autophagy of endoplasmic reticulum (ER)/ ER fragmentation, both of them have roles in different selective autophagy of ER pathways; while *ATG39* is responsible in perinuclear ER-phagy and nucleophagy, *ATG40* gene contributes to cortical (cell periphery) ER-phagy/cytoplasmic ER-phagy (Mochida et al., 2015). According to the microarray results, even though the increase in the expression level of the *ATG39* gene was 5.62-fold, there was no change in the expression level of the *ATG40* gene. The presence of the mutation at the c.-602G>A position, upstream of *ATG40* gene could affect the expression level change and the selective autophagy pathway use of the H7 evolved strain.

VBA1 encodes a permease that transfers the basic amino acids into the vacuolar membrane (Matsuura & Takagi, 2005; Shimazu et al., 2005). H7 had a mutation upstream of the coding region of *VBA1* gene (Table 3.16). Considering the expression level increse in *VBA1,* the proximity of the mutation to the gene could be important. This mutation should be investigated with the specific promoter prediction modelling to find its potential importance and role in expression profiling, and oxidative stress resistance.

Table 3.16 : Mutations of H7 that were located out of the coding sequences. Chromosome locations, gene (with the systematic name), changed nucleotide and amino acid, and information about the mutated gene of H7 are listed.

Chromosome	Gene name, nucleotide location	Information about gene
XV:618646	*ATG40 / YOR152C* c.-602G>A	Autophagy receptor with a role in endoplasmic reticulum degradation
XIII:86365	*UFO1 / YML088W* c.-591G>A	F-box receptor protein; subunit of the Skp1-Cdc53-F-box receptor (SCF) E3 ubiquitin ligase complex
VII:423438	*YGL039W* c.-364 G>A	Aldehyde reductase; reduces aliphatic aldehyde substrates using NADH as a cofactor;
III:113547	*RER1 / YCL001W* c.567+47G>A	Protein involved in retention of membrane proteins
III:177852	Between the *RPS14A* and snR189 (smallRNA) G>A	
XII:561294	*MSC3 / YLR219W* c.2187+234C>T	Protein of unknown function; green fluorescent protein (GFP)-fusion protein localizes to the cell periphery
XIII:439236	*VBA1 / YMR088C* c.-31G>A	Permease of basic amino acids in the vacuolar membrane
XIII:911274	*YMR321C* c.318+747G>A	Putative protein of unknown function; proposed to be a palmitoylated membrane protein
X:164001	*MCO6 / YJL127C-B* c.159+19C>T	Putative protein of unknown function; Mitochondrial Class One protein of 6 kDa
VIII:345696	*MSH1 / YHR120W* c.2880+69C>T	DNA-binding protein of the mitochondria; involved in repair of mitochondrial DNA
XI:136824	*MCD4 / YKL165C* c.2760+918C>T	Protein involved in GPI anchor synthesis; multi-membrane-spanning protein that localizes to the endoplasmic reticulum
IV:508645	*LYS14 / YDR034C* c.2373+53 C>T	Transcriptional activator involved in regulating lysine biosynthesis

FYV6, *TPS1*, *VHS3* and *HSP82* genes have silent mutations in the H7 genome (Table 3.17), and these genes were up-regulated. Although there are not many studies to understand the role of the protein encoded by *FYV6*, one study showed that this gene is required for yeast viability in response to K1 killer toxin (Wilson, 2002). *TPS1* encodes the Tre6P synthase catalytic subunit (François & Parrou, 2001). Previous physiological studies on H7 showed that trehalose production of H7 was much higher than the reference strain even without stress treatment. The silent mutation at *TPS1* could have led to an increase in the trehalose production. *VHS3* encodes the negative regulatory subunit of protein phosphatase 1 Ppz1p (Ruiz et al., 2004). Hsp90p has two isoforms which are encoded by *HSP82* and *HSC82*. Hsp90p is located in the nucleus in response to environmental stress (Morano et al., 2012). The silent mutation in the

HSP82 gene of H7 was found in the SSF54211 domain (ribosomal protein S5 domain 2-type fold). The silent mutation might not affect the protein structure.

Table 3.17 : Silent mutations found in H7. Chromosome locations, gene (with the systematic name) and changed nucleotide about mutated gene of H7 are listed.

Chromosome	Gene name, nucleotide and amino acid location
V:389882	*BOI2 / YER114C* c.1572G>A, p.P524=
II:257438	*IPP1 / YBR011C* c.225C>T, p.K75=
II:330243	*REB1 / YBR049C* c.336C>T, p.A12=
XIV:368268	*FYV6 / YNL133C* c.276C>T, p.K92=
XIII:787413	*TPS1 / YBR126C* c.366G>A, p.N122=
XV:428900	*VHS3 / YOR054C* c.954G>A, p.Y318=
V:557833	*PUG1 / YER185W* c.618C>T, p.E206=
XII:740002	*CDC25 / YLR310C* c.1605A>G, p.S535=
XIII:323503	*FAR8 / YMR029C* c.4158G>A, p.F486=
X:284453	*SMC3 / YJL074C* c.867C>T, p.K89=
XVI:97634	*HSP82 / YPL240C* c.927G>A, p.P309=
XIII:263870	*CDC5 / YMR001C* c.1998G>A, p.P666=

A nonsense mutation was detected in the *NRG1* gene of H7 (Table 3.14). Nrg1p is composed of 231 amino acids. There was a stop codon at the seventieth amino acid in the *NRG1* gene in H7 genome. Thus, the Nrg1 protein is produced as a truncated protein in H7. *NRG1* gene encodes a transcriptional repressor protein, and *NRG1* did not have more than 2-fold expression level change in H7. Ninety-four genes are the targets of the *NRG1* gene. Four of the target genes (*AMN1, FAF1, KTI12,* and *YBL029W*) have been down-regulated by more than 2-fold in H7. 23 genes (*BOP2, CCP1, CWP1, GAL7, GAT4, GSY1, HOR7, HSP30, HXT2, JID1, NCE103, NRG2, PPM1, RCN2, SED1, USV1, YBL029C-A, YIR014W, YJL107C, YLR012C, YMR084W, YMR085W, YOL014W*) have been up-regulated by more than 2-fold in H7. GO analysis was performed for both down-regulated and up-regulated genes (Tables 3.18 and 3.19). According to the deletion studies it was observed that nrg1Δ mutant strains could utilize different carbon sources. In addition, it was also shown that *NRG1* gene was not an essential gene for yeast growth (Zhou & Winston, 2001).

Table 3.18 : GO-slim process analysis results of the down-regulated (more than 2-fold) genes of H7 that are regulated by *NRG1*.

GO-Slim process name	Gene Name
biological process unknown	*YBL029W*
rRNA processing	*FAF1*
RNA modification	*KTI12*
regulation of cell cycle	*AMN1*
regulation of organelle organization	*AMN1*
organelle fission	*AMN1*
ribosomal small subunit biogenesis	*FAF1*
transcription from RNA polymerase II promoter	*KTI12*
mitotic cell cycle	*AMN1*
tRNA processing	*KTI12*

Table 3.19 : GO-slim process analysis results of the up-regulated (more than 2-fold) genes of H7 that are regulated by *NRG1*.

GO-Slim process name	Gene Name
biological process unknown	*BOP2, JID1, RCN2, YBL029C-A, YIR014W, YJL107C, YLR012C, YMR084W, YMR085W, YOL014W*
response to chemical	*CCP1, HSP30, NCE103, NRG2, USV1*
response to oxidative stress	*CCP1, HSP30, NCE103*
response to osmotic stress	*HSP30, NRG2, USV1*
transcription from RNA polymerase II promoter	*NRG2, USV1*
cell wall organization or biogenesis	*CWP1, SED1*
carbohydrate metabolic process	*GAL7, GSY1*
generation of precursor metabolites and energy	*GSY1*
carbohydrate transport	*HXT2*
pseudohyphal growth	*NRG2*
protein alkylation	*PPM1*
cellular response to DNA damage stimulus	*HSP30*
protein complex biogenesis	*PPM1*
invasive growth in response to glucose limitation	*NRG2*
sporulation	*CWP1*
mitochondrion organization	*SED1*
response to heat	*HSP30*
meiotic cell cycle	*CWP1*
cannot be mapped to a GO slim term	*GAT4, HOR7*

In H7 genome, another nonsense mutation occurred in *DUF1* (Table 3.14). Duf1p (DUB-associated Factor 1) is a ubiquitin-binding protein of unknown function. Many DUBs bind ubiquitin with a reasonable affinity, but others have little affinity for ubiquitin. WD40 domain of Duf1p interacts with ubiquitin (Kanga et al., 2012). Various databases indicated that the WD40 domain was involved with the first 417 amino acids of Duf1p (Table 3.20). The stop codon was found at the 722. codon of *DUF1* in the H7 genome. Thus, ubiquitinylation may not be affected by this mutation.

Table 3.20 : *DUF1* gene domains and classification.

Protein Coordinates	Accession ID of domain	Domain Description	Database source
8-312	G3DSA:2.130.10.10	WD40/YVTN repeat-like-containing domain	Gene3D
12-53	SM00320	WD40; WD40 repeat	SMART
15-125	SSF50978	WD40-repeat-containing domain	SUPERFAMILY
120-191	SM00320	WD40; WD40 repeat	SMART
160-204	SSF50978	WD40-repeat-containing domain	SUPERFAMILY
164-476	SSF50978	WD40-repeat-containing domain	SUPERFAMILY
257-296	SM00320	WD40; WD40 repeat	SMART
264-298	PS50082	WD_REPEATS_2; WD40 repeat	PROSITE
264-305	PS50294	WD_REPEATS_REGION; WD40-repeat-containing domain	PROSITE
283-297	PS00678	WD_REPEATS_1; WD40 repeat, conserved site	PROSITE
313-486	G3DSA:2.130.10.10	WD40/YVTN repeat-like-containing domain	Gene3D
382-417	SM00320	WD40; WD40 repeat	SMART
412-1110	PTHR19862		PANTHER
412-1110	PTHR19862:SF15		PANTHER
895-1099	PF11816	DUF3337; Protein of unknown function DUF3337	Pfam
995-1100	G3DSA:3.10.20.90		Gene3D

The genes with the missense mutations in H7 were also investigated, based on their up- and down-regulation levels and their biological roles. Roles of the down-regulated genes that have missense mutations in H7 were found as rRNA processing, cellular amino acid metabolic process, endosomal transport, protein acetylation, RNA catabolic process, carbohydrate metabolic process, nucleobase-containing small molecule metabolic process, and chromatin organization. Also, these gene products are located in the cytoplasm, nucleus, nucleolus, endomembrane system, cytoplasmic vesicles, and chromosome.

Up-regulated genes that have missense mutations in H7 were found to have a role in organelle fission, peroxisome, mitochondria cytoskeleton organization, protein phosphorylation, meiotic and mitotic cell cycle, and cell cycle regulation. Locations of these gene products are cytoplasm, mitochondrion, and mitochondrial envelope, cytoskeleton, peroxisome and membrane.

3.3 Lyticase Sensitivity Assay Results

By this assay, cell wall integrity of both strains in the absence and presence of the oxidative stress condition was evaluated. As a result, it was observed that the lyticase resistance of H7 was four-fold of the reference strain, in the absence of oxidative stress,

at the end of three hours. Additionally, oxidative stress treatment doubled the lyticase resistance of the reference strain. However, the stress treatment did not seem to affect the cell wall integrity of H7, unlike the reference strain (Table 3.21 and Figure 3.19).

Table 3.21 : Lyticase resistance values (%) of the reference and the evolved strain H7 in the absence and presence of oxidative stress, applied as 0.5 mM hydrogen peroxide.

Time (min)	Reference Strain	Reference Strain (H_2O_2)	H7	H7 (H_2O_2)
0	100±0	100±0	100±0	100±0
20	84.29±4.49	79.60±7.90	91.96±3.72	87.77±4.33
40	66.18±3.95	64.34±10.96	81.97±3.55	76.27±2.52
60	45.23±4.50	52.18±9.31	69.68±3.66	69.66±3.12
80	36.23±5.97	45.21±7.38	66.67±3.64	67.00±2.39
100	25.10±4.31	37.95±8.65	56.34±3.94	58.56±3.26
120	19.53±3.67	34.06±8.81	53.94±3.57	55.84±2.57
150	13.80±2.65	29.09±9.37	48.06±3.68	51.89±2.67
180	11.31±1.88	25.18±9.15	44.95±2.89	48.84±2.75

The lyticase sensitivity assay results showed that the evolved strain H7 showed significantly higher lyticase resistance than the reference strain, both in the absence and presence of oxidative stress condition. This result implies a significantly higher cell wall integrity or robustness of the evolved strain H7. It could be interpreted that the high cell wall integrity of H7 may contribute to its high resistance against oxidative stress. In addition, the other physiological data of H7 such as trehalose/glycogen amounts and other metabolic data suggest that H7 seems to behave as if it is always under stress conditions, and may have a more resistant cell wall than the reference strain (Kocaefe-Özşen et al., 2022).

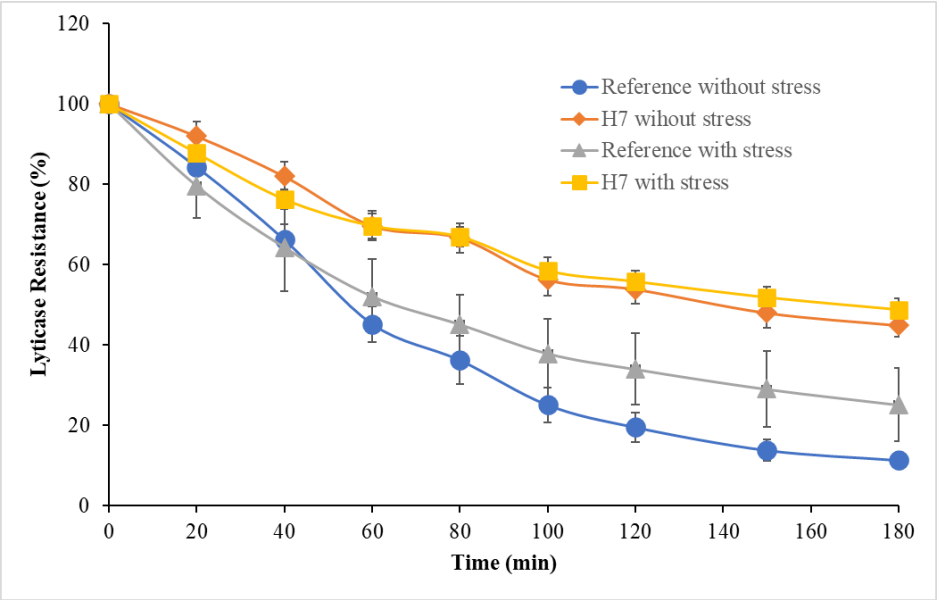

Figure 3.19 : Lyticase resistance of the reference and the evolved strain (H7) in the absence and presence of oxidative stress (0.5 mM H_2O_2). Lyticase sensitivity was assessed as the percent decrease in lyticase resistance. Initial resistance value was accepted as 100%.

4. CONCLUSIONS

In this thesis study, the genetic and complex molecular mechanisms of oxidative stress resistance in yeast were investigated by comparing an oxidative stress-resistant, evolved strain and the reference strain at genomic and transcriptomic level.

Lyticase sensitivity assay was carried out to determine cell wall integrity changes of the evolved strain, as part of the physiological analyses. Microarray experiments were performed for comprehensive transcriptomic analysis. Transcriptomic analysis was done by comparing the reference strain and the oxidative stress resistant evolved strain. GO analysis and metabolic pathway analysis were carried out, based on the identified transcriptomic differences. By this way, the effect of oxidative stress on *S. cerevisiae* and its response were identified. In addition, genomic analysis was carried out by next generation sequencing to find the mutations that occurred in the evolved strain H7 during evolutionary engineering selection under oxidative stress condition. The genomic and transcriptomic analysis results were then combined, and transcriptomic levels and the regulatory effects related to the mutated genes (if the gene is a transcription factor) were investigated.

The results of this study revealed that the oxidative stress-resistant strain had significant changes in its metabolic processes, especially in its oxidative stress response. The underlying changes providing this adaptive resistance were elucidated, using lyticase sensitivity assay, comparative transcriptomic analysis and comparative genomic analysis of the evolved strain.

Lyticase sensitivity assay results indicated the important role of the cell wall integrity in oxidative stress resistance of the evolved strain. It also emphasized the general importance of the cell wall integrity against environmental or physiological stress conditions.

Transcriptomic analysis of the evolved strain showed changes in expression profiles of genes associated with key cellular processes, including a wide variety of metabolic processes, autophagy, carbon metabolism, peroxisome and cell wall organization or biogenesis.

Many genes related with metabolite production and modification process were up-regulated in the oxidative stress-resistant, evolved strain. These outstanding processes are carbohydrate and oligosaccharide metabolic process, biosynthesis of precursor metabolites and processes for energy production, metabolic process of monocarboxylic acid and cofactor, the processes related with lipid metabolism, protein phosphorylation and biogenesis of protein complex, cell wall organization or biogenesis, protein modification by small protein conjugation or removal and protein folding. As expected, mitochondrion and peroxisome organization-related genes were also up-regulated in H7 to survive oxidative stress. In addition, the genes related with transportation mechanisms, except for nuclear transportation, were also up-regulated. The transport mechanisms mentioned are ion transport, transmembrane transport, protein targeting, carbohydrate transport, Golgi vesicle transport, membrane invagination, membrane fusion, lipid transport, amino acid transport and organelle fusion.

Genes of the evolved strain which are related with nuclear and nucleobase containing metabolite transportation were obviously down-regulated. In addition, genes associated with organelle and ribosome assembling process were down-regulated. The expression of the genes associated with mitosis and cell cycle was also at a low level. As expected, sporulation and stationary-phase genes were highly up-regulated.

ESR gene analysis revealed that the ESR-repressed genes and the genes that showed low levels of expression in the oxidative stress-resistant evolved strain share the same profile. Additionally, the up-regulated genes in the evolved strain had a similar profile to the ESR-induced genes. The ESR is identified in response to a wide variety of factors that cause stress in yeast, as indicated by the stereotyped alterations in the expression of the genes in this response.

Comparative genomic analysis of H7 showed mutations in diverse genes which are under the control of critical transcription factors. Down-regulated genes that have missense mutations in H7 have roles in rRNA processing, cellular amino acid metabolic process, endosomal transport, protein acetylation, RNA catabolic process, carbohydrate metabolic process, nucleobase-containing small molecule metabolic process, and chromatin organization. Besides, up-regulated genes that have missense mutations in H7 have roles in organelle fission, peroxisome, mitochondria cytoskeleton organization, protein phosphorylation, meiotic and mitotic cell cycle, and cell cycle regulation. These gene products are located in the cytoplasm, mitochondrion,

and mitochondrial envelope, cytoskeleton, peroxisome and membrane. *NRG1* gene, a transcriptional repressor protein, had a nonsense mutation in H7, which leads to the production of a truncated Nrg1p. The expression of many genes, which are regulated by *NRG1* gene product, was up- or down-regulated in the evolved strain. As *NRG1* encodes a transcriptional regulator, the reason for the expression level changes in many genes related with different processes could be the truncated *NRG1* product.

The evolved strain H7 had been studied previously at the physiological level (Kocaefe-Özşen et al., 2022; Kocaefe, 2012). The knowledge about the particular genes with mutations, the physiological and transcriptomic analysis results and the known phenotypic observations of this evolved strain are consistent. Especially, the observation of an increase in the production of the disaccharide trehalose which is known as a stress protectant in yeast, could be explained with the up-regulation of trehalose-associated genes, including *TPS1*, *TPS2* and *TSL1*. Besides, the decreased levels of glycerol and acetate were observed at late phases of growth in H7 cultures. It showed that H7 utilizes the previously produced non-fermentative carbon source. This can be explained as the evolved strain could adapt itself to grow by consuming the non-fermentative carbon source easier than the reference strain. A significant increase in the expression of the genes *HXK1*, *GLK1* and *MPC3* in H7, which are known to be expressed during growth on non-fermentable carbon sources, supports this situation. In addition, high levels of maltose production in H7, upon breakdown of glycogen residues to maltose disaccharide, also indicates a stress protection mechanism of the evolved strain. Hydrolysis of glycogen residues may also be related with the up-regulation of *SGA1* gene in H7, which has a role in degradation of glycogen. A previous study on the CLS of H7 showed that the evolved strain H7 was a long-lived strain (Arslan et al., 2018). In recent years, there is more evidence about the link between longevity, aging and the activation of the autophagy. The up-regulation of 30 of autophagy-related genes (within this group all *ATG* genes) support this longevity and the activation of the autophagy link. The results at physiological, genomic and transcriptomic level are in line with each other, as well as the literature (Kocaefe-Özşen et al., 2022; François and Parrou, 2001; Rodriguez et al., 2001; Cherry et al., 2012; Pugh et al., 1989; Arslan et al., 2018; Nakamura and Yoshimori, 2018).

To conclude, this study revealed important genomic and transcriptomic changes that may have an important role in oxidative stress resistance in yeast. To better understand the complex molecular mechanisms of oxidative stress resistance in *S. cerevisiae*, the

specific genomic changes of the evolved strain should be investigated further in more detail. For this purpose, the individual mutations observed in H7 and their combinations should be transferred to the reference strain by genome editing and reverse engineering strategies, and the resulting phenotypes should be analyzed. CRISPR-Cas9 genome editing strategy can be used as a powerful technique in reverse engineering, for the investigation of the effects of the identified mutations on desired phenotypes.

REFERENCES

Ames, B. N., Shigenaga, M. K., Hagen, T. M. (1993). Oxidants, antioxidants, and the degenerative diseases of aging. *Proceedings of the National Academy of Sciences*, *90*(17), 7915 LP – 7922. https://doi.org/10.1073/pnas.90.17.7915

Arslan, M., Turanli-Yildiz, B., Yilmaz, B., Kocaefe, N., & Cakar, Z. P. (2018). An improved semi-quantitative spot assay to analyse chronological lifespan in yeast. *Romanian Biotechnol Lett*, 23(3), 13551-13560.

Bailey, J. E. (1991). Toward a science of metabolic engineering. *Science*, *252*(5013), 1668–1675.

Bailey, J. E., Sburlati, A., Hatzimanikatis, V., Lee, K., Renner, W. A., & Tsai, P. S. (1996). Inverse metabolic engineering: a strategy for directed genetic engineering of useful phenotypes. *Biotechnology and Bioengineering*, *52*(1), 109–121.

Ballester-Tomás, L., Randez-Gil, F., Pérez-Torrado, R., & Prieto, J. A. (2015). Redox engineering by ectopic expression of glutamate dehydrogenase genes links NADPH availability and NADH oxidation with cold growth in *Saccharomyces cerevisiae*. *Microbial Cell Factories*, 14(1), 100. https://doi.org/10.1186/s12934-015-0289-2

Berterame, N. M., Martani, F., Porro, D., & Branduardi, P. (2018). Copper homeostasis as a target to improve *Saccharomyces* cerevisiae tolerance to oxidative stress. Metabolic Engineering. *Metabolic engineering*, 46, 43-50. https://doi.org/10.1016/j.ymben.2018.02.010

Bhatia-Kiššová, I., & Camougrand, N. (2010). Mitophagy in yeast: actors and physiological roles. *FEMS Yeast Research*, *10*(8), 1023–1034.

Bilsland, E., Molin, C., Swaminathan, S., Ramne, A., & Sunnerhagen, P. (2004). Rck1 and Rck2 MAPKAP kinases and the HOG pathway are required for oxidative stress resistance. *Molecular Microbiology*, *53*(6), 1743–1756.

Bisschops, M. M., Vos, T., Martínez-Moreno, R., Cortés, P. T., Pronk, J. T., & Daran-Lapujade, P. (2015). Oxygen availability strongly affects chronological lifespan and thermotolerance in batch cultures of *Saccharomyces cerevisiae*. *Microbial Cell*, *2*(11), 429.

Botstein, D., & Fink, G. R. (2011). Yeast: an experimental organism for 21st Century biology. *Genetics*, *189*(3), 695–704.

Brauer, M. J., Huttenhower, C., Airoldi, E. M., Rosenstein, R., Matese, J. C., Gresham, D., Boer, V. M., Troyanskaya, O. G., & Botstein, D. (2008). Coordination of growth rate, cell cycle, stress response, and metabolic activity in yeast. *Molecular Biology of the Cell*, *19*(1), 352–367.

B**ricker, D. K., Taylor, E. B., Schell, J. C., Orsak, T., Boutron, A., Chen, Y.-C., Cox, J. E., Cardon, C. M., Van Vranken, J. G., & Dephoure, N.** (2012). A mitochondrial pyruvate carrier required for pyruvate uptake in yeast, Drosophila, and humans. *Science*, *337*(6090), 96–100.

Briggs, M. W., Burkard, K. T. D., & Butler, J. S. (1998). Rrp6p, the Yeast Homologue of the Human PM-Scl 100-kDa Autoantigen, Is Essential for Efficient 5.8 S rRNA 3′ End Formation. *Journal of Biological Chemistry*, 273(21), 13255–13263. https://doi.org/10.1074/jbc.273.21.13255.

Briza, P., Bogengruber, E., Thür, A., Rützler, M., Münsterkötter, M., Dawes, I. W., & Breitenbach, M. (2002). Systematic analysis of sporulation phenotypes in 624 non-lethal homozygous deletion strains of *Saccharomyces cerevisiae*. *Yeast*, 19(5), 403-422.

Brown, J. A., Sherlock, G., Myers, C. L., Burrows, N. M., Deng, C., Wu, H. I., Brown, J. M. (2006). Global analysis of gene function in yeast by quantitative phenotypic profiling. *Molecular Systems Biology*, 2(1). https://doi.org/10.1038/msb4100043.

Brunelli, L., Yermilov, V., & Beckman, J. S. (2001). Modulation of catalase peroxidatic and catalatic activity by nitric oxide. *Free Radical Biology and Medicine*, *30*(7), 709–714.

Brunelli, P. V, Raitt, D. C., Allen, L. A., Kellogg, E. A., & Poyton, R. O. (1997). Effects of oxygen concentration on the expression of cytochrome c and cytochrome c oxidase genes in yeast. *Journal of Biological Chemistry*, *272*(23), 14705–14712.

B**yrne, K. P., & Wolfe, K. H.** (2005). The Yeast Gene Order Browser: combining curated homology and syntenic context reveals gene fate in polyploid species. *Genome Research*, *15*(10), 1456–1461. https://doi.org/10.1101/gr.3672305

Çakar, Z. P., Turanlı-Yıldız, B., Alkım, C., & Yılmaz, Ü. (2012). Evolutionary engineering of *Saccharomyces cerevisiae* for improved industrially important properties. *FEMS Yeast Research*, *12*(2), 171–182. https://doi.org/10.1111/j.1567-1364.2011.00775.x

Cheng, C., Huang, D., & Roach, P. J. (1997). Yeast PIG genes: *PIG1* encodes a putative type 1 phosphatase subunit that interacts with the yeast glycogen synthase Gsy2p. *Yeast (Chichester, England)*, 13(1), 1–8. https://doi.org/10.1002/(SICI)1097-0061(199701)13:1<1::AID-YEA49>3.0.CO;2-F

Chang, N., Yao, S., Chen, D., Zhang, L., Huang, J., & Zhang, L. (2018). The Hog1 positive regulated YCT1 gene expression under cadmium tolerance of budding yeast. *FEMS Microbiology Letters*, *365*(17), fny170.

Costa, V., & Moradas-Ferreira, P. (2001). Oxidative stress and signal transduction in *Saccharomyces cerevisiae*: insights into ageing, apoptosis and diseases. *Molecular Aspects of Medicine*, *22*(4–5), 217–246. https://doi.org/10.1016/S0098-2997(01)00012-7

Costa, V. M. V, Amorim, M. A., Quintanilha, A., & Moradas-Ferreira, P. (2002). Hydrogen peroxide-induced carbonylation of key metabolic enzymes in *Saccharomyces cerevisiae*: the involvement of the oxidative stress response regulators Yap1 and Skn7. *Free Radical Biology and Medicine*, *33*(11), 1507–1515.

Crawford, D. R. (2002). Regulation of mammalian gene expression by reactive oxygen species. In Reactive oxygen species in biological systems. *Springer*, (pp. 155–171), https://doi.org/10.1007/0-306-46806-9_6.

Dastidar, R., Hooda, J., Shah, A., Cao, T. M., Henke, R., & Zhang, L. (2012). The nuclear localization of SWI/SNF proteins is subjected to oxygen regulation. *Cell & Bioscience*, 2(1), 30. https://doi.org/10.1186/2045-3701-2-30.

Davies, K. J. (2000).Oxidative Stress, Antioxidant Defenses, and Damage Removal, Repair, and Replacement Systems, *UBMB life*, 50(4-5), 279-289.

de Nobel, H., Lawrie, L., Brul, S., Klis, F., Davis, M., Alloush, H., & Coote, P. (2001). Parallel and comparative analysis of the proteome and transcriptome of sorbic acid-stressed *Saccharomyces cerevisiae*. *Yeast*, *18*(15), 1413–1428.

DeMaster, E. G., Redfern, B., & Nagasawa, H. T. (1998). Mechanisms of inhibition of aldehyde dehydrogenase by nitroxyl, the active metabolite of the alcohol deterrent agent cyanamide. *Biochemical Pharmacology*, *55*(12), 2007–2015.

Doğan, A., Demirci, S., Aytekin, A. Ö., & Şahin, F. (2014). Improvements of tolerance to stress conditions by genetic engineering in *Saccharomyces cerevisiae* during ethanol production. *Applied Biochemistry and Biotechnology*, *174*(1), 28–42.

Downie, J. A., Stewart, J. W., Brockman, N., Schweingruber, A. M., & Sherman, F. (1977). Structural gene for yeast iso-2-cytochrome c. *Journal of Molecular Biology*, *113*(2), 369–384. https://doi.org/10.1016/0022-2836(77)90147-4

Erasmus, D. J., van der Merwe, G. K., & van Vuuren, H. J. J. (2003). Genome-wide expression analyses: metabolic adaptation of *Saccharomyces cerevisiae* to high sugar stress. *FEMS Yeast Research*, *3*(4), 375–399.

Finkel, T., & Holbrook, N. J. (2000). Oxidants, oxidative stress and the biology of ageing. *Nature*, *408*, 239.

François, J., & Parrou, J. L. (2001). Reserve carbohydrates metabolism in the yeast *Saccharomyces cerevisiae*. *FEMS Microbiology Reviews*, 25(1), 125–145. https://doi.org/10.1111/j.1574-6976.2001.tb00574.x

Fujimura, T., & Wickner, R. B. (1987). L-A double-stranded RNA viruslike particle replication cycle in *Saccharomyces cerevisiae*: Particle maturation in vitro and effects of mak10 and pet18 mutations. *Molecular and Cellular Biology*, 7(1), 420–426. https://doi.org/10.1128/MCB.7.1.420

Gandhi, S., & Abramov, A. Y. (2012). Mechanism of oxidative stress in neurodegeneration. *Oxidative Medicine and Cellular Longevity*, *2012*. https://doi.org/10.1155/2012/428010

Gasch, A. P. (2003). The environmental stress response: a common yeast response to diverse environmental stresses. In Yeast stress responses. *Springer*, (pp. 11–70).

Gershon, H., & Gershon, D. (2000). The budding yeast, *Saccharomyces cerevisiae*, as a model for aging research: a critical review. *Mechanisms of Ageing and Development*, *120*(1–3), 1–22.

Glover, J. R., & Lindquist, S. (1998). Hsp104, Hsp70, and Hsp40: a novel chaperone system that rescues previously aggregated proteins. *Cell*, *94*(1), 73–82.

Goffeau, A., Barrell, B. G., Bussey, H., Davis, R. W., Dujon, B., Feldmann, H., Galibert, F., Hoheisel, J. D., Jacq, C., & Johnston, M. (1996). Life with 6000 genes. *Science*, *274*(5287), 546–567.

Halliwell, B., & Gutteridge, J. M. C. (2007). *Free radicals in biology and medicine*. Oxford university press, USA.

Halliwell, B., & Whiteman, M. (2004). Measuring reactive species and oxidative damage in vivo and in cell culture: how should you do it and what do the results mean? *British Journal of Pharmacology*, *142*(2), 231–255. https://doi.org/10.1038/sj.bjp.0705776

Hasan, R., Leroy, C., Isnard, A., Labarre, J., Boy-Marcotte, E., & Toledano, M. B. (2002). The control of the yeast H_2O_2 response by the Msn2/4 transcription factors. *Molecular Microbiology*, *45*(1), 233–241.

Hess, D. C., Myers, C. L., Huttenhower, C., Hibbs, M. A., Hayes, A. P., Paw, J., Caudy, A. A. (2009). Computationally Driven, Quantitative Experiments Discover Genes Required for Mitochondrial Biogenesis. *PLoS Genetics*, 5(3), e1000407. https://doi.org/10.1371/journal.pgen.1000407

Hieronymus, H. (2004). Genome-wide mRNA surveillance is coupled to mRNA export. *Genes & Development*, 18(21), 2652–2662. https://doi.org/10.1101/gad.1241204

Hoffmann, M. E., & Meneghini, R. (1979). Action of hydrogen peroxide on human fibroblast in culture. *Photochemistry and Photobiology*, 30(1), 151-155.

Hohmann, S., & Mager, W. H. (2003). *Yeast stress responses* (Vol. 1). Springer Science & Business Media.

Hon, T., Dodd, A., Dirmeier, R., Gorman, N., Sinclair, P. R., Zhang, L., & Poyton, R. O. (2003). A mechanism of oxygen sensing in yeast: multiple oxygen-responsive steps in the heme biosynthetic pathway affect Hap1 activity. *Journal of Biological Chemistry*, *278*(50), 50771–50780.

Hong, S.-Y., Roze, L. V, & Linz, J. E. (2013a). Oxidative stress-related transcription factors in the regulation of secondary metabolism. *Toxins*, *5*(4), 683–702.

Hong, S., Roze, L. V, Wee, J., & Linz, J. E. (2013b). Evidence that a transcription factor regulatory network coordinates oxidative stress response and secondary metabolism in aspergilli. *MicrobiologyOpen*, *2*(1), 144–160.

Huang, D. W., Sherman, B. T., & Lempicki, R. A. (2008). Bioinformatics enrichment tools: paths toward the comprehensive functional analysis of large gene lists. *Nucleic Acids Research*, *37*(1), 1–13. https://doi.org/10.1093/nar/gkn923

Huang, D. W., Sherman, B. T., & Lempicki, R. A. (2009a). Bioinformatics enrichment tools: paths toward the comprehensive functional analysis of large gene lists. *Nucleic Acids Research*, *37*(1), 1–13.

Huang, D. W., Sherman, B. T., & Lempicki, R. A. (2009b). Systematic and integrative analysis of large gene lists using DAVID bioinformatics resources. *Nature Protocols*, *4*(1), 44–57. https://doi.org/10.1038/nprot.2008.211

Hwang, P. K., Tugendreich, S., & Fletterick, R. J. (1989). Molecular analysis of GPH1, the gene encoding glycogen phosphorylase in *Saccharomyces cerevisiae*. *Molecular and Cellular Biology*, *9*(4), 1659–1666.

Jamieson, D. J. (1998). Oxidative stress responses of the yeast *Saccharomyces cerevisiae*. *Yeast*, *14*(16), 1511–1527. https://doi.org/10.1002/(SICI)1097-0061(199812)14:16<1511::AID-YEA356>3.0.CO;2-S

Jordan, P. W., Klein, F., & Leach, D. R. F. (2007). Novel Roles for Selected Genes in Meiotic DNA Processing. *PLoS Genetics*, 3(12), e222. https://doi.org/10.1371/journal.pgen.0030222

Kanga, S., Bernard, D., Mager-Heckel, A.-M., Erpapazoglou, Z., Mattiroli, F., Sixma, T. K., Leon, S., Urban-Grimal, D., Tarassov, I., & Haguenauer-Tsapis, R. (2012). A deubiquitylating complex required for neosynthesis of a yeast mitochondrial ATP synthase subunit. *PLoS One*, *7*(6), e38071.

Kavšček, M., Stražar, M., Curk, T., Natter, K., & Petrovič, U. (2015). Yeast as a cell factory: current state and perspectives. *Microbial Cell Factories*, *14*(1), 1–10.

Keyes, B. E., & Burke, D. J. (2009). Irc15 Is a Microtubule-Associated Protein that Regulates Microtubule Dynamics in *Saccharomyces cerevisiae*. *Current Biology*, 19(6), 472–478. https://doi.org/10.1016/j.cub.2009.01.068.

Kitagaki, H., Araki, Y., Funato, K., & Shimoi, H. (2007). Ethanol-induced death in yeast exhibits features of apoptosis mediated by mitochondrial fission pathway. *FEBS Letters*, *581*(16), 2935–2942. https://doi.org/10.1016/j.febslet.2007.05.048

Kobayashi, N., & McEntee, K. (1990). Evidence for a heat shock transcription factor-independent mechanism for heat shock induction of transcription in *Saccharomyces cerevisiae*. Proceedings of the National Academy of Sciences, 87(17), 6550-6554.

Kocaefe, N. (2012). *Molecular Characterization of Oxidatıve Stress Resistant Yeast* (M.Sc. Thesis). Istanbul Technical University, Graduate School of Science Engineerıng and Technology.

Kocaefe-Özşen, N., Yilmaz, B., Alkım, C., Arslan, M., Topaloğlu, A., İbrahim Kısakesen, H., Gülsev, E., & Çakar, Z. P. (2022). Physiological and Molecular Characterization of an Oxidative Stress-Resistant *Saccharomyces cerevisiae* Strain Obtained by Evolutionary Engineering. *Frontiers in Microbiology*, *13*, 822864.

Koch, K., Strandback, E., Jha, S., Richter, G., Bourgeois, B., Madl, T., & Macheroux, P. (2018). Oxidative stress induced structural changes in the microtubule-associated flavoenzyme Irc15p from *Saccharomyces cerevisiae*. *Protein Science*, pro.3517. https://doi.org/10.1002/pro.3517.

Kuranda K, Leberre V, Sokol S. (2006). Investigating the caffeine effects in the yeast Saccharomyces cerevisiae brings new insights into the connection between TOR, PKC and Ras/cAMP signalling pathways. *Mol Microbiol* 2006;61:1147-66.

Lee, J., Godon, C., Lagniel, G., Spector, D., Garin, J., Labarre, J., & Toledano, M. B. (1999). Yap1 and Skn7 control two specialized oxidative stress response regulons in yeast. *Journal of Biological Chemistry*, *274*(23), 16040–16046.

Lee, M.-W., Kim, B.-J., Choi, H.-K., Ryu, M.-J., Kim, S.-B., Kang, K.-M., Kim, S.-T. (2007). Global protein expression profiling of budding yeast in response to DNA damage. *Yeast*, *24*(3), 145–154. https://doi.org/10.1002/yea.1446

Ma, C., Wei, X., Sun, C., Zhang, F., Xu, J., Zhao, X., & Bai, F. (2015). Improvement of acetic acid tolerance of *Saccharomyces cerevisiae* using a zinc-finger-based artificial transcription factor and identification of novel genes involved in acetic acid tolerance. *Applied Microbiology and Biotechnology*, 99(5), 2441–2449. https://doi.org/10.1007/s00253-014-6343-x.

Mariani, E., Polidori, M. C., Cherubini, A., & Mecocci, P. (2005). Oxidative stress in brain aging, neurodegenerative and vascular diseases: an overview. *Journal of Chromatography B*, *827*(1), 65–75.

Martinez-Pastor, M. T., Marchler, G., Schüller, C., Marchler-Bauer, A., Ruis, H., & Estruch, F. (1996). The *Saccharomyces cerevisiae* zinc finger proteins Msn2p and Msn4p are required for transcriptional induction through the stress response element (STRE). *The EMBO Journal*, *15*(9), 2227–2235.

Martinez, M. J., Roy, S., Archuletta, A. B., Wentzell, P. D., Anna-Arriola, S. S., Rodriguez, A. L., Aragon, A. D., Quiñones, G. A., Allen, C., & Werner-Washburne, M. (2004). Genomic analysis of stationary-phase and exit in *Saccharomyces cerevisiae*: gene expression and identification of novel essential genes. *Molecular Biology of the Cell*, *15*(12), 5295–5305. https://doi.org/10.1091/mbc.e03-11-0856

Matsuura, K., & Takagi, H. (2005). Vacuolar functions are involved in stress-protective effect of intracellular proline in *Saccharomyces cerevisiae*. *Journal of Bioscience and Bioengineering*, 100(5), 538–544. https://doi.org/10.1263/jbb.100.538

Mello Filho, A. C., Hoffmann, M. E., & Meneghini, R. (1984). Cell killing and DNA damage by hydrogen peroxide are mediated by intracellular iron. *Biochemical Journal*, *218*(1), 273.

Mendes, V., Vilaça, R., de Freitas, V., Ferreira, P. M., Mateus, N., & Costa, V. (2015). Effect of myricetin, pyrogallol, and phloroglucinol on yeast resistance to oxidative stress. *Oxidative Medicine and Cellular Longevity*, *2015*.

Miller, S. M., & Magasanik, B. (1990). Role of NAD-linked glutamate dehydrogenase in nitrogen metabolism in *Saccharomyces cerevisiae*. *Journal of Bacteriology*, 172(9), 4927–4935. https://doi.org/10.1128/jb.172.9.4927-4935.1990

Mochida, K., Oikawa, Y., Kimura, Y., Kirisako, H., Hirano, H., Ohsumi, Y., & Nakatogawa, H. (2015). Receptor-mediated selective autophagy degrades the endoplasmic reticulum and the nucleus. *Nature*, *522*(7556), 359–362. https://doi.org/10.1038/nature14506

Moradas-Ferreira, P., & Costa, V. (2000). Adaptive response of the yeast *Saccharomyces cerevisiae* to reactive oxygen species: Defences, damage and death. *Redox Report*, *5*(5), 277–285. https://doi.org/10.1179/135100000101535816

Morano, K. A., Grant, C. M., & Moye-Rowley, W. S. (2012). The Response to Heat Shock and Oxidative Stress in *Saccharomyces cerevisiae*. *Genetics*, 190(4), 1157–1195. https://doi.org/10.1534/genetics.111.128033

Morita, D., Miyoshi, K., Matsui, Y., Toh-e, A., Shinkawa, H., Miyakawa, T., & Mizuta, K. (2002). Rpf2p, an Evolutionarily Conserved Protein, Interacts with Ribosomal Protein L11 and Is Essential for the Processing of 27 SB Pre-rRNA to 25 S rRNA and the 60 S Ribosomal Subunit Assembly in *Saccharomyces cerevisiae. Journal of Biological Chemistry*, 277(32), 28780–28786. https://doi.org/10.1074/jbc.M203399200

Moye-Rowley, W. S., Harshman, K. D., & Parker, C. S. (1989). Yeast *YAP1* encodes a novel form of the jun family of transcriptional activator proteins. *Genes & Development*, *3*(3), 283–292.

Mozdy, A. D., McCaffery, J. M., & Shaw, J. M. (2000). Dnm1p GTPase-mediated mitochondrial fission is a multi-step process requiring the novel integral membrane component Fis1p. *The Journal of Cell Biology*, 151(2), 367–380. https://doi.org/10.1083/jcb.151.2.367

Murphy, J. P., Stepanova, E., Everley, R. A., Paulo, J. A., & Gygi, S. P. (2015). Comprehensive temporal protein dynamics during the diauxic shift in *Saccharomyces cerevisiae*. *Molecular & Cellular Proteomics*, *14*(9), 2454–2465.

Nakamura S, Yoshimori T. (2018). Autophagy and Longevity. *Mol Cells.* 2018 Jan 31;41(1):65-72. doi: 10.14348/molcells.2018.2333. Epub 2018 Jan 23. PMID: 29370695; PMCID: PMC5792715.

Nordberg, G. F., Sandstrom, B., Becking, G., & Goyer, R. A. (2002). Essentiality and toxicity of metals. *Heavy Metals in the Environment*.

Okada, N., Ogawa, J., & Shima, J. (2014). Comprehensive analysis of genes involved in the oxidative stress tolerance using yeast heterozygous deletion collection. *FEMS Yeast Research*, *14*(3), 425–434. https://doi.org/10.1111/1567-1364.12136

Okazaki, S., Tachibana, T., Naganuma, A., Mano, N., & Kuge, S. (2007). Multistep disulfide bond formation in Yap1 is required for sensing and transduction of H_2O_2 stress signal. *Molecular Cell*, *27*(4), 675–688.

Potukuchi, A., Addepally, U., Sindhu, K., & Manchala, R. (2018). Increased total DNA damage and oxidative stress in brain are associated with decreased longevity in high sucrose diet fed WNIN/Gr-Ob obese rats. *Nutritional Neuroscience*, *21*(9), 648–656.

Pugh, T. A., Shah, J. C., Magee, P. T., and Clancy, M. J. (1989). Characterization and localization of the sporulation glucoamylase of *Saccharomyces cerevisiae*. Biochimica et Biophysica Acta - Protein Structure. *Molecular Enzymology*, 994, 200–209. doi:https://doi.org/10.1016/0167-4838(89)90294-X.

Rafalski, J. A., & Falco, S. C. (1988). Structure of the yeast *HOM3* gene which encodes aspartokinase. *The Journal of Biological Chemistry*, 263(5), 2146–2151.

Rieger, K. J., El-Alama, M., Stein, G., Bradshaw, C., Slonimski, P. P., & Maundrell, K. (1999). Chemotyping of yeast mutants using robotics. *Yeast (Chichester, England)*, 15(10B), 973–986. https://doi.org/10.1002/(SICI)1097-0061(199907)15:10B<973::AID-YEA402>3.0.CO;2-L.

Rona, G., Herdeiro, R., Mathias, C. J., Torres, F. A., Pereira, M. D., & Eleutherio, E. (2015). CTT1 overexpression increases life span of calorie-restricted *Saccharomyces cerevisiae* deficient in Sod1. *Biogerontology*, *16*(3), 343–351.

Ruiz, A., Muñoz, I., Serrano, R., González, A., Simón, E., & Ariño, J. (2004). Functional characterization of the *Saccharomyces cerevisiae* VHS3 gene: A regulatory subunit of the Ppz1 protein phosphatase with novel, phosphatase-unrelated functions. *The Journal of Biological Chemistry*, 279(33), 34421–34430. https://doi.org/10.1074/jbc.M400572200.

Sales, K., Brandt, W., Rumbak, E., & Lindsey, G. (2000). The LEA-like protein HSP 12 in *Saccharomyces cerevisiae* has a plasma membrane location and protects membranes against desiccation and ethanol-induced stress. *Biochimica et Biophysica Acta (BBA)-Biomembranes*, *1463*(2), 267–278.

Shi, Y., Stefan, C. J., Rue, S. M., Teis, D., & Emr, S. D. (2011). Two novel WD40 domain–containing proteins, Ere1 and Ere2, function in the retromer-mediated endosomal recycling pathway. *Molecular Biology of the Cell*, 22(21), 4093–4107. https://doi.org/10.1091/mbc.e11-05-0440

Shimazu, M., Sekito, T., Akiyama, K., Ohsumi, Y., & Kakinuma, Y. (2005). A family of basic amino acid transporters of the vacuolar membrane from *Saccharomyces cerevisiae*. *The Journal of Biological Chemistry*, 280(6), 4851–4857. https://doi.org/10.1074/jbc.M412617200

Schmitt, A. P., & McEntee, K. (1996). Msn2p, a zinc finger DNA-binding protein, is the transcriptional activator of the multistress response in *Saccharomyces cerevisiae. Proceedings of the National Academy of Sciences*, *93*(12), 5777–5782.

Schuller, C., Mamnun, Y. M., Mollapour, M., Krapf, G., Schuster, M., Bauer, B. E., Piper, P. W., & Kuchler, K. (2004). Global phenotypic analysis and transcriptional profiling defines the weak acid stress response regulon in *Saccharomyces cerevisiae*. *Molecular Biology of the Cell*, *15*(2), 706–720.

Sies, H. (1997). Physiological society symposium: Impaired endothelial and smooth muscle cell function in oxidative stress. *Experimental Physiology*, *82*, 291–295.

Stahl, F. (1996). Meiotic recombination in yeast: coronation of the double-strand-break repair model. *Cell*, *87*(6), 965–968.

Tartik, M. (2013). *Molecular Characterization of a Boron-Resistant Yeast Mutant Obtained by Evolutionary Engineering* (M.Sc. Thesis). Istanbul Technical University, Graduate School of Science Engineerıng and Technology.

Toyokuni, S., Okamoto, K., Yodoi, J., & Hiai, H. (1995). Persistent oxidative stress in cancer. *FEBS Letters*, *358*(1), 1–3. https://doi.org/10.1016/0014-5793(94)01368-B

Trotter, E. W. (2002). *Studies on the Heat Shock Response in Saccharomyces cerevisiae and Arabidopsis thaliana* (Ph.D Thesis).University of Glasgow, Faculty of Biomedical and Life Sciences.

URL-1. https://www.yeastgenome.org/#, date retrieved 16.05.2023

URL-2. http://fungi.ensembl.org/index.html, date retrieved 04.12.2017

URL-3. https://www.ensembl.org/index.html, date retrieved 16.05.2023

URL-4. http://growthrate.princeton.edu/transcriptome/analyze.shtml, date retrieved 10.01.2019

URL-5. https://www.wikipathways.org/index.php/WikiPathways, date retrieved 29.06.2019

URL-6. https://david.ncifcrf.gov/, date retrieved 29.06.2019

URL-7. http://www.yeastract.com/, date retrieved 29.06.2019

Wallace-Salinas, V., Brink, D. P., Ahrén, D., & Gorwa-Grauslund, M. F. (2015). Cell periphery-related proteins as major genomic targets behind the adaptive evolution of an industrial *Saccharomyces cerevisiae* strain to combined heat and hydrolysate stress. *BMC Genomics*, *16*(1), 1–16.

Walsh, R. B., Kawasaki, G., & Fraenkel, D. G. (1983). Cloning of genes that complement yeast hexokinase and glucokinase mutants. *Journal of Bacteriology*, *154*(2), 1002–1004.

Whitmarsh, A. J., & Davis, R. J. (1998). Structural organization of MAP-kinase signaling modules by scaffold proteins in yeast and mammals. *Trends in Biochemical Sciences*, *23*(12), 481–485.

Wilson, T. E. (2002). A genomics-based screen for yeast mutants with an altered recombination/end-joining repair ratio. *Genetics*, 162(2), 677–688.

Woodbine, L., Brunton, H., Goodarzi, A. A., Shibata, A., & Jeggo, P. A. (2011). Endogenously induced DNA double strand breaks arise in heterochromatic DNA regions and require ataxia telangiectasia mutated and Artemis for their repair. *Nucleic Acids Research*, *39*(16), 6986–6997.

Woods, R. A., Roberts, D. G., Friedman, T., Jolly, D., & Filpula, D. (1983). Hypoxanthine: Guanine phosphoribosyltransferase mutants in Saccharomyces cerevisiae. MGG Molecular & General Genetics, 191(3), 407–412. https://doi.org/10.1007/BF00425755

Yılmaz, B. (2009). *Investigation of Oxidative Stress Response in Yeast and Rat*. Istanbul Technical University, Institute of Science and Technology.

Young, M. E., Karpova, T. S., Brügger, B., Moschenross, D. M., Wang, G. K., Schneiter, R., Wieland, F. T., & Cooper, J. A. (2002). The Sur7p family defines novel cortical domains in *Saccharomyces cerevisiae*, affects sphingolipid metabolism, and is involved in sporulation. *Molecular and Cellular Biology*, *22*(3), 927–934. https://doi.org/10.1128/mcb.22.3.927-934.2002

Zhao, H., Chen, J., Liu, J., & Han, B. (2015). Transcriptome analysis reveals the oxidative stress response in *Saccharomyces cerevisiae*. *RSC Advances*, *5*(29), 22923–22934.

Zhou, H., & Winston, F. (2001). *NRG1* is required for glucose repression of the *SUC2* and *GAL* genes of *Saccharomyces cerevisiae*. *BMC Genetics*, *2*, 5. https://doi.org/10.1186/1471-2156-2-5

Zitomer, R. S., Carrico, P., & Deckert, J. (1997). Regulation of hypoxic gene expression in yeast. *Kidney International*, *51*(2), 507–513.

Zuzuarregui, A., Monteoliva, L., Gil, C., & del Olmo, M. lí. (2006). Transcriptomic and proteomic approach for understanding the molecular basis of adaptation of *Saccharomyces cerevisiae* to wine fermentation. *Applied and Environmental Microbiology*, *72*(1), 836–847.

APPENDICES

APPENDIX A: Microarray results of H7 (about two-fold and higher ganges in H7).
APPENDIX B : NGS results showing the mutation regions in H7 genome.

APPENDIX A: Microarray results of H7 (about two-fold and higher ganges in H7).

Table A. 1 : Down-regulated genes (about two-fold and higher) in H7 based on microarray results, according to metabolic processes.

Process Name	Systematic Gene Symbol	Standard Gene Symbol	Gene Name	Fold Change (absolute)	Fold Change (log2)
rRNA processing	YDR299W	BFR2	BreFeldin A Resistance	3.31	9.93
	YPL217C	BMS1	BMh Sensitive	3.31	9.92
	YIL096C	BMT5	Base Methyltransferase of Twenty five S rRNA 5	3.05	8.26
	YMR014W	BUD22	BUD site selection	2.48	5.60
	YCR047C	BUD23	BUD site selection	2.39	5.24
	YLR175W	CBF5	Centromere Binding Factor	3.61	12.20
	YGL029W	CGR1	Coiled-coil Growth-Regulated	2.72	6.57
	YDL031W	DBP10	Dead Box Protein	2.57	5.95
	YNL112W	DBP2	Dead Box Protein	5.24	37.72
	YGL078C	DBP3	Dead Box Protein	3.18	9.08
	YKR024C	DBP7	Dead Box Protein	2.93	7.63
	YHR169W	DBP8	Dead Box Protein	3.48	11.15
	YLR276C	DBP9	Dead Box Protein	3.14	8.81
	YKL078W	DHR2	DEAH-box RNA helicase	4.33	20.10
	YPL266W	DIM1	DIMethylase	2.54	5.83
	YLR129W	DIP2	DOM34 Interacting Protein	2.58	5.99
	YLL008W	DRS1	Deficiency of Ribosomal Subunits	3.46	11.00
	YKL172W	EBP2	EBNA1-binding protein (homolog)	2.75	6.73
	YMR128W	ECM16	ExtraCellular Mutant	2.88	7.35
	YGR271C-A	EFG1	Exit From G1	2.67	6.34
	YLR186W	EMG1	Essential for Mitotic Growth	2.54	5.83
	YBR247C	ENP1	Essential Nuclear Protein	2.81	7.00
	YGR145W	ENP2	Essential Nuclear Protein	3.03	8.15
	YMR049C	ERB1	Eukaryotic Ribosome Biogenesis	3.02	8.10
	YNR054C	ESF2	Eighteen S rRNA Factor 2	2.80	6.95
	YIL019W	FAF1	Forty (40) S Assembly Factor	2.62	6.14
	YDR021W	FAL1	eukaryotic translation initiation factor Four A Like	2.59	6.02
	YLR068W	FYV7	Function required for Yeast Viability	2.71	6.55
	YHR089C	GAR1	Glycine Arginine Rich	3.10	8.60
	YLL035W	GRC3		4.54	23.18
	YMR290C	HAS1	Helicase Associated with Set1	3.29	9.81
	YJL033W	HCA4	Helicase CA	3.25	9.51
	YHR148W	IMP3	Interacting with Mpp10p	2.46	5.48
	YNL075W	IMP4	Interacting with Mpp10p	3.14	8.84

Table A. 1 (continued) : Down-regulated genes (about two-fold and higher) in H7 based on microarray results, according to metabolic processes.

rRNA processing	YCL059C	KRR1	contains KRR-R motif	2.62	6.14
	YER127W	LCP5	Lethal with Conditional Pap1	2.84	7.16
	YAL025C	MAK16	MAintenance of Killer	3.37	10.36
	YBR142W	MAK5	MAintenance of Killer	2.81	7.00
	YJR002W	MPP10	M Phase Phosphoproteins	3.00	8.01
	YPR112C	MRD1	Multiple RNA-binding domain	2.71	6.53
	YKL009W	MRT4	mRNA Turnover 4	3.06	8.32
	YJL050W	MTR4	MrnaTRansport	2.83	7.11
	YPL211W	NIP7	Nuclear ImPort	3.02	8.11
	YLR002C	NOC3	NucleOlar Complex associated	2.64	6.21
	YPR144C	NOC4	NucleOlar Complex associated	2.44	5.41
	YPL093W	NOG1	NucleOlar G-protein	3.58	11.92
	YDL014W	NOP1	NucleOlar Protein	3.33	10.03
	YOL041C	NOP12	NucleOlar Protein	2.86	7.26
	YNL061W	NOP2	NucleOlar Protein	3.73	13.27
	YPL043W	NOP4	NucleOlar Protein	3.14	8.82
	YLR197W	NOP56	NucleOlar Protein of 56.8 kDa	2.41	5.31
	YOR310C	NOP58	NucleOlar Protein of 58 kDa	3.55	11.69
	YGR103W	NOP7	NucleOlar Protein	3.13	8.73
	YOL144W	NOP8	NucleOlar Protein	2.66	6.33
	YJL010C	NOP9	NucleOlar Protein	3.24	9.43
	YER126C	NSA2	Nop Seven Associated	2.54	5.83
	YGR159C	NSR1		4.81	28.13
	YER006W	NUG1	NUclearGTPase	2.98	7.87
	YOR145C	PNO1	Partner of NOb1	2.55	5.84
	YGL120C	PRP43	Pre-mRNA Processing	2.78	6.87
	YOR243C	PUS7	PseudoUridine Synthase	2.55	5.84
	YLR196W	PWP1	Periodic tryptophan (W) Protein	2.85	7.22
	YCR057C	PWP2	Periodic tryptophan (W) Protein	3.06	8.34
	YOL010W	RCL1	Rna 3'-terminal phosphate Cyclase Like	2.99	7.96
	YOL080C	REX4	RnaEXonuclease	2.85	7.20
	YHR197W	RIX1	RIbosomeeXport	2.71	6.55
	YGL171W	ROK1	Rescuer Of Kem1	2.67	6.36
	YKR081C	RPF2	Ribosome Production Factor	2.85	7.19
	YHR062C	RPP1	Ribonuclease P Protein	2.40	5.28
	YPL012W	RRP12	Ribosomal RNA Processing	3.18	9.04
	YOR287C	RRP36	Ribosomal RNA Processing	2.44	5.43
	YMR229C	RRP5	Ribosomal RNA Processing	2.93	7.63
	YDR083W	RRP8	Ribosomal RNA Processing	3.12	8.69
	YPR137W	RRP9	Ribosomal RNA Processing	2.72	6.60

Table A. 1 (continued) : Down-regulated genes (about two-fold and higher) in H7 based on microarray results, according to metabolic processes.

rRNA processing	YOR294W	RRS1	Regulator of Ribosome Synthesis	3.59	12.05
	YDL153C	SAS10	Something About Silencing	2.45	5.47
	YEL026W	SNU13	Small NUclear ribonucleoprotein associated	3.64	12.49
	YLL011W	SOF1	Suppressor Of Fibrillarin	2.42	5.36
	YCL054W	SPB1	Suppressor of PaB1 mutant	2.80	6.95
	YFL002C	SPB4	Suppressor of PAB1	2.43	5.39
	YNL209W	SSB2	Stress-Seventy subfamily B	2.39	5.24
	YHR066W	SSF1	Suppressor of ste4 (Four)	2.58	5.97
	YPR016C	TIF6	Translation Initiation Factor	2.34	5.05
	YDL060W	TSR1	Twenty S rRNA accumulation	2.70	6.48
	YLR435W	TSR2	Twenty S rRNA accumulation	2.65	6.29
	YJL109C	UTP10	U Three Protein	2.60	6.08
	YLR222C	UTP13	U Three Protein	2.84	7.18
	YML093W	UTP14	U Three Protein	2.40	5.29
	YMR093W	UTP15	U Three Protein	2.39	5.24
	YJL069C	UTP18	U Three Protein	2.74	6.68
	YLR409C	UTP21	U Three Protein	2.76	6.78
	YOR004W	UTP23	U Three-associated Protein	3.82	14.13
	YIL091C	UTP25	U Three Protein	2.90	7.45
	YDR324C	UTP4	U Three Protein	2.82	7.08
	YDR398W	UTP5	U Three Protein	3.25	9.50
	YDR449C	UTP6	U Three Protein	2.55	5.87
	YGR128C	UTP8	U Three Protein	2.75	6.74
ribosomal small subunit biogenesis	YDR299W	BFR2	BreFeldin A Resistance	3.31	9.93
	YPL217C	BMS1	BMh Sensitive	3.31	9.92
	YMR014W	BUD22	BUD site selection	2.48	5.60
	YCR047C	BUD23	BUD site selection	2.39	5.24
	YHR169W	DBP8	Dead Box Protein	3.48	11.15
	YKL078W	DHR2	DEAH-box RNA helicase	4.33	20.10
	YPL266W	DIM1	DIMethylase	2.54	5.83
	YLR129W	DIP2	DOM34 Interacting Protein	2.58	5.99
	YMR128W	ECM16	ExtraCellular Mutant	2.88	7.35
	YGR271C-A	EFG1	Exit From G1	2.67	6.34
	YLR186W	EMG1	Essential for Mitotic Growth	2.54	5.83
	YBR247C	ENP1	Essential Nuclear Protein	2.81	7.00
	YGR145W	ENP2	Essential Nuclear Protein	3.03	8.15
	YNR054C	ESF2	Eighteen S rRNA Factor 2	2.80	6.95
	YIL019W	FAF1	Forty (40) S Assembly Factor	2.62	6.14
	YDR021W	FAL1	eukaryotic translation initiation factor Four A Like	2.59	6.02
	YLR068W	FYV7	Function required for Yeast Viability	2.71	6.55

Table A. 1 (continued) : Down-regulated genes (about two-fold and higher) in H7 based on microarray results, according to metabolic processes.

ribosomal small subunit biogenesis	YMR290C	HAS1	Helicase Associated with Set1	3.29	9.81
	YHR148W	IMP3	Interacting with Mpp10p	2.46	5.48
	YNL075W	IMP4	Interacting with Mpp10p	3.14	8.84
	YNL132W	KRE33	Killer toxin REsistant	4.37	20.66
	YCL059C	KRR1	contains KRR-R motif	2.62	6.14
	YER127W	LCP5	Lethal with Conditional Pap1	2.84	7.16
	YJR002W	MPP10	M Phase Phosphoproteins	3.00	8.01
	YPR112C	MRD1	Multiple RNA-binding domain	2.71	6.53
	YPL226W	NEW1	Nu+	2.88	7.34
	YPR144C	NOC4	NucleOlar Complex associated	2.44	5.41
	YOR310C	NOP58	NucleOlar Protein of 58 kDa	3.55	11.69
	YGR103W	NOP7	NucleOlar Protein	3.13	8.73
	YJL010C	NOP9	NucleOlar Protein	3.24	9.43
	YGR159C	NSR1		4.81	28.13
	YOR145C	PNO1	Partner of NOb1	2.55	5.84
	YGL120C	PRP43	Pre-mRNA Processing	2.78	6.87
	YCR057C	PWP2	Periodic tryptophan (W) Protein	3.06	8.34
	YOL010W	RCL1	Rna 3'-terminal phosphate Cyclase Like	2.99	7.96
	YGL171W	ROK1	Rescuer Of Kem1	2.67	6.36
	YPL012W	RRP12	Ribosomal RNA Processing	3.18	9.04
	YOR287C	RRP36	Ribosomal RNA Processing	2.44	5.43
	YMR229C	RRP5	Ribosomal RNA Processing	2.93	7.63
	YOR294W	RRS1	Regulator of Ribosome Synthesis	3.59	12.05
	YDL153C	SAS10	Something About Silencing	2.45	5.47
	YLR336C	SGD1	Suppressor of Glycerol Defect	2.74	6.67
	YEL026W	SNU13	Small NUclear ribonucleoprotein associated	3.64	12.49
	YLL011W	SOF1	Suppressor Of Fibrillarin	2.42	5.36
	YDL060W	TSR1	Twenty S rRNA accumulation	2.70	6.48
	YLR435W	TSR2	Twenty S rRNA accumulation	2.65	6.29
	YJL109C	UTP10	U Three Protein	2.60	6.08
	YLR222C	UTP13	U Three Protein	2.84	7.18
	YML093W	UTP14	U Three Protein	2.40	5.29
	YMR093W	UTP15	U Three Protein	2.39	5.24
	YJL069C	UTP18	U Three Protein	2.74	6.68
	YLR409C	UTP21	U Three Protein	2.76	6.78
	YOR004W	UTP23	U Three-associated Protein	3.82	14.13
	YIL091C	UTP25	U Three Protein	2.90	7.45
	YDR324C	UTP4	U Three Protein	2.82	7.08
	YDR398W	UTP5	U Three Protein	3.25	9.50
	YDR449C	UTP6	U Three Protein	2.55	5.87

Table A. 1 (continued) : Down-regulated genes (about two-fold and higher) in H7 based on microarray results, according to metabolic processes.

ribosomal small subunit biogenesis	YGR128C	UTP8	U Three Protein	2.75	6.74
ribosomal large subunit biogenesis	YLR397C	AFG2	ATPase Family Gene	2.87	7.29
	YJL122W	ALB1	Arx1 Little Brother	4.04	16.50
	YOL077C	BRX1	Xenopuslaevis Brix (Biogenesis of Ribosomes in Xenopus) homolog	2.75	6.73
	YDL031W	DBP10	Dead Box Protein	2.57	5.95
	YGL078C	DBP3	Dead Box Protein	3.18	9.08
	YKR024C	DBP7	Dead Box Protein	2.93	7.63
	YLR276C	DBP9	Dead Box Protein	3.14	8.81
	YLL008W	DRS1	Deficiency of Ribosomal Subunits	3.46	11.00
	YMR049C	ERB1	Eukaryotic Ribosome Biogenesis	3.02	8.10
	YLL035W	GRC3		4.54	23.18
	YMR290C	HAS1	Helicase Associated with Set1	3.29	9.81
	YHR085W	IPI1	Involved in Processing ITS2	2.85	7.21
	YNL182C	IPI3	Involved in Processing ITS2	3.57	11.87
	YGL099W	LSG1	Large-Subunit Gtpase	2.51	5.71
	YAL025C	MAK16	MAintenance of Killer	3.37	10.36
	YDR060W	MAK21	MAintenance of Killer	3.14	8.84
	YBR142W	MAK5	MAintenance of Killer	2.81	7.00
	YKL009W	MRT4	mRNA Turnover 4	3.06	8.32
	YPL211W	NIP7	Nuclear ImPort	3.02	8.11
	YOR206W	NOC2	NucleOlar Complex associated	2.50	5.67
	YPL093W	NOG1	NucleOlar G-protein	3.58	11.92
	YOL041C	NOP12	NucleOlar Protein	2.86	7.26
	YNL061W	NOP2	NucleOlar Protein	3.73	13.27
	YPL043W	NOP4	NucleOlar Protein	3.14	8.82
	YGR103W	NOP7	NucleOlar Protein	3.13	8.73
	YOL144W	NOP8	NucleOlar Protein	2.66	6.33
	YER126C	NSA2	Nop Seven Associated	2.54	5.83
	YER006W	NUG1	NUclearGTPase	2.98	7.87
	YGL120C	PRP43	Pre-mRNA Processing	2.78	6.87
	YDR496C	PUF6	PUmilio-homology domain Family	2.98	7.88
	YBR267W	REI1	REquired for Isotropic bud growth	3.18	9.08
	YOL080C	REX4	RnaEXonuclease	2.85	7.20
	YHR197W	RIX1	RIbosomeeXport	2.71	6.55
	YLL034C	RIX7	RIbosomeeXport	3.27	9.63
	YDR091C	RLI1	RNase L Inhibitor	2.73	6.64
	YLR009W	RLP24	Ribosomal-Like Protein	3.97	15.63
	YKR081C	RPF2	Ribosome Production Factor	2.85	7.19
	YMR229C	RRP5	Ribosomal RNA Processing	2.93	7.63
	YDR083W	RRP8	Ribosomal RNA Processing	3.12	8.69

Table A. 1 (continued) : Down-regulated genes (about two-fold and higher) in H7 based on microarray results, according to metabolic processes.

ribosomal large subunit biogenesis RNA modification	YOR294W	RRS1	Regulator of Ribosome Synthesis	3.59	12.05
	YCR072C	RSA4	RiboSome Assembly	4.53	23.05
	YGR245C	SDA1	Severe Depolymerization of Actin	5.70	51.87
	YCL054W	SPB1	Suppressor of PaB1 mutant	2.80	6.95
	YFL002C	SPB4	Suppressor of PAB1	2.43	5.39
	YIR012W	SQT1	Suppressor of QSR1 Truncations	2.43	5.40
	YHR066W	SSF1	Suppressor of ste4 (Four)	2.58	5.97
	YDL063C	SYO1	SYnchronizedimpOrt or SYmpOrtin	3.39	10.46
	YPR016C	TIF6	Translation Initiation Factor	2.34	5.05
	YOR272W	YTM1		3.44	10.82
	YIR026C	YVH1	Yeast vaccinia virus VH1 Homolog	3.14	8.80
	YIL096C	BMT5	Base Methyltransferase of Twenty five S rRNA 5	3.05	8.26
	YCR047C	BUD23	BUD site selection	2.39	5.24
	YLR175W	CBF5	Centromere Binding Factor	3.61	12.20
	YPL266W	DIM1	DIMethylase	2.54	5.83
	YML080W	DUS1	DihydroUridine Synthase	2.37	5.18
	YGR200C	ELP2	ELongator Protein	2.66	6.31
	YLR186W	EMG1	Essential for Mitotic Growth	2.54	5.83
	YHR089C	GAR1	Glycine Arginine Rich	3.10	8.60
	YNL062C	GCD10	General Control Derepressed	2.81	7.01
	YLR384C	IKI3	Insensitive to KIller toxin	2.46	5.49
	YBL024W	NCL1	NuCLear protein	2.80	6.99
	YDL014W	NOP1	NucleOlar Protein	3.33	10.03
	YNL061W	NOP2	NucleOlar Protein	3.73	13.27
	YLR197W	NOP56	NucleOlar Protein of 56.8 kDa	2.41	5.31
	YPL212C	PUS1	PseudoUridine Synthase	2.78	6.87
	YOR243C	PUS7	PseudoUridine Synthase	2.55	5.84
	YDR083W	RRP8	Ribosomal RNA Processing	3.12	8.69
	YPR137W	RRP9	Ribosomal RNA Processing	2.72	6.60
	YCL054W	SPB1	Suppressor of PaB1 mutant	2.80	6.95
	YGL169W	SUA5	Suppressor of Upstream AUG	2.36	5.12
	YDR120C	TRM1	tRNA Methyltransferase	3.36	10.25
	YOL124C	TRM11	TRna Methyltransferase	2.44	5.42
	YOL125W	TRM13	TRna Methyltransferase	3.64	12.46
	YPL030W	TRM44	TRna Methyltransferase	2.91	7.51
	YDL201W	TRM8	Transfer RNA Methyltransferase	2.75	6.75
	YDR165W	TRM82	Transfer RNA Methyltransferase	2.77	6.81
nuclear transport	YDR101C	ARX1	Associated with Ribosomal eXport complex	3.47	11.09
	YCR047C	BUD23	BUD site selection	2.39	5.24
	YAL059W	ECM1	ExtraCellular Mutant	2.41	5.32

Table A. 1 (continued) : Down-regulated genes (about two-fold and higher) in H7 based on microarray results, according to metabolic processes.

nuclear transport	YBR034C	HMT1	HnRNPMethylTransferase	3.80	13.90
	YER110C	KAP123	KAryoPherin	3.35	10.23
	YGL099W	LSG1	Large-Subunit Gtpase	2.51	5.71
	YPL226W	NEW1	Nu+	2.88	7.34
	YHR170W	NMD3	Nonsense-Mediated mRNA Decay	2.36	5.15
	YPL093W	NOG1	NucleOlar G-protein	3.58	11.92
	YNR053C	NOG2	NucleOlar G-protein	3.82	14.15
	YJL010C	NOP9	NucleOlar Protein	3.24	9.43
	YER006W	NUG1	NUclearGTPase	2.98	7.87
	YBR267W	REI1	REquired for Isotropic bud growth	3.18	9.08
	YHR197W	RIX1	RIbosomeeXport	2.71	6.55
	YLL034C	RIX7	RIbosomeeXport	3.27	9.63
	YDR091C	RLI1	RNase L Inhibitor	2.73	6.64
	YOR294W	RRS1	Regulator of Ribosome Synthesis	3.59	12.05
	YGR245C	SDA1	Severe Depolymerization of Actin	5.70	51.87
	YKR092C	SRP40	Serine Rich Protein	2.59	6.04
	YNL209W	SSB2	Stress-Seventy subfamily B	2.39	5.24
	YDL063C	SYO1	SYnchronizedimpOrt or SYmpOrtin	3.39	10.46
	YPR016C	TIF6	Translation Initiation Factor	2.34	5.05
	YGR128C	UTP8	U Three Protein	2.75	6.74
organelle assembly	YOL077C	BRX1	Xenopuslaevis Brix (Biogenesis of Ribosomes in Xenopus) homolog	2.75	6.73
	YLL008W	DRS1	Deficiency of Ribosomal Subunits	3.46	11.00
	YNR054C	ESF2	Eighteen S rRNA Factor 2	2.80	6.95
	YHR085W	IPI1	Involved in Processing ITS2	2.85	7.21
	YNL182C	IPI3	Involved in Processing ITS2	3.57	11.87
	YGL099W	LSG1	Large-Subunit Gtpase	2.51	5.71
	YDR060W	MAK21	MAintenance of Killer	3.14	8.84
	YPR112C	MRD1	Multiple RNA-binding domain	2.71	6.53
	YKL009W	MRT4	mRNA Turnover 4	3.06	8.32
	YGR159C	NSR1		4.81	28.13
	YOL080C	REX4	RnaEXonuclease	2.85	7.20
	YHR197W	RIX1	RIbosomeeXport	2.71	6.55
	YKR081C	RPF2	Ribosome Production Factor	2.85	7.19
	YCR072C	RSA4	RiboSome Assembly	4.53	23.05
	YFL002C	SPB4	Suppressor of PAB1	2.43	5.39
	YIR012W	SQT1	Suppressor of QSR1 Truncations	2.43	5.40
	YHR066W	SSF1	Suppressor of ste4 (Four)	2.58	5.97
	YIR026C	YVH1	Yeast vaccinia virus VH1 Homolog	3.14	8.80
ribosome assembly	YOL077C	BRX1	Xenopuslaevis Brix (Biogenesis of Ribosomes in Xenopus) homolog	2.75	6.73
	YLL008W	DRS1	Deficiency of Ribosomal Subunits	3.46	11.00

Table A. 1 (continued) : Down-regulated genes (about two-fold and higher) in H7 based on microarray results, according to metabolic processes.

ribosome assembly	YNR054C	ESF2	Eighteen S rRNA Factor 2	2.80	6.95
	YHR085W	IPI1	Involved in Processing ITS2	2.85	7.21
	YNL182C	IPI3	Involved in Processing ITS2	3.57	11.87
	YGL099W	LSG1	Large-Subunit Gtpase	2.51	5.71
	YDR060W	MAK21	MAintenance of Killer	3.14	8.84
	YPR112C	MRD1	Multiple RNA-binding domain	2.71	6.53
	YKL009W	MRT4	mRNA Turnover 4	3.06	8.32
	YGR159C	NSR1		4.81	28.13
	YOL080C	REX4	RnaEXonuclease	2.85	7.20
	YHR197W	RIX1	RIbosomeeXport	2.71	6.55
	YKR081C	RPF2	Ribosome Production Factor	2.85	7.19
	YCR072C	RSA4	RiboSome Assembly	4.53	23.05
	YFL002C	SPB4	Suppressor of PAB1	2.43	5.39
	YIR012W	SQT1	Suppressor of QSR1 Truncations	2.43	5.40
	YHR066W	SSF1	Suppressor of ste4 (Four)	2.58	5.97
	YIR026C	YVH1	Yeast vaccinia virus VH1 Homolog	3.14	8.80
ribosomal subunit export from nucleus	YDR101C	ARX1	Associated with Ribosomal eXport complex	3.47	11.09
	YCR047C	BUD23	BUD site selection	2.39	5.24
	YAL059W	ECM1	ExtraCellular Mutant	2.41	5.32
	YGL099W	LSG1	Large-Subunit Gtpase	2.51	5.71
	YHR170W	NMD3	Nonsense-Mediated mRNA Decay	2.36	5.15
	YPL093W	NOG1	NucleOlar G-protein	3.58	11.92
	YNR053C	NOG2	NucleOlar G-protein	3.82	14.15
	YJL010C	NOP9	NucleOlar Protein	3.24	9.43
	YER006W	NUG1	NUclearGTPase	2.98	7.87
	YHR197W	RIX1	RIbosomeeXport	2.71	6.55
	YLL034C	RIX7	RIbosomeeXport	3.27	9.63
	YDR091C	RLI1	RNase L Inhibitor	2.73	6.64
	YOR294W	RRS1	Regulator of Ribosome Synthesis	3.59	12.05
	YGR245C	SDA1	Severe Depolymerization of Actin	5.70	51.87
	YNL209W	SSB2	Stress-Seventy subfamily B	2.39	5.24
	YPR016C	TIF6	Translation Initiation Factor	2.34	5.05
tRNA processing	YML080W	DUS1	DihydroUridine Synthase	2.37	5.18
	YGR200C	ELP2	ELongator Protein	2.66	6.31
	YNL062C	GCD10	General Control Derepressed	2.81	7.01
	YLR384C	IKI3	Insensitive to KIller toxin	2.46	5.49
	YBL024W	NCL1	NuCLear protein	2.80	6.99
	YPL212C	PUS1	PseudoUridine Synthase	2.78	6.87
	YOR243C	PUS7	PseudoUridine Synthase	2.55	5.84
	YHR062C	RPP1	Ribonuclease P Protein	2.40	5.28

Table A. 1 (continued) : Down-regulated genes (about two-fold and higher) in H7 based on microarray results, according to metabolic processes.

tRNA processing	YGL169W	SUA5	Suppressor of Upstream AUG	2.36	5.12
	YDR120C	TRM1	tRNA Methyltransferase	3.36	10.25
	YOL124C	TRM11	TRna Methyltransferase	2.44	5.42
	YOL125W	TRM13	TRna Methyltransferase	3.64	12.46
	YPL030W	TRM44	TRna Methyltransferase	2.91	7.51
	YDL201W	TRM8	Transfer RNA Methyltransferase	2.75	6.75
	YDR165W	TRM82	Transfer RNA Methyltransferase	2.77	6.81
transcription from RNA polymerase I promoter	YLL035W	GRC3		4.54	23.18
	YPR010C	RPA135	RNA Polymerase A	2.64	6.21
	YJL148W	RPA34	RNA Polymerase A	2.32	5.00
	YOR340C	RPA43	RNA Polymerase A	3.61	12.25
	YNL248C	RPA49	RNA Polymerase A	2.85	7.20
	YBR154C	RPB5	RNA Polymerase B	2.60	6.08
	YPR110C	RPC40	RNA Polymerase C	2.52	5.73
	YJL109C	UTP10	U Three Protein	2.60	6.08
	YMR093W	UTP15	U Three Protein	2.39	5.24
	YDR324C	UTP4	U Three Protein	2.82	7.08
	YDR398W	UTP5	U Three Protein	3.25	9.50
	YGR128C	UTP8	U Three Protein	2.75	6.74
nucleobase-containing small molecule metabolic process	YNL141W	AAH1	Adenine AminoHydrolase	4.13	17.50
	YMR300C	ADE4	ADEnine requiring	2.44	5.42
	YGL234W	ADE5,7	ADEnine requiring	2.94	7.68
	YMR217W	GUA1	GUanine Auxotroph	2.60	6.06
	YLR432W	IMD3	IMP Dehydrogenase	2.47	5.53
	YLR134W	PDC5	Pyruvate DeCarboxylase	4.05	16.59
	YLR014C	PPR1	Pyrimidine Pathway Regulation	2.45	5.45
	YOR101W	RAS1	homologous to RAS proto-oncogene	3.02	8.12
	YOR095C	RKI1	Ribose-5-phosphate Ketol-Isomerase	3.26	9.57
	YOR047C	STD1	Suppressor of Tbp Deletion	2.65	6.26
	YKL216W	URA1	URAcil requiring	2.73	6.62
	YBL039C	URA7	URAcil requiring	3.36	10.26
response to chemical	YDR161W	ACL4	Assembly Chaperone of RpL4	2.43	5.38
	YLR397C	AFG2	ATPase Family Gene	2.87	7.29
	YGR177C	ATF2	AcetylTransFerase	2.62	6.17
	YML116W	ATR1	AminoTriazole Resistance	2.56	5.89
	YPL256C	CLN2	CycLiN	2.51	5.69
	YGR271C-A	EFG1	Exit From G1	2.67	6.34
	YJL157C	FAR1	Factor ARrest	2.59	6.04
	YMR052W	FAR3	Factor ARrest	2.55	5.85
	YBL024W	NCL1	NuCLear protein	2.80	6.99

Table A. 1 (continued) : Down-regulated genes (about two-fold and higher) in H7 based on microarray results, according to metabolic processes.

response to chemical	YDR091C	RLI1	RNase L Inhibitor	2.73	6.64
	YFL026W	STE2	STErile	2.50	5.64
cellular amino acid metabolic process	YKL106W	AAT1	Aspartate AminoTransferase	2.69	6.44
	YGL256W	ADH4	Alcohol DeHydrogenase	5.36	41.21
	YDR321W	ASP1	ASParaginase	2.64	6.24
	YNL256W	FOL1	FOLic acid synthesis	2.37	5.18
	YER086W	ILV1	IsoLeucine-plus-Valine requiring	2.55	5.84
	YJR016C	ILV3	IsoLeucine-plus-Valine requiring	2.57	5.96
cellular amino acid metabolic process	YLR355C	ILV5	IsoLeucine-plus-Valine requiring	2.42	5.35
	YOR108W	LEU9	LEUcine biosynthesis	2.83	7.11
	YDR234W	LYS4	LYSine requiring	2.93	7.65
	YLR134W	PDC5	Pyruvate DeCarboxylase	4.05	16.59
	YHR020W	YHR020W		2.56	5.90
regulation of cell cycle	YBR158W	AMN1	Antagonist of Mitotic exit Network	2.36	5.13
	YMR199W	CLN1	CycLiN	2.83	7.13
	YPL256C	CLN2	CycLiN	2.51	5.69
	YKR083C	DAD2	Duo1 And Dam1 interacting	3.06	8.35
	YJL157C	FAR1	Factor ARrest	2.59	6.04
	YDR130C	FIN1	Filaments In between Nuclei	2.53	5.79
	YOR233W	KIN4	KINase	3.21	9.27
	YNL289W	PCL1	Pho85 CycLin	2.40	5.26
	YLR263W	RED1	REDuctional division	2.46	5.50
	YGR245C	SDA1	Severe Depolymerization of Actin	5.70	51.87
mitotic cell cycle	YBR158W	AMN1	Antagonist of Mitotic exit Network	2.36	5.13
	YDR184C	ATC1	Aip Three Complex	2.79	6.93
	YCR047C	BUD23	BUD site selection	2.39	5.24
	YCR063W	BUD31	BUD site selection	2.39	5.25
	YDR130C	FIN1	Filaments In between Nuclei	2.53	5.79
	YOR233W	KIN4	KINase	3.21	9.27
	YBR267W	REI1	REquired for Isotropic bud growth	3.18	9.08
	YDR180W	SCC2	Sister Chromatid Cohesion	2.37	5.17
	YGR245C	SDA1	Severe Depolymerization of Actin	5.70	51.87
	YOR315W	SFG1	SuperFicialpseudohyphal Growth	2.73	6.62
signaling	YPL256C	CLN2	CycLiN	2.51	5.69
	YGR271C-A	EFG1	Exit From G1	2.67	6.34
	YJL157C	FAR1	Factor ARrest	2.59	6.04
	YMR052W	FAR3	Factor ARrest	2.55	5.85

Table A. 1 (continued) : Down-regulated genes (about two-fold and higher) in H7 based on microarray results, according to metabolic processes.

signaling	YDR144C	MKC7	Multicopy suppressor of Kex2 Cold sensitivity	2.86	7.26
	YOR101W	RAS1	homologous to RAS proto-oncogene	3.02	8.12
	YOR107W	RGS2	Regulator of heterotrimeric G protein Signaling	2.82	7.05
	YOR047C	STD1	Suppressor of Tbp Deletion	2.65	6.26
	YFL026W	STE2	STErile	2.5	5.64
	YIR026C	YVH1	Yeast vaccinia virus VH1 Homolog	3.14	8.80
conjugation	YPL256C	CLN2	CycLiN	2.51	5.69
	YGR271C-A	EFG1	Exit From G1	2.67	6.34
	YJL157C	FAR1	Factor ARrest	2.59	6.04
	YMR052W	FAR3	Factor ARrest	2.55	5.85
	YGL099W	LSG1	Large-Subunit Gtpase	2.51	5.71
	YDL039C	PRM7	Pheromone-Regulated Membrane protein	4.28	19.46
	YHR066W	SSF1	Suppressor of ste4 (Four)	2.58	5.97
	YFL026W	STE2	STErile	2.50	5.64
RNA catabolic process	YIL079C	AIR1	Arginine methyltransferase-Interacting RING finger protein	3.22	9.35
	YNL112W	DBP2	Dead Box Protein	5.24	37.72
	YKL009W	MRT4	mRNA Turnover 4	3.06	8.32
	YJL050W	MTR4	MrnaTRansport	2.83	7.11
	YJL208C	NUC1	NUClease	2.56	5.90
	YHR062C	RPP1	Ribonuclease P Protein	2.40	5.28
	YNL299W	TRF5	Topoisomerase one-Related Function	2.59	6.04
	YOR359W	VTS1	VTi1-2 Suppressor	2.35	5.10
transcription from RNA polymerase II promoter	YER045C	ACA1	ATF/CREB Activator	2.42	5.36
	YGR200C	ELP2	ELongator Protein	2.66	6.31
	YBR034C	HMT1	HnRNPMethylTransferase	3.80	13.90
	YLR384C	IKI3	Insensitive to KIller toxin	2.46	5.49
	YLR014C	PPR1	Pyrimidine Pathway Regulation	2.45	5.45
	YBR154C	RPB5	RNA Polymerase B	2.60	6.08
	YOR047C	STD1	Suppressor of Tbp Deletion	2.65	6.26
	YBL054W	TOD6	Twin Of Dot6p	3.27	9.65
organelle fission	YBR158W	AMN1	Antagonist of Mitotic exit Network	2.36	5.13
	YKL172W	EBP2	EBNA1-binding protein (homolog)	2.75	6.73
	YDR130C	FIN1	Filaments In between Nuclei	2.53	5.79
	YOR233W	KIN4	KINase	3.21	9.27
	YLR263W	RED1	REDuctional division	2.46	5.50
	YDR180W	SCC2	Sister Chromatid Cohesion	2.37	5.17

Table A. 1 (continued) : Down-regulated genes (about two-fold and higher) in H7 based on microarray results, according to metabolic processes.

organelle fission	YPL130W	SPO19	SPOrulation	3.11	8.65
	YIR026C	YVH1	Yeast vaccinia virus VH1 Homolog	3.14	8.80
regulation of organelle organization	YBR158W	AMN1	Antagonist of Mitotic exit Network	2.36	5.13
	YKR083C	DAD2	Duo1 And Dam1 interacting	3.06	8.35
	YDR130C	FIN1	Filaments In between Nuclei	2.53	5.79
	YLR449W	FPR4	FKBP Proline Rotamase (isomerase)	3.00	8.03
	YOR233W	KIN4	KINase	3.21	9.27
	YLR263W	RED1	REDuctional division	2.46	5.50
	YIR026C	YVH1	Yeast vaccinia virus VH1 Homolog	3.14	8.80
transmembrane transport	YML116W	ATR1	AminoTriazole Resistance	2.56	5.89
	YBR291C	CTP1	Citrate Transport Protein	2.47	5.54
	YER056C	FCY2	FluoroCYtosine resistance	3.16	8.93
	YBL042C	FUI1	5-FlUorourIdine resistance	3.56	11.77
	YJR054W	KCH1	Potassium (K) regulator of CcH1	2.90	7.45
	YBR104W	YMC2	Yeast Mitochondrial Carrier	2.73	6.62
	YGL255W	ZRT1	Zinc-Regulated Transporter	5.64	49.79
peptidyl-amino acid modification	YHL039W	EFM1	Elongation Factor Methyltransferase	3.42	10.69
	YBR271W	EFM2	Elongation Factor Methyltransferase	3.72	13.16
	YIL064W	EFM4	Elongation Factor Methyltransferase	2.58	6.00
	YLR449W	FPR4	FKBP Proline Rotamase (isomerase)	3.00	8.03
	YBR034C	HMT1	HnRNPMethylTransferase	3.80	13.90
	YJR070C	LIA1	Ligand of eIF5A	2.71	6.53
	YDR465C	RMT2	aRginineMeThyltransferase	3.02	8.09
protein alkylation	YHL039W	EFM1	Elongation Factor Methyltransferase	3.42	10.69
	YBR271W	EFM2	Elongation Factor Methyltransferase	3.72	13.16
	YIL064W	EFM4	Elongation Factor Methyltransferase	2.58	6.00
	YLR449W	FPR4	FKBP Proline Rotamase (isomerase)	3.00	8.03
	YBR034C	HMT1	HnRNPMethylTransferase	3.80	13.90
	YDL014W	NOP1	NucleOlar Protein	3.33	10.03
	YDR465C	RMT2	aRginineMeThyltransferase	3.02	8.09
ion transport	YML116W	ATR1	AminoTriazole Resistance	2.56	5.89
	YBR291C	CTP1	Citrate Transport Protein	2.47	5.54
	YJR054W	KCH1	Potassium (K) regulator of CcH1	2.90	7.45
	YOR306C	MCH5	MonoCarboxylate transporter Homologue	3.10	8.56
	YGR138C	TPO2	Transporter of POlyamines	2.83	7.12

Table A. 1 (continued) : Down-regulated genes (about two-fold and higher) in H7 based on microarray results, according to metabolic processes.

ion transport	YMR241W	YHM2	Yeast suppressor of HM mutant	2.78	6.85
	YGL255W	ZRT1	Zinc-Regulated Transporter	5.64	49.79
DNA replication	YHR085W	IPI1	Involved in Processing ITS2	2.85	7.21
	YNL182C	IPI3	Involved in Processing ITS2	3.57	11.87
	YLR002C	NOC3	NucleOlar Complex associated	2.64	6.21
	YGR103W	NOP7	NucleOlar Protein	3.13	8.73
	YML060W	OGG1	8-OxoGuanine Glycosylase/lyase	2.61	6.09
	YHR197W	RIX1	RIbosomeeXport	2.71	6.55
cytoskeleton organization	YKR083C	DAD2	Duo1 And Dam1 interacting	3.06	8.35
	YDR130C	FIN1	Filaments In between Nuclei	2.53	5.79
	YJR070C	LIA1	Ligand of eIF5A	2.71	6.53
	YNL289W	PCL1	Pho85 CycLin	2.40	5.26
	YGR245C	SDA1	Severe Depolymerization of Actin	5.70	51.87
mRNA processing	YCR063W	BUD31	BUD site selection	2.39	5.25
	YMR268C	PRP24	Pre-mRNA Processing	4.52	22.88
	YGL120C	PRP43	Pre-mRNA Processing	2.78	6.87
	YMR061W	RNA14	poly(A) mRNA metabolism	3.45	10.92
	YEL026W	SNU13	Small NUclear ribonucleoprotein associated	3.64	12.49
RNA splicing	Q0110	BI2		6.36	82.20
	YCR063W	BUD31	BUD site selection	2.39	5.25
	YMR268C	PRP24	Pre-mRNA Processing	4.52	22.88
	YGL120C	PRP43	Pre-mRNA Processing	2.78	6.87
	YEL026W	SNU13	Small NUclear ribonucleoprotein associated	3.64	12.49
regulation of protein modification process	YMR199W	CLN1	CycLiN	2.83	7.13
	YPL256C	CLN2	CycLiN	2.51	5.69
	YDR130C	FIN1	Filaments In between Nuclei	2.53	5.79
	YLR449W	FPR4	FKBP Proline Rotamase (isomerase)	3.00	8.03
	YNL289W	PCL1	Pho85 CycLin	2.40	5.26
snoRNA processing	YLR175W	CBF5	Centromere Binding Factor	3.61	12.20
	YJL050W	MTR4	MrnaTRansport	2.83	7.11
	YDL014W	NOP1	NucleOlar Protein	3.33	10.03
	YHR062C	RPP1	Ribonuclease P Protein	2.40	5.28
	YNL299W	TRF5	Topoisomerase one-Related Function	2.59	6.04
generation of precursor metabolites and energy	YGL256W	ADH4	Alcohol DeHydrogenase	5.36	41.21
	YGR177C	ATF2	AcetylTransFerase	2.62	6.17

Table A. 1 (continued) : Down-regulated genes (about two-fold and higher) in H7 based on microarray results, according to metabolic processes.

generation of precursor metabolites and energy	YLR134W	PDC5	Pyruvate DeCarboxylase	4.05	16.59
	YLR273C	PIG1	Protein Interacting with Gsy2p	4.83	28.36
	YBR238C	YBR238C		2.64	6.25
chromosome segregation	YKR083C	DAD2	Duo1 And Dam1 interacting	3.06	8.35
	YDR130C	FIN1	Filaments In between Nuclei	2.53	5.79
	YOR233W	KIN4	KINase	3.21	9.27
	YLR263W	RED1	REDuctional division	2.46	5.50
	YDR180W	SCC2	Sister Chromatid Cohesion	2.37	5.17
nucleobase-containing compound transport	YER056C	FCY2	FluoroCYtosine resistance	3.16	8.93
	YBL042C	FUI1	5-FlUorourIdine resistance	3.56	11.77
	YBR034C	HMT1	HnRNPMethylTransferase	3.80	13.90
	YPL226W	NEW1	Nu+	2.88	7.34
	YGR128C	UTP8	U Three Protein	2.75	6.74
regulation of translation	YBR271W	EFM2	Elongation Factor Methyltransferase	3.72	13.16
	YDR496C	PUF6	PUmilio-homology domain Family	2.98	7.88
	YDR091C	RLI1	RNase L Inhibitor	2.73	6.64
	YNL209W	SSB2	Stress-Seventy subfamily B	2.39	5.24
	YGL169W	SUA5	Suppressor of Upstream AUG	2.36	5.12
protein phosphorylation	YMR199W	CLN1	CycLiN	2.83	7.13
	YPL256C	CLN2	CycLiN	2.51	5.69
	YOR233W	KIN4	KINase	3.21	9.27
	YNL289W	PCL1	Pho85 CycLin	2.40	5.26
lipid metabolic process	YDR147W	EKI1	Ethanolamine KInase	2.90	7.47
	YJL167W	ERG20	ERGosterol biosynthesis	6.99	127.04
	YBL039C	URA7	URAcil requiring	3.36	10.26
	YGR177C	ATF2	AcetylTransFerase	2.62	6.17
protein complex biogenesis	YFL026W	STE2	STErile	2.50	5.64
	YOR145C	PNO1	Partner of NOb1	2.55	5.84
	YKR083C	DAD2	Duo1 And Dam1 interacting	3.06	8.35
	YLR449W	FPR4	FKBP Proline Rotamase (isomerase)	3.00	8.03
meiotic cell cycle	YGL099W	LSG1	Large-Subunit Gtpase	2.51	5.71
	YLR263W	RED1	REDuctional division	2.46	5.50
	YPL130W	SPO19	SPOrulation	3.11	8.65
	YIR026C	YVH1	Yeast vaccinia virus VH1 Homolog	3.14	8.80
cell wall organization or biogenesis	YNL313C	EMW1	Essential for Maintenance of the cell Wall	2.55	5.87

Table A. 1 (continued) : Down-regulated genes (about two-fold and higher) in H7 based on microarray results, according to metabolic processes.

cell wall organization or biogenesis	YDR144C	MKC7	Multicopy suppressor of Kex2 Cold sensitivity	2.86	7.26
	YHL011C	PRS3	PhosphoRibosylpyrophosphateSynthetase	2.52	5.74
	YIR026C	YVH1	Yeast vaccinia virus VH1 Homolog	3.14	8.80
regulation of DNA metabolic process	YHR085W	IPI1	Involved in Processing ITS2	2.85	7.21
	YNL182C	IPI3	Involved in Processing ITS2	3.57	11.87
	YHR197W	RIX1	RIbosomeeXport	2.71	6.55
	YOR359W	VTS1	VTi1-2 Suppressor	2.35	5.10
cytoplasmic translation	YAL036C	RBG1	RiBosome interacting Gtpase	2.72	6.59
	YBR079C	RPG1		3.43	10.78
	YCL037C	SRO9	Suppressor of rho3	2.43	5.37
	YNL209W	SSB2	Stress-Seventy subfamily B	2.39	5.24
cellular response to DNA damage stimulus	YER038C	KRE29	Killer toxin REsistant	3.41	10.65
	YML060W	OGG1	8-OxoGuanine Glycosylase/lyase	2.61	6.09
	YDR180W	SCC2	Sister Chromatid Cohesion	2.37	5.17
carbohydrate metabolic process	YLR134W	PDC5	Pyruvate DeCarboxylase	4.05	16.59
	YLR273C	PIG1	Protein Interacting with Gsy2p	4.83	28.36
	YOR047C	STD1	Suppressor of Tbp Deletion	2.65	6.26
translational initiation	YDR091C	RLI1	RNase L Inhibitor	2.73	6.64
	YBR079C	RPG1		3.43	10.78
	YGR054W	YGR054W		2.95	7.75
DNA repair	YER038C	KRE29	Killer toxin REsistant	3.41	10.65
	YML060W	OGG1	8-OxoGuanine Glycosylase/lyase	2.61	6.09
	YDR180W	SCC2	Sister Chromatid Cohesion	2.37	5.17
cytokinesis	YDR184C	ATC1	Aip Three Complex	2.79	6.93
	YCR047C	BUD23	BUD site selection	2.39	5.24
	YCR063W	BUD31	BUD site selection	2.39	5.25
transcription from RNA polymerase III promoter	YBR154C	RPB5	RNA Polymerase B	2.60	6.08
	YPR110C	RPC40	RNA Polymerase C	2.52	5.73
	YDL150W	RPC53	RNA Polymerase C	3.93	15.29
sporulation	YGL099W	LSG1	Large-Subunit Gtpase	2.51	5.71
	YPL130W	SPO19	SPOrulation	3.11	8.65
	YIR026C	YVH1	Yeast vaccinia virus VH1 Homolog	3.14	8.80
translational elongation	YNL209W	SSB2	Stress-Seventy subfamily B	2.39	5.24
	YGL169W	SUA5	Suppressor of Upstream AUG	2.36	5.12
	YLR249W	YEF3	Yeast Elongation Factor	2.67	6.37

Table A. 1 (continued) : Down-regulated genes (about two-fold and higher) in H7 based on microarray results, according to metabolic processes.

proteolysis involved in cellular protein catabolic process	YDR161W	ACL4	Assembly Chaperone of RpL4	2.43	5.38
	YDR130C	FIN1	Filaments In between Nuclei	2.53	5.79
	YOR233W	KIN4	KINase	3.21	9.27
cofactor metabolic process	YNL256W	FOL1	FOLic acid synthesis	2.37	5.18
	YLR134W	PDC5	Pyruvate DeCarboxylase	4.05	16.59
	YOR095C	RKI1	Ribose-5-phosphate Ketol-Isomerase	3.26	9.57
DNA-templated transcription, elongation	YBR034C	HMT1	HnRNPMethylTransferase	3.80	13.90
	YJL148W	RPA34	RNA Polymerase A	2.32	5.00
	YNL248C	RPA49	RNA Polymerase A	2.85	7.20
pseudohyphal growth	YLR083C	EMP70		2.38	5.21
	YER110C	KAP123	KAryoPherin	3.35	10.23
	YOR315W	SFG1	SuperFicialpseudohyphal Growth	2.73	6.62
DNA-templated transcription, termination	YLL035W	GRC3		4.54	23.18
	YBR034C	HMT1	HnRNPMethylTransferase	3.80	13.90
protein targeting	YER110C	KAP123	KAryoPherin	3.35	10.23
	YDL063C	SYO1	SYnchronizedimpOrt or SYmpOrtin	3.39	10.46
histone modification	YLR449W	FPR4	FKBP Proline Rotamase (isomerase)	3.00	8.03
	YDL014W	NOP1	NucleOlar Protein	3.33	10.03
chromatin organization	YLR449W	FPR4	FKBP Proline Rotamase (isomerase)	3.00	8.03
	YDL014W	NOP1	NucleOlar Protein	3.33	10.03
endosomal transport	YLR083C	EMP70		2.38	5.21
	YPL183C	RTT10	Regulator of Ty1 Transposition	2.83	7.13
DNA recombination	YJL208C	NUC1	NUClease	2.56	5.90
	YDR180W	SCC2	Sister Chromatid Cohesion	2.37	5.17
response to oxidative stress	YBL024W	NCL1	NuCLear protein	2.80	6.99
	YDR091C	RLI1	RNase L Inhibitor	2.73	6.64
cell budding	YDR184C	ATC1	Aip Three Complex	2.79	6.93
	YBR267W	REI1	REquired for Isotropic bud growth	3.18	9.08
cellular ion homeostasis	YDR184C	ATC1	Aip Three Complex	2.79	6.93
	YLR083C	EMP70		2.38	5.21
response to osmotic stress	YLR336C	SGD1	Suppressor of Glycerol Defect	2.74	6.67
	YOR047C	STD1	Suppressor of Tbp Deletion	2.65	6.26
response to starvation	YAL036C	RBG1	RiBosome interacting Gtpase	2.72	6.59
	YNL209W	SSB2	Stress-Seventy subfamily B	2.39	5.24
protein folding	YBR155W	CNS1	CyclophiliN Seven suppressor	2.55	5.87

Table A. 1 (continued) : Down-regulated genes (about two-fold and higher) in H7 based on microarray results, according to metabolic processes.

protein folding	YNL209W	SSB2	Stress-Seventy subfamily B	2.39	5.24
mitochondrion organization	YLR355C	ILV5	IsoLeucine-plus-Valine requiring	2.42	5.35
	YMR241W	YHM2	Yeast suppressor of HM mutant	2.78	6.85
protein dephosphorylation	YGR123C	PPT1	Protein Phosphatase T	2.89	7.41
	YIR026C	YVH1	Yeast vaccinia virus VH1 Homolog	3.14	8.80
protein modification by small protein conjugation or removal	YGR200C	ELP2	ELongator Protein	2.66	6.31
	YDR130C	FIN1	Filaments In between Nuclei	2.53	5.79
telomere organization	YML060W	OGG1	8-OxoGuanine Glycosylase/lyase	2.61	6.09
	YGL169W	SUA5	Suppressor of Upstream AUG	2.36	5.12
cellular respiration	YBR238C	YBR238C		2.64	6.25
vacuole organization	YIR026C	YVH1	Yeast vaccinia virus VH1 Homolog	3.14	8.80
monocarboxylic acid metabolic process	YLR134W	PDC5	Pyruvate DeCarboxylase	4.05	16.59
invasive growth in response to glucose limitation	YLR083C	EMP70		2.38	5.21
vitamin metabolic process	YOR095C	RKI1	Ribose-5-phosphate Ketol-Isomerase	3.26	9.57
endocytosis	YBR266C	SLM6	Synthetic Lethal with Mss4	3.52	11.46
tRNAaminoacylation for protein translation	YHR020W	YHR020W		2.56	5.90

Table A. 2 : Up-regulated genes (two-fold and higher) in H7, based on microarray results, accroding to metabolic processes.

Process Name	Systematic Gene Symbol	Standard Gene Symbol	Gene Name	Fold Change (absolute)	Fold Change (log2)
carbohydrate metabolic process	YGL156W	AMS1	Alpha-MannoSidase	3.32	9.96
	YBR149W	ARA1	D-ARAbinose dehydrogenase	2.34	5.06
	YPR026W	ATH1	Acid TreHalase	3.25	9.49
	YMR280C	CAT8	CATabolite repression	4.10	17.17
	YLR377C	FBP1	Fructose-1,6-BisPhosphatase	3.10	8.58
	YIL097W	FYV10	Function required for Yeast Viability	2.78	6.88
	YOR178C	GAC1	Glycogen ACcumulation	3.78	13.73
	YLR081W	GAL2	GALactose metabolism	3.33	10.07
	YBR018C	GAL7	GALactose metabolism	4.23	18.70
	YOR120W	GCY1	Galactose-inducible Crystallin-like Yeast protein	3.86	14.57
	YPR184W	GDB1	Glycogen DeBranching	3.24	9.42
	YER054C	GIP2	Glc7-Interacting Protein	3.67	12.76
	YEL011W	GLC3	GLyCogen	4.28	19.43
	YCL040W	GLK1	GLucoKinase	3.90	14.89
	YPR160W	GPH1	Glycogen PHosphorylase	6.83	113.86
	YHR104W	GRE3	Genes de Respuesta a Estres (stress responsive genes)	2.78	6.89
	YFR015C	GSY1	Glycogen SYnthase	4.76	27.17
	YLR258W	GSY2	Glycogen SYnthase	3.55	11.72
	YIL155C	GUT2	Glycerol UTilization	4.07	16.78
	YFR053C	HXK1	HeXoKinase	7.63	198.00
	YER065C	ICL1	IsoCitrateLyase	2.72	6.59
	YFR017C	IGD1	Inhibitor of Glycogen Debranching	4.55	23.43
	YGR289C	MAL11	MALtose fermentation	3.94	15.39
	YGR292W	MAL12	MALtose fermentation	4.85	28.82
	YBR299W	MAL32	MALtose	4.51	22.75
	YOL126C	MDH2	Malate DeHydrogenase	2.82	7.05
	YNL117W	MLS1	MaLate Synthase	3.16	8.94
	YDL085W	NDE2	NADH Dehydrogenase, External	4.16	17.82
	YDR001C	NTH1	Neutral TreHalase	2.37	5.16
	YOL032W	OPI10	OverProducer of Inositol	2.61	6.10
	YKR097W	PCK1	Phosphoenolpyruvate CarboxyKinase	3.55	11.70
	YMR105C	PGM2	PhosphoGlucoMutase	5.33	40.19
	YDR255C	RMD5	Required for Meiotic nuclear Division	2.56	5.91
	YDR511W	SDH7	Succinate DeHydrogenase	2.36	5.14
	YIL099W	SGA1	Sporulation-specific GlycoAmylase	4.84	28.72
	YJL089W	SIP4	SNF1-Interacting Protein	2.53	5.77

Table A. 2 (continued): Up-regulated genes (two-fold and higher) in H7, based on microarray results, accroding to metabolic processes.

carbohydrate metabolic process	YBR126C	TPS1	Trehalose-6-Phosphate Synthase	2.45	5.45
	YDR074W	TPS2	Trehalose-6-Phosphate Synthase/phosphatase	2.98	7.91
	YML100W	TSL1	Trehalose Synthase Long chain	5.39	42.01
	YEL012W	UBC8	UBiquitin-Conjugating	2.99	7.96
	YKL035W	UGP1	UDP-glucose pyrophosphorylase	2.63	6.20
	YGR194C	XKS1	XyluloKinaSe	3.00	7.99
	YLR070C	XYL2		2.44	5.41
	YJR096W	YJR096W		4.27	19.26
	YLR345W	YLR345W		2.61	6.12
response to chemical	YDR216W	ADR1	Alcohol Dehydrogenase II synthesis Regulator	3.08	8.45
	YPR026W	ATH1	Acid TreHalase	3.25	9.49
	YNL305C	BXI1	BaX Inhibitor	2.62	6.13
	YMR280C	CAT8	CATabolite repression	4.10	17.17
	YKR066C	CCP1	Cytochrome c Peroxidase	2.48	5.56
	YOR028C	CIN5	Chromosome INstability	4.51	22.79
	YGR088W	CTT1	CaTalase T	5.37	41.30
	YHR053C	CUP1-1	Cu, copper, CUPrum	2.77	6.84
	YHR055C	CUP1-2	Cu, copper, CUPrum	2.71	6.52
	YOL052C-A	DDR2	DNA Damage Responsive	7.00	127.65
	YMR250W	GAD1	GlutAmate Decarboxylase	4.03	16.29
	YOR120W	GCY1	Galactose-inducible Crystallin-like Yeast protein	3.86	14.57
	YKL026C	GPX1	Glutathione PeroXidase	3.45	10.92
	YHR104W	GRE3	Genes de Respuesta a Estres (stress responsive genes)	2.78	6.89
	YCL035C	GRX1	GlutaRedoXin	3.91	15.08
	YDR513W	GRX2	GlutaRedoXin	3.59	12.05
	YDL223C	HBT1	HuB1 Target	3.99	15.94
	YFL014W	HSP12	Heat Shock Protein	8.44	348.27
	YCR091W	KIN82	protein KINase	2.51	5.69
	YKL150W	MCR1	Mitochondrial NADH-Cytochrome b5 Reductase	2.50	5.65
	YNL036W	NCE103	NonClassical Export	4.86	29.01
	YGR043C	NQM1	Non-Quiescent Mutant	6.36	82.18
	YBR066C	NRG2	Negative Regulator of Glucose-controlled genes	2.52	5.73
	YDR001C	NTH1	Neutral TreHalase	2.37	5.16
	YPL196W	OXR1	OXidation Resistance	2.39	5.24
	YDR406W	PDR15	Pleiotropic Drug Resistance	2.70	6.48
	YDL214C	PRR2	Pheromone Response Regulator	5.77	54.73
	YBL064C	PRX1	PeroxiRedoXin	3.73	13.31
	YOL117W	RRI2		2.68	6.40
	YMR175W	SIP18	Salt Induced Protein	4.56	23.63
	YJL089W	SIP4	SNF1-Interacting Protein	2.53	5.77

Table A. 2 (continued): Up-regulated genes (two-fold and higher) in H7, based on microarray results, accroding to metabolic processes.

response to chemical	YKL086W	SRX1	SulfiRedoXin	4.31	19.85
	YGR008C	STF2	STabilizing Factor	3.36	10.28
	YBR126C	TPS1	Trehalose-6-Phosphate Synthase	2.45	5.45
	YDR453C	TSA2	Thiol-Specific Antioxidant	3.45	10.94
	YPL230W	USV1	Up in StarVation	4.53	23.03
	YIL101C	XBP1	XhoI site-Binding Protein	4.12	17.36
	YJL144W	YJL144W		3.82	14.11
	YJR096W	YJR096W		4.27	19.26
	YBR046C	ZTA1	ZeTA-crystallin	3.11	8.62
generation of precursor metabolites and energy	YNR001C	CIT1	CITrate synthase	2.34	5.08
	Q0105	COB	CytochrOme B	2.56	5.88
	Q0045	COX1	Cytochrome c OXidase	2.65	6.29
	YIL111W	COX5B	Cytochrome c OXidase	3.99	15.85
	YMR256C	COX7	Cytochrome c OXidase	2.82	7.08
	YEL039C	CYC7	CYtochrome C	9.09	544.69
	YBR026C	ETR1	2-Enoyl Thioester Reductase	3.31	9.94
	YOR178C	GAC1	Glycogen ACcumulation	3.78	13.73
	YPR184W	GDB1	Glycogen DeBranching	3.24	9.42
	YER054C	GIP2	Glc7-Interacting Protein	3.67	12.76
	YEL011W	GLC3	GLyCogen	4.28	19.43
	YCL040W	GLK1	GLucoKinase	3.90	14.89
	YPR160W	GPH1	Glycogen PHosphorylase	6.83	113.86
	YFR015C	GSY1	Glycogen SYnthase	4.76	27.17
	YLR258W	GSY2	Glycogen SYnthase	3.55	11.72
	YFR053C	HXK1	HeXoKinase	7.63	198.00
	YFR017C	IGD1	Inhibitor of Glycogen Debranching	4.55	23.43
	YMR081C	ISF1	Increasing Suppression Factor	5.82	56.53
	YKL093W	MBR1	Mitochondrial Biogenesis Regulation	5.41	42.57
	YDL085W	NDE2	NADH Dehydrogenase, External	4.16	17.82
	YML120C	NDI1	NADH Dehydrogenase Internal	2.37	5.16
	YMR105C	PGM2	PhosphoGlucoMutase	5.33	40.19
	YHR001W-A	QCR10	ubiQuinol-cytochrome C oxidoReductase	2.55	5.86
	YGR183C	QCR9	ubiQuinol-cytochrome C oxidoReductase	2.37	5.17
	YER067W	RGI1	Respiratory Growth Induced	6.00	64.09
	YIL057C	RGI2	Respiratory growth induced	7.69	206.80
	YIL099W	SGA1	Sporulation-specific GlycoAmylase	4.84	28.72
	YLR164W	SHH4	SDH4 Homolog	2.86	7.25
	YKL035W	UGP1	UDP-glucose pyrophosphorylase	2.63	6.20
	YLR345W	YLR345W		2.61	6.12
	YFR049W	YMR31	Yeast Mitochondrial Ribosomal protein	2.54	5.83

Table A. 2 (continued): Up-regulated genes (two-fold and higher) in H7, based on microarray results, accroding to metabolic processes.

nucleobase-containing small molecule metabolic process	YOR374W	ALD4	ALdehyde Dehydrogenase	5.22	37.39
	Q0105	COB	CytochrOme B	2.56	5.88
	Q0045	COX1	Cytochrome c OXidase	2.65	6.29
	YIL111W	COX5B	Cytochrome c OXidase	3.99	15.85
	YMR256C	COX7	Cytochrome c OXidase	2.82	7.08
	YEL039C	CYC7	CYtochrome C	9.09	544.69
	YCL040W	GLK1	GLucoKinase	3.90	14.89
	YGR256W	GND2	6-phosphoGlucoNateDehydrogenase	4.73	26.59
	YDL022W	GPD1	Glycerol-3-Phosphate Dehydrogenase	2.56	5.90
	YIL155C	GUT2	Glycerol UTilization	4.07	16.78
	YFR053C	HXK1	HeXoKinase	7.63	198.00
	YDL085W	NDE2	NADH Dehydrogenase, External	4.16	17.82
	YML120C	NDI1	NADH Dehydrogenase Internal	2.37	5.16
	YER037W	PHM8	PHosphate Metabolism	2.58	5.96
	YGL037C	PNC1	Pyrazinamidase and NiCotinamidase	2.96	7.80
	YHR001W-A	QCR10	ubiQuinol-cytochrome C oxidoReductase	2.55	5.86
	YGR183C	QCR9	ubiQuinol-cytochrome C oxidoReductase	2.37	5.17
	YLR164W	SHH4	SDH4 Homolog	2.86	7.25
	YGR248W	SOL4	Suppressor Of Los1-1	5.17	36.03
	YBR117C	TKL2	TransKetoLase	6.52	91.77
	YMR271C	URA10	URAcil requiring	3.77	13.65
	YKL151C	YKL151C		3.75	13.44
	YLR345W	YLR345W		2.61	6.12
	YNL200C	YNL200C		3.49	11.22
response to oxidative stress	YKR066C	CCP1	Cytochrome c Peroxidase	2.48	5.56
	YGR088W	CTT1	CaTalase T	5.37	41.30
	YHR053C	CUP1-1	Cu, copper, CUPrum	2.77	6.84
	YHR055C	CUP1-2	Cu, copper, CUPrum	2.71	6.52
	YOL052C-A	DDR2	DNA Damage Responsive	7.00	127.65
	YMR250W	GAD1	GlutAmate Decarboxylase	4.03	16.29
	YOR120W	GCY1	Galactose-inducible Crystallin-like Yeast protein	3.86	14.57
	YKL026C	GPX1	Glutathione PeroXidase	3.45	10.92
	YHR104W	GRE3	Genes de Respuesta a Estres (stress responsive genes)	2.78	6.89
	YCL035C	GRX1	GlutaRedoXin	3.91	15.08
	YDR513W	GRX2	GlutaRedoXin	3.59	12.05
	YFL014W	HSP12	Heat Shock Protein	8.44	348.27
	YKL150W	MCR1	Mitochondrial NADH-Cytochrome b5 Reductase	2.50	5.65
	YNL036W	NCE103	NonClassical Export	4.86	29.01
	YGR043C	NQM1	Non-Quiescent Mutant	6.36	82.18
	YPL196W	OXR1	OXidation Resistance	2.39	5.24

Table A. 2 (continued): Up-regulated genes (two-fold and higher) in H7, based on microarray results, accroding to metabolic processes.

response to oxidative stress	YBL064C	PRX1	PeroxiRedoXin	3.73	13.31
	YKL086W	SRX1	SulfiRedoXin	4.31	19.85
	YBR126C	TPS1	Trehalose-6-Phosphate Synthase	2.45	5.45
	YDR453C	TSA2	Thiol-Specific Antioxidant	3.45	10.94
	YIL101C	XBP1	XhoI site-Binding Protein	4.12	17.36
	YJR096W	YJR096W		4.27	19.26
	YBR046C	ZTA1	ZeTA-crystallin	3.11	8.62
transmembrane transport	YCR010C	ADY2	Accumulation of DYads	6.24	75.37
	YBR132C	AGP2	high-Affinity Glutamine Permease	3.31	9.91
	YPR192W	AQY1	AQuaporin from Yeast	3.89	14.86
	YDR039C	ENA2	ExitusNAtru (Latin, "exit sodium")	5.22	37.24
	YDL022W	GPD1	Glycerol-3-Phosphate Dehydrogenase	2.56	5.90
	YDL245C	HXT15	HeXose Transporter	2.80	6.98
	YDR343C	HXT6	HeXose Transporter	6.38	83.18
	YDR342C	HXT7	HeXose Transporter	6.30	78.62
	YKL217W	JEN1		6.12	69.70
	YOL126C	MDH2	Malate DeHydrogenase	2.82	7.05
	YGL080W	MPC1	Mitochondrial Pyruvate Carrier	2.50	5.65
	YGR243W	MPC3	Mitochondrial Pyruvate Carrier	6.77	109.47
	YNL214W	PEX17	PEroXisome related	2.36	5.15
	YHR160C	PEX18	PEroXin	4.02	16.24
	YAL005C	SSA1	Stress-Seventy subfamily A	2.70	6.50
	YER103W	SSA4	Stress-Seventy subfamily A	4.18	18.14
	YDR536W	STL1	Sugar Transporter-Like protein	6.91	119.88
	YGL104C	VPS73	Vacuolar Protein Sorting	2.59	6.00
	YFL054C	AQY3	AQuaporin from Yeast	3.37	10.35
meiotic cell cycle	YPR192W	AQY1	AQuaporin from Yeast	3.89	14.86
	YPL200W	CSM4	Chromosome Segregation in Meiosis	4.44	21.75
	YKL096W	CWP1	Cell Wall Protein	4.64	24.95
	YDR516C	EMI2	Early Meiotic Induction	4.81	27.98
	YDL222C	FMP45	Found in Mitochondrial Proteome	7.89	238.02
	YOR178C	GAC1	Glycogen ACcumulation	3.78	13.73
	YGL192W	IME4	Inducer of MEiosis	3.19	9.10
	YPL017C	IRC15	Increased Recombination Centers	4.27	19.36
	YOR351C	MEK1	MEiotic Kinase	3.37	10.35
	YML128C	MSC1	Meiotic Sister-Chromatid recombination	5.12	34.66
	YLR054C	OSW2	Outer Spore Wall	3.05	8.26
	YHL024W	RIM4	Regulator of IME2	3.17	8.98
	YGL250W	RMR1	Reduced Meiotic Recombination	2.98	7.87
	YOL048C	RRT8	Regulator of rDNA Transcription	4.15	17.72

Table A. 2 (continued): Up-regulated genes (two-fold and higher) in H7, based on microarray results, accroding to metabolic processes.

meiotic cell cycle	YNL196C	SLZ1		7.27	154.70
	YGR059W	SPR3	SPorulation Regulated	2.60	6.08
	YLL039C	UBI4	Ubiquitin	3.04	8.25
	YNL194C	YNL194C		8.30	315.45
monocarboxylic acid metabolic process	YBL015W	ACH1	Acetyl CoA Hydrolase	2.72	6.61
	YDR216W	ADR1	Alcohol Dehydrogenase II synthesis Regulator	3.08	8.45
	YOR374W	ALD4	ALdehyde Dehydrogenase	5.22	37.39
	YML042W	CAT2	Carnitine AcetylTransferase	3.52	11.50
	YMR280C	CAT8	CATabolite repression	4.10	17.17
	YOR100C	CRC1	CaRnitine Carrier	4.24	18.94
	YML054C	CYB2	CYtochrome B	4.46	22.01
	YBR026C	ETR1	2-Enoyl Thioester Reductase	3.31	9.94
	YKR009C	FOX2	Fatty acid OXidation	2.53	5.76
	YCL040W	GLK1	GLucoKinase	3.90	14.89
	YML004C	GLO1	GLyOxalase	3.38	10.40
	YFR053C	HXK1	HeXoKinase	7.63	198.00
	YER065C	ICL1	IsoCitrateLyase	2.72	6.59
	YNL117W	MLS1	MaLate Synthase	3.16	8.94
	YDL085W	NDE2	NADH Dehydrogenase, External	4.16	17.82
	YIL160C	POT1	PeroxisomalOxoacylThiolase	5.23	37.50
	YLR345W	YLR345W		2.61	6.12
ion transport	YCR010C	ADY2	Accumulation of DYads	6.24	75.37
	YBR132C	AGP2	high-Affinity Glutamine Permease	3.31	9.91
	YNR002C	ATO2	Ammonia (Ammonium) Transport Outward	5.99	63.54
	YGR142W	BTN2	BaTteN disease	3.39	10.48
	YDR039C	ENA2	ExitusNAtru (Latin, "exit sodium")	5.22	37.24
	YKL187C	FAT3	FATty acid transporter 3	2.42	5.34
	YKL217W	JEN1		6.12	69.70
	YCR091W	KIN82	protein KINase	2.51	5.69
	YPL060W	MFM1	Mrs2 Function Modulating factor	2.33	5.02
	YGL080W	MPC1	Mitochondrial Pyruvate Carrier	2.50	5.65
	YGR243W	MPC3	Mitochondrial Pyruvate Carrier	6.77	109.47
	YKR052C	MRS4	Mitochondrial RNA Splicing	2.36	5.14
	YOR348C	PUT4	Proline UTilization	4.04	16.46
	YOR049C	RSB1	Resistance to Sphingoid long-chain Base	3.79	13.84
	YJR095W	SFC1	Succinate-Fumarate Carrier	5.05	33.06
	YLL055W	YCT1	Yeast Cysteine Transporter	2.63	6.19
cofactor metabolic process	YOR374W	ALD4	ALdehyde Dehydrogenase	5.22	37.39
	YNR001C	CIT1	CITrate synthase	2.34	5.08
	YCL040W	GLK1	GLucoKinase	3.90	14.89

Table A. 2 (continued): Up-regulated genes (two-fold and higher) in H7, based on microarray results, accroding to metabolic processes.

cofactor metabolic process	YGR256W	GND2	6-phosphoGlucoNateDehydrogenase	4.73	26.59
	YDL022W	GPD1	Glycerol-3-Phosphate Dehydrogenase	2.56	5.90
	YIL155C	GUT2	Glycerol UTilization	4.07	16.78
	YFR053C	HXK1	HeXoKinase	7.63	198.00
	YDL085W	NDE2	NADH Dehydrogenase, External	4.16	17.82
	YML120C	NDI1	NADH Dehydrogenase Internal	2.37	5.16
	YGL037C	PNC1	Pyrazinamidase and NiCotinamidase	2.96	7.80
	YGR248W	SOL4	Suppressor Of Los1-1	5.17	36.03
	YBR117C	TKL2	TransKetoLase	6.52	91.77
	YKL151C	YKL151C		3.75	13.44
	YLR345W	YLR345W		2.61	6.12
	YNL200C	YNL200C		3.49	11.22
protein targeting	YBR128C	ATG14	AuTophaGy related	2.79	6.90
	YBL078C	ATG8	AuTophaGy related	2.99	7.93
	YDR358W	GGA1	Golgi-localized, Gamma-adaptin ear homology, Arf-binding protein	2.67	6.38
	YDL022W	GPD1	Glycerol-3-Phosphate Dehydrogenase	2.56	5.90
	YPL240C	HSP82	Heat Shock Protein	2.87	7.29
	YOL126C	MDH2	Malate DeHydrogenase	2.82	7.05
	YBR230C	OM14	Outer Membrane Protein of 14 kDa	5.18	36.25
	YNL214W	PEX17	PEroXisome related	2.36	5.15
	YHR160C	PEX18	PEroXin	4.02	16.24
	YHR136C	SPL2	Suppressor of PLc1 deletion	3.32	9.98
	YAL005C	SSA1	Stress-Seventy subfamily A	2.70	6.50
	YER103W	SSA4	Stress-Seventy subfamily A	4.18	18.14
	YGL104C	VPS73	Vacuolar Protein Sorting	2.59	6.00
	YNL093W	YPT53	Yeast Protein Two	5.40	42.27
cellular respiration	YNR001C	CIT1	CITrate synthase	2.34	5.08
	Q0105	COB	CytochrOme B	2.56	5.88
	Q0045	COX1	Cytochrome c OXidase	2.65	6.29
	YIL111W	COX5B	Cytochrome c OXidase	3.99	15.85
	YMR256C	COX7	Cytochrome c OXidase	2.82	7.08
	YEL039C	CYC7	CYtochrome C	9.09	544.69
	YBR026C	ETR1	2-Enoyl Thioester Reductase	3.31	9.94
	YMR081C	ISF1	Increasing Suppression Factor	5.82	56.53
	YKL093W	MBR1	Mitochondrial Biogenesis Regulation	5.41	42.57
	YML120C	NDI1	NADH Dehydrogenase Internal	2.37	5.16
	YHR001W-A	QCR10	ubiQuinol-cytochrome C oxidoReductase	2.55	5.86
	YGR183C	QCR9	ubiQuinol-cytochrome C oxidoReductase	2.37	5.17
	YLR164W	SHH4	SDH4 Homolog	2.86	7.25
	YFR049W	YMR31	Yeast Mitochondrial Ribosomal protein	2.54	5.83

Table A. 2 (continued): Up-regulated genes (two-fold and higher) in H7, based on microarray results, accroding to metabolic processes.

transcription from RNA polymerase II promoter	YDR216W	ADR1	Alcohol Dehydrogenase II synthesis Regulator	3.08	8.45
	YMR280C	CAT8	CATabolite repression	4.10	17.17
	YOR028C	CIN5	Chromosome INstability	4.51	22.79
	YPR030W	CSR2	Chs5 Spa2 Rescue	4.55	23.42
	YDR516C	EMI2	Early Meiotic Induction	4.81	27.98
	YDR096W	GIS1	GIg1-2 Suppressor	2.36	5.13
	YIR017C	MET28	METhionine	2.4	5.28
	YDR253C	MET32	METhionine requiring	2.94	7.69
	YBR066C	NRG2	Negative Regulator of Glucose-controlled genes	2.52	5.73
	YDL214C	PRR2	Pheromone Response Regulator	5.77	54.73
	YBR050C	REG2	REsistance to Glucose repression	3.89	14.83
	YJL089W	SIP4	SNF1-Interacting Protein	2.53	5.77
	YPL230W	USV1	Up in StarVation	4.53	23.03
	YIL101C	XBP1	XhoI site-Binding Protein	4.12	17.36
cellular amino acid metabolic process	YFL030W	AGX1	Alanine:Glyoxylateaminotrans(X)ferase	3.87	14.66
	YMR169C	ALD3	ALdehyde Dehydrogenase	6.75	107.85
	YHR137W	ARO9	AROmatic amino acid requiring	3.74	13.34
	YPL111W	CAR1	Catabolism of ARginine	3.53	11.59
	YLR438W	CAR2	Catabolism of ARginine	3.20	9.18
	YNR001C	CIT1	CITrate synthase	2.34	5.08
	YMR250W	GAD1	GlutAmate Decarboxylase	4.03	16.29
	YAL062W	GDH3	Glutamate DeHydrogenase	3.06	8.34
	YIR017C	MET28	METhionine	2.40	5.28
	YDR253C	MET32	METhionine requiring	2.94	7.69
	YGR087C	PDC6	Pyruvate DeCarboxylase	2.71	6.54
	YLR142W	PUT1	Proline UTilization	3.16	8.95
mitochondrion organization	YHL021C	AIM17	Altered Inheritance rate of Mitochondria	4.44	21.67
	YPL166W	ATG29	AuTophaGy related	2.34	5.06
	YBL078C	ATG8	AuTophaGy related	2.99	7.93
	YDR258C	HSP78	Heat Shock Protein	3.26	9.58
	YPL240C	HSP82	Heat Shock Protein	2.87	7.29
	YBR230C	OM14	Outer Membrane Protein of 14 kDa	5.18	36.25
	YGR183C	QCR9	ubiQuinol-cytochrome C oxidoReductase	2.37	5.17
	YDR379C-A	SDH6		4.36	20.54
	YDR511W	SDH7	Succinate DeHydrogenase	2.36	5.14
	YAL005C	SSA1	Stress-Seventy subfamily A	2.70	6.50
	YFR049W	YMR31	Yeast Mitochondrial Ribosomal protein	2.54	5.83
	YOR019W	YOR019W		3.41	10.61
lipid metabolic process	YDR216W	ADR1	Alcohol Dehydrogenase II synthesis Regulator	3.08	8.45
	YCR068W	ATG15	AuTophaGy related	2.92	7.59

Table A. 2 (continued): Up-regulated genes (two-fold and higher) in H7, based on microarray results, accroding to metabolic processes.

lipid metabolic process	YGR110W	CLD1	CardioLipin-specific Deacylase	3.36	10.27
	YOR100C	CRC1	CaRnitine Carrier	4.24	18.94
	YBR026C	ETR1	2-Enoyl Thioester Reductase	3.31	9.94
	YKR009C	FOX2	Fatty acid OXidation	2.53	5.76
	YDR096W	GIS1	GIg1-2 Suppressor	2.36	5.13
	YKR067W	GPT2	Glycerol-3-Phosphate acylTransferase	2.47	5.54
	YKL150W	MCR1	Mitochondrial NADH-Cytochrome b5 Reductase	2.50	5.65
	YIL160C	POT1	PeroxisomalOxoacylThiolase	5.23	37.50
	YDR018C	YDR018C		4.37	20.65
oligosaccharide metabolic process	YGL156W	AMS1	Alpha-MannoSidase	3.32	9.96
	YPR026W	ATH1	Acid TreHalase	3.25	9.49
	YGR289C	MAL11	MALtose fermentation	3.94	15.39
	YGR292W	MAL12	MALtose fermentation	4.85	28.82
	YBR299W	MAL32	MALtose	4.51	22.75
	YDR001C	NTH1	Neutral TreHalase	2.37	5.16
	YMR105C	PGM2	PhosphoGlucoMutase	5.33	40.19
	YBR126C	TPS1	Trehalose-6-Phosphate Synthase	2.45	5.45
	YDR074W	TPS2	Trehalose-6-Phosphate Synthase/phosphatase	2.98	7.91
	YML100W	TSL1	Trehalose Synthase Long chain	5.39	42.01
	YKL035W	UGP1	UDP-glucose pyrophosphorylase	2.63	6.20
carbohydrate transport	YLR081W	GAL2	GALactose metabolism	3.33	10.07
	YCL040W	GLK1	GLucoKinase	3.90	14.89
	YFR053C	HXK1	HeXoKinase	7.63	198.00
	YDL245C	HXT15	HeXose Transporter	2.80	6.98
	YMR011W	HXT2	HeXose Transporter	4.82	28.22
	YHR096C	HXT5	HeXose Transporter	6.62	98.13
	YDR343C	HXT6	HeXose Transporter	6.38	83.18
	YDR342C	HXT7	HeXose Transporter	6.30	78.62
	YGR289C	MAL11	MALtose fermentation	3.94	15.39
	YDR277C	MTH1	MSN Three Homolog	4.22	18.67
	YDR536W	STL1	Sugar Transporter-Like protein	6.91	119.88
response to heat	YPR158W	CUR1	Curing of [URe3]	2.66	6.33
	YOL052C-A	DDR2	DNA Damage Responsive	7.00	127.65
	YOR178C	GAC1	Glycogen ACcumulation	3.78	13.73
	YFL014W	HSP12	Heat Shock Protein	8.44	348.27
	YBR072W	HSP26	Heat Shock Protein	7.32	160.31
	YDR258C	HSP78	Heat Shock Protein	3.26	9.58
	YPL004C	LSP1	Long chain bases Stimulate Phosphorylation	2.41	5.33
	YDL079C	MRK1	Mds1p Related Kinase	6.31	79.14
	YER103W	SSA4	Stress-Seventy subfamily A	4.18	18.14

Table A. 2 (continued): Up-regulated genes (two-fold and higher) in H7, based on microarray results, accroding to metabolic processes.

response to heat	YBR126C	TPS1	Trehalose-6-Phosphate Synthase	2.45	5.45
	YDR074W	TPS2	Trehalose-6-Phosphate Synthase/phosphatase	2.98	7.91
protein phosphorylation	YJL057C	IKS1		3.44	10.83
	YCR091W	KIN82	protein KINase	2.51	5.69
	YPL004C	LSP1	Long chain bases Stimulate Phosphorylation	2.41	5.33
	YOR351C	MEK1	MEiotic Kinase	3.37	10.35
	YDL079C	MRK1	Mds1p Related Kinase	6.31	79.14
	YDL214C	PRR2	Pheromone Response Regulator	5.77	54.73
	YIL113W	SDP1	Stress-inducible Dual specificity Phosphatase	3.42	10.70
	YGL208W	SIP2	SNF1-Interacting Protein	2.36	5.12
	YMR291W	TDA1	Topoisomerase I Damage Affected	2.40	5.28
	YJL164C	TPK1	Takashi's Protein Kinase	2.95	7.70
sporulation	YPR192W	AQY1	AQuaporin from Yeast	3.89	14.86
	YKL096W	CWP1	Cell Wall Protein	4.64	24.95
	YDR516C	EMI2	Early Meiotic Induction	4.81	27.98
	YDL222C	FMP45	Found in Mitochondrial Proteome	7.89	238.02
	YLR054C	OSW2	Outer Spore Wall	3.05	8.26
	YHL024W	RIM4	Regulator of IME2	3.17	8.98
	YOL048C	RRT8	Regulator of rDNA Transcription	4.15	17.72
	YGR059W	SPR3	SPorulation Regulated	2.60	6.08
	YLL039C	UBI4	Ubiquitin	3.04	8.25
	YNL194C			8.30	315.45
signaling	YNL305C	BXI1	BaX Inhibitor	2.62	6.13
	YGL121C	GPG1	G Protein Gamma	4.41	21.29
	YDR277C	MTH1	MSN Three Homolog	4.22	18.67
	YGR070W	ROM1	RhO1 Multicopy suppressor	2.48	5.59
	YOL117W	RRI2		2.68	6.40
	YIL113W	SDP1	Stress-inducible Dual specificity Phosphatase	3.42	10.70
	YGL208W	SIP2	SNF1-Interacting Protein	2.36	5.12
	YIL105C	SLM1	Synthetic Lethal with Mss4	2.82	7.04
	YLR178C	TFS1	cdc Twenty-Five Suppressor	4.54	23.23
	YJL164C	TPK1	Takashi's Protein Kinase	2.95	7.70
protein complex biogenesis	YPL240C	HSP82	Heat Shock Protein	2.87	7.29
	YPL017C	IRC15	Increased Recombination Centers	4.27	19.36
	YGL087C	MMS2	Methyl MethaneSulfonate sensitivity	2.49	5.60
	YPR154W	PIN3	Psi+ INducibility	2.49	5.61
	YGR183C	QCR9	ubiQuinol-cytochrome C oxidoReductase	2.37	5.17
	YDR379C-A	SDH6		4.36	20.54
	YDR511W	SDH7	Succinate DeHydrogenase	2.36	5.14
	YGL208W	SIP2	SNF1-Interacting Protein	2.36	5.12
	YDL110C	TMA17	Translation Machinery Associated	3.54	11.63
response to osmotic stress	YOR028C	CIN5	Chromosome INstability	4.51	22.79
	YGR088W	CTT1	CaTalase T	5.37	41.30
	YDL022W	GPD1	Glycerol-3-Phosphate Dehydrogenase	2.56	5.90
	YHR104W	GRE3	Genes de Respuesta a Estres (stress responsive genes)	2.78	6.89
	YFL014W	HSP12	Heat Shock Protein	8.44	348.27
	YPL240C	HSP82	Heat Shock Protein	2.87	7.29

Table A. 2 (continued): Up-regulated genes (two-fold and higher) in H7, based on microarray results, accroding to metabolic processes.

response to osmotic stress	YDL079C	MRK1	Mds1p Related Kinase	6.31	79.14
	YBR066C	NRG2	Negative Regulator of Glucose-controlled genes	2.52	5.73
	YPL230W	USV1	Up in StarVation	4.53	23.03
organelle fission	YPL200W	CSM4	Chromosome Segregation in Meiosis	4.44	21.75
	YOR178C	GAC1	Glycogen ACcumulation	3.78	13.73
	YGL192W	IME4	Inducer of MEiosis	3.19	9.10
	YPL017C	IRC15	Increased Recombination Centers	4.27	19.36
	YOR351C	MEK1	MEiotic Kinase	3.37	10.35
	YML128C	MSC1	Meiotic Sister-Chromatid recombination	5.12	34.66
	YHL024W	RIM4	Regulator of IME2	3.17	8.98
	YGL250W	RMR1	Reduced Meiotic Recombination	2.98	7.87
	YNL196C	SLZ1		7.27	154.70
protein modification by small protein conjugation or removal	YNL077W	APJ1	Anti-Prion DnaJ	3.05	8.26
	YOR178C	GAC1	Glycogen ACcumulation	3.78	13.73
	YGL087C	MMS2	Methyl MethaneSulfonate sensitivity	2.49	5.60
	YDR255C	RMD5	Required for Meiotic nuclear Division	2.56	5.91
	YOL117W	RRI2		2.68	6.40
	YAL005C	SSA1	Stress-Seventy subfamily A	2.70	6.50
	YEL012W	UBC8	UBiquitin-Conjugating	2.99	7.96
	YLL039C	UBI4	Ubiquitin	3.04	8.25
	YPL003W	ULA1	Ubiquitin-Like protein Activation	2.44	5.44
cell wall organization or biogenesis	YPR030W	CSR2	Chs5 Spa2 Rescue	4.55	23.42
	YKL096W	CWP1	Cell Wall Protein	4.64	24.95
	YDL222C	FMP45	Found in Mitochondrial Proteome	7.89	238.02
	YLR054C	OSW2	Outer Spore Wall	3.05	8.26
	YOL048C	RRT8	Regulator of rDNA Transcription	4.15	17.72
	YIL113W	SDP1	Stress-inducible Dual specificity Phosphatase	3.42	10.70
	YNL160W	YGP1	Yeast GlycoProtein	4.52	23.02
	YIR039C	YPS6	YaPSin	3.82	14.15
peroxisome organization	YDR216W	ADR1	Alcohol Dehydrogenase II synthesis Regulator	3.08	8.45
	YBR128C	ATG14	AuTophaGy related	2.79	6.90
	YJL185C	ATG36	AuTophaGy related	3.36	10.25
	YDL022W	GPD1	Glycerol-3-Phosphate Dehydrogenase	2.56	5.90
	YKL026C	GPX1	Glutathione PeroXidase	3.45	10.92
	YOL126C	MDH2	Malate DeHydrogenase	2.82	7.05
	YNL214W	PEX17	PEroXisome related	2.36	5.15
	YHR160C	PEX18	PEroXin	4.02	16.24

Table A. 2 (continued): Up-regulated genes (two-fold and higher) in H7, based on microarray results, accroding to metabolic processes.

regulation of organelle organization	YDR216W	ADR1	Alcohol Dehydrogenase II synthesis Regulator	3.08	8.45
	YPL200W	CSM4	Chromosome Segregation in Meiosis	4.44	21.75
	YOR178C	GAC1	Glycogen ACcumulation	3.78	13.73
	YPL240C	HSP82	Heat Shock Protein	2.87	7.29
	YOR351C	MEK1	MEiotic Kinase	3.37	10.35
	YPR154W	PIN3	Psi+ INducibility	2.49	5.61
	YIL101C	XBP1	XhoI site-Binding Protein	4.12	17.36
protein folding	YGR142W	BTN2	BaTteN disease	3.39	10.48
	YPR158W	CUR1	Curing of [URe3]	2.66	6.33
	YBR072W	HSP26	Heat Shock Protein	7.32	160.31
	YDR258C	HSP78	Heat Shock Protein	3.26	9.58
	YPL240C	HSP82	Heat Shock Protein	2.87	7.29
	YAL005C	SSA1	Stress-Seventy subfamily A	2.70	6.50
	YER103W	SSA4	Stress-Seventy subfamily A	4.18	18.14
DNA recombination	YPL200W	CSM4	Chromosome Segregation in Meiosis	4.44	21.75
	YPL017C	IRC15	Increased Recombination Centers	4.27	19.36
	YML128C	MSC1	Meiotic Sister-Chromatid recombination	5.12	34.66
	YDL059C	RAD59	RADiation sensitive	2.43	5.38
	YHL024W	RIM4	Regulator of IME2	3.17	8.98
	YGL250W	RMR1	Reduced Meiotic Recombination	2.98	7.87
cytoskeleton organization	YDR171W	HSP42	Heat Shock Protein	2.83	7.11
	YPL017C	IRC15	Increased Recombination Centers	4.27	19.36
	YPR154W	PIN3	Psi+ INducibility	2.49	5.61
	YIL105C	SLM1	Synthetic Lethal with Mss4	2.82	7.04
	YHR016C	YSC84		2.74	6.66
regulation of cell cycle	YPL200W	CSM4	Chromosome Segregation in Meiosis	4.44	21.75
	YOR178C	GAC1	Glycogen ACcumulation	3.78	13.73
	YPL017C	IRC15	Increased Recombination Centers	4.27	19.36
	YOR351C	MEK1	MEiotic Kinase	3.37	10.35
	YDR253C	MET32	METhionine requiring	2.94	7.69
proteolysis involved in cellular protein catabolic process	YIL097W	FYV10	Function required for Yeast Viability	2.78	6.88
	YOR178C	GAC1	Glycogen ACcumulation	3.78	13.73
	YDR358W	GGA1	Golgi-localized, Gamma-adaptin ear homology, Arf-binding protein	2.67	6.38
	YDR255C	RMD5	Required for Meiotic nuclear Division	2.56	5.91
	YEL012W	UBC8	UBiquitin-Conjugating	2.99	7.96
Golgi vesicle transport	YBL078C	ATG8	AuTophaGy related	2.99	7.93
	YLR080W	EMP46		3.23	9.41
	YDR358W	GGA1	Golgi-localized, Gamma-adaptin ear homology, Arf-binding protein	2.67	6.38
	YGR209C	TRX2	ThioRedoXin	2.79	6.93
	YNL093W	YPT53	Yeast Protein Two	5.40	42.27
invasive growth in response to glucose limitation	YDL024C	DIA3	Digs Into Agar	4.05	16.61
	YGL121C	GPG1	G Protein Gamma	4.41	21.29
	YBR066C	NRG2	Negative Regulator of Glucose-controlled genes	2.52	5.73
	YGL208W	SIP2	SNF1-Interacting Protein	2.36	5.12
	YJL089W	SIP4	SNF1-Interacting Protein	2.53	5.77

Table A. 2 (continued): Up-regulated genes (two-fold and higher) in H7, based on microarray results, accroding to metabolic processes.

endocytosis	YPR030W	CSR2	Chs5 Spa2 Rescue	4.55	23.42
	YPL004C	LSP1	Long chain bases Stimulate Phosphorylation	2.41	5.33
	YBR214W	SDS24	homolog of S. pombe SDS23	3.64	12.44
	YNL093W	YPT53	Yeast Protein Two	5.40	42.27
	YHR016C	YSC84		2.74	6.66
cellular response to DNA damage stimulus	YOL052C-A	DDR2	DNA Damage Responsive	7.00	127.65
	YMR173W	DDR48	DNA Damage Responsive	2.50	5.64
	YGL087C	MMS2	Methyl MethaneSulfonate sensitivity	2.49	5.60
	YDL059C	RAD59	RADiation sensitive	2.43	5.38
conjugation	YDL223C	HBT1	HuB1 Target	3.99	15.94
	YCR091W	KIN82	protein KINase	2.51	5.69
	YDL214C	PRR2	Pheromone Response Regulator	5.77	54.73
	YOL117W	RRI2		2.68	6.40
regulation of protein modification process	YOR178C	GAC1	Glycogen ACcumulation	3.78	13.73
	YPL004C	LSP1	Long chain bases Stimulate Phosphorylation	2.41	5.33
	YIL113W	SDP1	Stress-inducible Dual specificity Phosphatase	3.42	6.40
	YIL101C	XBP1	XhoI site-Binding Protein	4.12	17.36
chromatin organization	YDR216W	ADR1	Alcohol Dehydrogenase II synthesis Regulator	3.08	8.45
	YDR096W	GIS1	GIg1-2 Suppressor	2.36	5.13
	YGL037C	PNC1	Pyrazinamidase and NiCotinamidase	2.96	7.80
	YIL101C	XBP1	XhoI site-Binding Protein	4.12	17.36
endosomal transport	YGR142W	BTN2	BaTteN disease	3.39	10.48
	YDR358W	GGA1	Golgi-localized, Gamma-adaptin ear homology, Arf-binding protein	2.67	6.38
	YIL105C	SLM1	Synthetic Lethal with Mss4	2.82	7.04
membrane invagination	YBL078C	ATG8	AuTophaGy related	2.99	7.93
	YBR128C	ATG14	AuTophaGy related	2.79	6.90
	YCR068W	ATG15	AuTophaGy related	2.92	7.59
response to starvation	YDR096W	GIS1	GIg1-2 Suppressor	2.36	5.13
	YER037W	PHM8	PHosphate Metabolism	2.58	5.96
	YGL208W	SIP2	SNF1-Interacting Protein	2.36	5.12
vacuole organization	YBL078C	ATG8	AuTophaGy related	2.99	7.93
	YGR209C	TRX2	ThioRedoXin	2.79	6.93
	YHR138C	YHR138C		3.63	12.41
mitotic cell cycle	YOR178C	GAC1	Glycogen ACcumulation	3.78	13.73
	YDR253C	MET32	METhionine requiring	2.94	7.69
	YGL229C	SAP4	Sit4 Associated Protein	2.88	7.36
pseudohyphal growth	YDL024C	DIA3	Digs Into Agar	4.05	16.61
	YGL192W	IME4	Inducer of MEiosis	3.19	9.10
	YBR066C	NRG2	Negative Regulator of Glucose-controlled genes	2.52	5.73
membrane fusion	YBL078C	ATG8	AuTophaGy related	2.99	7.93
	YGR209C	TRX2	ThioRedoXin	2.79	6.93
	YHR138C	YHR138C		3.63	12.41

Table A. 2 (continued): Up-regulated genes (two-fold and higher) in H7, based on microarray results, accroding to metabolic processes.

lipid transport	YKL187C	FAT3	FATty acid transporter 3	2.42	5.34
	YCR091W	KIN82	protein KINase	2.51	5.69
	YOR049C	RSB1	Resistance to Sphingoid long-chain Base	3.79	13.84
DNA repair	YMR173W	DDR48	DNA Damage Responsive	2.50	5.64
	YGL087C	MMS2	Methyl MethaneSulfonate sensitivity	2.49	5.60
	YDL059C	RAD59	RADiation sensitive	2.43	5.38
RNA catabolic process	YLR270W	DCS1	DeCapping Scavenger	2.55	5.84
	YOR173W	DCS2	DeCapping Scavenger	4.76	27.01
	YPL123C	RNY1	RiboNuclease from Yeast	3.30	9.85
chromosome segregation	YPL200W	CSM4	Chromosome Segregation in Meiosis	4.44	21.75
	YOR178C	GAC1	Glycogen ACcumulation	3.78	13.73
	YPL017C	IRC15	Increased Recombination Centers	4.27	19.36
regulation of DNA metabolic process	YPL200W	CSM4	Chromosome Segregation in Meiosis	4.44	21.75
	YPL240C	HSP82	Heat Shock Protein	2.87	7.29
	YGL037C	PNC1	Pyrazinamidase and NiCotinamidase	2.96	7.80
amino acid transport	YGR142W	BTN2	BaTteN disease	3.39	10.48
	YOR348C	PUT4	Proline UTilization	4.04	16.46
	YLL055W	YCT1	Yeast Cysteine Transporter	2.63	6.19
organelle fusion	YNL015W	PBI2	Proteinase B Inhibitor	3.63	12.37
	YGR209C	TRX2	ThioRedoXin	2.79	6.93
	YHR138C	YHR138C		3.63	12.41
RNA modification	YGL192W	IME4	Inducer of MEiosis	3.19	9.10
	YNL196C	SLZ1		7.27	154.70
histone modification	YDR096W	GIS1	GIg1-2 Suppressor	2.36	5.13
	YIL101C	XBP1	XhoI site-Binding Protein	4.12	17.36
cell morphogenesis	YDL223C	HBT1	HuB1 Target	3.99	15.94
	YPL123C	RNY1	RiboNuclease from Yeast	3.30	9.85
DNA replication	YPL240C	HSP82	Heat Shock Protein	2.87	7.29
	YHL024W	RIM4	Regulator of IME2	3.17	8.98
nuclear transport	YNR034W	SOL1	Suppressor Of Los1-1	2.38	5.21
	YAL005C	SSA1	Stress-Seventy subfamily A	2.70	6.50
telomere organization	YDL059C	RAD59	RADiation sensitive	2.43	5.38
	YPL240C	HSP82	Heat Shock Protein	2.87	7.29
nucleus organization	YOR185C	GSP2	Genetic Suppressor of Prp20-1	2.63	6.20
organelle assembly	YBL078C	ATG8	AuTophaGy related	2.99	7.93
peptidyl-amino acid modification	YNL077W	APJ1	Anti-Prion DnaJ	3.05	8.26
organelle inheritance	YGR209C	TRX2	ThioRedoXin	2.79	6.93
cellular ion homeostasis	YMR105C	PGM2	PhosphoGlucoMutase	5.33	40.19
protein alkylation	YNL092W	YNL092W		2.61	6.13
nucleobase-containing compound transport	YNR034W	SOL1	Suppressor Of Los1-1	2.38	5.21
mitochondrial translation	YFR049W	YMR31	Yeast Mitochondrial Ribosomal protein	2.54	5.83
regulation of transport	YBR132C	AGP2	high-Affinity Glutamine Permease	3.31	9.91
protein dephosphorylation	YER054C	GIP2	Glc7-Interacting Protein	3.67	12.76
protein maturation	YCR068W	ATG15	AuTophaGy related	2.92	7.59
cytoplasmic translation	YAL005C	SSA1	Stress-Seventy subfamily A	2.70	6.50

APPENDIX B: NGS results showing the mutation regions in H7 genome.

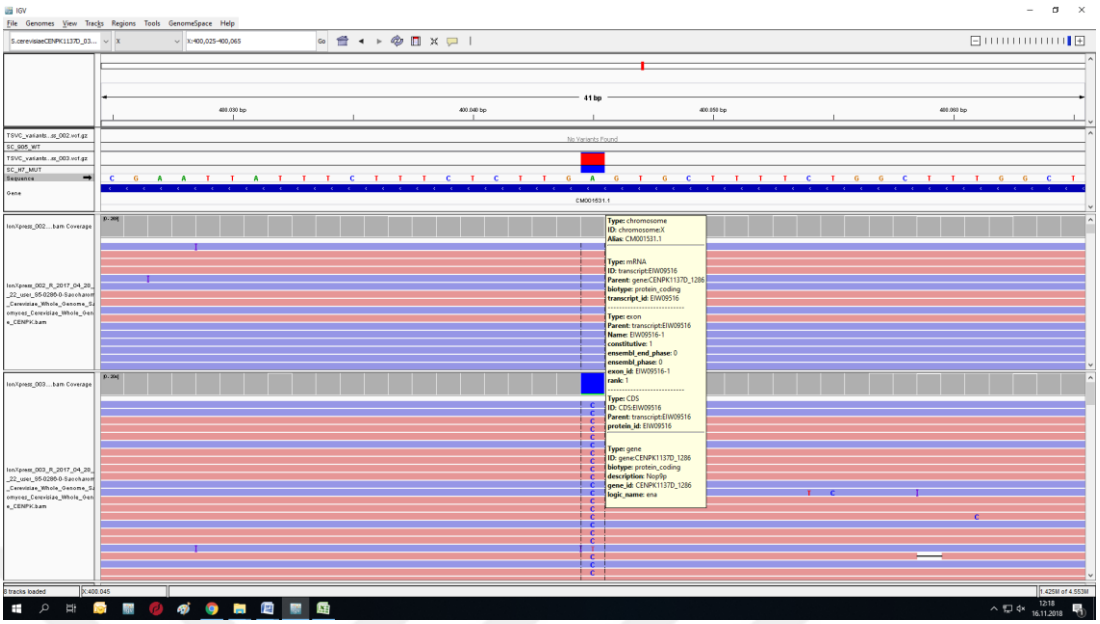

Figure B.1 : IGV image of mutation *NOP9 / YJL010C* c.1939A>C, p.S647A (ChrX:400045). IonXpress_002 indicates reference strain (upper part of the image) and IonXpress_003 (lower part of the image) indicates H7.

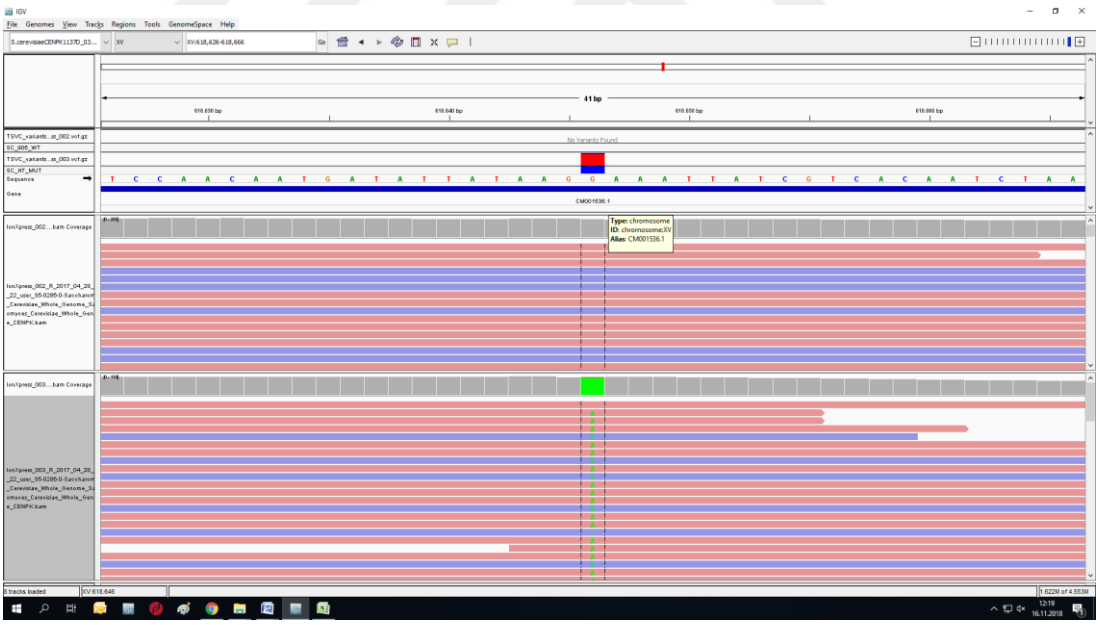

Figure B.2 : IGV image of mutation *ATG40 / YOR152C* c.-602G>A (ChrXV:618646). IonXpress_002 indicates reference strain (upper part of the image) and IonXpress_003 (lower part of the image) indicates H7.

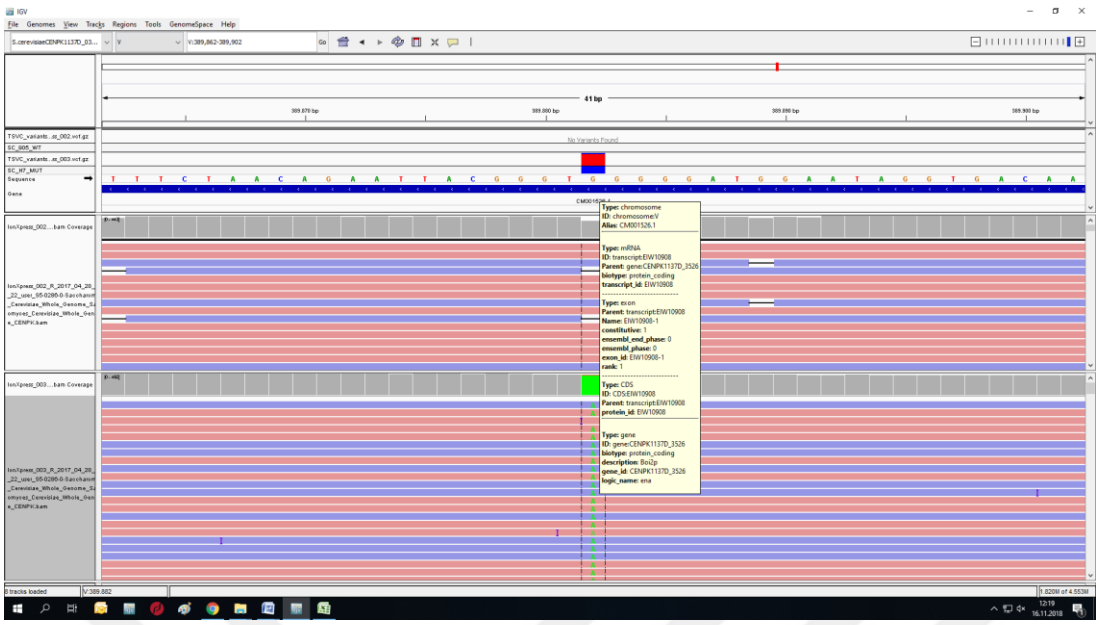

Figure B.3 : IGV image of mutation *BOI2 / YER114C* c.1572G>A p.P524= (ChrV:389882). IonXpress_002 indicates reference strain (upper part of the image) and IonXpress_003 (lower part of the image) indicates H7.

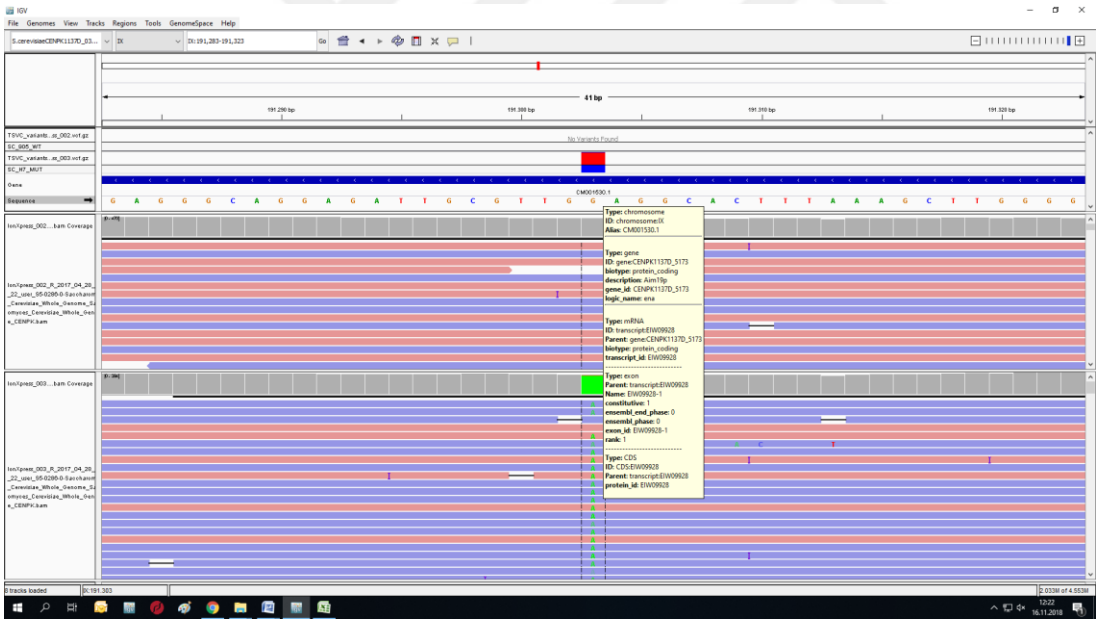

Figure B.4 : IGV image of mutation *AIM19 / YIL087C* c.154G>A, p.P52S (ChrIX:191303). IonXpress_002 indicates reference strain (upper part of the image) and IonXpress_003 (lower part of the image) indicates H7.

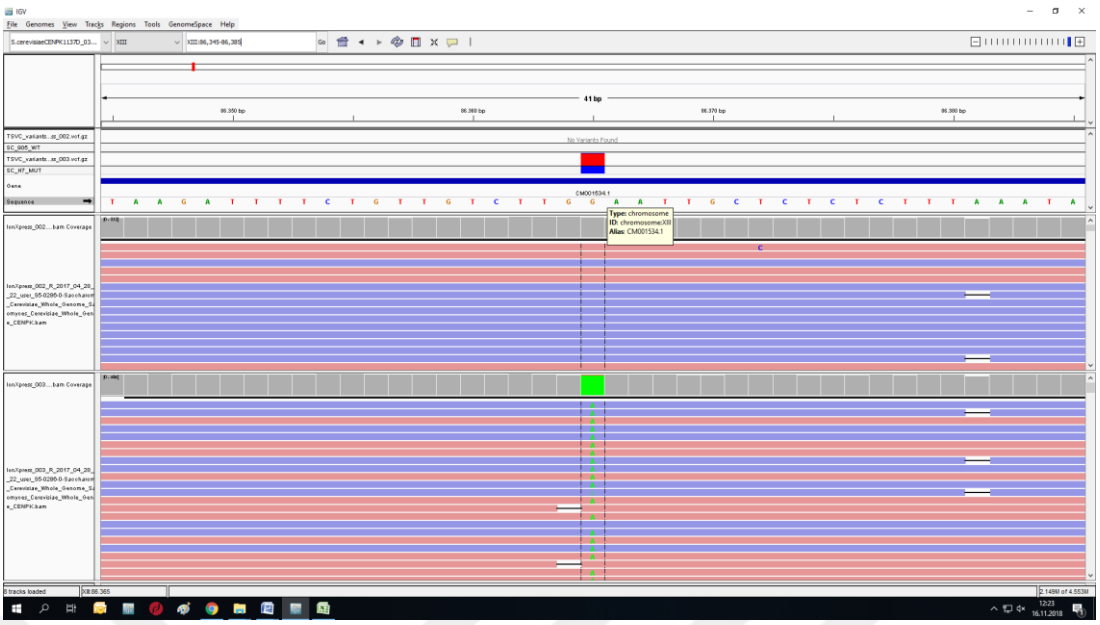

Figure B.5 : IGV image of mutation *UFO1 / YML088W* c.-591G>A, p.P52S (Chr XIII:86365). IonXpress_002 indicates reference strain (upper part of the image) and IonXpress_003 (lower part of the image) indicates H7.

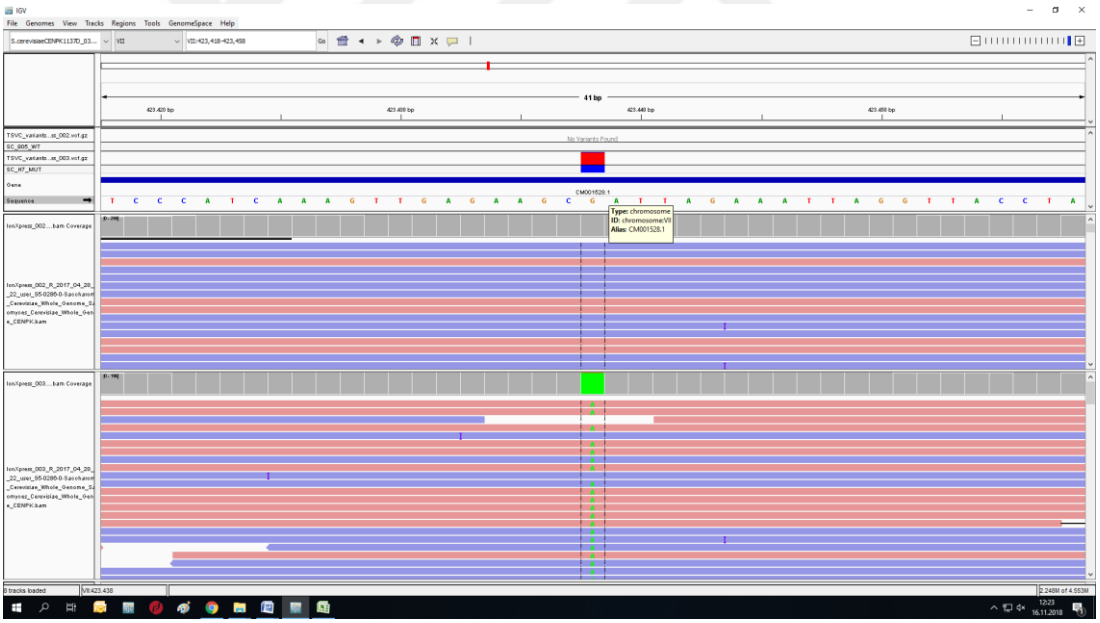

Figure B.6 : IGV image of mutation *YGL039W* c.-364 G>A (ChrVII:423438). IonXpress_002 indicates reference strain (upper part of the image) and IonXpress_003 (lower part of the image) indicates H7.

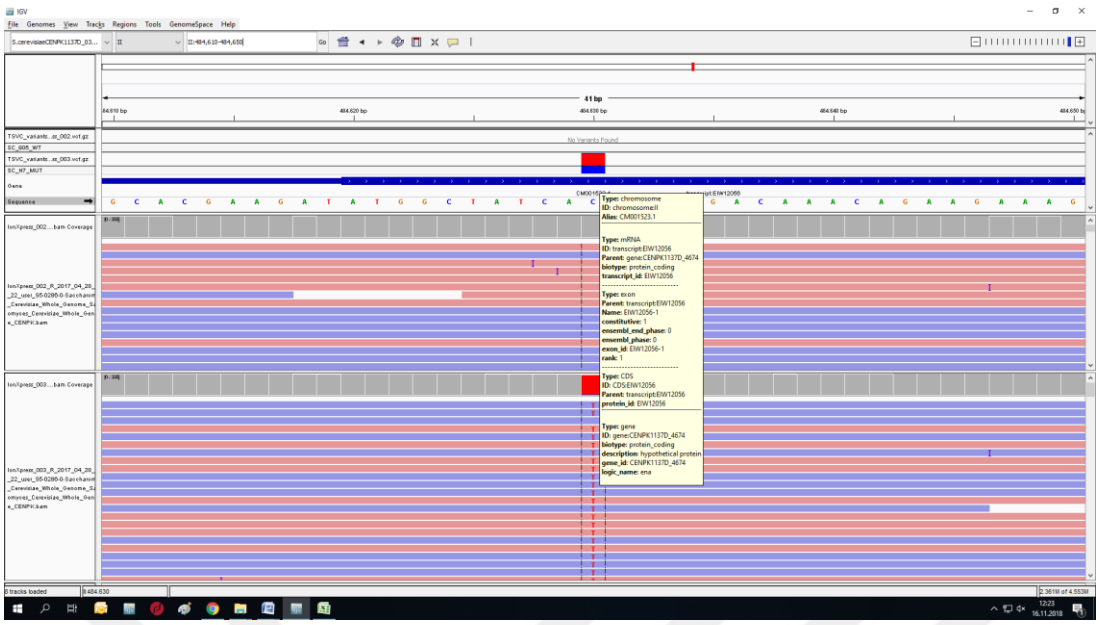

Figure B.7 : IGV image of mutation *MEO1 / YBR126W-A* c.11C>T, p.T4I (ChrII:484630). IonXpress_002 indicates reference strain (upper part of the image) and IonXpress_003 (lower part of the image) indicates H7.

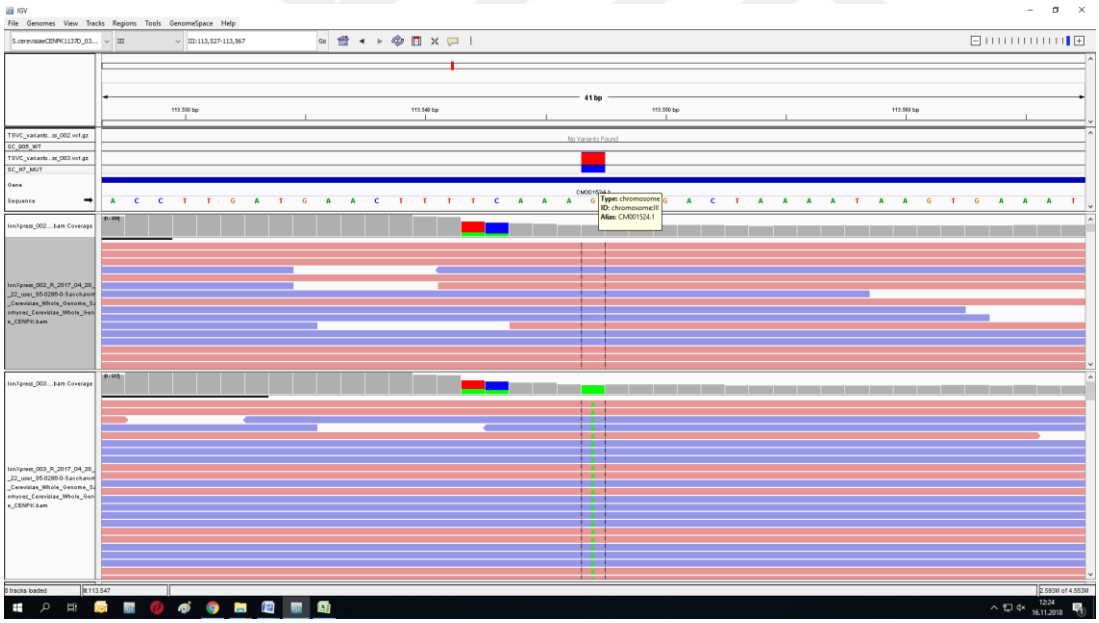

Figure B.8 : IGV image of mutation *RER1 / YCL001W* c.567+47 G>A (ChrIII:113547). IonXpress_002 indicates reference strain (upper part of the image) and IonXpress_003 (lower part of the image) indicates H7.

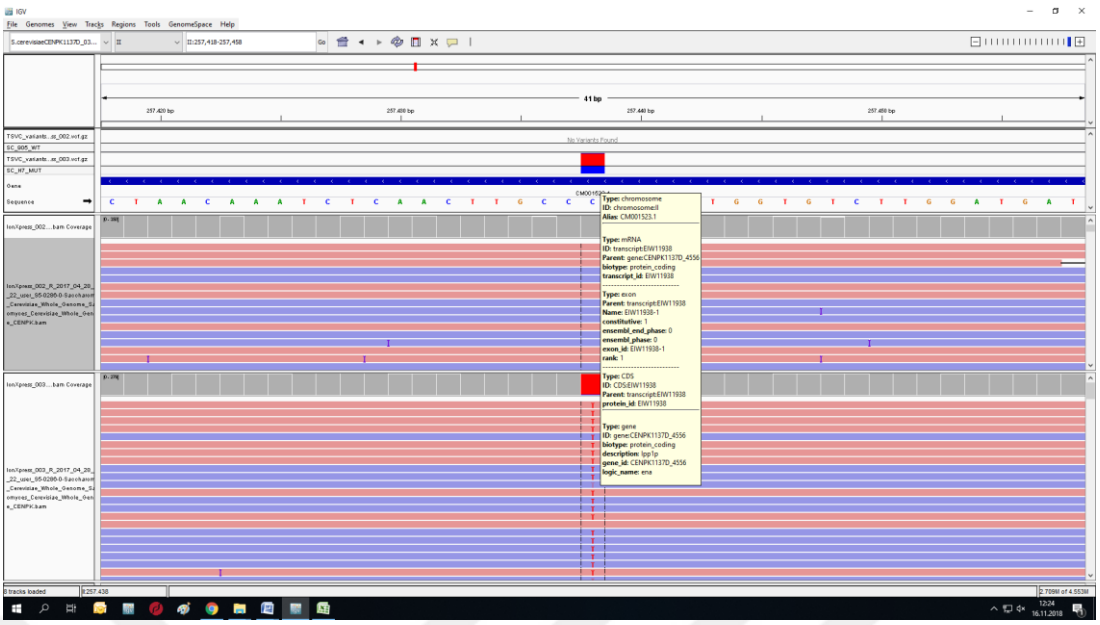

Figure B.9 : IGV image of mutation *IPP1 / YBR011C* c.225C>T p.K75= (ChrII:257438). IonXpress_002 indicates reference strain (upper part of the image) and IonXpress_003 (lower part of the image) indicates H7.

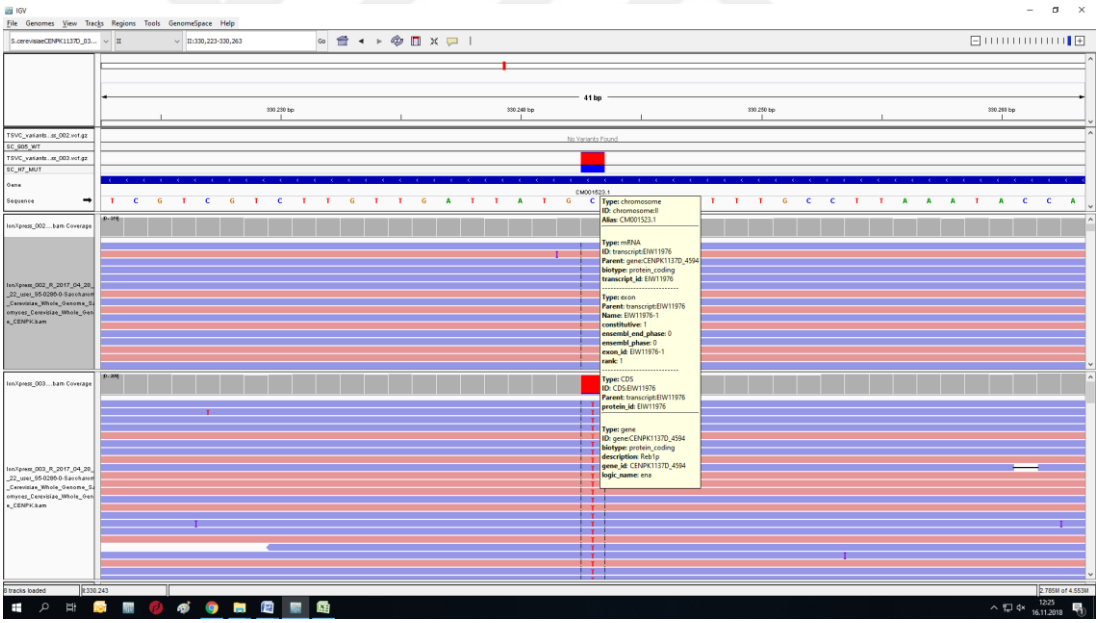

Figure B.10 : IGV image of mutation *REB1 / YBR049C* c.336C>T p.A12= (ChrII:330243). IonXpress_002 indicates reference strain (upper part of the image) and IonXpress_003 (lower part of the image) indicates H7.

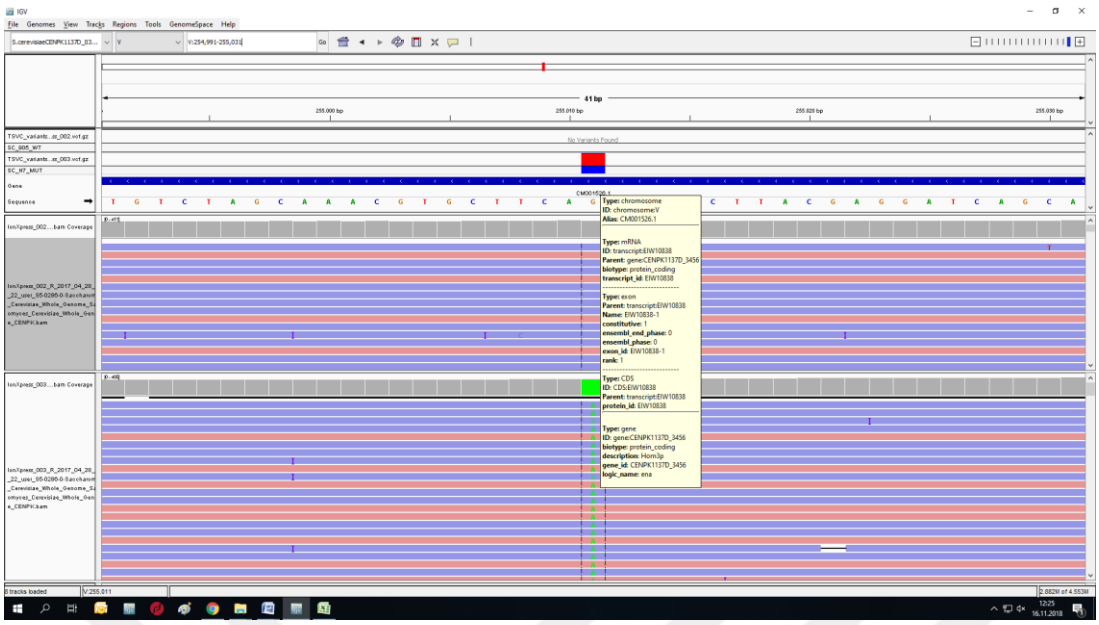

Figure B.11 : IGV image of mutation *HOM3 / YER052C* c.801G>A, p.P267L (ChrV:255011). IonXpress_002 indicates reference strain (upper part of the image) and IonXpress_003 (lower part of the image) indicates H7.

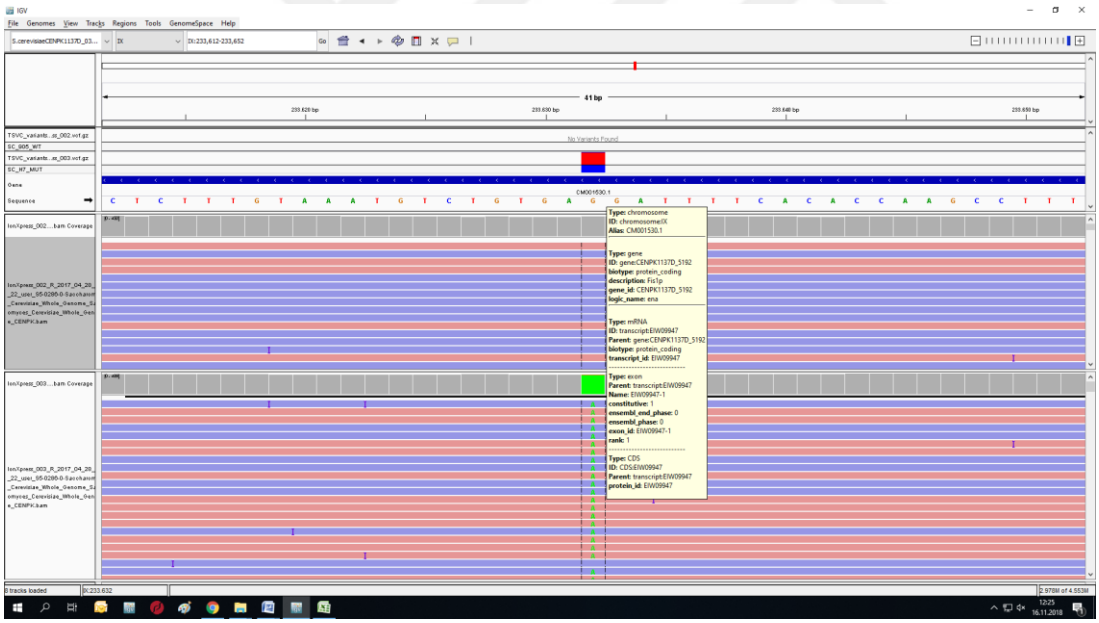

Figure B.12 : IGV image of mutation *FIS1 / YIL065C* c.193G>A, p.L65F (ChrIX:233632). IonXpress_002 indicates reference strain (upper part of the image) and IonXpress_003 (lower part of the image) indicates H7.

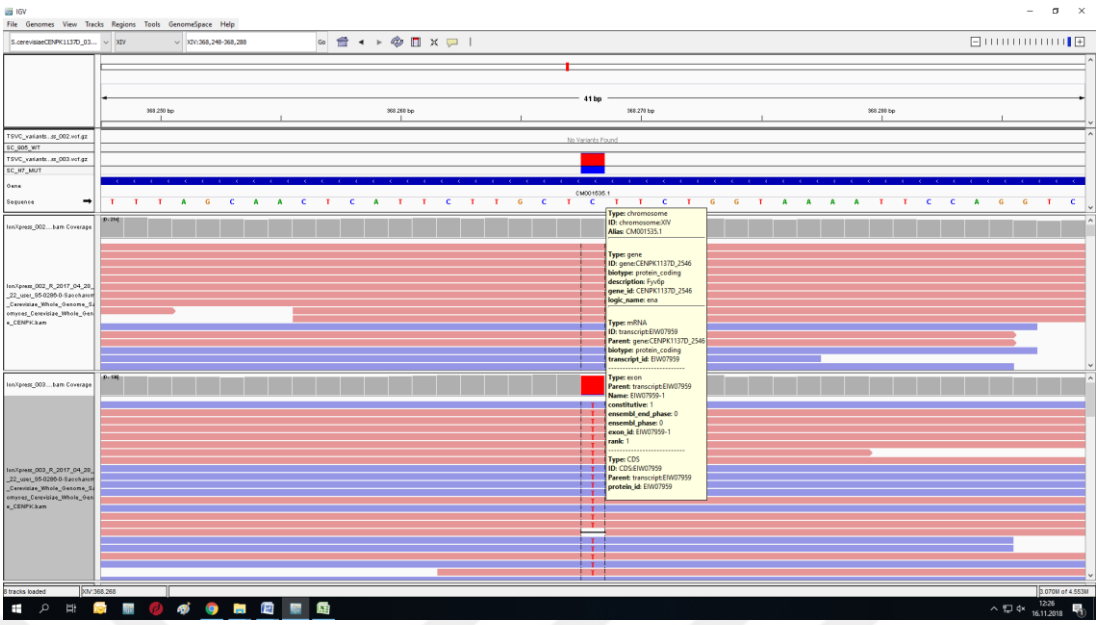

Figure B.13 : IGV image of mutation *FYV6 / YNL133C* c.276C>T p.K92= (ChrXIV:368268). IonXpress_002 indicates reference strain (upper part of the image) and IonXpress_003 (lower part of the image) indicates H7.

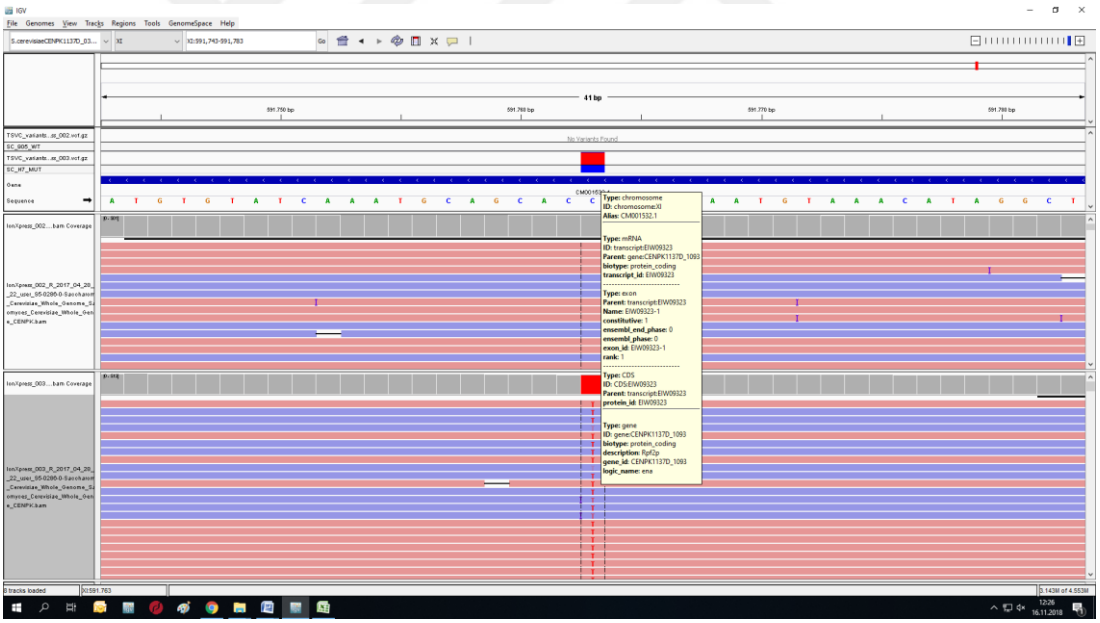

Figure B.14 : IGV image of mutation *RPF2 / YKR081C* c.453C>T p.G145S (ChrXI:591763). IonXpress_002 indicates reference strain (upper part of the image) and IonXpress_003 (lower part of the image) indicates H7.

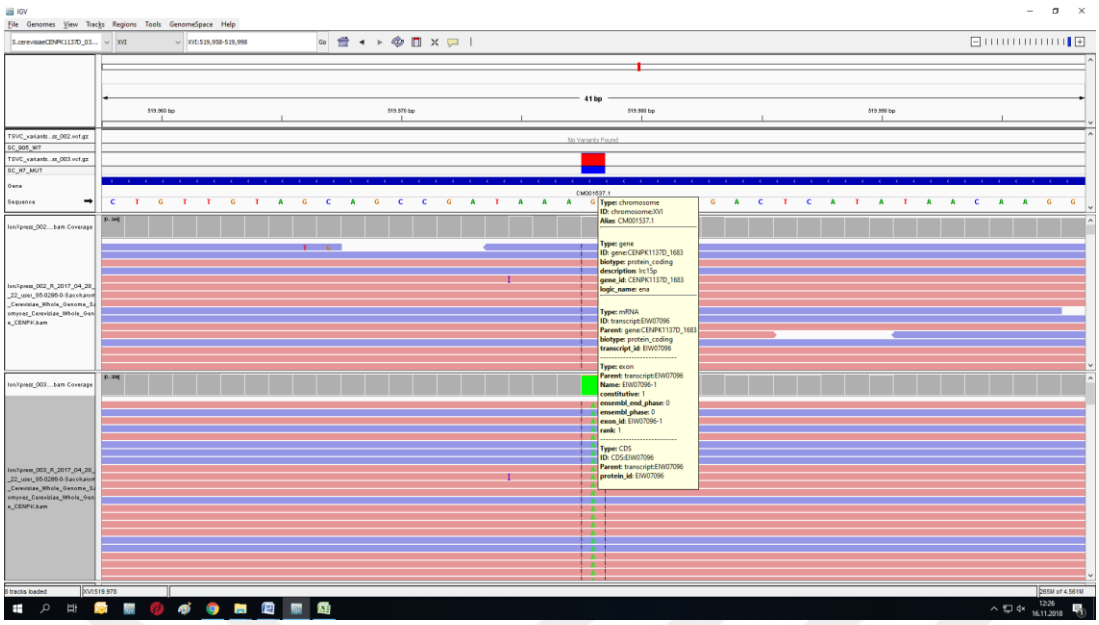

Figure B.15 : IGV image of mutation *IRC15 / YPL017C* c.217G>A, p.L73F (ChrXVI:519978). IonXpress_002 indicates reference strain (upper part of the image) and IonXpress_003 (lower part of the image) indicates H7.

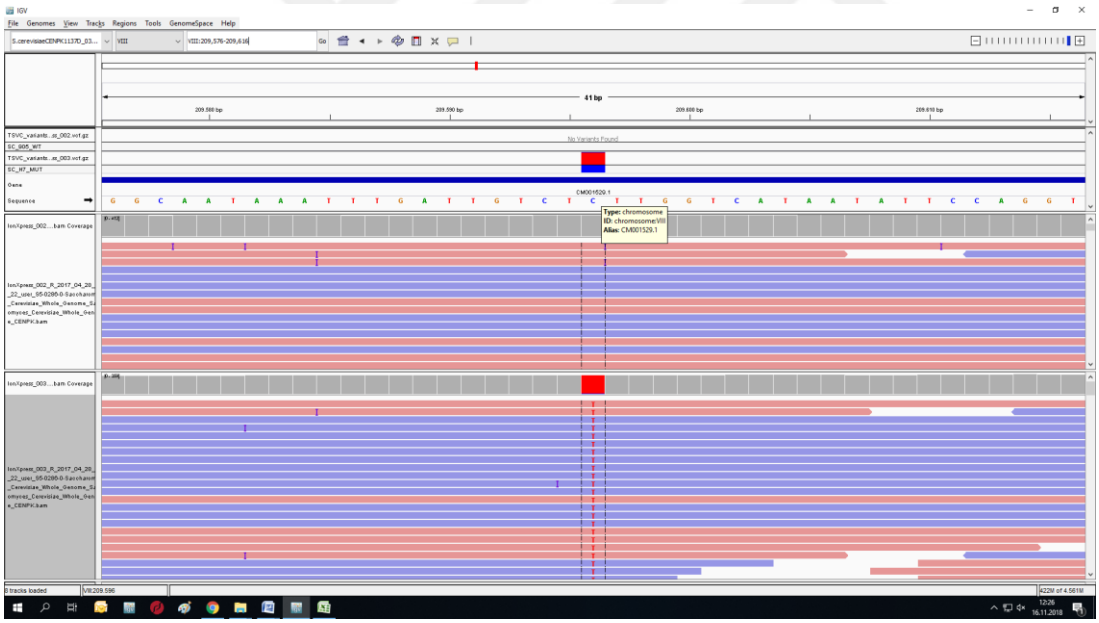

Figure B.16 : IGV image of mutation *RSC30 / YHR056C* c.1402C>T p. E68K (ChrVIII:209596). IonXpress_002 indicates reference strain (upper part of the image) and IonXpress_003 (lower part of the image) indicates H7.

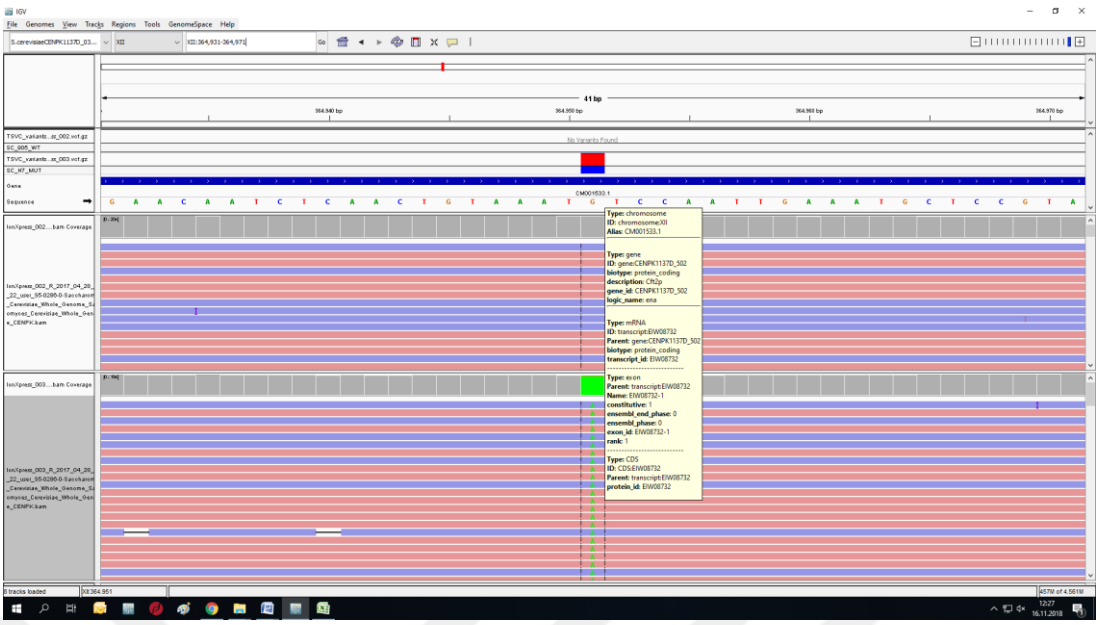

Figure B.17 : IGV image of mutation *CFT2 / YLR115W* c.1945G>A, p.G145S (ChrXII:364951). IonXpress_002 indicates reference strain (upper part of the image) and IonXpress_003 (lower part of the image) indicates H7.

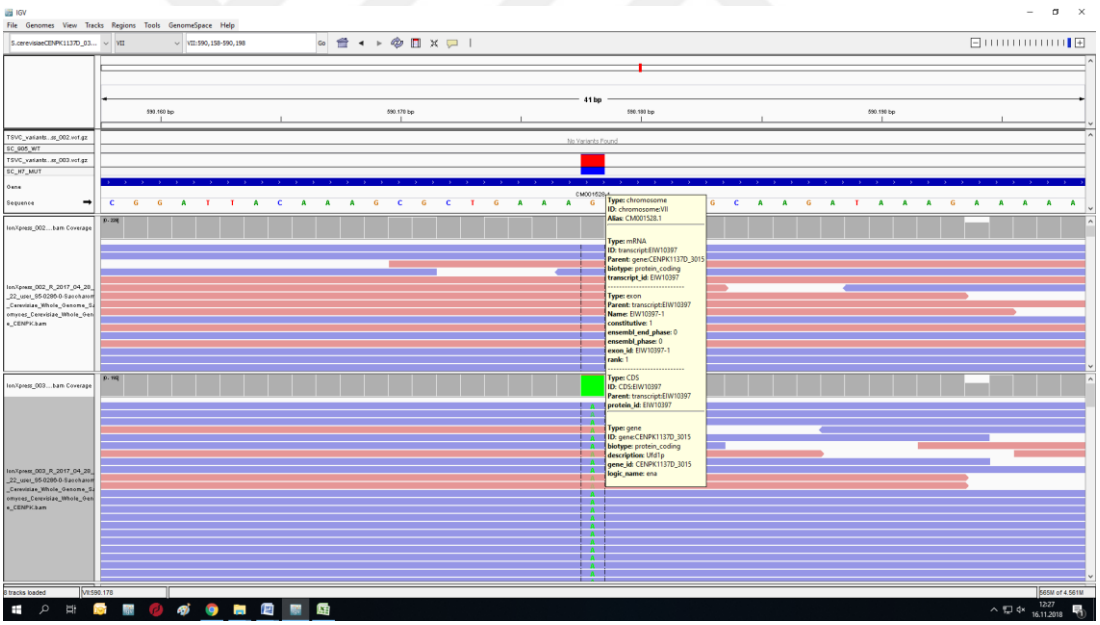

Figure B.18 : IGV image of mutation *UFD1 / YGR048W* c.634G>A, p.A212T (ChrVII:590178). IonXpress_002 indicates reference strain (upper part of the image) and IonXpress_003 (lower part of the image) indicates H7.

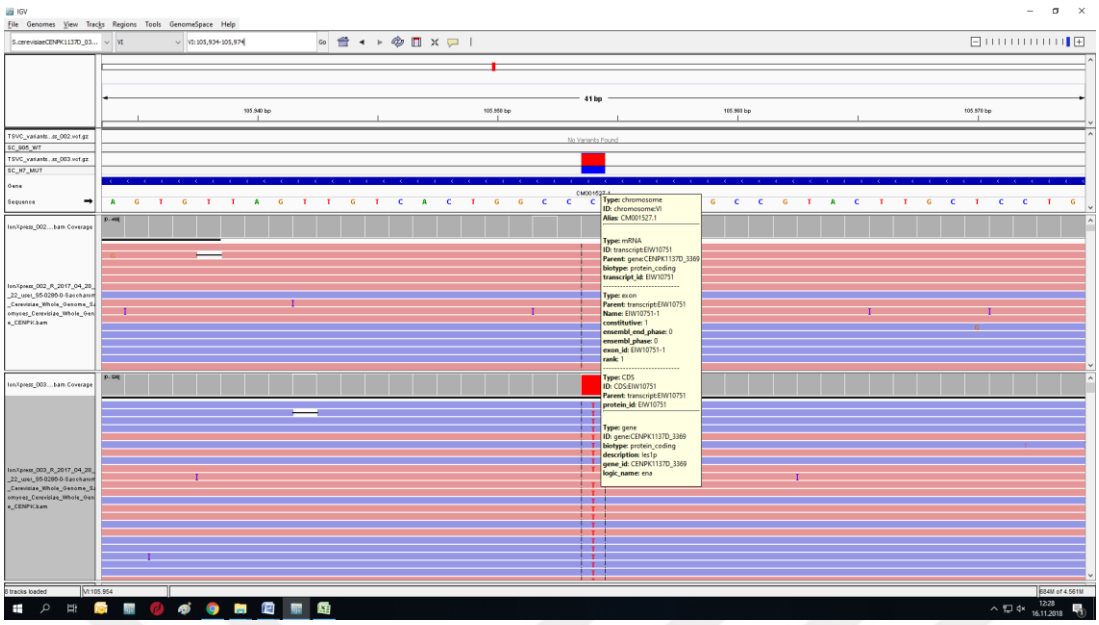

Figure B.19 : IGV image of mutation *IES1 / YFL013C* c.307C>T, p.G103R (ChrVI:105954). IonXpress_002 indicates reference strain (upper part of the image) and IonXpress_003 (lower part of the image) indicates H7.

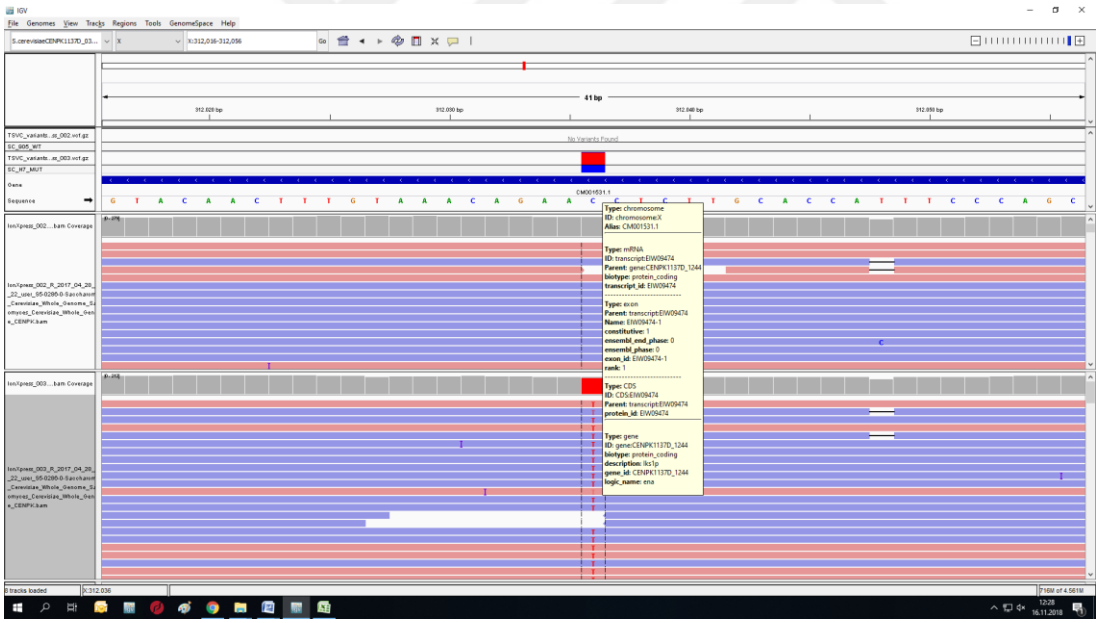

Figure B.20 : IGV image of mutation *IKS1 / YJL057C* c.554C>T, p.G185D (ChrX:312036). IonXpress_002 indicates reference strain (upper part of the image) and IonXpress_003 (lower part of the image) indicates H7.

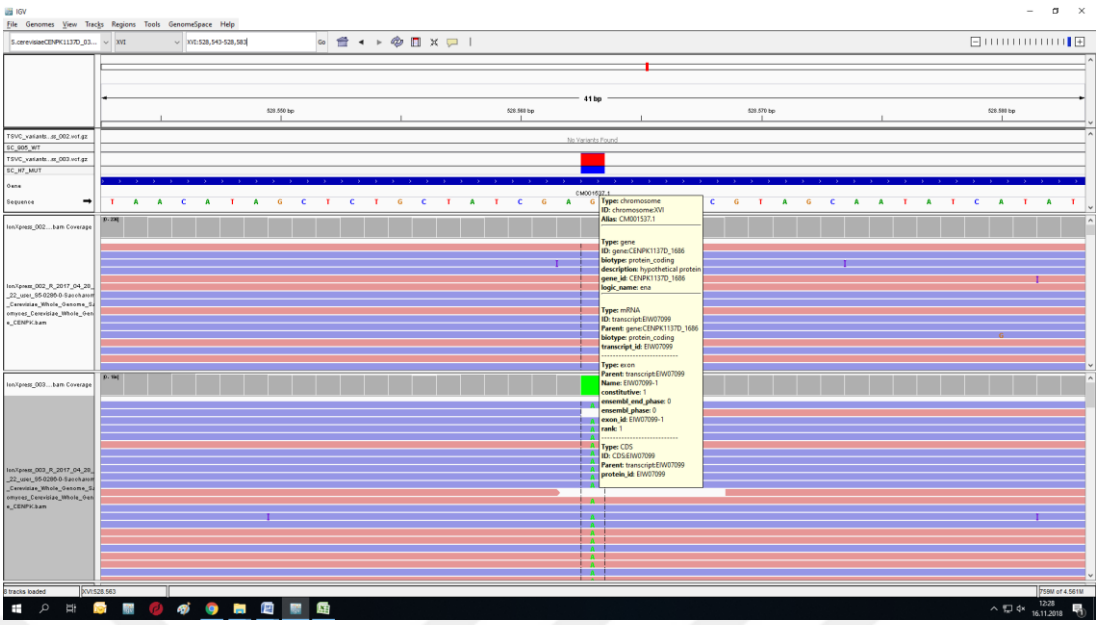

Figure B.21 : IGV image of mutation *CIP1 / YPL014W* c.1010G>A p.R337K (ChrXVI:528563). IonXpress_002 indicates reference strain (upper part of the image) and IonXpress_003 (lower part of the image) indicates H7.

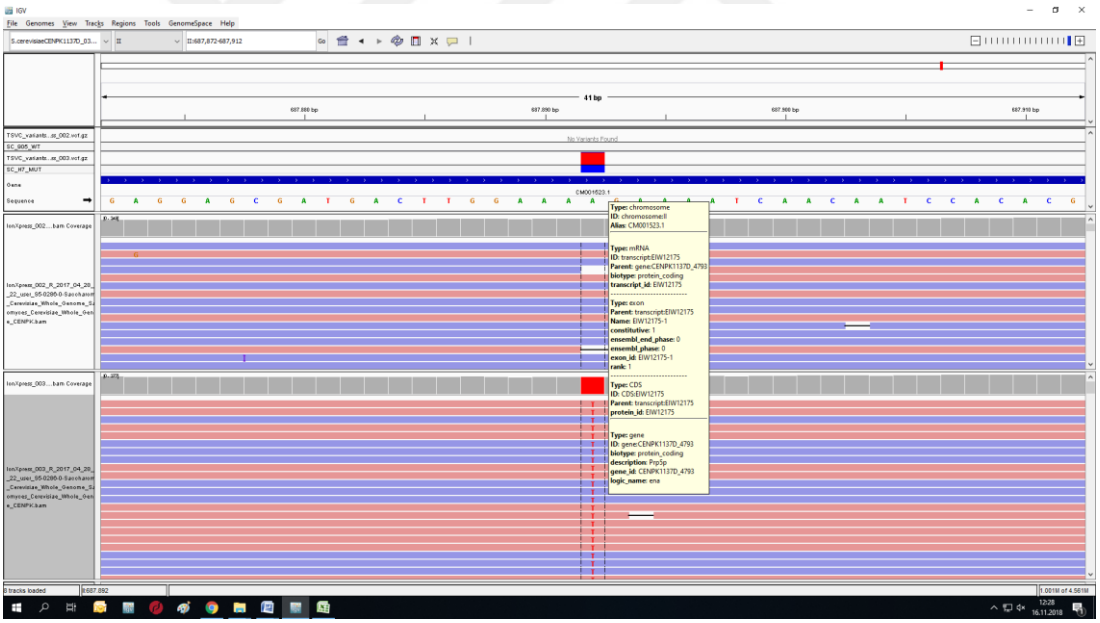

Figure B.22 : IGV image of mutation *PRP5 / YBR237W* c.2147A>T, p.K716M (ChrII:687892). IonXpress_002 indicates reference strain (upper part of the image) and IonXpress_003 (lower part of the image) indicates H7.

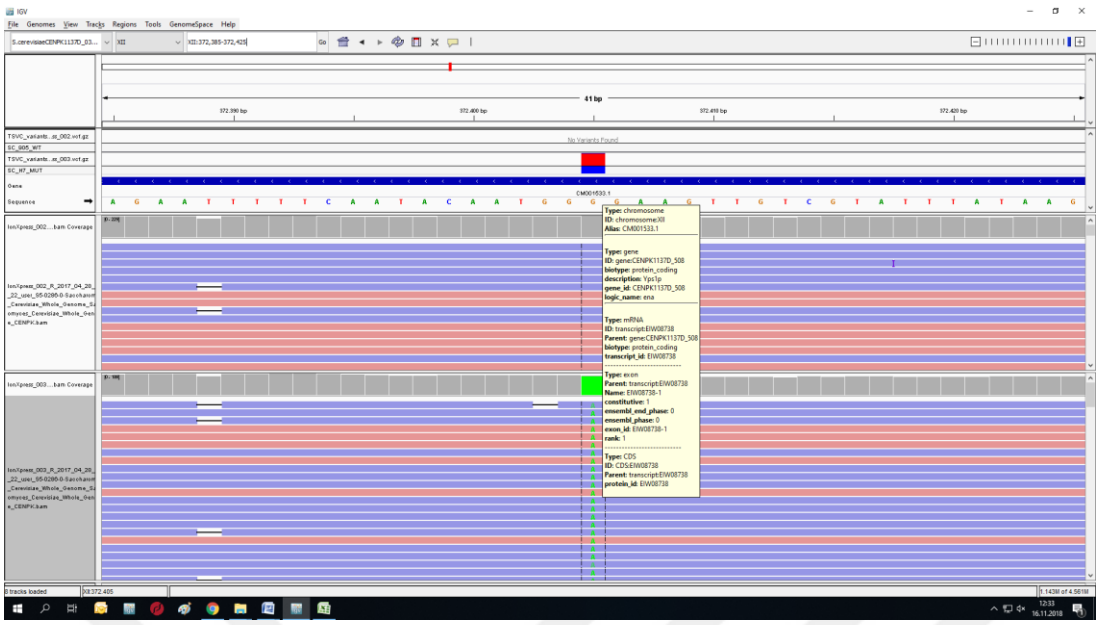

Figure B.23 : IGV image of mutation *YPS1 / YLR120C* c.838G>A, p.P280S(ChrXII:372405). IonXpress_002 indicates reference strain (upper part of the image) and IonXpress_003 (lower part of the image) indicates H7.

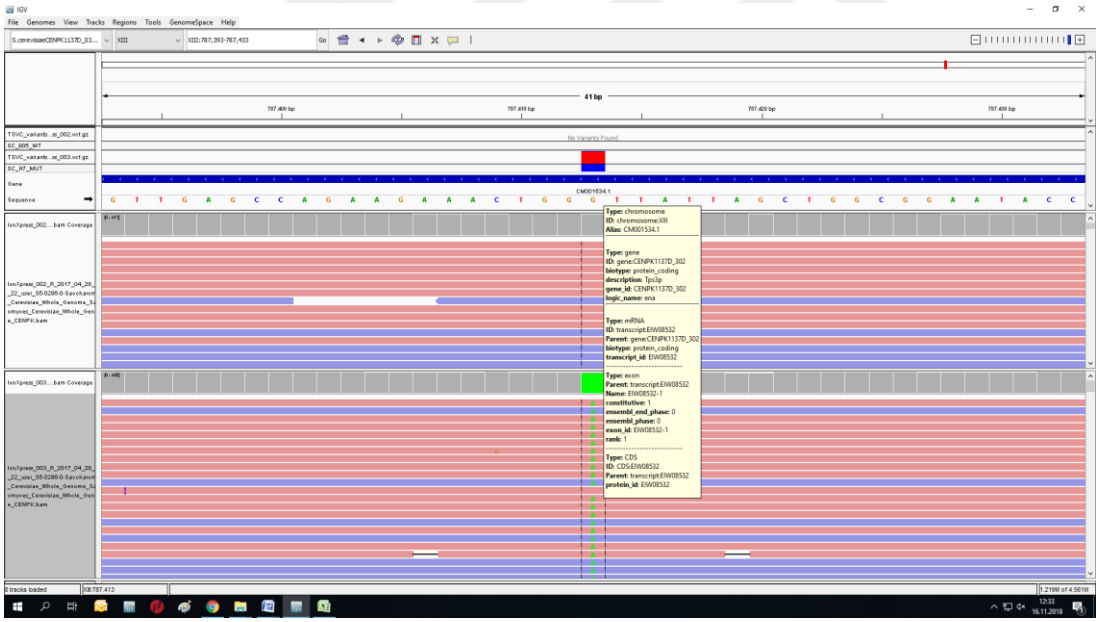

Figure B.24 : IGV image of mutation *TPS1 / YBR126C* c.366G>A p.N122= (ChrXIII:787413). IonXpress_002 indicates reference strain (upper part of the image) and IonXpress_003 (lower part of the image) indicates H7.

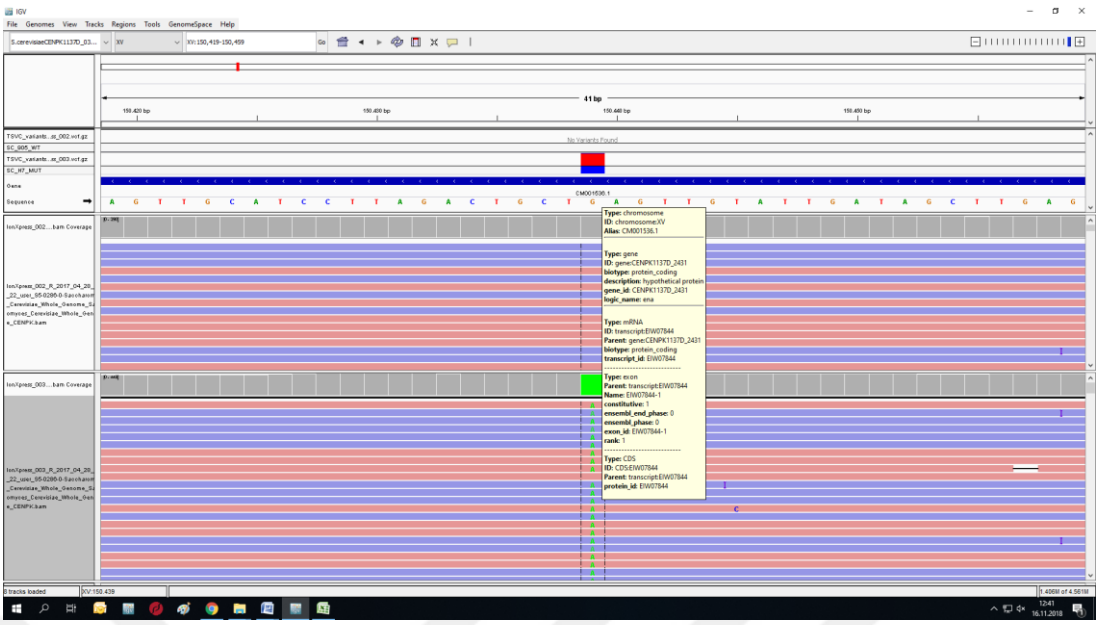

Figure B.25 : IGV image of mutation *DUF1 / YOL087C* c.2164G>A p.Q722*(ChrXV:150439). IonXpress_002 indicates reference strain (upper part of the image) and IonXpress_003 (lower part of the image) indicates H7.

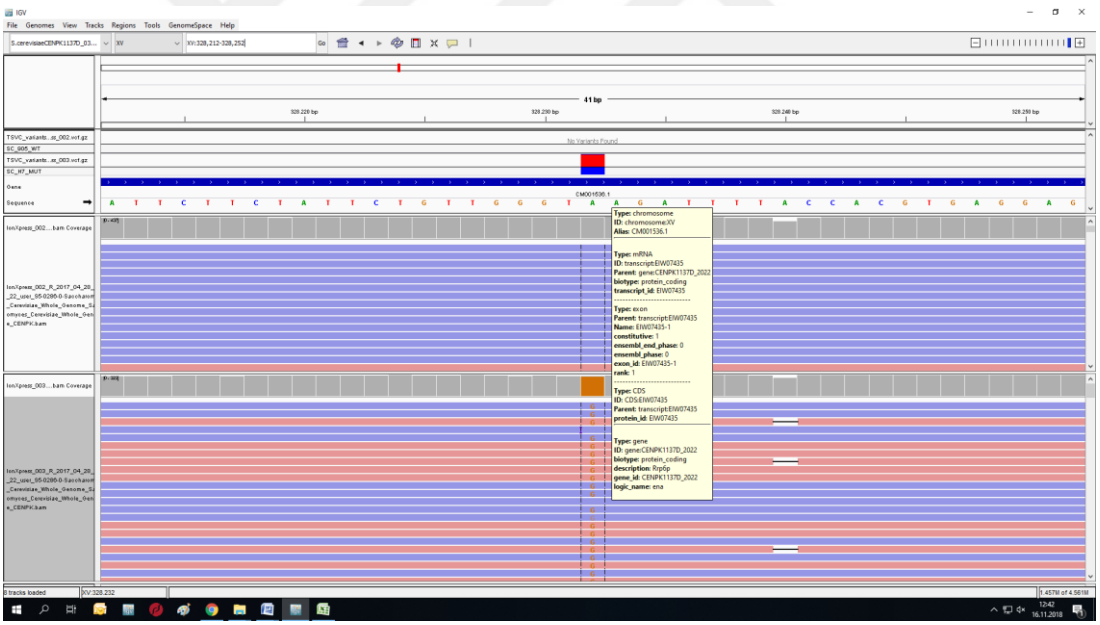

Figure B.26 : IGV image of mutation *RRP6 / YOR001W* c.1720A>G, p.K574E (ChrXV:328232). IonXpress_002 indicates reference strain (upper part of the image) and IonXpress_003 (lower part of the image) indicates H7.

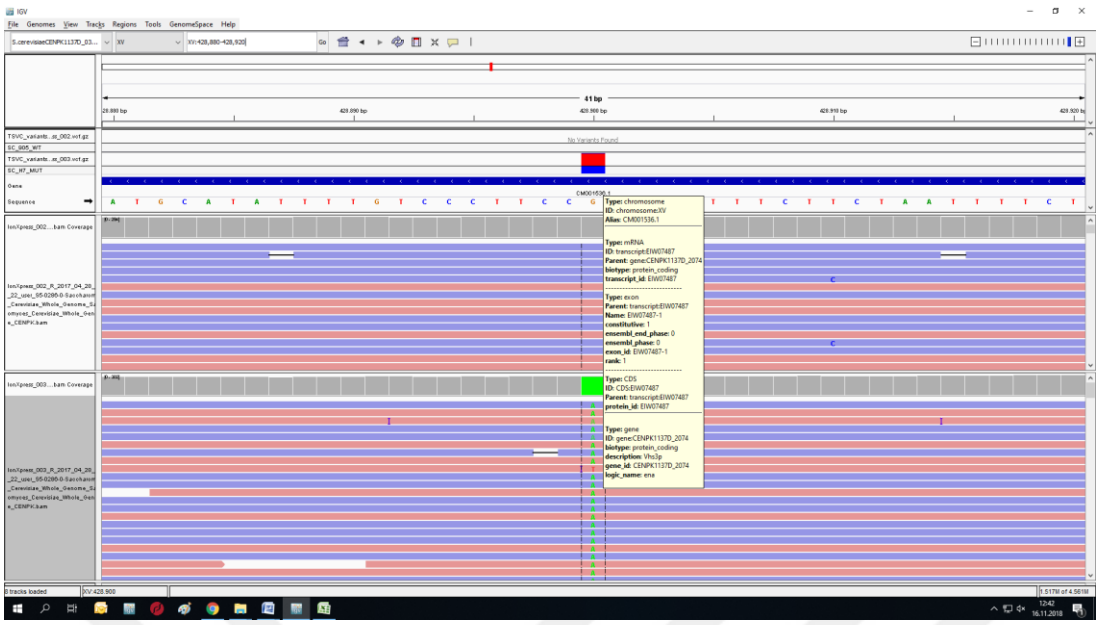

Figure B.27 : IGV image of mutation *VHS3 / YOR054C* c.954G>A, p.Y318= (XV:428900). IonXpress_002 indicates reference strain (upper part of the image) and IonXpress_003 (lower part of the image) indicates H7.

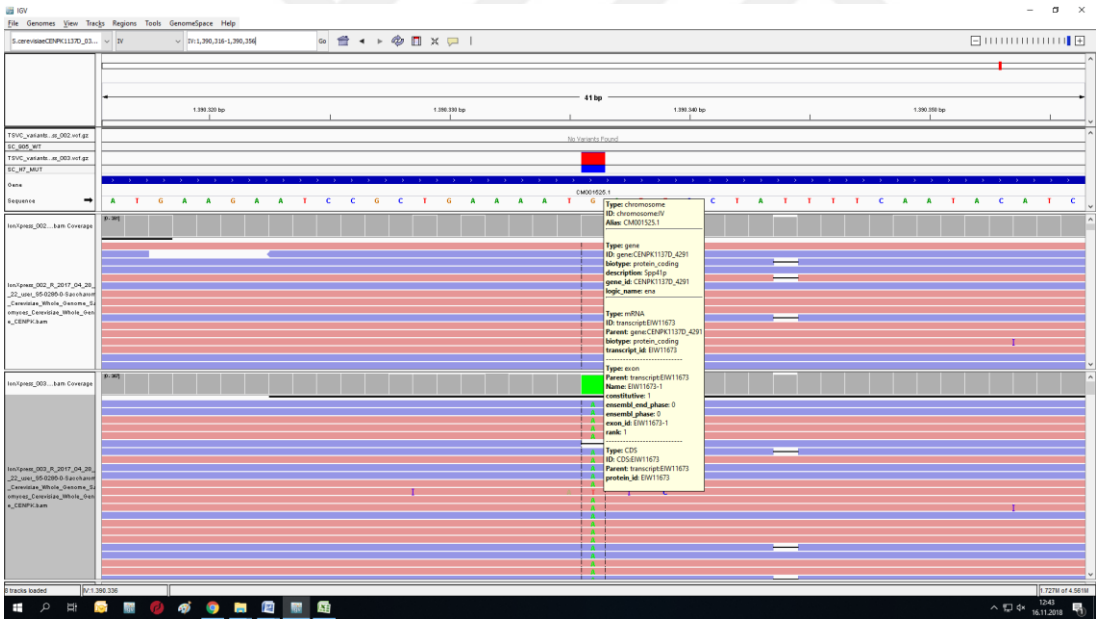

Figure B.28 : IGV image of mutation *SPP41 / YDR464W* c.2769G>A, p.M923I (ChrIV:1390336). IonXpress_002 indicates reference strain (upper part of the image) and IonXpress_003 (lower part of the image) indicates H7.

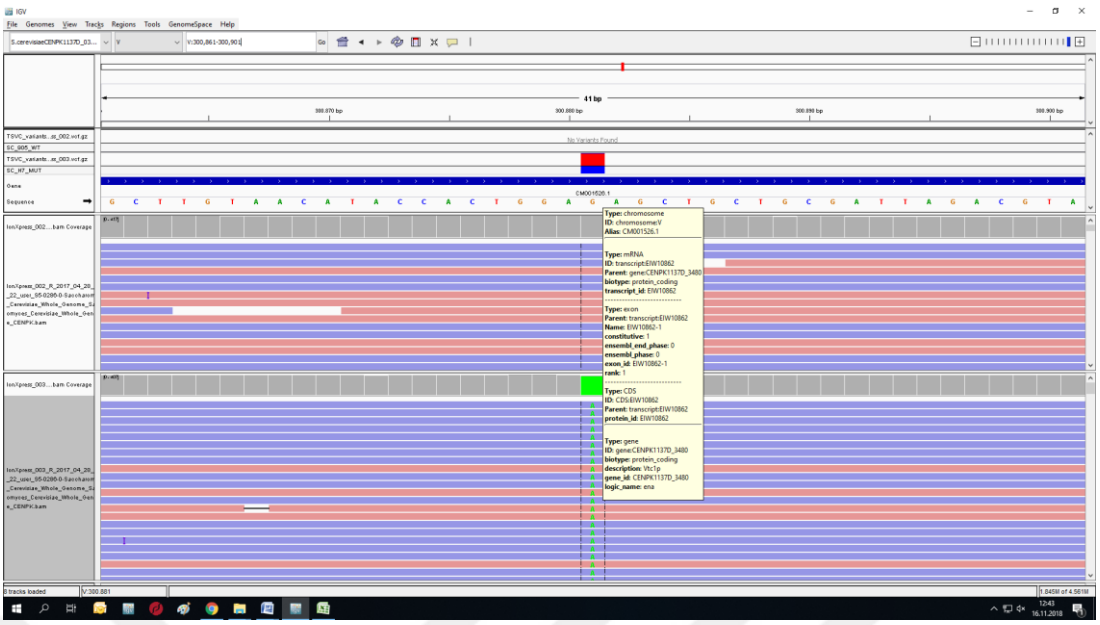

Figure B.29 : IGV image of mutation *VTC1 / YER072W* c.248G>A, p.R83K (ChrV:300881). IonXpress_002 indicates reference strain (upper part of the image) and IonXpress_003 (lower part of the image) indicates H7.

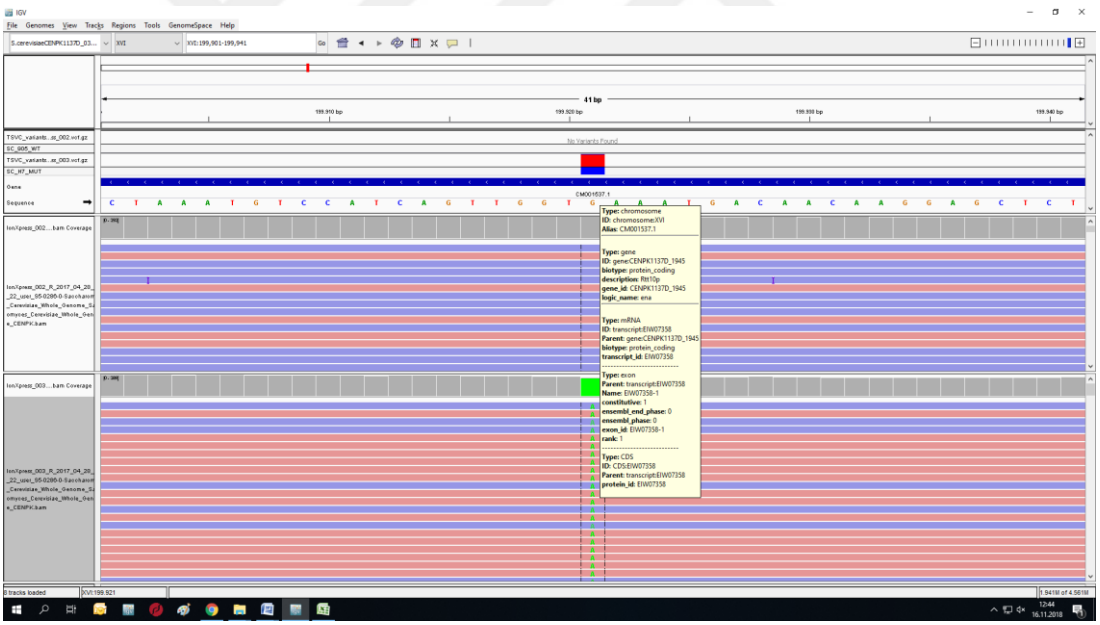

Figure B.30 : IGV image of mutation *RTT10 / YPL183C* c.2498G>A, p.S833L (ChrXVI:199921). IonXpress_002 indicates reference strain (upper part of the image) and IonXpress_003 (lower part of the image) indicates H7.

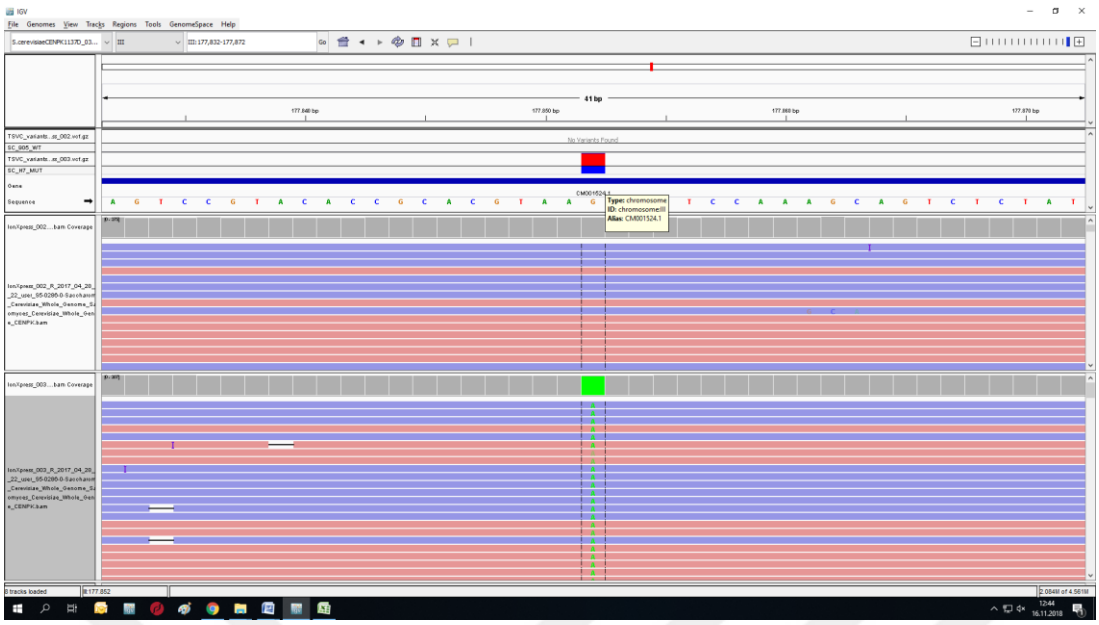

Figure B.31 : IGV image of mutation between the *RPS14A* and *snR189* (smallRNA) G>A (III:177852). IonXpress_002 indicates reference strain (upper part of the image) and IonXpress_003 (lower part of the image) indicates H7.

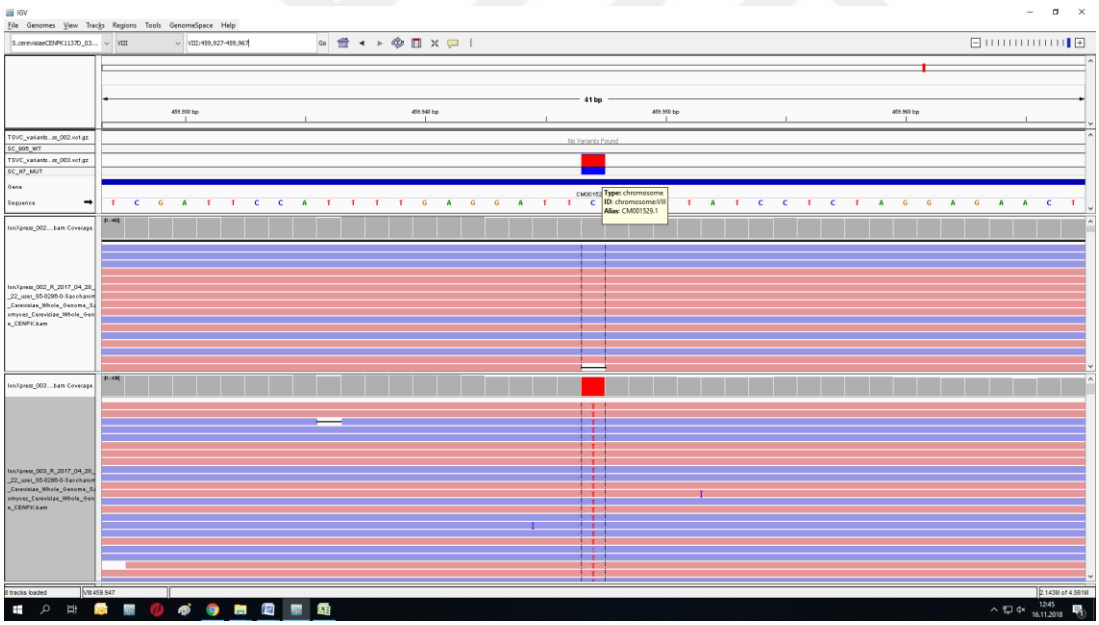

Figure B.32 : IGV image of mutation *YHRWdelta13* c.211C>T (ChrVIII:459947). IonXpress_002 indicates reference strain (upper part of the image) and IonXpress_003 (lower part of the image) indicates H7.

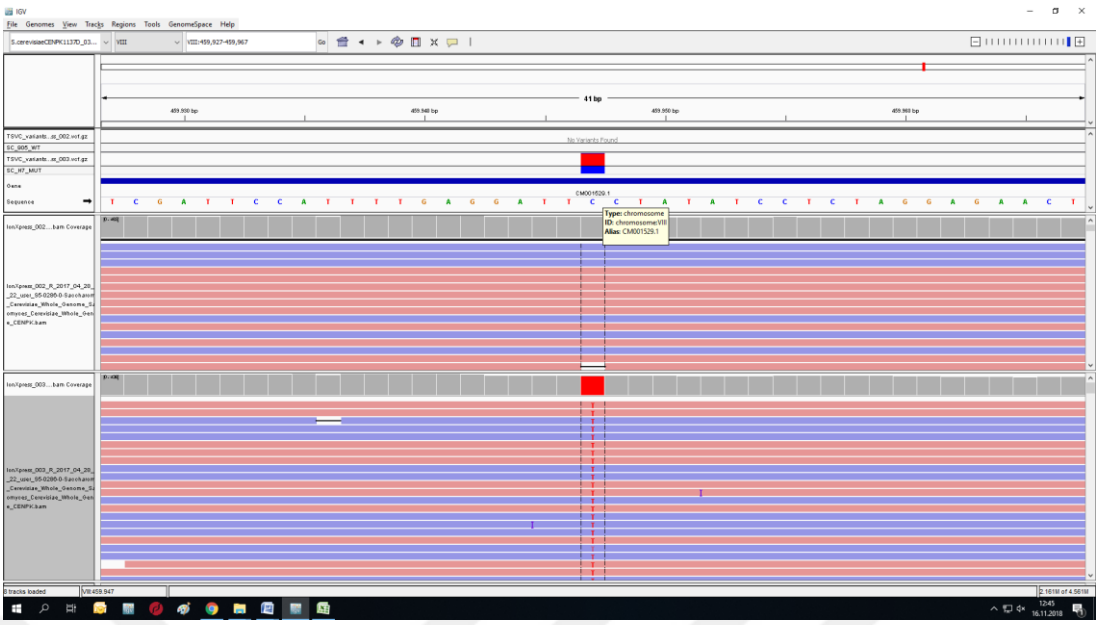

Figure B.33 : IGV image of mutation *PUG1 / YER185W* c.618C>T p.E206= (ChrV:557833). IonXpress_002 indicates reference strain (upper part of the image) and IonXpress_003 (lower part of the image) indicates H7.

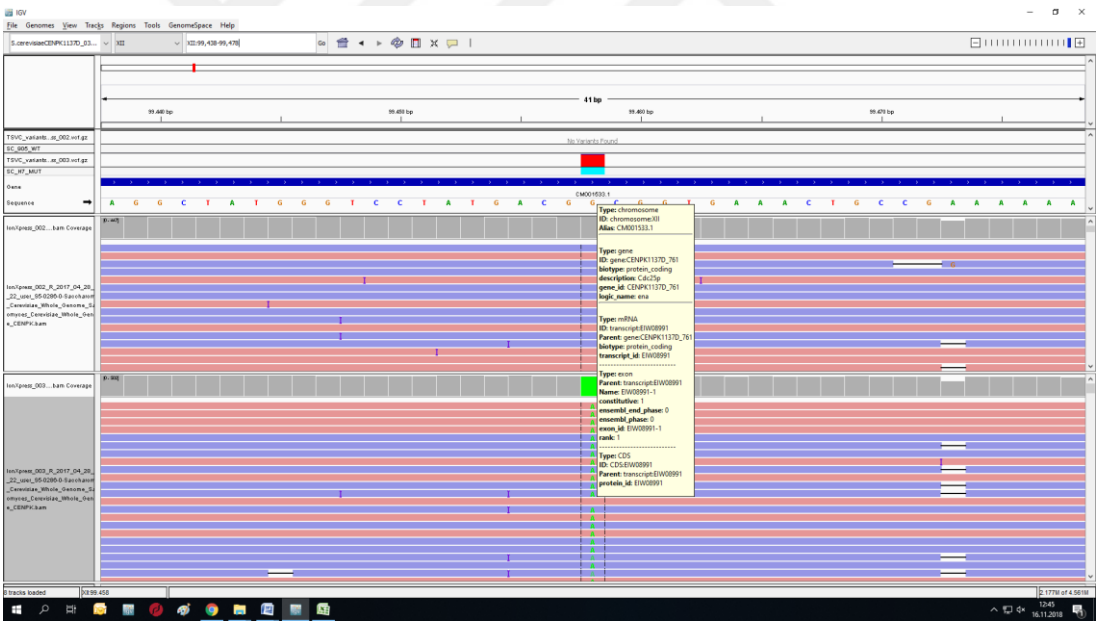

Figure B.34 : IGV image of mutation *CDC25 / YLR310C* c.2204G>A p. G735D (ChrXII:99458). IonXpress_002 indicates reference strain (upper part of the image) and IonXpress_003 (lower part of the image) indicates H7.

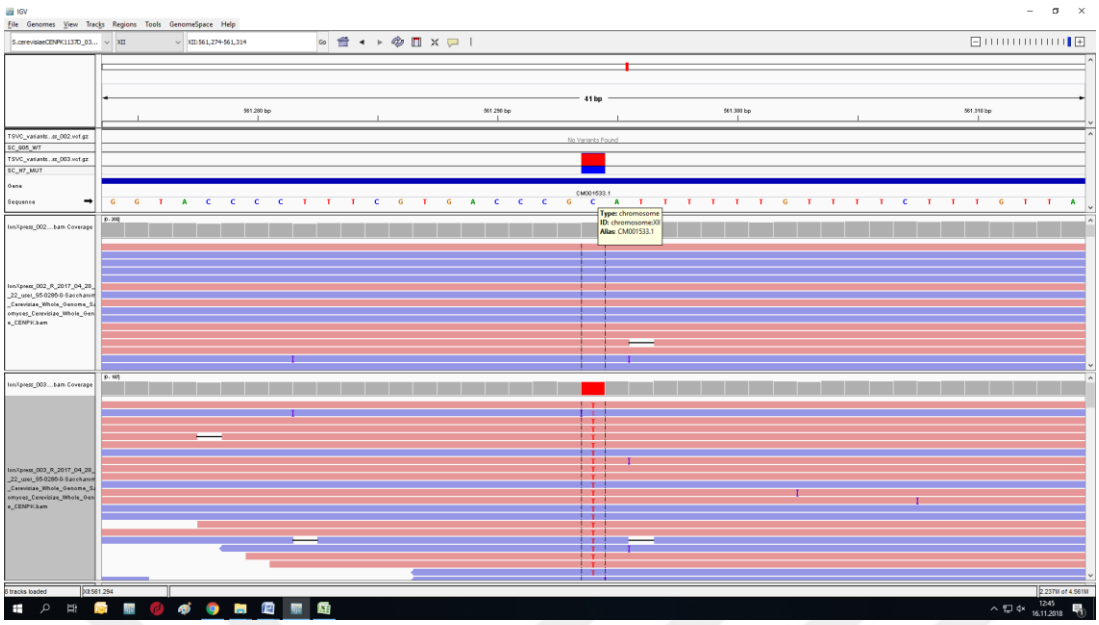

Figure B.35 : IGV image of mutation *MSC3 c.2187+234C>T* (Chr XII:561294). IonXpress_002 indicates reference strain (upper part of the image) and IonXpress_003 (lower part of the image) indicates H7.

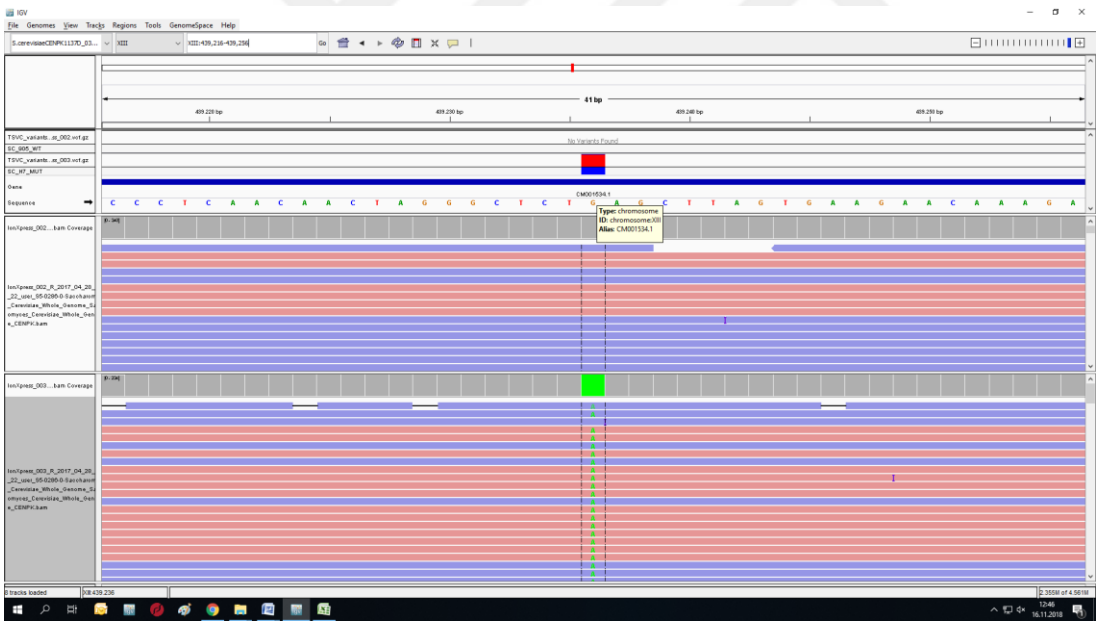

Figure B.36 : IGV image of mutation *VBA1 / YMR088C* c.-31G>A (ChrXIII:439236). IonXpress_002 indicates reference strain (upper part of the image) and IonXpress_003 (lower part of the image) indicates H7.

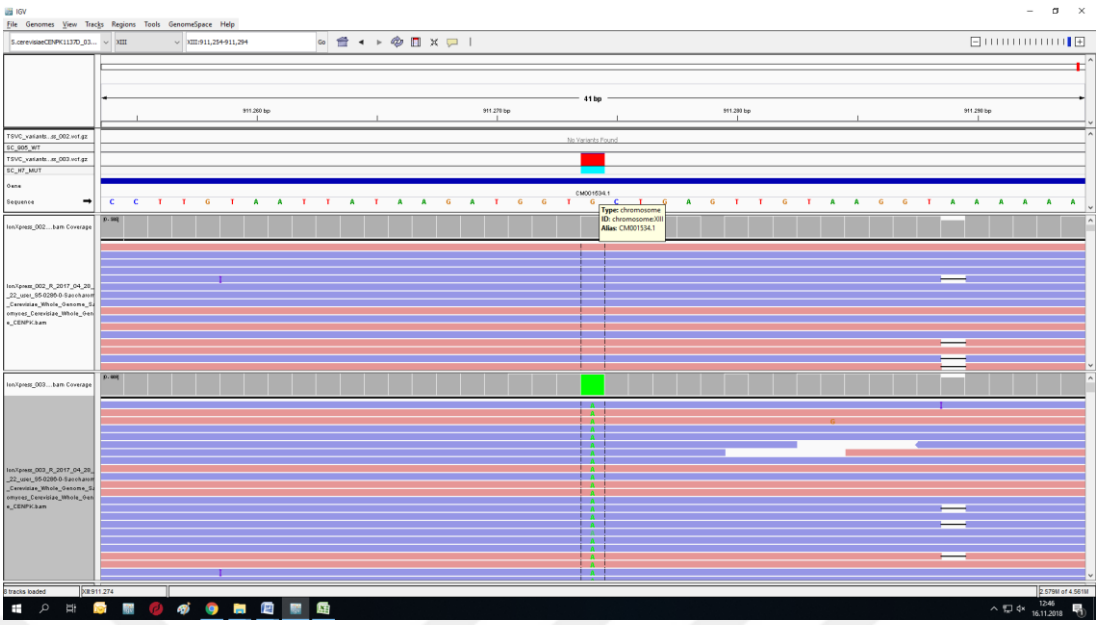

Figure B.37 : IGV image of mutation *YMR321C c. 318+747G>A* (ChrXIII:911274). IonXpress_002 indicates reference strain (upper part of the image) and IonXpress_003 (lower part of the image) indicates H7.

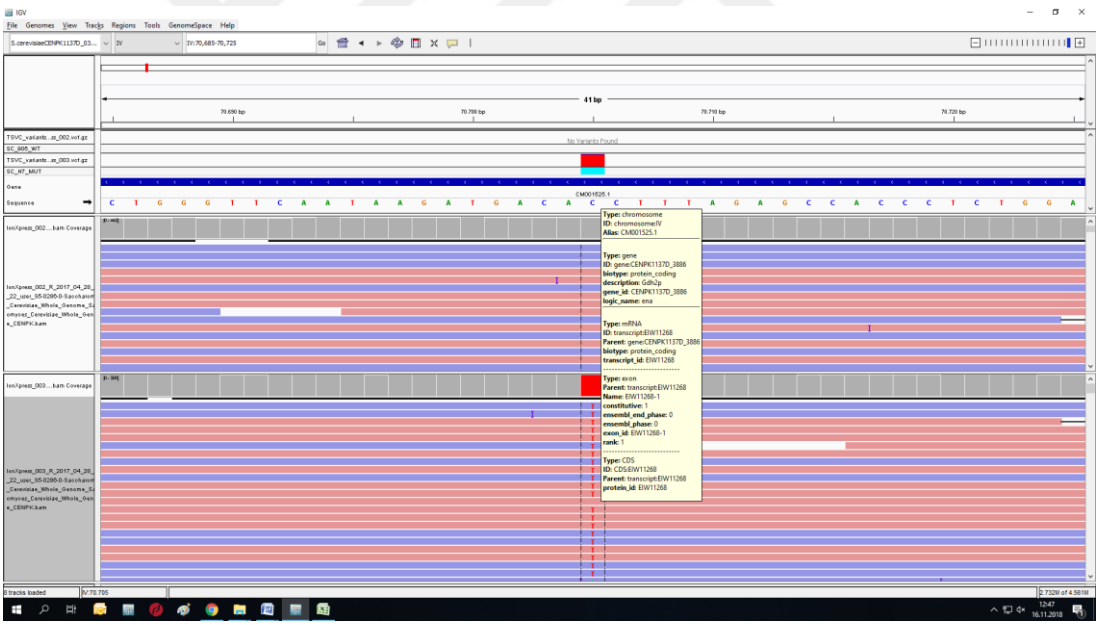

Figure B.38 : IGV image of mutation *GDH2 / YDL215C* c.1880C>T, p.G627D(ChrIV:70705). IonXpress_002 indicates reference strain (upper part of the image) and IonXpress_003 (lower part of the image) indicates H7.

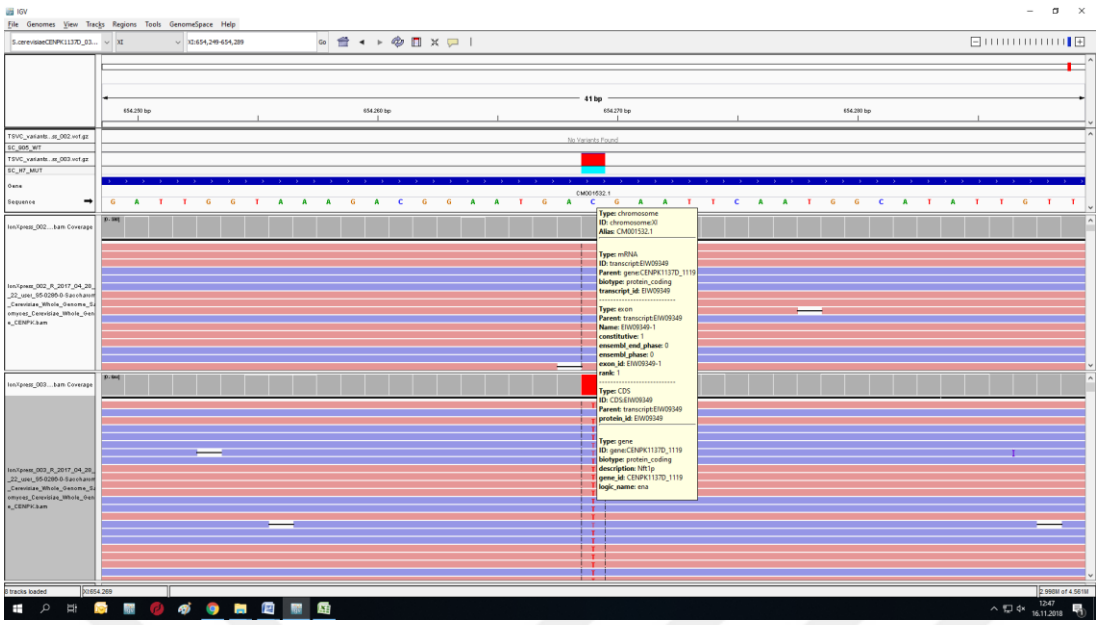

Figure B.39 : IGV image of mutation *NFT1 / YKR103W* c.2186C>T, p.T729M (ChrXI:654269). IonXpress_002 indicates reference strain (upper part of the image) and IonXpress_003 (lower part of the image) indicates H7.

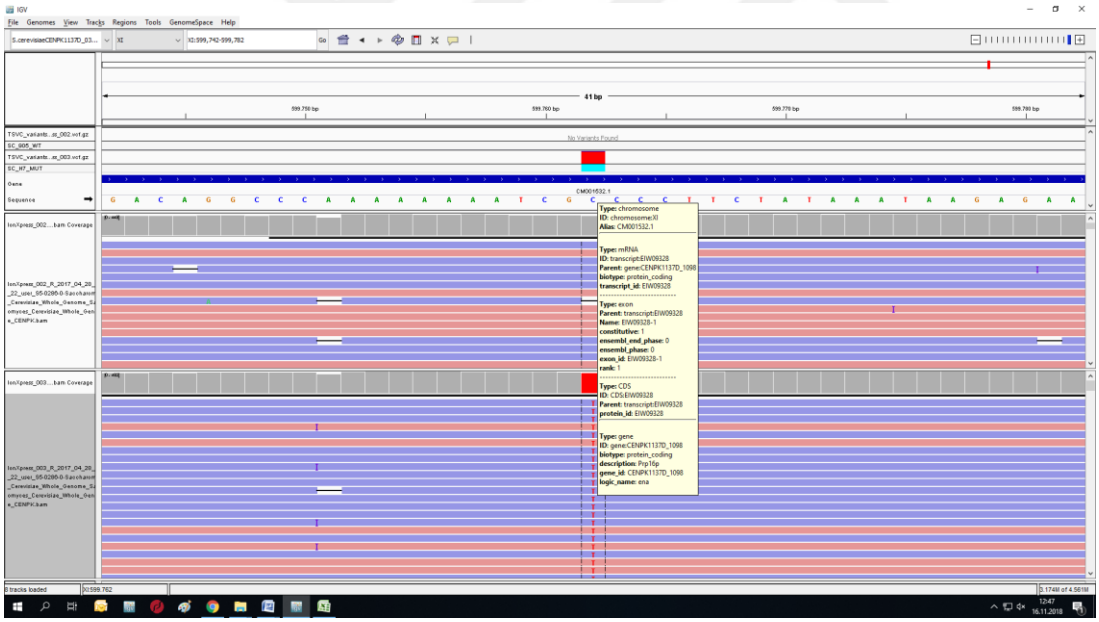

Figure B.40 : IGV image of mutation *PRP16 / YKR086W* c.251C>T, p.A84V (ChrXI:599762). IonXpress_002 indicates reference strain (upper part of the image) and IonXpress_003 (lower part of the image) indicates H7.

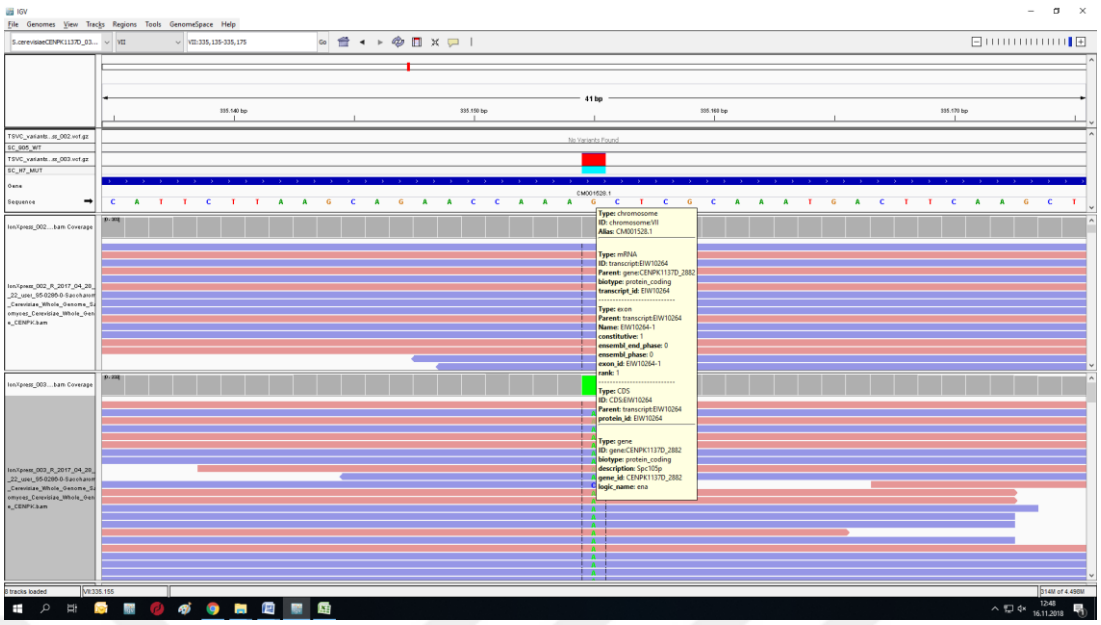

Figure B.41 : IGV image of mutation *SPC105 / YGL093W* c.83G>A, p.S28N (ChrVII:335155). IonXpress_002 indicates reference strain (upper part of the image) and IonXpress_003 (lower part of the image) indicates H7.

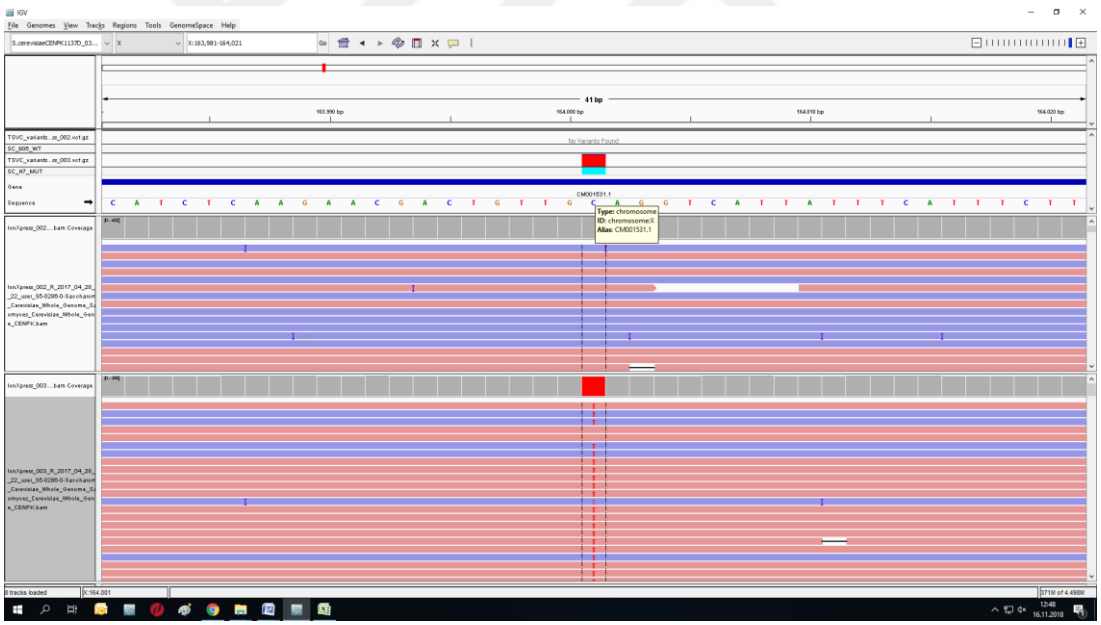

Figure B.42 : IGV image of mutation *MCO6 / YJL127C-B* c.159+19C>T (ChrX:164001). IonXpress_002 indicates reference strain (upper part of the image) and IonXpress_003 (lower part of the image) indicates H7.

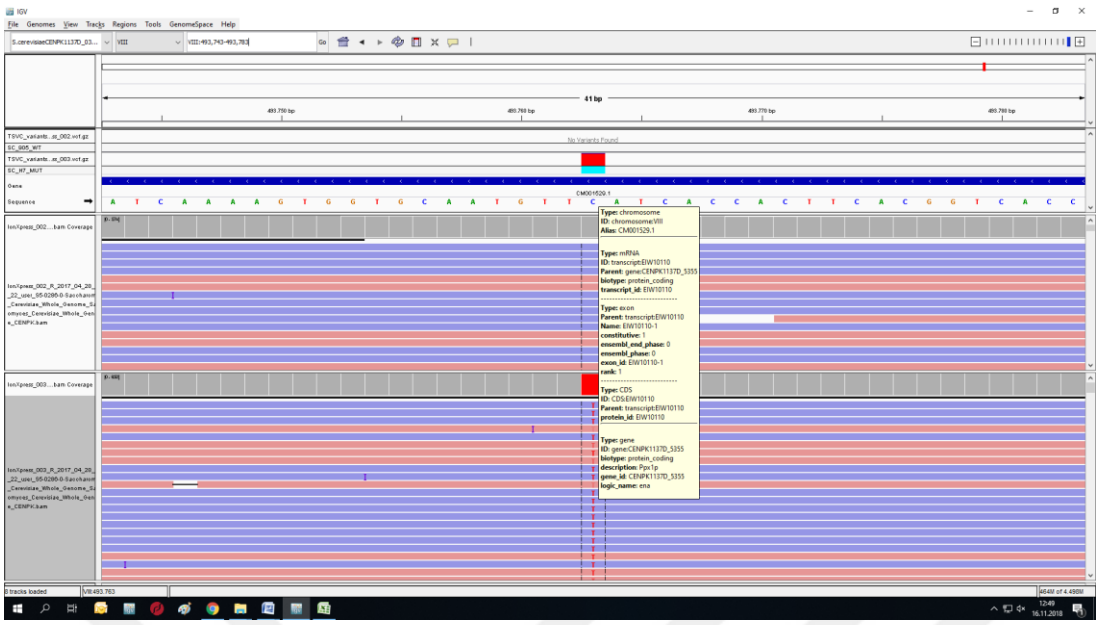

Figure B.43 : IGV image of mutation *PPX1 / YHR201C* c.567C>T, p.M189I(ChrVIII:493763). IonXpress_002 indicates reference strain (upper part of the image) and IonXpress_003 (lower part of the image) indicates H7.

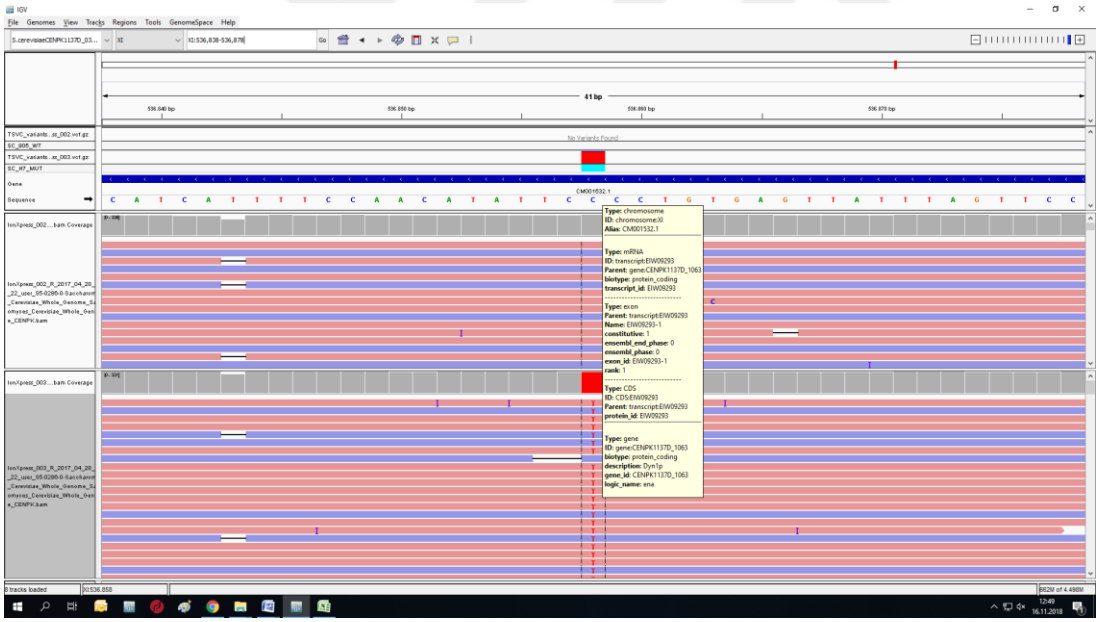

Figure B.44 : IGV image of mutation *DYN1 / YKR054C* c.10724C>T, p.G3575E (ChrXI:536858). IonXpress_002 indicates reference strain (upper part of the image) and IonXpress_003 (lower part of the image) indicates H7.

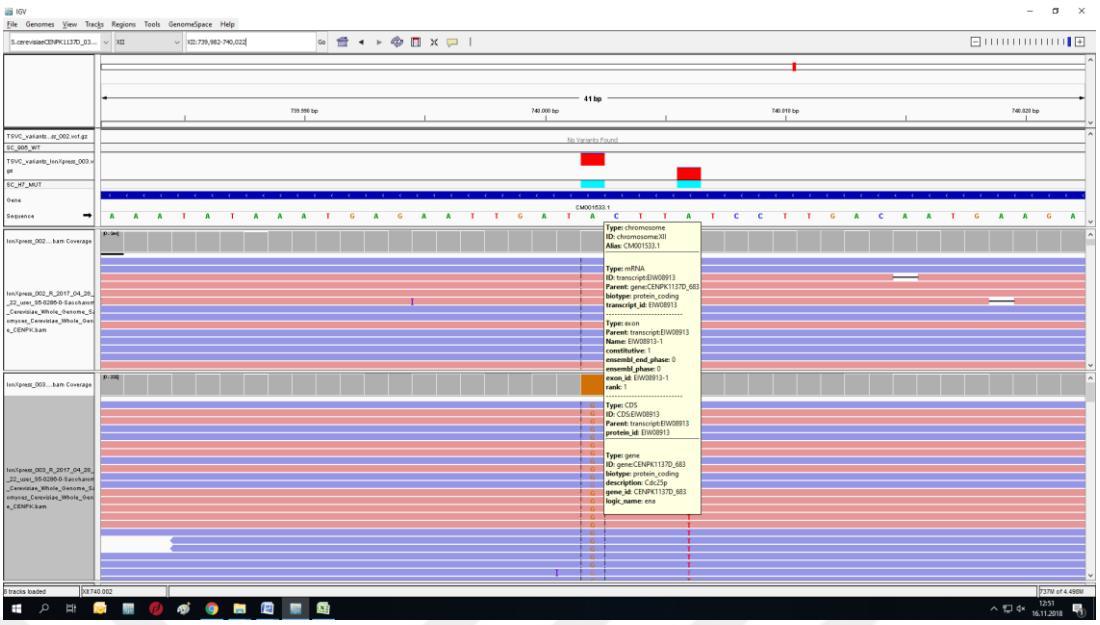

Figure B.45 : IGV image of mutation *CDC25 / YLR310C* c.1605A>G p.S535= (ChrXII:740002). IonXpress_002 indicates reference strain (upper part of the image) and IonXpress_003 (lower part of the image) indicates H7.

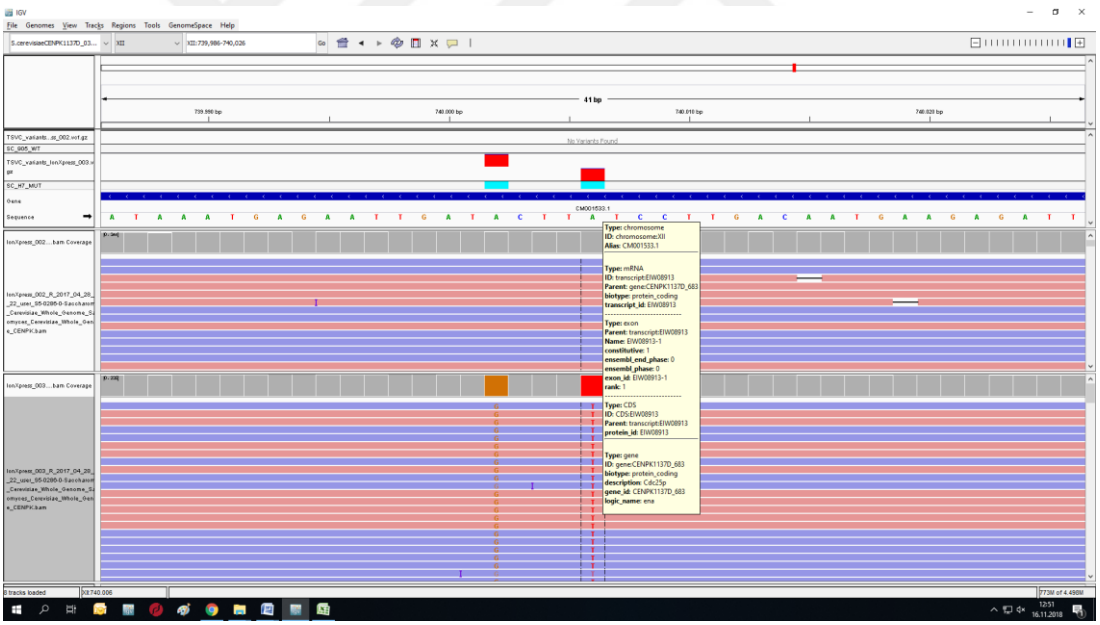

Figure B.46 : IGV image of mutation *CDC25 / YLR310C* c.1601A>T p.I534K (ChrXII:740006). IonXpress_002 indicates reference strain (upper part of the image) and IonXpress_003 (lower part of the image) indicates H7.

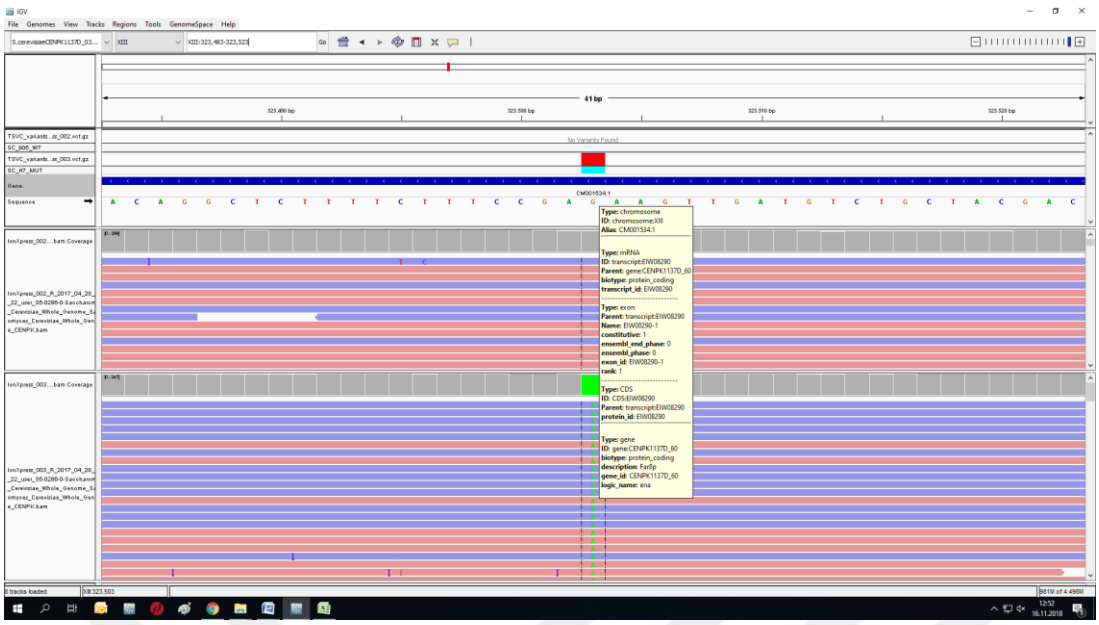

Figure B.47 : IGV image of mutation *FAR8 / YMR029C* c.4158G>A p.F486= (ChrXIII:323503). IonXpress_002 indicates reference strain (upper part of the image) and IonXpress_003 (lower part of the image) indicates H7.

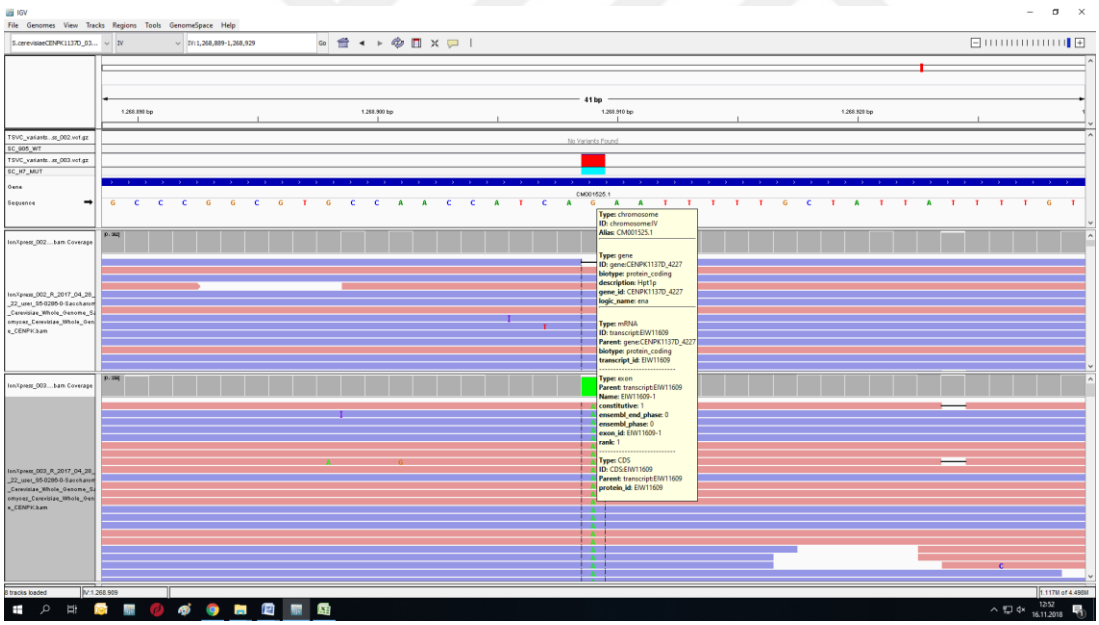

Figure B.48 : IGV image of mutation *HPT1 / YDR399W* c.179G>A, p.R60K (ChrIV:1268909). IonXpress_002 indicates reference strain (upper part of the image) and IonXpress_003 (lower part of the image) indicates H7.

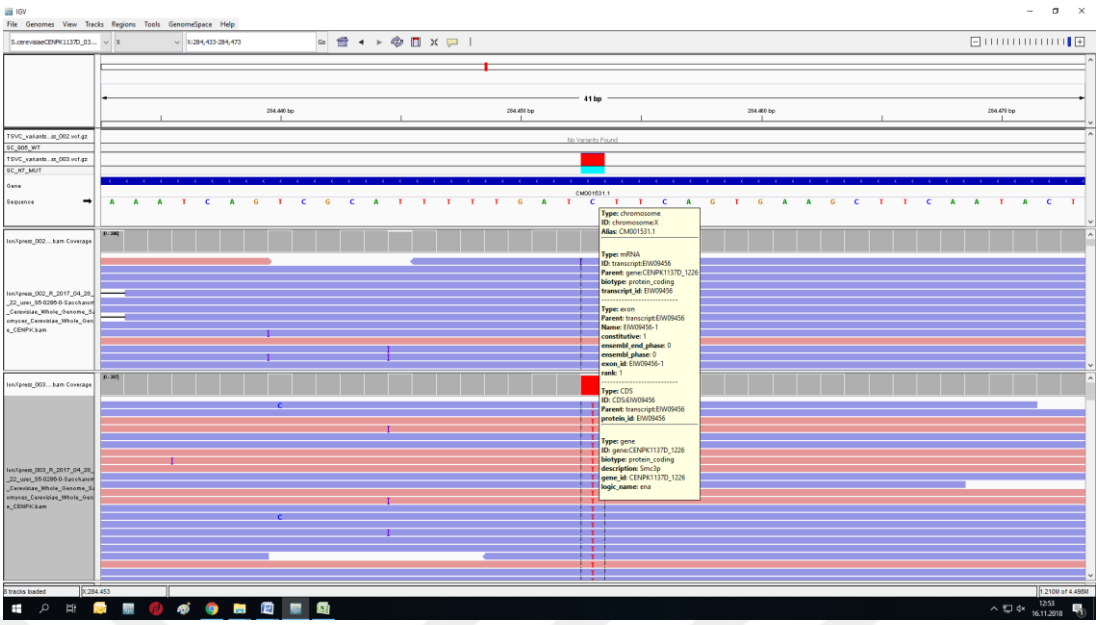

Figure B.49 : IGV image of mutation *SMC3 / YJL074C* c.867C>T, p.K89= (ChrX:284453). IonXpress_002 indicates reference strain (upper part of the image) and IonXpress_003 (lower part of the image) indicates H7.

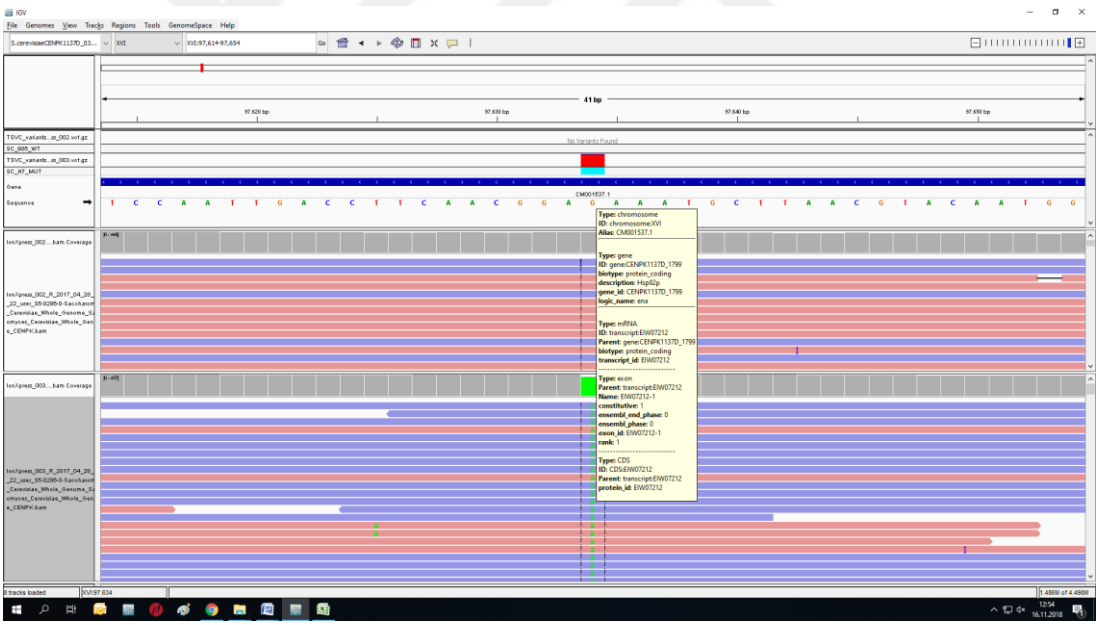

Figure B.50 : IGV image of mutation *HSP82 / YPL240C* c.927G>A p.P309= (ChrXVI:97634). IonXpress_002 indicates reference strain (upper part of the image) and IonXpress_003 (lower part of the image) indicates H7.

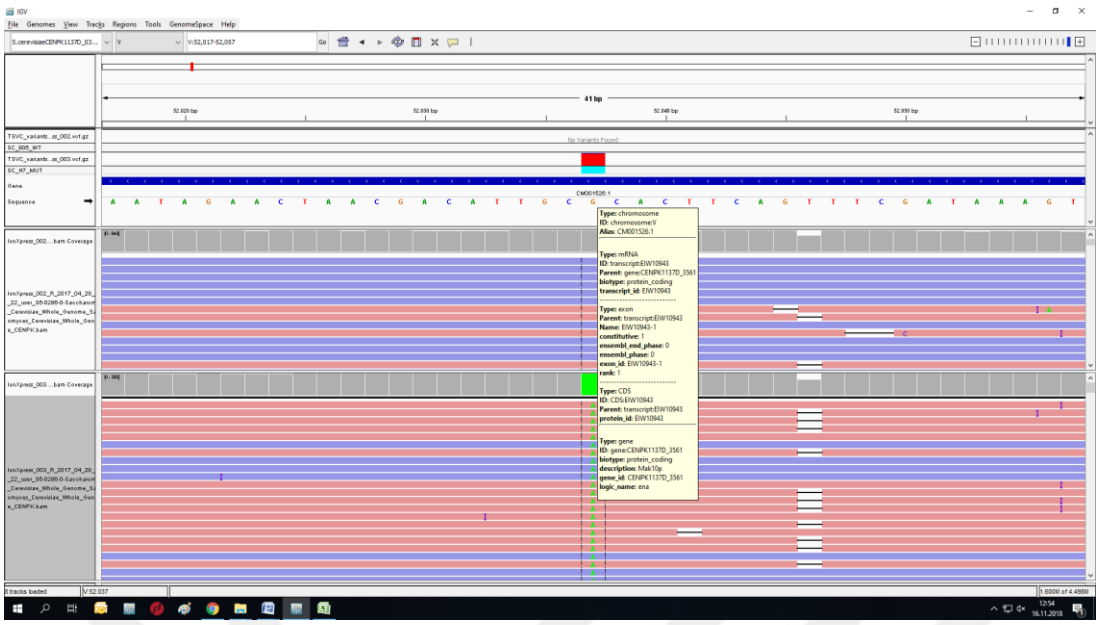

Figure B.51 : IGV image of mutation *MAK10 / YEL053C* c.1906G>A, p.R636K (Chr V:52037). IonXpress_002 indicates reference strain (upper part of the image) and IonXpress_003 (lower part of the image) indicates H7.

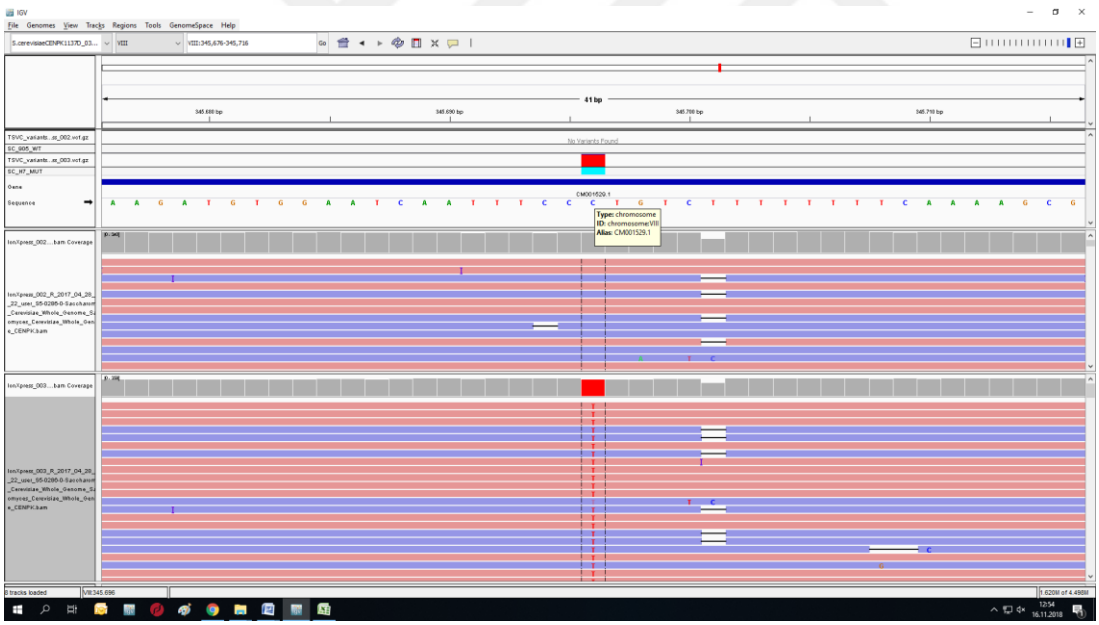

Figure B.52 : IGV image of mutation *MSH1 / YHR120W* c.2880+69C>T (ChrVIII:345696). IonXpress_002 indicates reference strain (upper part of the image) and IonXpress_003 (lower part of the image) indicates H7.

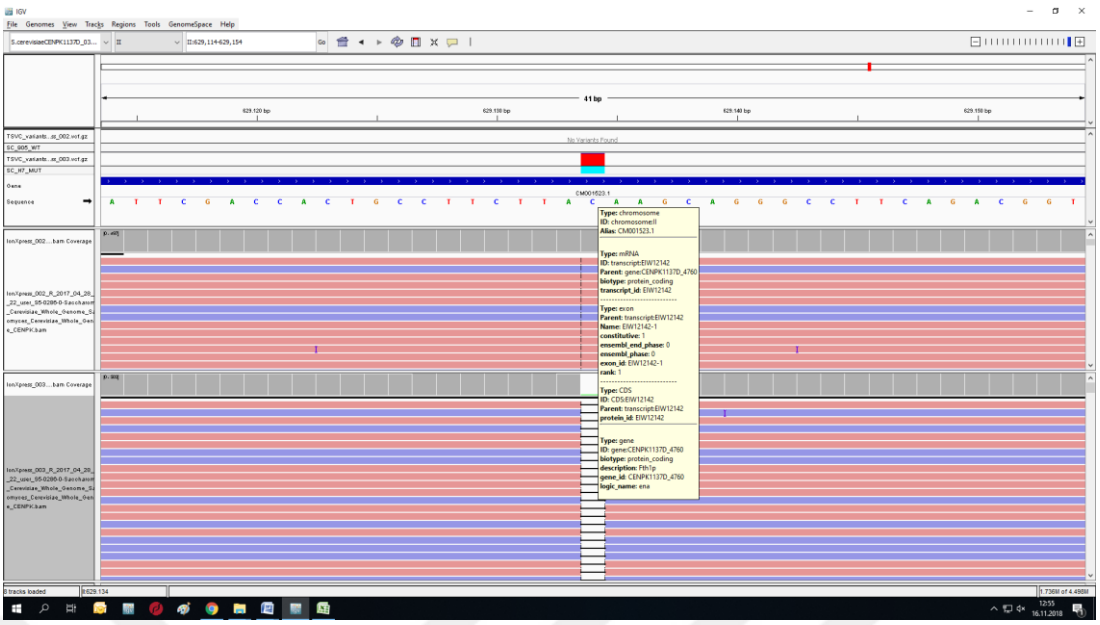

Figure B.53 : IGV image of mutation *FTH1 / YBR207W* c.211delC, p.Q71Kfs (ChrII:629134). IonXpress_002 indicates reference strain (upper part of the image) and IonXpress_003 (lower part of the image) indicates H7.

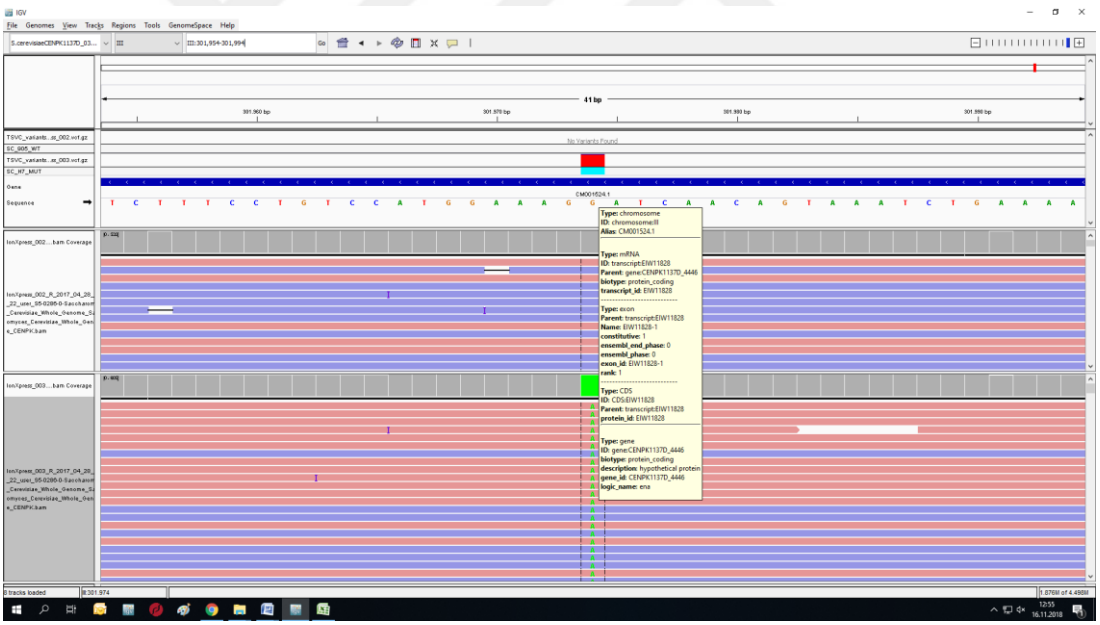

Figure B.54 : IGV image of mutation *YCR101C c.250C>T*, p.P84S (ChrIII:301974). IonXpress_002 indicates reference strain (upper part of the image) and IonXpress_003 (lower part of the image) indicates H7.

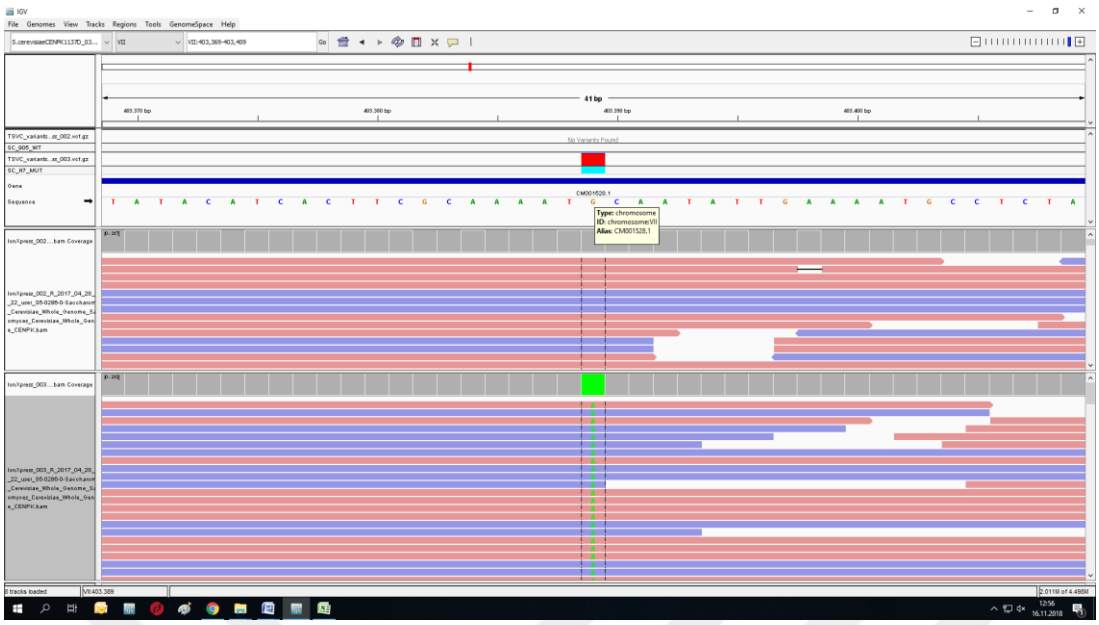

Figure B.55 : IGV image of mutation *YGL052W* c. 112G>A, p.A38T (ChrVII:403389). IonXpress_002 indicates reference strain (upper part of the image) and IonXpress_003 (lower part of the image) indicates H7.

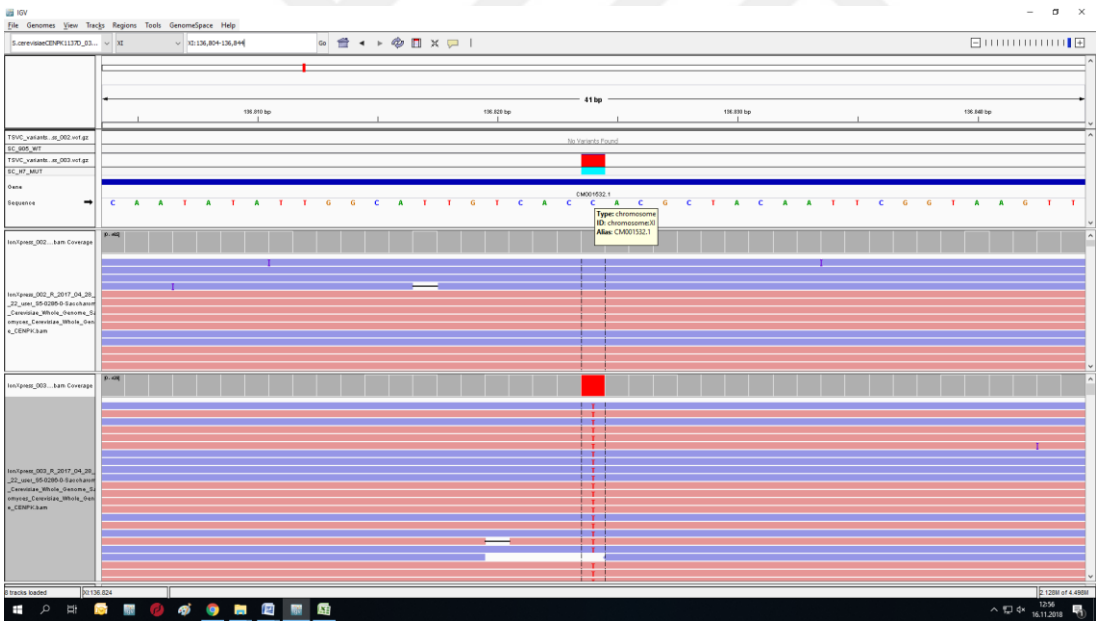

Figure B.56 : IGV image of mutation *MCD4 / YKL165C* c.2760+918C>T (ChrXI:136824). IonXpress_002 indicates reference strain (upper part of the image) and IonXpress_003 (lower part of the image) indicates H7.

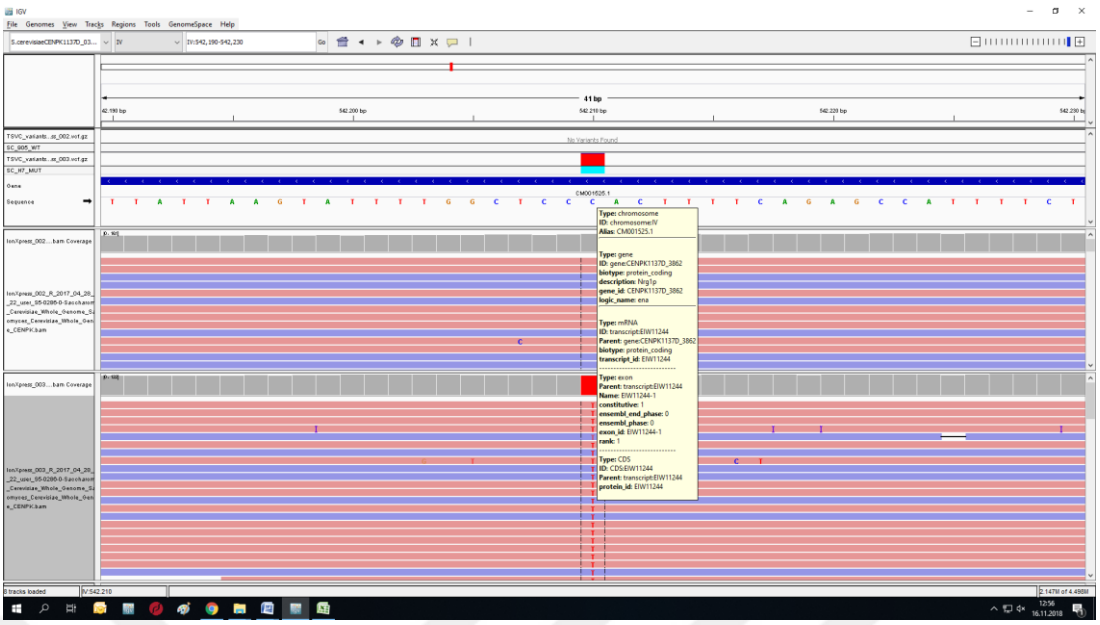

Figure B.57 : IGV image of mutation *NRG1 / YDR043C* c.245C>T p.W82* (ChrIV:542210). IonXpress_002 indicates reference strain (upper part of the image) and IonXpress_003 (lower part of the image) indicates H7.

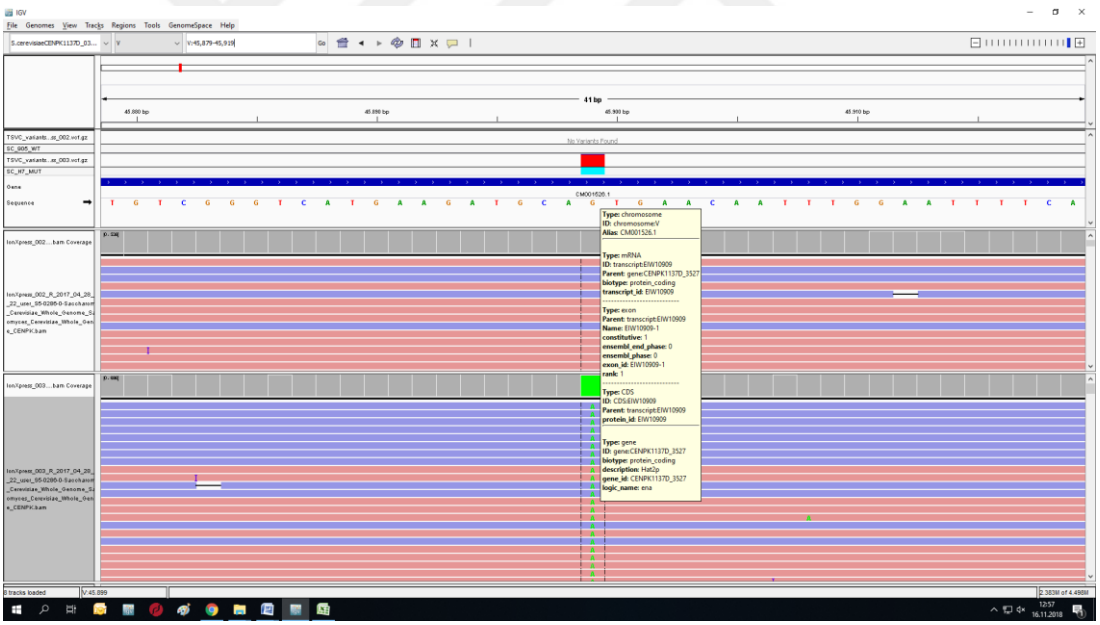

Figure B.58 : IGV image of mutation *HAT2 / YEL056W* c.892G>A, p.V298M (ChrV:45899). IonXpress_002 indicates reference strain (upper part of the image) and IonXpress_003 (lower part of the image) indicates H7.

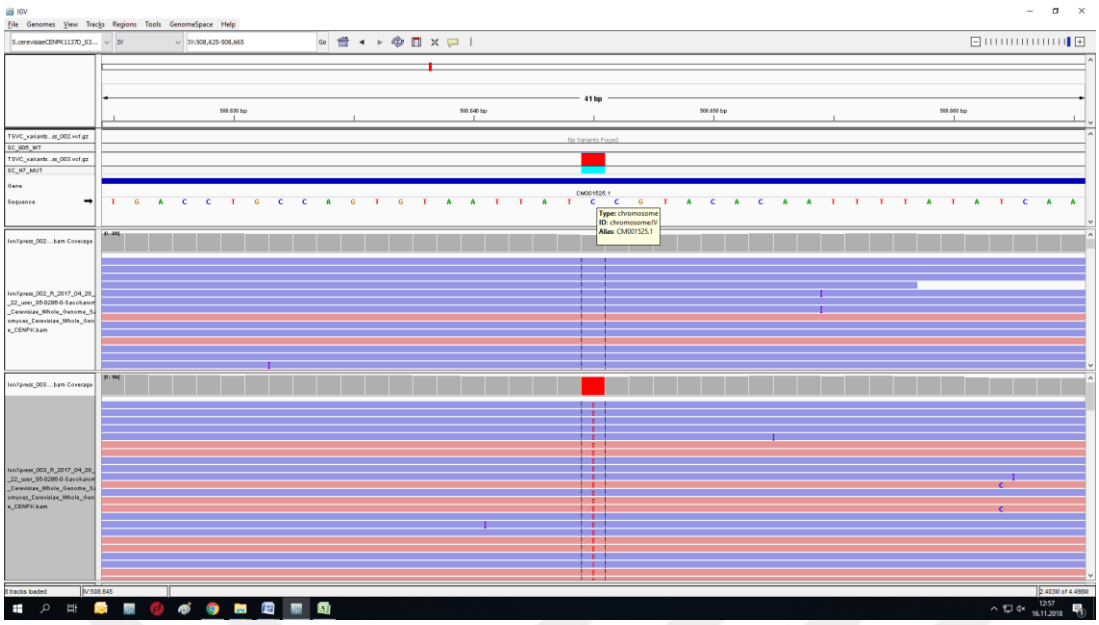

Figure B.59 : IGV image of mutation *LYS14 / YDR034C* c.2373+53 C>T (ChrIV:508645). IonXpress_002 indicates reference strain (upper part of the image) and IonXpress_003 (lower part of the image) indicates H7.

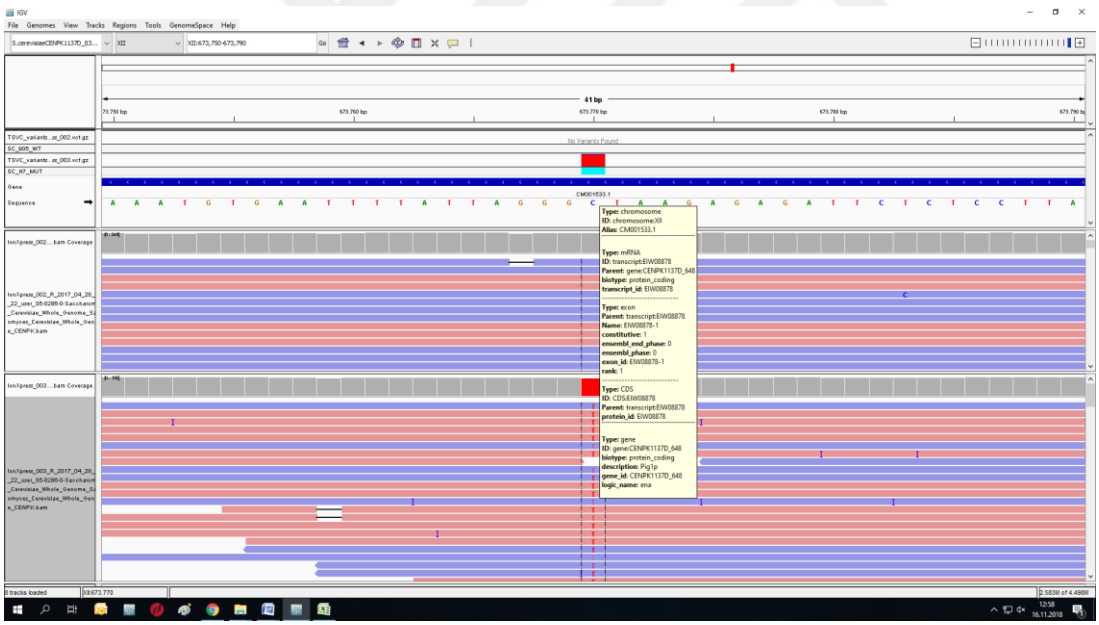

Figure B.60 : IGV the image of mutation *PIG1 / YLR273C* c.1892C>T, p.S631N (ChrXII:673770). IonXpress_002 indicates reference strain (upper part of the image) and IonXpress_003 (lower part of the image) indicates H7.

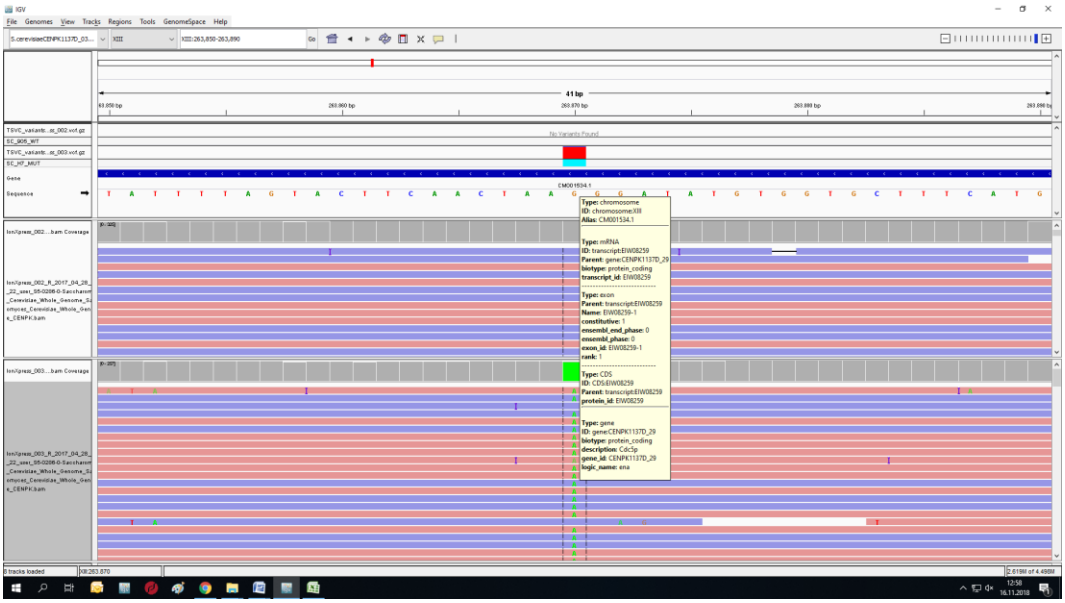

Figure B.61 : IGV image of mutation *CDC5 / YMR001C* c.1998G>A p.P666= (ChrXIII:263870). IonXpress_002 indicates reference strain (upper part of the image) and IonXpress_003 (lower part of the image) indicates H7.

CURRICULUM VITAE

Name Surname **:** Nazlı KOCAEFE ÖZŞEN

EDUCATION:

- **B.Sc.** **:** 2009, Istanbul University, Science and Literature Faculty, Department of Molecular Biology and Genetics
- **M.Sc.** **:** 2012, Istanbul Technical University, Graduate School of Science Engineering and Technology, Department of Advanced Technologies

PROFESSIONAL EXPERIENCE AND REWARDS:

- 17.12.2019 TTGV (Türkiye Teknoloji Geliştirme Vakfı) 250K Sağlık Teknolojilerinde Müşteri ve İş Geliştirme Programı/İstanbul-"Hayvanlarda Viral Hastalıkların Tanısı Amaçlı Kişiselleştirilmiş Kit"

PUBLICATIONS, PRESENTATIONS AND PATENTS ON THE THESIS:

- **Kocaefe-Özşen, N.,** Yilmaz, B., Alkım, C., Arslan, M., Topaloğlu, A., İbrahim Kısakesen, H., Gülsev, E., & Çakar, Z. P. (2022). Physiological and Molecular Characterization of an Oxidative Stress-Resistant *Saccharomyces cerevisiae* Strain Obtained by Evolutionary Engineering. Frontiers in Microbiology, 13, 822864.

OTHER PUBLICATIONS, PRESENTATIONS AND PATENTS:

- **Kocaefe N.,** Yilmaz U, Alkim C., Cakar Z. P. (2011): Physiological and Genetic Analyses of an Oxidative Stress-Resistant *Saccharomyces cerevisiae* Mutant. International Conference on Enzyme Science and Technology, ICEST 2011, Abstract book, 31 October – 4 November, İzmir, Türkiye.
- Holyavkin C., Alkim C., Yilmaz U., Balaban B. G., Kucukgoze G., **Kocaefe N.,** Gunduz S., Akman S., Cakar Z. P. **(**2011): Metal Content and *COT1*/*AFT1* Expression of Cobalt-Resistant *Saccharomyces cerevisiae* Mutant Obtained by Evolutionary Engineering. ICEST 2011, Abstract book, 31 October – 4 November, İzmir, Türkiye.
- Arslan, M., Turanli-Yildiz, B., Yilmaz, B., **Kocaefe, N.,** and Cakar, Z. P. (2018). An improved semi-quantitative spot assay to analyse chronological lifespan in yeast. *Romanian Biotechnology Letters*, 23, 13551.
- Arslan, M., **Kocaefe, N.,** and İleri, M. (2022). W locus alleles of the KIT Gene in Turkish Van Cats and Their Association with Certain Phenotypes. *Van Sağlık Bilimleri Dergisi*, Van Yüzüncü Yıl Üniversitesi 40. Kuruluş Yılı Özel Sayısı , 206-214 . DOI: 10.52976/vansaglik.1141256